AMIRA REPORT

AUGUST 1987

CONTROLS ON GOLD AND SILVER GRADES IN VOLCANOGENIC SULPHIDE DEPOSITS (84/P210)

CONTENTS

ASSOCIATED REPORTS distributed at the August, 1987 AMIRA Meeting

INTRODUCTION

Restatement of Aims:

To investigate the geological and geochemical controls on the distribution of precious metals within volcanic hosted massive sulphide deposits, with the objective of developing exploration models useful for the discovery of further precious metal-rich deposits.

Progress in 1987

This is the third major report on the research results to emerge from this project, and marks the end of the second year of a three year programme. The project is on schedule and, although we lost two of our team members to industry earlier in the year, progress in other areas has been excellent. Our progress since the previous meeting in November, 1986 is listed below (* items are reported in this volume).

1.* Studies on the Que River precious metal zone are virtually complete, and a final report is included herein.

2.* Gold distribution studies on the F-lens pyrrhotite, magnetite and tourmaline zones is complete. Mineralogical and geochemical work is continuing.

3.* Mapping, petrological and alteration studies on the Lake Selina system are complete.

4.* Whole rock geochemistry and R.E.E. research on the Mount Read Volcanics is near completion.

5,* Gold distribution and metal ratio studies on the Scuddles deposits, W.A., are complete.

6.* Structure and metal distribution studies at Balcooma, Qld, are complete.

7. Investigations on precious metal distribution in the Thalanga massive sulphide deposit, Qld, have commenced.

8. Literature research on gold in the Canadian Precambrian deposits is complete (see associated report).

9.* A discussion paper on the source and movement of gold in submarine volcanic environments has been completed.

Parallel with this AMIRA research, an ARGS-funded study on the thermodynamics of gold transport and deposition mechanisms in VMS systems has been completed and is circulated as a separate report.

In conclusion I would like to thank all members of the AMIRA team: Peter McGoldrick, Tony Crawford, David Huston, Khin Zaw, Steve Hunns, John Pemberton and Stewart Capp, in addition to June Pongratz and Phil Robinson, all of whom have given their unfailing support to the project in 1987.

Ross Large
Project Leader

SUMMARY OF PROJECTS

Final Report on the Footwall Precious Metal Zone, Que River

(Peter J. McGoldrick and Ross R. Large)

Geological and geochemical results of an ongoing study of the unusual Au-anomalous mineralised zone (PMZ) in the eastern footwall of PQ lens at Que River are discussed. The PMZ is best developed in a coarse pyritic polymictic andesitic volcaniclastic which has characteristic patches of 'white alteration' in hand specimen. In thin section secondary K feldspar (often sericitised) is prominent in samples from the PMZ. As well as elevated Au contents, many samples from the PMZ have anomalous Sb, As and Ba. Sulphur in pyrite from the PMZ is distinctive isotopically. $\partial^{34}S$ values decrease from PMZ to 'normal' stringer to massive ore. All these features place constraints on the genesis of the PMZ and have important implications for exploration for similar style mineralisation.

The PMZ is interpreted to be part of the alteration zone developed in andesitic volcaniclastic footwall rocks during formation of the PQ-P north massive sulphide orebody. This stringer mineralisation is crudely zoned from a Cu-rich core surrounded by Pb-Zn bearing stringer to a distal Pb-Zn-Ag-Au-As-Sb stringer. Best development of the distal Au-bearing stringer occurs in more porous and permeable volcanisclastics (e.g. the PMZ). Gold remained in solution in the more proximal parts of the stringer because physico-chemical conditions in the hydrothermal fluids forming the stringer favoured Au transport as bisulfide complexes. Gold could not precipitate until the fluids were oxidised or dramatically cooled in the outer parts of the stringer zone.

F-lens Metal Zonation - Rosebery Mine

(Khin Zaw)

Recent metal zonation studies of the 'F' lens, south-end orebody, Rosebery Mine have revealed three major replacement zones: (1) Tourmaline-quartz ± magnetite zone (2) Pyrrhotite-pyrite zone, and (3) Magnetite-biotite ± chalcopyrite zone. Core logging and metal distribution studies also indicate that gold deposited in the Rosebery orebody during Cambrian exhalation was redistributed and preferentially concentrated in the pyrrhotite-pyrite zone during the later Devonian replacement event.

Progress Report on the Lake Selina Prospect

(Steven R. Hunns)

In the past year work has concentrated on the structure, geochemistry, alteration assemblages and sulphide paragenesis. The Selina Volcanics dip steeply and face towards the west. Poles to cleavage contour plots indicate that the Dora Conglomerate occupies the core of an anticline. At least one and possibly two mylonites have been mapped.

Two styles of mineralization have been recognized:

a. Magnetite-pyrite ± chalcopyrite assemblages, reflecting higher fluid temperatures - To $\geq$ 300°C.

b. Sphalerite-chalcopyrite-galena assemblages, reflecting lower fluid temperatures, i.e. To $\leq$ 250°C.

These mineralizing episodes have been related to rhyo-dacitic porphyry intrusions and later high level intrusion of Murchison Granite equivalents. K-feldspar, chlorite, pyrite and sericite alteration resulted from these intrusive events.

Geochemistry of the Mount Read Volcanics : Internal Correlations and Tectonic Implications

(Anthony Crawford)

Representative least-altered Mount Read Volcanics analyzed for major and trace elements (April, 1986 AMIRA Report) have been analyzed for their rare earth elements. Trace and major geochemical features of the Central Volcanic Complex andesites to rhyolites indicate affinities with high-K calc-alkaline orogenic lavas presently erupting through relatively thick crust at active continental margins (e.g. Mexico, Central America, the Andes). Tyndall Group lavas and associated subvolcanic granites are compositionally closely similar to the Central Volcanic Complex rocks. The Western Volcanic Sequence includes in the area south of Queenstown possible basement composed of depleted tholeiites (Miners Ridge basalts) with strong compositional similarities to the upper lavas in the Serpentine Hill mafic-ultramafic complex. Overlying these tholeiites is

a sequence of lavas, with voluminous basalts in places, which range from high-K basalts to LREE- and P205-enriched shoshonites. This sequence extends from south of Queenstown to the Que-Hellyer area, and has geochemical affinities with lavas associated with arc-continent collision, such as those in Eastern Papua.

A new tectonic model for western Tasmania is briefly described, in which the so-called ophiolites originally formed an extensive allochthon over much of western and central Tasmania. These were emplaced during arc-continent collision in the Middle Cambrian. Mount Read Volcanics erupted through and onto the allochthon. The high gold tenor of the Tasmanian VMS deposits may be due to the fact that hydrothermal fluids associated with Mount Read volcanism and shallow intrusive activity penetrated into the basement allochthon, which is composed of second-stage melt magnesian lavas which are likely to have higher gold contents than normal basalts.

Progress Report on the Alteration Geochemistry of the Mount Read Volcanics

(Peter J. McGoldrick, Stewart C. Capp and Ross R. Large)

This report briefly discusses important alteration processes that have affected the MRV. Analytical data for all the important host rock types at Que River are presented and summarised. These include 'fresh' andesites, highly altered footwall volcaniclastic rocks and less altered hanging wall dacites and the fuchsite-carbonate altered 'breccia'. Data for samples of MRV from Lake Selina, the Sterling Valley and Mt Jukes-Mt Darwin areas are presented. Proposed future directions for this study are briefly discussed.

Gold-base metal Relationships at Scuddles, W.A.

(Peter Ruxton)

Scuddles is a highly deformed VMS deposit which contains moderate levels of gold and base metals (1.2 ppm Au, 78 ppm Ag, 9.5% Zn, 0.7% Pb, 0.8% Cu) which are generally typical of Archean deposits elsewhere. Gold is evenly distributed throughout the massive sulphide (0.5 to 3 ppm) and depleted in the copper-rich stringer zone (< 0.5 ppm). The gold is enriched in the middle to lower parts of the zinc-rich zone, and not at the top of the massive sulphide (cf. Rosebery, Hellyer). On detailed downhole assay plots, it is evident that variations in copper grades are paralleled by variations in gold grade which suggests a fundamental association between the two metals. These relationships are confirmed by metal versus gold plots on three sections through the deposit.

Balcooma Prospect, Northern Queensland

(David L. Huston)

The Balcooma prospect contains four mineralized horizons within a pelitic lens hosted by metagreywackes and volcaniclastics. The central copper horizon contains most of the known mineralization (3.5 mt of 3.0% Cu), while the other three horizons contain massive Zn-Pb-Ag-(Cu-Au) sulphides. Four phases of folding have resulted in a complex structural picture. Three distinct types of massive mineralisation have been defined: (1) massive magnetite (2) massive pyrite-chalcopyrite, and (3) massive sphalerite-galena-pyrite. All types contain very little gold (less than 1 ppm), however there is a moderate to good correlation between copper and gold. It is concluded that the chemistry of the ore fluid (low pH and low fO_2) was unfavourable for gold transport in this system.

Source and Movement of Gold in Submarine Volcanic Environments - A Discussion Paper

(Ross R. Large)

Preliminary calculations suggest that gold, silver and base metals have been leached from a volume of about 60 km^3 of footwall source rocks to provide the quantity of metals in deposits such as Hellyer and Rosebery. The zone of leaching is approximated by an inverted cone with the deposit at the apex of the cone. Convective seawater leaching probably penetrated 4-6 km into the footwall sequence and leached metal from the Central Volcanic Sequence and underlying early Cambrian(?) and Precambrian basement rocks. Calculated amounts of metals required to be leached are 0.25 ppm Cu, 4.3 ppm Pb, 8 ppm Zn, 18 ppm S, 0.01 ppm Ag and 0.2 ppb. Trace element data suggests that rhyolite-andesite volcanics within the CVS are an adequate source of all metals including the gold and silver.

Solubility calculations suggest that gold, silver and base metals are mobilised as chloride complexes, deep in the high temperature part of the convection cone. In response to dropping temperature and buffering by the volcanics, gold transport switches from $AuCl_2^-$ to $Au(HS)_2^-$ in the upper part of the volcanic pile. The level of gold saturation and the elevation of the switchover of gold complexes in the convective cone has a major control on the ultimate gold content of the seafloor massive sulphide deposits.

Review of the Canadian Precambrian Deposits, with emphasis on Precious Metals

(separate report by John Pemberton)

Precambrian volcanogenic massive sulphides are found in greenstone belts of volcanic and sedimentary rock types in Superior, Churchill and Slave Provinces. Tonnage and grade data for 127 deposits shows an enrichment in Cu and depletion in Pb, Zn, Au and Ag compared to the Tasmanian deposits. Au is enriched in four deposits in the Noranda area, and Ag is enriched in the Wabigoon belt of Superior and in Slave Province.

Nine deposits are discussed with regard to precious metal distribution. Cu is enriched in the footwall stringer zone and base of the massive sulphides while Zn is enriched towards the hanging wall and laterally. Precious metals show two patterns of enrichment being associated with Cu in the base of the orebodies or with Zn towards the top. Metal zoning and morphology of the deposits is dependent on the controls on hydrothermal solutions, environment of deposition, activity and chemistry of host rocks and source rock chemistry.

FINAL REPORT ON THE FOOTWALL PRECIOUS METAL ZONE, QUE RIVER

Peter J. McGoldrick and Ross.R. Large

AMIRA Report

August 1987

FINAL REPORT ON THE FOOTWALL PRECIOUS METAL ZONE, QUE RIVER

Peter J. McGoldrick and Ross R. Large

Summary

In this report geological and geochemical results of an ongoing study of the unusual Au-anomalous mineralised zone (PMZ) in the eastern footwall of PQ lens at Que River are discussed. The PMZ is best developed in a coarse pyritic polymictic andesitic volcaniclastic which has characteristic patches of "white alteration" in hand specimen. In thin section secondary K feldspar (often sericitised) is prominent in samples from the PMZ. As well as elevated Au contents, many samples from the PMZ have anomalous Sb, As and Ba. Sulphur in pyrite from the PMZ is distinctive isotopically. $\partial^{34}S$ values decrease from PMZ to "normal" stringer to massive ore. All these features place constraints on the genesis of the PMZ and have important implications for exploration for similar style mineralisation.

The PMZ is interpreted to be part of the alteration zone developed in andesitic volcaniclastic footwall rocks during formation of the PQ - P north massive sulphide orebody. This stringer mineralisation is crudely zoned from a Cu-rich core surrounded by Pb-Zn bearing stringer to a distal Pb-Zn-Ag-Au-As-Sb stringer. Best development of the distal Au-bearing stringer occurs in more porous and permeable vocaniclastics (eg., the PMZ). Gold remained in solution in the more proximal parts of the stringer because physico-chemical conditions in the hydrothermal fluids forming the stringer favoured Au transport as bisulfide complexes. Gold could not precipite until the fluids were oxidised or dramatically cooled in the outer parts of the stringer zone.

Introduction

Since the previous report on the unusual Au anomalous zone in the footwall to the east of the main PQ massive sulphide lens at Que River the main thrust of our investigation has been geochemical. Whole rock analyses for major and trace elements have been

carried out at the University of Tasmania for a number of samples of altered andesitic fragmental rocks from the footwall stringer zone. Commercial assays were obtained for small samples from two meter lengths of "white altered" core and data for a large group of elements were available for drill core from two holes through the precious metal zone (PMZ) and normal footwall stringer (QR 631 and QR 417 respectively). A preliminary sulphur isotope study has been undertaken. A fluid inclusion study and follow-up sulphur isotope work will be carried out as soon as practicable. It is also planned to analyse the QR 631 and QR 417 samples for Tl and developmental work for a Tl analytical procedure is well underway at the University. These three programs will complete the current investigation of the Que River PMZ.

Extent of PMZ

A knowledge of the extent and distribution of the PMZ in relation to "normal" stringer and the massive ore at Que River is important to understanding the formation of this zone.

For much of the PMZ the host is a distinctive coarse polymictic fragmental rock of andesitic bulk composition The nature of this unit is problematical but it is interpreted here as a mass flow facies of the andesitic epiclastic units that form the footwall rocks at Que River. It has been suggested (R. Henley, pers. comm., 1987) that this unit could have formed as a hydrothermal explosion breccia. However, this is unlikely for two reasons, firstly, the unit is sheet-like in shape and conformable with other epiclastic units, and secondly, explosive hydrothermal activity might be expected to coincide with the zone of maximum fluid input but the PMZ is north of the main focus of the massive sulphide forming activity.

In the last report the PMZ was shown as open to the north, with this in mind two more sections (7725 and 7800 N) north of the most northern section reported previously (McGoldrick and Large, 1986) were examined. Section 7725 N shows similar geology (Fig. 1) and metal distribution to 7700 N. The PMZ is well developed with anomalous Au occurring below and east of the main orebody (Fig. 2). It is worth noting that on this section the anomalous Au extends west of the infered syncline axis. Similarly, on the 7700 N section zones of anomalous Au in the footwall stringer are distributed either side of a Cu "high" which may correspond to the centre of the stringer system. Although patches of "white alteration", a characteristic feature of much of the PMZ, are well developed in many holes from 7725 N, it is not as extensive on this section as 7700 N.

To the north (7800 N) the geology becomes more complex, although the "ore position" can certainly be recognised. Thin massive sulphide horizons are present in the footwall stringer and much of the mineralisation is lower grade and diluted by clastic gangue. Volcanic and epiclastic processes appear to have been co-eval with the hydrothermal activity responsible for the massive ore. The PMZ cannot be recognised as a separate entity on this section and "white alteration" was not observed. Insufficient data were available to produce contour diagrams of element distributions but sporadic high Au assays are reported from core in the stratigraphic footwall of the massive ore on both eastern and western limbs of the fold on this section.

At higher levels in the mine some drill-holes extend west from the P-north position and patchy low grade mineralization is common, including some with anomalous Au. At lower levels, however, the number of drill holes to the west is limited (eg., 7725 N section - Fig. 2) which allows for the possibility that a fold repetition of the PMZ mineralisation could occur there.

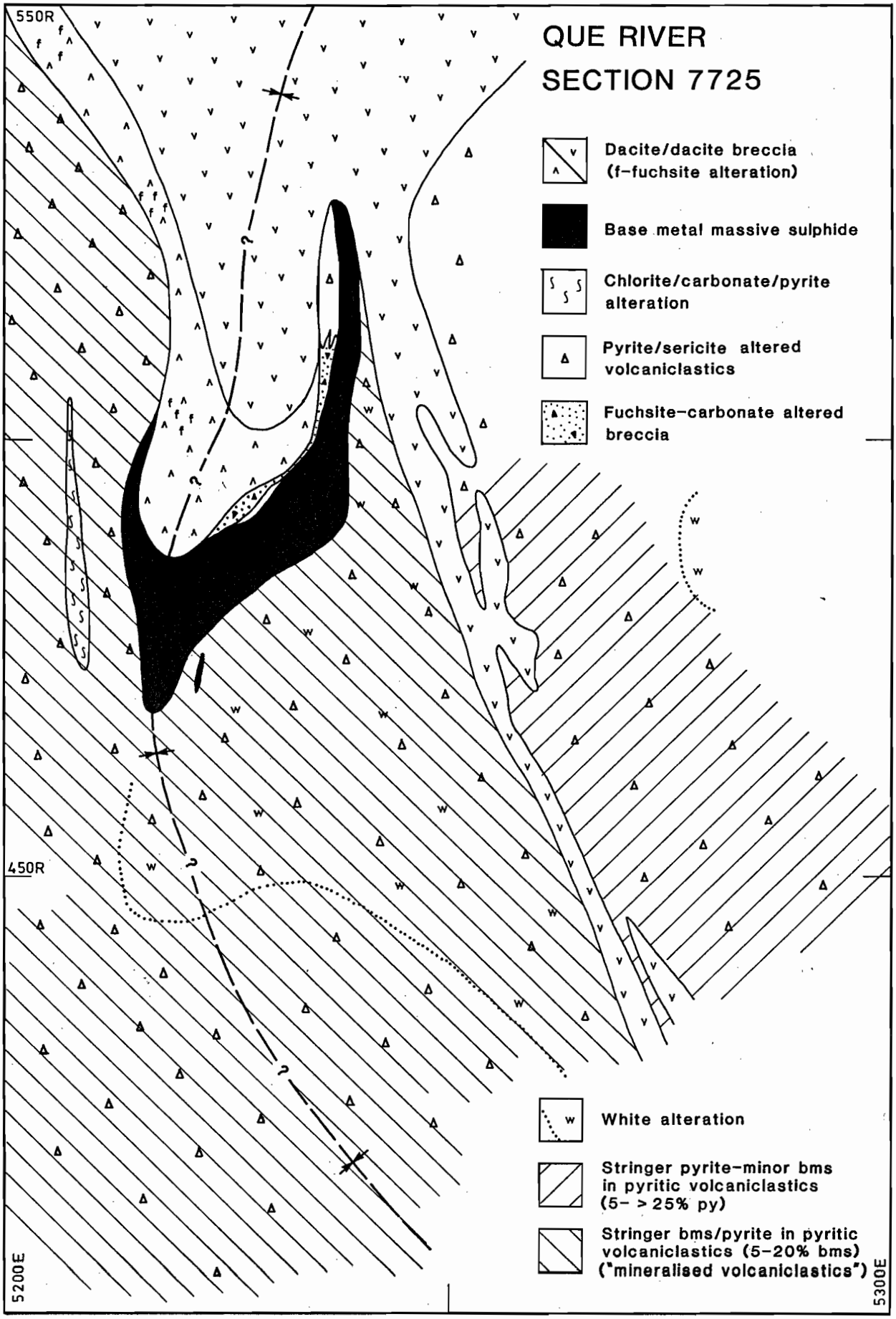

Fig. 1 Interpreted geology from 7725 N section Que River.

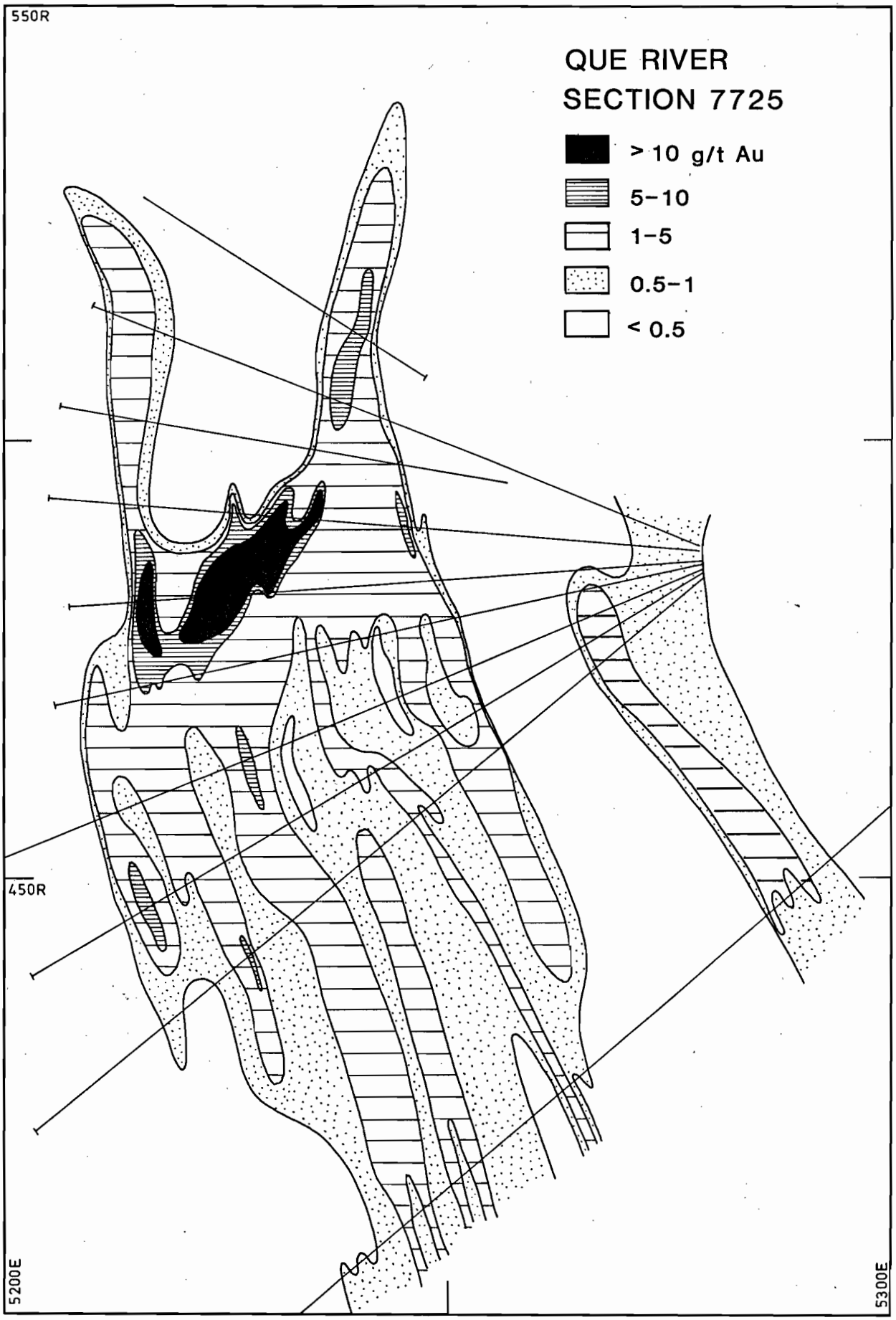

Fig. 2 Gold distribution from 7725 N section Que River.

In conclusion although the best development of PMZ style mineralisation occurs in the eastern footwall of PQ lens between about 7600 and 7800 N, similar mineralization may possibly occur elsewhere in the Que River stringer system

Petrography

The important petrographic features of the PMZ, "normal" footwall stringer samples and "fresh" andesites have been discussed in the last report (McGoldrick and Large, 1986) and their observation are summarised on Table 1.

TABLE 1: Important mineralogic and petrographic features of the footwall rocks at Que River.

	Andesites	Normal Stringer	PMZ Stringer
Hand Specimen:	- massive grey-green rocks - mnr disseminated pyrite	- fn to crs grained polymictic volcaniclastic rocks - pyrite (± base metal sulphides) in veins (± quartz and carbonate) and disseminations - often silicified and / or sericitised	- crs and med. grained volcaniclastic rocks - pyrite and base metal sulphides in veins and disseminations - "white alteration" patches (few mm square) are common
Thin Section:	- fn grained albite / chlorite / quartz / carbonate - albite phenocrysts common - often sheared and altered but both lavas and monomict fragmentals (autobreccias?) are recognised	- quartz / sericite / carbonate / py / ±bms / rare K feldspar - no albite - primary textures poorly preserved (esp. in matrix)	- quartz / K feldspar / sericite / pyrite / bms - "white alteration" comprises crs sericite - sphalerite intergrowths - no albite (relict phenocryst are silicified or replaced by K feldspar)

Geochemistry

In order to investigate if the PMZ has a distinctive geochemical signature that could be related to its formation a number of different analytical investigations were carried out.

-Small samples

In core from the PMZ there is an observed correspondance at the scale of meter length assay samples between core with "white alteration" patches and elevated Au grades. To test if the "white alteration" is the site for the extra Au, two metre lengths of core

showing excellent patchy development of "white alteration" were cut into smaller segments (white altered and non-white altered) and each piece analysed for a range of elements.

Sample # 261761 (QR 557 24.1 - 25.1m) was cut into three and sample # 261765 (QR 557 28.1 - 29.1m) was cut into seven pieces for a total of five "white altered" samples and five "non-white altered" samples. The results are displayed in Table 2 and on Figure 3 which shows raw assay data that have been normalised using an "average" Que River least altered andesite composition (Table 3). The patterns for both groups are remarkably similiar except that the "white altered" samples are somewhat enriched in Zn (this observation is consistent with the white alteration patches being coarse sericite - sphalerite intergrowths; McGoldrick and Large, 1986). The lack of any real difference in Au contents between the two samples groups indicates that Au is not directly hosted by the white alteration patches.

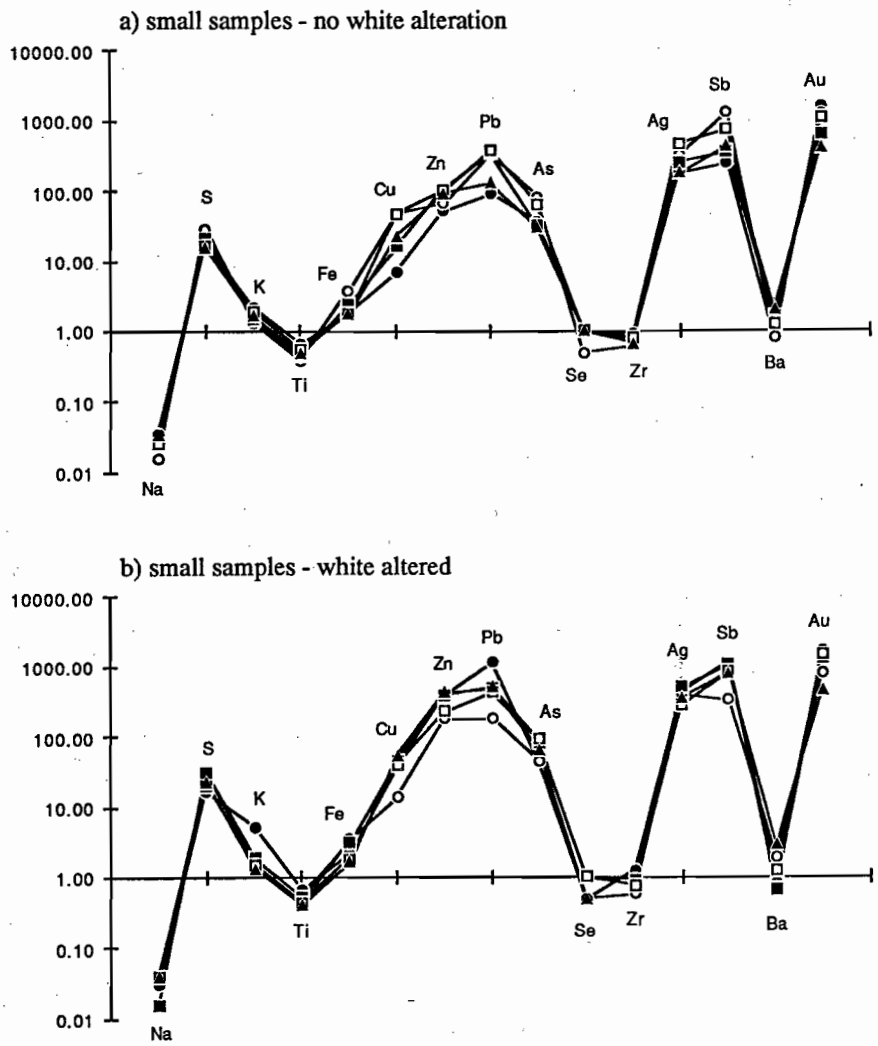

Fig. 3. Normalised element variations in small samples from the PMZ

TABLE 2: Small samples from PMZ core, Qur River.

Sample No.	Na2O (wt%)	S (wt%)	K2O (wt%)	TIO2 (wt%)	Fe (wt%)
26761.1	0.09	9.85	4.46	0.41	9.50
26761.2w	0.08	8.90	10.36	0.40	11.00
26761.3	0.04	15.60	2.71	0.24	19.00
26765.1w	0.04	16.00	3.13	0.27	18.00
26765.2	0.07	11.50	2.98	0.28	12.50
26765.3w	0.04	16.10	3.79	0.33	16.00
26765.4	0.07	9.15	3.91	0.35	9.00
26765.5w	0.11	10.80	2.95	0.28	9.50
26765.6	0.09	8.25	3.34	0.31	9.00
26765.7w	0.11	12.00	2.65	0.25	8.50

	Zn (wt%)	Pb (wt%)	Cu (wt%)	As (ppm)	Se (ppm)
26761.1	0.45	0.18	0.02	540	0.10
26761.2w	3.48	2.10	0.09	630	0.05
26761.3	0.58	0.63	0.12	1200	0.05
26765.1w	1.55	0.34	0.04	630	0.05
26765.2	0.95	0.65	0.04	480	0.10
26765.3w	3.33	0.90	0.11	1200	0.10
26765.4	0.90	0.70	0.12	930	0.10
26765.5w	1.98	0.78	0.10	1300	0.10
26765.6	0.83	0.24	0.06	450	0.10
26765.7w	3.68	0.93	0.13	930	0.05

	Zr (ppm)	Ag (ppm)	Sb (ppm)	Ba (ppm)	Au (ppm)
26761.1	120	13	50	730	1.53
26761.2w	170	30	230	770	1.70
26761.3	85	23	260	770	1.25
26765.1w	80	28	65	1850	0.80
26765.2	100	18	70	1550	0.63
26765.3w	120	35	210	670	1.28
26765.4	110	33	150	1200	1.06
26765.5w	100	20	170	1200	1.42
26765.6	90	13	85	2000	0.41
26765.7w	10	25	160	2800	0.47

-Whole rock geochemistry

Over 50 samples from Que River were analysed by XRF at the University of Tasmania for major and trace elements. Selected analyses from the CSIRO Que River reports were combined with these data to generate a data base of 84 analyses. The twelve fresh (i.e., least altered - see McGoldrick and Large, this report) andesites (Table 3) comprise eleven massive green-grey rocks and one coarse volcaniclastic, and all were collected from drill core some distance from the extensive footwall alteration zone of the massive ore.

TABLE 3: Que River Andesites.

Sample #	69717	69718	69900	71464	72014	502650	72023	72504	72514
Section	7400	7400	7400	7400	7400	7525	7400	8600	8600
DDH	QR46	QR46	QR2	QR11	QR46W	QR87	QR46W	QR110	QR110
Depth (m)	118.65	124.75	286.8	157.2	432.5	109.5	512.8	211.6	341.4
Rock type	andesite	andesite	andesite	andesite	andesite	andesite	andesite	andesite	andesite
SiO2	57.94	67.09	61.6	50.1	58.1	60.93	47.7	49.7	49.4
TiO2	0.68	0.54	0.53	0.8	0.64	0.55	0.49	0.69	0.61
Al2O3	17.03	13.51	14.2	18.3	14.5	14.57	13.5	18.4	13.7
Fe2O3	9.07	3.15	6.66	7.55	7.81	7.66	8.44	9.81	9.2
MnO	0.1	0.1	0.45	0.1	0.14	0.11	0.25	0.18	0.18
MgO	2.07	0.83	5.6	10.4	3.69	3.7	2.48	6.18	5.49
CaO	1.95	3.93	0.97	0.62	4.48	3.09	10.3	5.84	8.18
Na2O	3.98	3.17	0.03	2.32	2.16	3.32	1	4.99	0.13
K2O	2.12	2.57	3.67	0.48	1.92	1.14	2.77	0.22	2.34
P2O5	0.16	0.13	0.18	0.1	0.17	0.15	0.15	0.12	0.19
LOI						4.81			
S	0.04	0.06	0.67	0.2	0.9	0.44	2.7	0.1	0.1
CO2	0.5	2.3	3	0.7	3.66		8.79	0.18	6.6
H2O-	0.4	0.3	0.2	0.9	0.3		0.3	0.3	0.4
H2O+	3.9	1.9	4	7.7	3.7		3.3	4.3	5.3
Sum	99.84	99.48	101.8	100.1	101.8	100.1	101.2	100.9	101.8
Rb	68	92	118	19	56	32	82	10	85
Sr	302	314	31	53	133	166	154	760	110
Ba	1080	1090	1580	301		667			
La	74	75	47	69	40		56	41	55
Ce	111	133							
Y	37	28	30	35	24	23	31	27	21
Zr	178	151	136	219	115	103	108	143	104
Nb	9	8	8	13		7			
Cr	54	73	23	5	152	146	69	133	407
V	91	92	116	198	216	217	164	236	217
Pb	11	9	352	19	32	10	38	30	24
As	10	14	16	14	20	12	45	15	5
Zn						128			
Cu						21			
Ni						25			
Sc						31			

Sample #	502644	502651	502647	AVERAGE QUE RIVER ANDESITE
Section	7537.5	7525	7700	
DDH	QR35	QR87	QR39	
Depth (m)	144	209	289.2	
Rock type	andesite	andesite	vc	
SiO2	56.91	56.33	58.64	56.20
TiO2	0.7	0.45	0.7	0.62
Al2O3	18.59	15.08	15.99	15.61
Fe2O3	6.9	6.12	6.14	7.38
MnO	0.18	0.12	0.04	0.16
MgO	1.66	3.58	0.79	3.87
CaO	4.06	6.51	3.45	4.45
Na2O	2.87	2.42	5.35	2.65
K2O	3	2.15	1.69	2.01
P2O5	0.2	0.1	0.21	0.16
LOI	5.96	7.99	6.11	6.22
S	1.73	0.65	3.84	0.95
CO2				3.22
H2O-				0.39
H2O+				4.26
Sum	101.13	100.91	99.22	100.69
Rb	91	55	57	64
Sr	154	121	335	219
Ba	918	581	1027	906
La				57
Ce				122
Y	32	23	33	29
Zr	160	102	132	138
Nb	10	7	10	8
Cr	102	69	127	113
V	247	195	250	187
Pb	11	8	18	47
As	22	11	35	18
Zn	111	63	64	92
Cu	24	49	26	30
Ni	21	17	24	22
Sc	34	28	37	33

TABLE 4: Que River , footwall volcaniclastics.

Sample #	502813	502804	502823	502822	502818	502657	502902	502917
Section	7400	7400	7400	7400	7400	7525	7550	7550
DDH	QR712	QR65	QR444	QR324	QR323	QR87	QR276	QR278
Depth (m)	30.00	62.00	34.00	22.00	29.00	613.00	17.00	88.00
Rock type	vc	vc	vc	vc	vc	vc	vc	vc
SIO2	61.20	64.03	68.38	66.77	61.92	62.72	75.63	48.07
TIO2	0.55	0.44	0.36	0.42	0.40	0.51	0.35	0.23
Al2 O3	17.37	14.82	11.39	10.81	9.75	16.81	9.68	5.50
Fe2 O3	4.51	5.26	7.21	8.71	15.17	5.71	5.54	16.82
MnO	0.09	0.30	0.02	0.23	0.01	0.18	0.02	0.14
MgO	1.87	1.62	0.75	2.49	0.47	4.19	0.53	3.95
CaO	2.88	3.04	0.32	0.46	0.13	0.54	0.21	1.18
Na2O	0.24	<.20	0.09	<.20	<.20	<.20	<.20	0.06
K2 O	4.34	3.88	3.39	2.81	2.73	4.15	2.90	0.79
P2 O5	0.18	0.12	0.11	0.15	0.08	0.31	0.08	0.04
LOI	6.53	7.01	5.88	7.11	9.26	4.88	4.49	12.64
S	1.36	0.64	5.95	4.11	11.66	0.59	4.32	14.56
Sum	100.00	100.67	99.49	100.03	100.01	100.25	99.53	99.15
Rb	130	116	133	101	105	136	108	35
Sr	135	29	10	8	6	17	6	164
Ba	25	1299	2351	629	660	2240	854	13855
La								
Ce								
Y	50	34	15	15	16	22	13	<2
Zr	161	183	78	89	84	132	78	24
Nb	11	10	5	6	6	5	5	4
Cr	146	7	52	119	55	15	63	37
V	2145	45	158	144	148	229	164	54
Pb		42	1723	301	614	7	76	23500
As	1198	101	334	100	381	37	179	459
Zn	24	939	9200	351	120	164	52	45400
Cu	7	15	264	24	52	19	29	2900
Ni	37	3	15	21	14	5	12	21
Sc	1307	20	26	21	19	27	21	12

Sample #	502921	502937	502998	503000	502686	502680	502668
Section	7550	7550	7550	7550	7700	7700	7700
DDH	QR312	QR310	QR68	QR71	QR558	QR632	QR631
Depth (m)	15.00	15.00	73.00	35.00	64.00	45.70	9.00
Rock type	vc	vc	vc	vc	vc	vc	vc
SIO2	33.94	71.51	60.63	63.87	66.28	74.12	68.90
TIO2	0.93	0.41	0.60	0.69	0.50	0.32	0.47
Al2 O3	21.61	9.77	16.34	18.11	12.95	8.10	11.93
Fe2 O3	20.93	7.82	8.53	4.76	7.43	6.60	7.01
MnO	0.02	0.01	0.01	0.01	0.02	0.02	0.01
MgO	0.99	0.51	1.23	0.91	0.95	0.56	0.52
CaO	0.59	0.15	0.19	0.36	0.26	0.15	0.18
Na2O	<.2	0.40	<.20	0.25	<.2	0.11	<.2
K2 O	6.30	2.79	4.94	4.83	3.92	2.46	5.16
P2 O5	0.42	0.08	0.10	0.16	0.11	0.09	0.12
LOI	14.40	5.72	7.21	5.58	6.28	4.98	4.89
S	16.53	6.35	6.46	3.46	5.98	5.58	5.52
Sum	100.41	100.10	99.85	99.73	99.81	100.55	99.40
Rb	215	104	190	170	158	94	147
Sr	11	4	7	25	12	11	21
Ba	1112	617	656	1789	2141	1568	1879
La							
Ce							
Y	40	16	26	37	19	10	25
Zr	180	87	137	210	124	75	121
Nb	13	6	9	14	8	6	8
Cr	80	22	141	31	35	24	57
V	222	99	237	111	135	93	165
Pb	744	2820	146	61	2094	13000	116
As	752	442	214	116	342	403	259
Zn	528	4447	54	33	5167	11800	41
Cu	1537	71	40	68	286	399	26
NI	25	7	24	7	12	9	14
Sc	36	14	36	23	23	16	23

TABLE 5: Que River , 'white altered' volcaniclasics.

Samp.No.	502682	502683	502676	502671	502672	502627	502642	502643	18-4-86-2
Section	7700	7700	7700	7700	7700	7700	7700	7700	ugs
DDH	QR558	QR558	QR632	QR631	QR631	QR767	QR14	QR14	
Depth (m)	3.00	17.00	15.60	38.00	41.00	26.00	261.40	281.70	
Rock type	wht alt vc	wht alt vc	wht alt vc	wht alt vc	wht alt vc	wht alt vc	wht alt vc	wht alt vc	wht alt vc
SiO2	64.23	62.76	62.20	60.29	51.90	57.41	70.42	64.52	58.31
TiO2	0.45	0.37	0.39	0.29	0.35	0.47	0.41	0.46	0.40
Al2 O3	11.56	10.19	10.06	6.79	9.89	14.06	11.37	13.01	9.99
Fe2 O3	7.67	9.30	12.23	11.80	16.49	8.85	5.17	7.03	13.28
MnO	0.03	<.01	0.01	0.07	0.01	0.03	0.01	0.08	0.04
MgO	0.51	0.41	0.75	0.58	0.64	0.54	0.48	0.67	0.61
CaO	0.63	0.13	0.11	0.44	0.09	0.38	0.29	1.37	0.50
Na2 O	0.30	0.38	0.04	0.04	0.06	0.17	0.42	<.2	0.09
K2 O	5.42	3.71	3.55	2.16	3.13	6.61	5.38	5.88	3.07
P2 O5	0.11	0.09	0.07	0.06	0.07	0.03	0.15	0.13	0.23
LOI	5.90	6.30	7.67	8.27	10.63	6.61	4.04	5.73	8.84
S	6.35	8.11	9.76	10.93	14.72	8.11	4.48	5.24	11.68
Sum	99.14	99.23	99.31	99.19	99.05	99.72	100.33	99.12	99.94
Rb	151	118	140	74	117	181	133	159	117
Sr	295	8	3	18	8	56	56	61	24
Ba	13924	974	734	1588	1951	4112	4023	2148	2472
La									
Ce									
Y	20	12	18	<2	<2	15	32	24	18
Zr	115	71	92	26	47	112	112	126	83
Nb	8	7	7	4	5	8	8	9	7
Cr	41	29	29	87	113	64	57	88	43
V	113	86	104	141	187	148	107	135	227
Pb	1737	19900	4900	26200	23900	5500	2670	165	8400
As	334	890	1068	549	754	671	277	171	545
Zn	4838	26900	9600	43400	24100	28200	11700	89	27300
Cu	615	1499	199	834	429	1120	414	43	949
Ni	14	16	12	27	33	14	15	13	23
Sc	24	16	16	23	30	32	22	24	23

Samp.No.	18-4-86-3c	18-4-86-3f	10-10-86-1
Section	ugs	ugs	ugs
DDH			
Depth (m)			
Rock type	wht alt vc	wht alt vc	wht alt vc
SiO2	52.21	38.17	66.91
TiO2	0.42	0.69	0.47
Al2 O3	10.54	25.79	12.09
Fe2 O3	12.57	13.28	7.20
MnO	0.09	0.03	0.03
MgO	1.05	1.15	0.54
CaO	1.07	0.32	0.54
Na2 O	0.11	<.2	0.31
K2 O	3.16	7.35	5.06
P2 O5	0.02	0.14	0.15
LOI	10.10	10.75	5.46
S	10.86	10.51	5.80
Sum	98.80	99.52	99.76
Rb	120	246	135
Sr	255	23	94
Ba	23049	8779	8659
La			
Ce			
Y	24	38	23
Zr	91	369	119
Nb	8	23	8
Cr	55	171	74
V	92	107	144
Pb	16400	4200	647
As	803	1017	238
Zn	25100	3200	936
Cu	1012	182	46
Ni	23	58	16
Sc	34	30	23

TABLE 6: Que River dacites (hanging wall "dacite wedge").

Sample #	69782	69783	72522	72524	72525	72527	502999	502900	502778
Section	7900	7900	7700?	7700	7700	7700	7550	7550	7700
DDH	QR32	QR32	QR478	QR478	QR478	QR478	QR68	QR405	QR494
Depth (m)	263.90	266.50	53.60	70.10	78.60	96.70	43.00	47.00	80.00
Rock type	dacite	dacite	dacite	dacite	dacite	dacite	dacite	dacite	dacite
SiO2	59.60	67.20	60.60	60.60	67.70	66.60	69.77	68.99	71.21
TiO2	0.35	0.25	0.29	0.35	0.25	0.32	0.27	0.27	0.30
Al2O3	16.40	12.00	14.10	15.30	12.10	14.20	13.67	13.12	14.86
Fe2O3	3.83	3.15	4.00	3.91	3.02	4.40	2.54	3.02	2.00
MnO	0.10	0.10	0.22	0.25	0.20	0.19	0.38	0.08	305.00
MgO	1.59	0.99	2.27	1.28	1.19	0.88	1.02	0.09	0.72
CaO	4.73	5.75	4.57	4.03	3.93	2.44	2.65	3.89	1.40
Na2O	1.98	1.44	0.17	1.55	0.97	0.47	<.2	0.73	2.24
K2O	3.15	2.21	4.47	3.81	3.01	3.91	3.91	3.09	3.25
P2O5	0.17	0.13	0.10	0.10	0.10	0.11	0.07	0.09	0.08
LOI							5.80	5.78	3.73
S	0.19	0.02	0.10	0.50	0.10	1.60	0.14	1.66	0.65
CO2	5.30	4.70	7.70	6.23	6.05	3.66			
H2O-	0.30	0.40	0.40	0.30	0.40	0.30			
H2O+	2.90	2.50	2.90	2.50	2.20	2.60			
Sum	100.50	100.80	101.70	100.40	101.10	101.10	100.14	99.47	100.00
Rb	96	60	139	110	82	112	121	96	94
Sr	122	135	83	74	74	45	21	102	57
Ba	964	728	nd	nd	nd	nd	561	1046	1461
La	144	90	107	125	90	153			
Ce	nd	nd	nd	nd	nd	nd			
Y	28	21	30	32	25	31	27	26	26
Zr	176	129	177	163	151	162	172	168	180
Nb	8	5	nd	nd	nd	nd	9	9	9
Cr	42	25	33	49	24	33	7	8	5
V	43	17	33	50	29	50	31	30	28
Pb	11	7	15	40	18	284	16	37	26
As	23	13	99	83	110	141	35	156	34
Zn							35	23	28
Cu							6	13	7
Ni							2	1	1
Sc							9	11	11

Sample #	502721	502704	502708	21-3-86d	18-4-86-1a
Section	7700	7700	7700	ugs	ugs
DDH	QR483	QR492	QR492		
Depth (m)	75.00	67.00	105.00		
Rock type	dacite	dacite	dacite	dacite dyke	dacite in fs-car bx
SiO2	70.58	69.64	68.32	64.11	73.68
TiO2	0.29	0.29	0.27	0.49	0.26
Al2O3	14.09	13.80	13.51	16.13	11.68
Fe2O3	2.01	2.41	2.80	3.74	1.86
MnO	0.04	0.10	0.17	0.27	0.06
MgO	0.24	0.32	1.17	1.19	1.44
CaO	2.93	3.17	3.50	2.36	2.14
Na2O	3.29	2.42	1.08	0.79	<.2
K2O	2.42	2.97	3.28	4.32	3.61
P2O5	0.09	0.09	0.08	0.24	0.12
LOI	3.91	4.69	6.45	6.08	4.98
S	1.08	<.05	0.05	0.34	0.07
Sum	100.01	99.99	100.85	100.31	99.99
Rb	70	92	92	144	113
Sr	132	112	69	70	40
Ba	892	826	1988	5305	1079
La					
Ce					
Y	24	30	27	31	20
Zr	172	174	164	196	130
Nb	9	9	9	8	6
Cr	8	3	4	10	2
V	26	31	26	137	27
Pb	50	8	23	37	3
As	78	12	11	55	34
Zn	211	27	37	46	19
Cu	10	5	8	23	2
Ni	2	1	1	2	14
Sc	13	10	11	20	12

TABLE 7: Que River , western dacites.

Sample #	69866	69867	69869	69870	69871	69872	69873	69874	69875
Section	7400	7400	7400	7400	7400	7400	7400	7400	7400
DDH	QR58	QR58	QR58	QR58	QR58	QR58	QR58	QR58	QR58
Depth (m)	56.70	58.90	70.80	75.40	84.70	92.00	98.40	109.00	119.00
Rock type	dcw	dcw	dcw	dcw	dcw	dcw	dcw	dcw	dcw
SiO2	66.50	67.30	66.60	66.90	66.60	63.44	66.70	65.30	66.02
TiO2	0.39	0.39	0.38	0.36	0.37	0.35	0.37	0.36	0.36
Al2O3	13.40	13.70	13.20	12.70	12.80	12.08	12.80	13.10	12.90
Fe2O3	4.94	4.24	4.32	4.32	3.95	8.40	4.25	3.36	4.50
MnO	0.15	0.10	0.16	0.31	0.21	0.56	0.22	0.25	0.14
MgO	1.19	1.19	1.34	1.04	0.95	0.64	1.03	1.08	1.48
CaO	1.67	2.04	2.16	2.38	2.64	1.22	2.51	2.89	2.46
Na2O	3.37	0.86	1.48	2.02	2.49	2.09	2.43	2.22	2.29
K2O	2.16	2.21	2.95	2.73	2.56	2.55	2.63	2.81	2.56
P2O5	0.10	0.10	0.10	0.10	0.10	0.10	0.10	0.10	0.10
S	0.01	0.01	0.01	0.02	0.03	0.13	0.01	0.01	0.01
CO2	3.30	3.20	3.40	4.30	5.00	5.70	4.00	4.50	3.90
H2O-	0.20	0.30	0.30	0.30	0.30	0.20	0.20	0.20	0.30
H2O+	1.70	1.80	2.30	1.30	1.50	1.60	1.70	1.70	1.60
Sum	99.00	97.20	98.60	98.70	99.40	98.96	98.80	97.80	98.00
Rb	77	78	104	86	84	83	90	101	95
Sr	125	148	90	109	150	90	134	90	115
Ba	951	941	1120	1100	1270	1450	1300	1260	1570
La	54	54	32	59	62	49	75	83	74
Ce	163	182	139	169	168	178	160	188	173
Y	28	30	32	29	29	33	30	31	28
Zr	168	164	163	158	161	154	160	168	164
Nb	9	8	8	7	6	7	7	8	8
Cr	53	44	37	39	35	29	67	49	46
V	31	35	26	28	28	24	26	30	28
Pb	7	6	5	11	10	20	8	5	6
As	10	10	12	10	10	19	11	11	10

Sample #	69876	69878	71469	71955	72533
Section	7400	7400	7400	6700	7700
DDH	QR58	QR58	QR11	QR29	QR478
Depth (m)	120.40	144.85	203.90	252.90	66.80
Rock type	dcw	dcw	dcw	dcw	dcw
SiO2	63.10	66.29	64.80	63.10	66.80
TiO2	0.36	0.40	0.47	0.29	0.30
Al2O3	12.40	13.78	16.20	13.50	14.70
Fe2O3	4.24	3.89	3.70	4.31	2.79
MnO	0.17	0.24	0.13	0.10	0.10
MgO	1.77	1.56	1.77	1.93	1.03
CaO	3.74	3.21	2.61	4.42	2.39
Na2O	1.62	0.15	0.26	0.26	2.63
K2O	2.83	3.84	3.98	4.22	2.35
P2O5	0.10	0.14	0.42	0.13	0.10
S	0.01	0.14	1.35	0.10	0.20
CO2	5.80	4.40	3.10	6.96	4.21
H2O-	0.30	0.30	0.20	0.40	0.30
H2O+	1.70	1.80	2.70	2.40	2.20
Sum	98.00	100.14	101.70	102.00	99.80
Rb	104	143	144	115	68
Sr	114	43	106	80	122
Ba	1590	1840	2780	1510	
La	69	77	117	182	146
Ce	132	145	nd	nd	nd
Y	29	33	31	26	29
Zr	156	159	174	109	181
Nb	6	7	7	7	nd
Cr	52	45	5	61	20
V	26	32	268	93	35
Pb	8	9	22	17	20
As	14	12	110	6	18

TABLE 8: Que River , fuchsite - carbonate altered volcaniclastic (hanging wall).

Sample #	502992	502975	502976	502773	502775	502777	8-4-86-1b	8-4-86-1c
Section	7550	7550	7550	7700	7700	7700	ugs	ugs
DDH	QR311	QR433	QR433	QR581	QR581	QR494		
Depth (m)	49.00	24.00	25.00	50.00	56.00	65.00		
Rock type	fs-car bx	fs-car bx	fs-car bx	fs-car bx	fs-car bx	fs-car bx	fs-car bx mafic frag.	fs-car bx matrix
SiO2	44.22	55.65	56.90	48.03	48.34	48.54	45.65	47.69
TiO2	0.59	0.65	0.55	0.63	0.52	0.54	0.31	0.47
Al2 O3	15.61	18.39	16.12	18.59	15.17	17.37	9.45	13.26
Fe2 O3	6.33	8.47	6.92	10.84	7.81	8.68	6.70	8.28
MnO	0.42	0.65	0.60	0.17	0.23	0.17	0.27	0.16
MgO	3.78	1.48	1.51	1.49	4.11	2.42	6.17	4.89
CaO	10.04	0.75	3.16	3.62	6.95	5.43	10.72	7.32
Na2 O	0.20	0.17	<.2	<.2	<.2	<.2	<.2	<.2
K2 O	4.07	4.93	4.49	5.49	4.75	5.25	2.90	4.06
P2 O5	0.49	0.20	0.26	0.33	0.27	0.25	0.68	0.11
LOI	14.30	6.95	8.57	10.27	11.82	11.03	16.95	14.29
S	0.81	1.86	2.01	6.37	1.99	3.11	0.85	1.14
Sum	100.35	100.93	99.52	100.09	100.56	100.38	99.92	100.69
Rb	135	181	147	173	172	180	97	138
Sr	106	16	36	68	173	110	261	148
Ba	2727	2076	1824	5125	1853	6152	1028	1344
La								
Ce								
Y	30	22	25	29	25	30	19	18
Zr	162	140	135	145	119	149	65	106
Nb	7	8	8	6	5	7	3	5
Cr	1356	850	471	826	984	217	1054	1128
V	388	347	274	348	310	207	207	308
Pb	52	8000	744	295	119	21	23	12
As	183	203	162	350	232	99	65	116
Zn	64	12400	1272	264	3000	80	99	81
Cu	396	217	71	62	685	18	42	26
Ni	188	159	99	106	143	21	124	133
Sc	64	58	46	55	53	32	37	Lost

TABLE 9: Que River , chlorite - carbonate altered rocks.

Sample #	71942	71943	71957	72519	72530	502781	502737	502949	502819
Section	6700	6700	6700	7700?	7700?	7700	7700	7550	7400
DDH	QR29	QR29	QR29	QR478	QR478	QR494	QR557	QR310	QR323
Depth (m)	142	145.8	277	38.4	141.8	139	68	59	19
Rock type	chlorite r.	chlorite r. - bxted	chl-car-py	hydrothermally altd tuff - chltic	chl-car	chl-car altd r.	chl-car altd r.	chl-car altd r.	chl-car altd r.
SiO2	34.2	27.2	44.4	36.5	28.3	38.78	23.28	28.96	17.33
TiO2	0.52	0.81	0.52	0.5	0.79	0.48	0.54	0.45	0.5
Al2O3	14.5	20.6	14.9	13.7	20.2	11.42	15.24	16.23	13.77
Fe2O3	15.4	17.1	17.2	9.38	16.2	17.9	13.27	17.73	32.45
MnO	0.47	0.29	0.27	0.3	0.26	0.47	0.7	0.51	0.25
MgO	14.3	16.4	6.16	8.14	13.4	14.1	20.55	15.76	12.75
CaO	3.39	0.34	1.04	9.28	0.8	0.26	7.05	2.08	2.5
Na2O	0.01	0.02	0.04	0.04	0.06	<.2	<.2	0.09	<.2
K2O	0.49	1.7	3.19	3.65	2.25	0.77	0.53	1.15	0.48
P2O5	0.17	0.14	0.18	0.1	0.13	0.12	0.12	0.07	0.12
LOI						16.01	18.78	15.6	19.85
S	4.5	4.4	7.2	1.5	5.4	5.42	2.7	7.83	18.64
CO2	5.5	3.66	4.03	15.2	7.15				
H2O-	0.9	0.6	0.6	0.5	0.6				
H2O+	7.9	9.4	4.6	3.4	7.6				
Sum	100.6	101	101.6	101.6	101.1	100.43	100.21	100.19	100.02
Rb	12	46	80	130	79	27	22	42	21
Sr	28	7	20	227	18	7	97	26	23
Ba	85	343	1170	nd	nd	538	468	1381	154
La	49	77	35	96	45				
Ce	nd	nd	nd	nd	nd				
Y	29	37	25	25	36	18	28	19	24
Zr	135	140	98	108	175	88	156	110	112
Nb	11	16	7	nd	nd	7	10	7	8
Cr	5	8	54	1420	34	79	8	81	105
V	83	126	219	323	184	182	91	124	265
Pb	103	61	155	42	94	71	67	309	461
As	70	51	109	84	52	157	38	112	545
Zn						465	704	11100	328
Cu						25	42	144	52
Ni						17	2	16	25
Sc						Lost	20	20	40

These andesites are remarkably similar in composition to the "average orogenic andesite" composition compiled by Ewart (1982). Hence, they provide a reference set of "fresh" rocks with which to compare the altered andesitic fragmental rocks (mass flow and other epiclastic deposits) of the footwall stringer zone from 7550 N section ("normal" stringer zone - fifteen samples - Table 4) and similar rocks from the PMZ stringer with characteristic "white alteration" (7700 N section and underground samples - twelve samples - Table 5).

As well as the andesitic footwall rocks, 28 dacites analyses were available (Tables 6 and 7), these comprise fourteen from the "dacite wedge" which stratigraphically overlies the northern part of the massive sulphide separating PQ from P-north lenses, and fourteen from the dacite mass to the west of the Que River orebodies. Eight samples from the fuschite-carbonate altered polymict volcanic fragmental which forms the immediate stratigraphic hanging wall of the massive ores were analysed (Table 8) as well as nine black fine-grained chlorite-pyrite altered rocks from the stratigraphic footwall (Table 9).

Figure 4 displays the elemental variation of the footwall volcaniclastics and "fresh" andesite with respect to their Ti/Zr ratio. For a fresh igneous rock composition the range of individual elements will be limited at any given Ti/Zr ratio and as Ti and Zr are elements that are immobile under all but the most extreme alteration conditions these diagrams can give a good indication of relative element mobility in altered rock types. For the major lithophile elements the footwall alteration halo at Que River is characterised by pronounced Na_2O, and some MgO and CaO depletion and K_2O and SiO_2 enrichment . The white altered samples are very similar to the normal stringer samples and this similarity in major element bulk chemical similarity reflects the similar gross mineralogy of the footwall alteration zone. There is, arguably, lower Al_2O_3 in the PMZ samples and this may be reflecting a higher K feldspar/sericite ratio in the PMZ. Despite this there is generally considerable overlap between the chemical variation

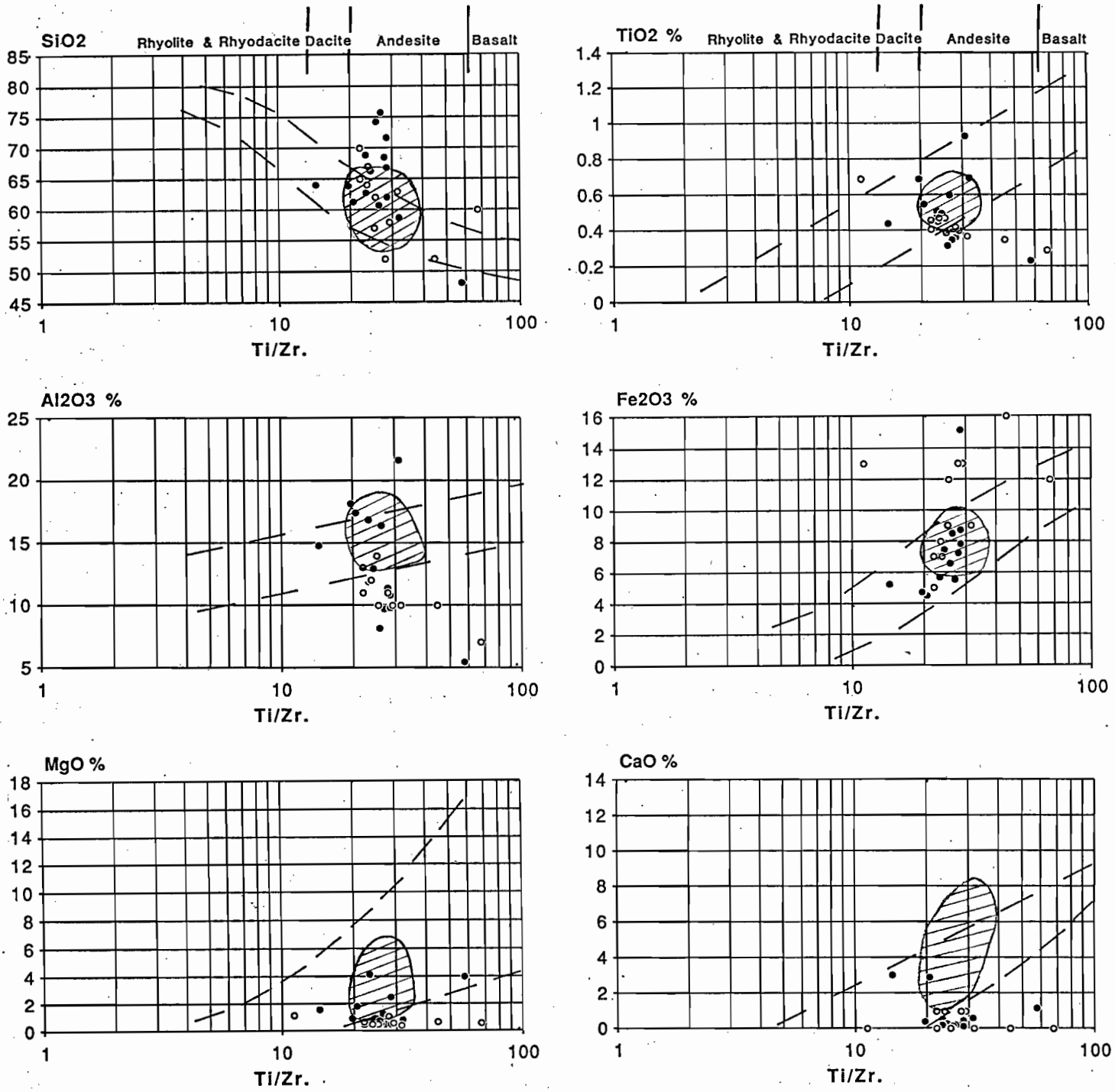

Fig. 4 Element - Ti/Zr plots for "normal" footwall volcaniclastics (solid circles) and white altered volcaniclastics (open circles); the shaded field corresponds to least altered andesites from Que River (Table 2).

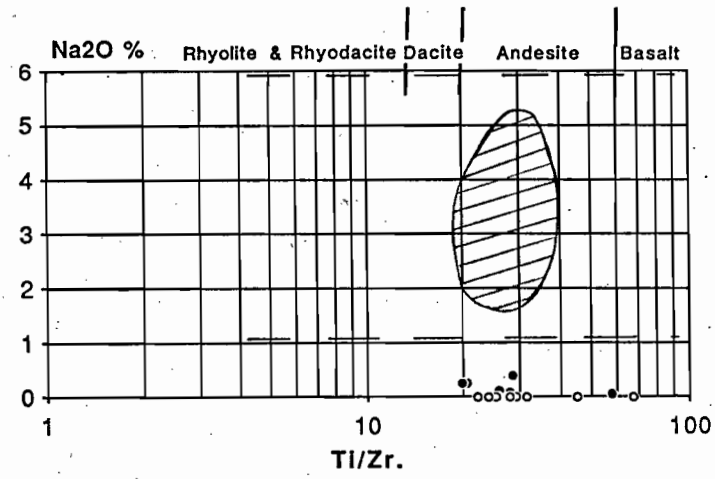
Na2O %
Rhyolite & Rhyodacite
Dacite
Andesite
Basalt
0
1
2
3
4
5
6
1
10
100
Ti/Zr.

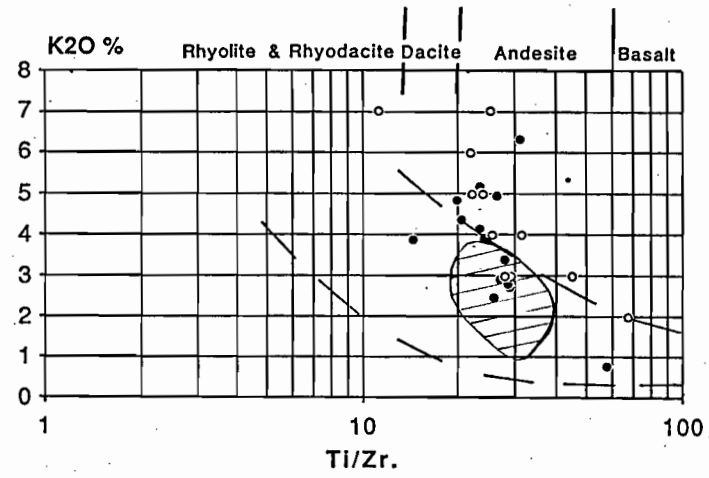
K2O %
Rhyolite & Rhyodacite
Dacite
Andesite
Basalt
0
1
2
3
4
5
6
7
8
1
10
100
Ti/Zr.

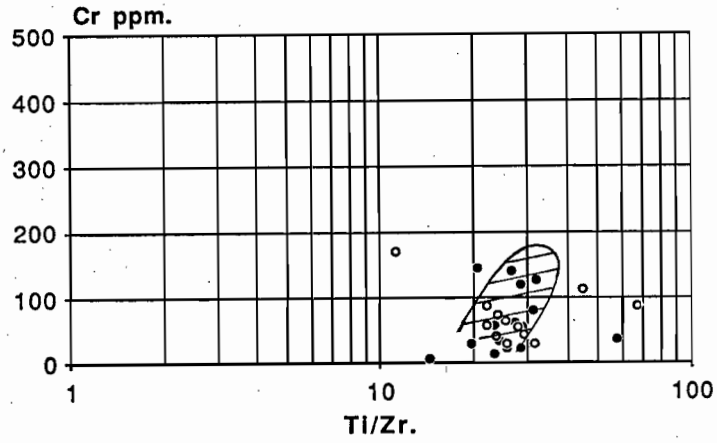
Cr ppm.
0
100
200
300
400
500
1
10
100
Ti/Zr.

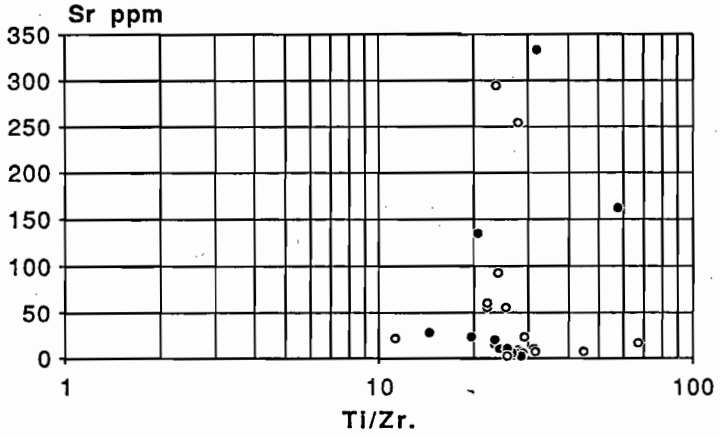
Sr ppm
0
50
100
150
200
250
300
350
1
10
100
Ti/Zr.

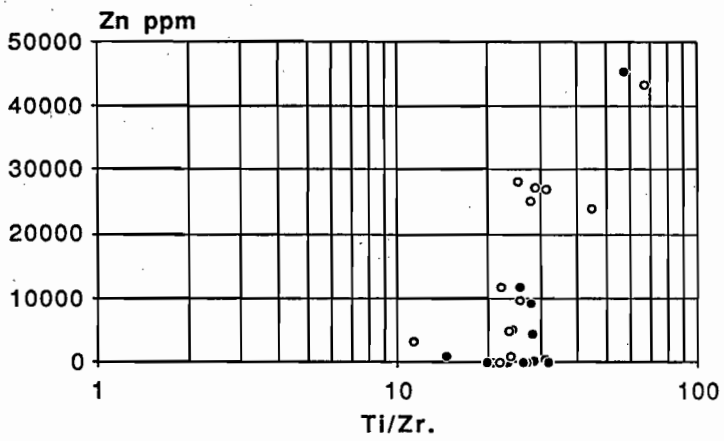
Zn ppm
0
10000
20000
30000
40000
50000
1
10
100
Ti/Zr.

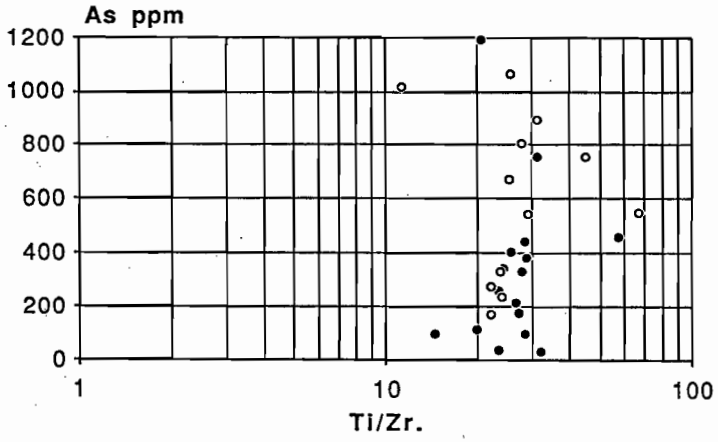
As ppm
0
200
400
600
800
1000
1200
1
10
100
Ti/Zr.

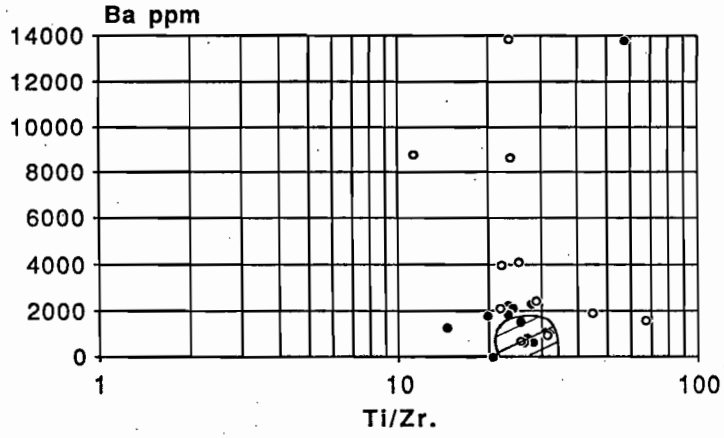
Ba ppm
0
2000
4000
6000
8000
10000
12000
14000
1
10
100
Ti/Zr.

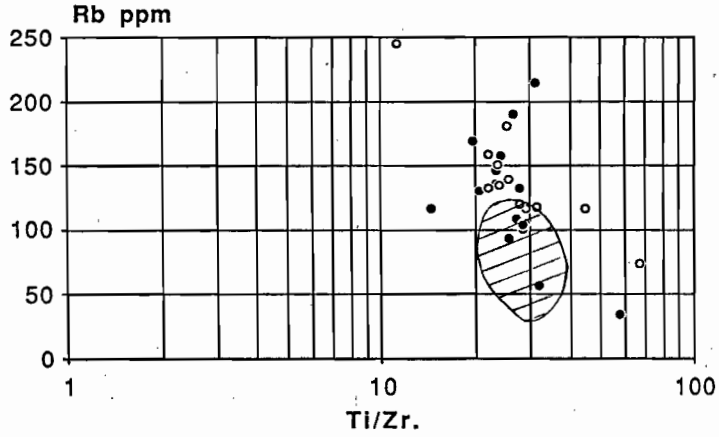
Rb ppm
0
50
100
150
200
250
1
10
100
Ti/Zr.

Fig. 4 (con).

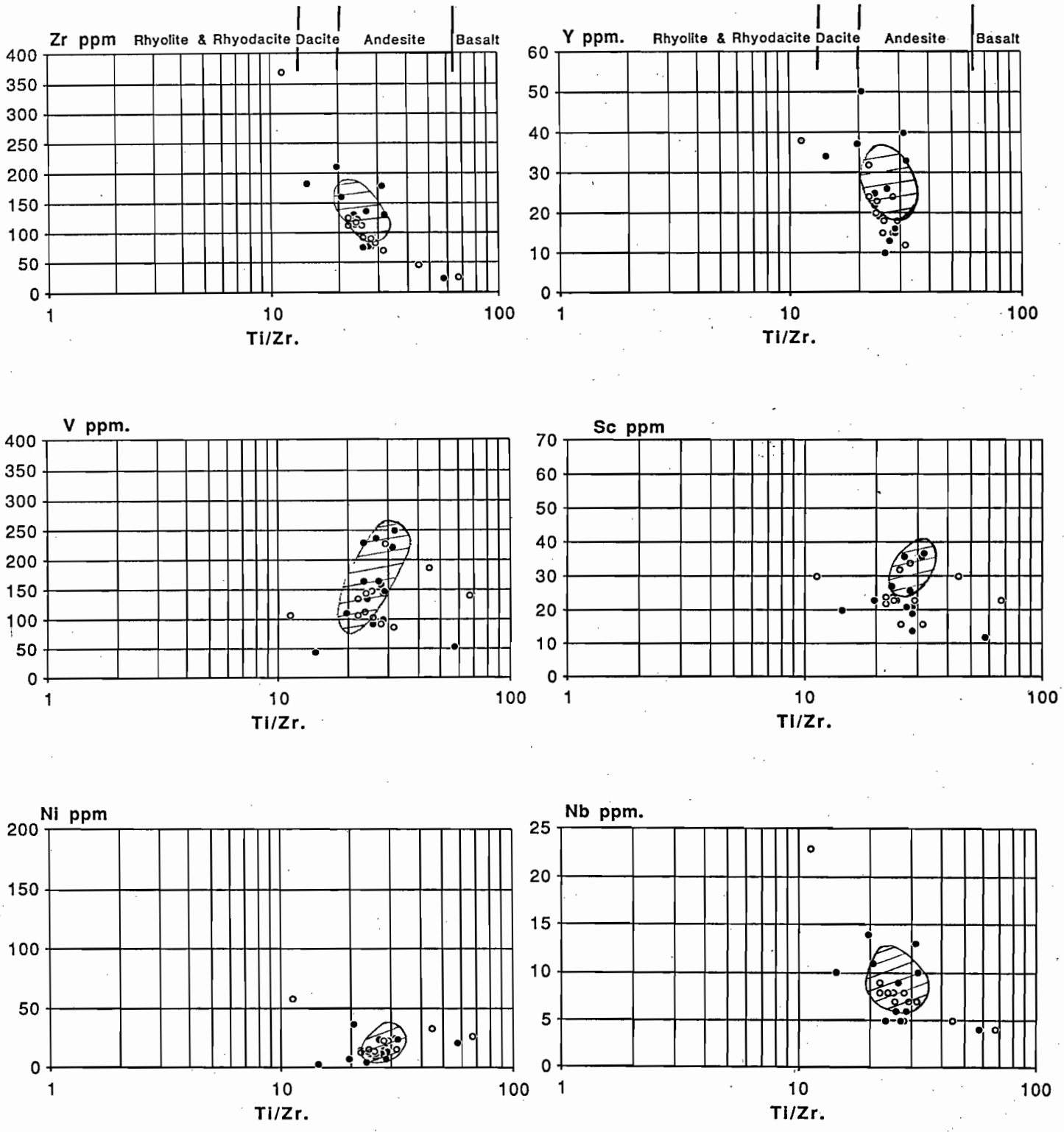
Zr ppm
Rhyolite & Rhyodacite
Dacite
Andesite
Basalt
400
350
300
250
200
150
100
50
0
1
10
100
Ti/Zr.
Y ppm.
Rhyolite & Rhyodacite
Dacite
Andesite
Basalt
60
50
40
30
20
10
0
1
10
100
Ti/Zr.
V ppm.
400
350
300
250
200
150
100
50
0
1
10
100
Ti/Zr.
Sc ppm
70
60
50
40
30
20
10
0
1
10
100
Ti/Zr.
Ni ppm
200
150
100
50
0
1
10
100
Ti/Zr.
Nb ppm.
25
20
15
10
5
0
1
10
100
Ti/Zr.

Fig. 4 (con).

shown by PMZ and "normal" stringer, hence, the PMZ does not have a distinctive whole rock geochemical signature.

-Au-Zn-Pb relationships in stringer and massive ore

In the previous report (McGoldrick and Large, 1986) Au v Zn+Pb plots for a large sample set were used to show that much of the PMZ stringer mineralisation on 7700 N section had a distinctive high Au content compared to stringer from 7550 and 7400 N sections. These data are re-presented here on Figure 5 and it is apparent that the PMZ has lower base metal : Au ratios (< 25,000 : 1) than "normal" stringer and much of the massive ores. However, a significant number of massive ore samples also have low base metal : Au ratios which suggests that similar processes may have acted to control Au and base metal behaviour in both types of mineralisation.

-Chalcophile elements in QR 417, QR 631

A second data set comprising chalcophile major and trace element analyses was available for samples from two drill holes (QR 417 and QR 631). Commercial analyses for Cu, Pb, Zn, Ag, Au, S, Fe, As, Sb, Se and Bi were obtained for eighteen samples of "normal" footwall stringer from 7550 N section (QR 417) and fourty six samples of PMZ stringer from 7700 N section (QR 631). Both drill-holes penetrated into PQ lens so similar data were also available for massive ore samples.

Most of the stringer samples were at or below the detection limit for Bi (0.4 ppm) as were samples of massive ore, the only samples with consistently elevated Bi values (~20 to 30 ppm) were from massive pyrite within PQ lens. Selenium is also very low (<0.1 ppm) in both stringer and massive ore and only a few samples from the PMZ stringer have slightly elevated values (0.2 to 0.8 ppm).

In contrast to Bi and Se the patterns displayed by other elements in the two holes are distinctive (Figs 6 and 7) and have important implications for understanding the PMZ.

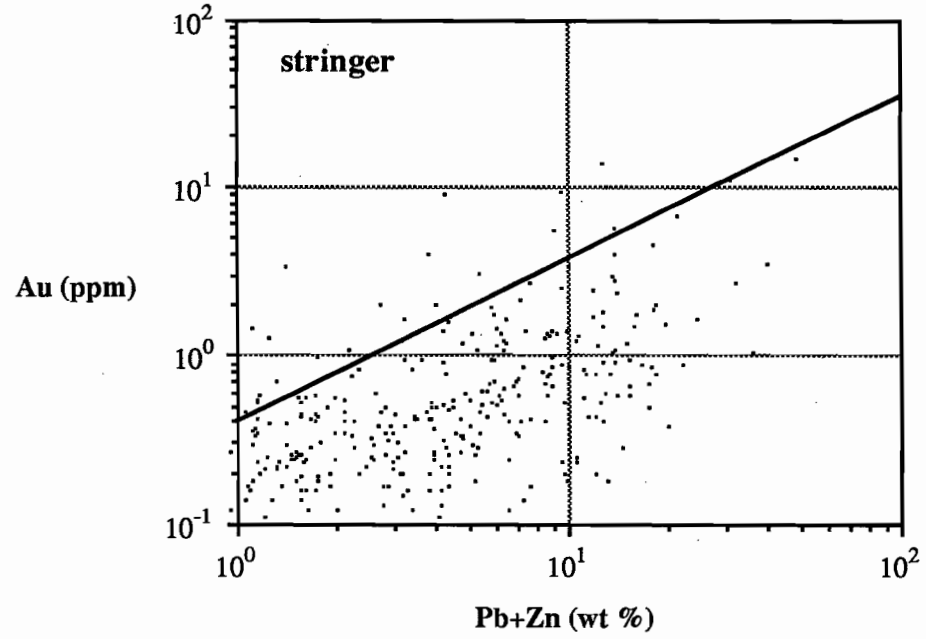

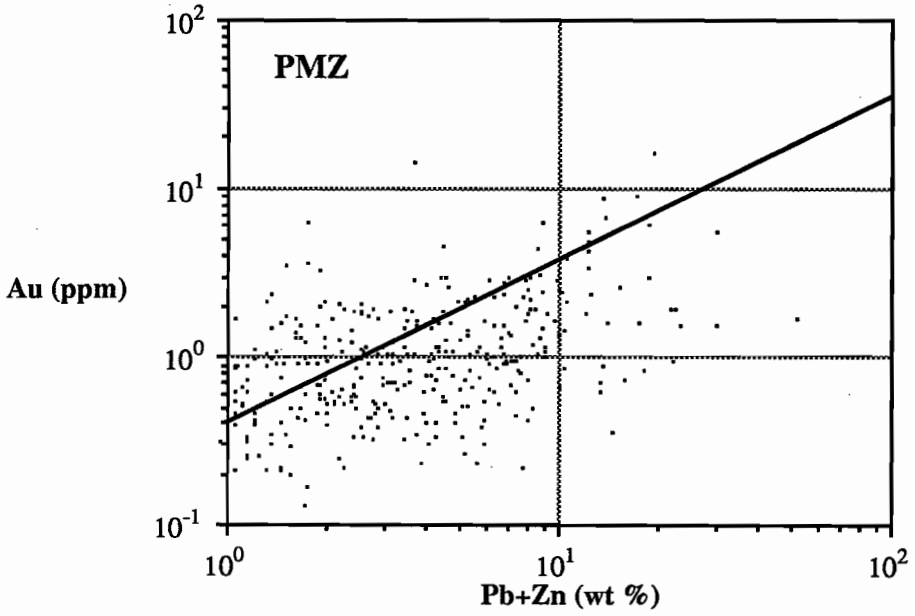

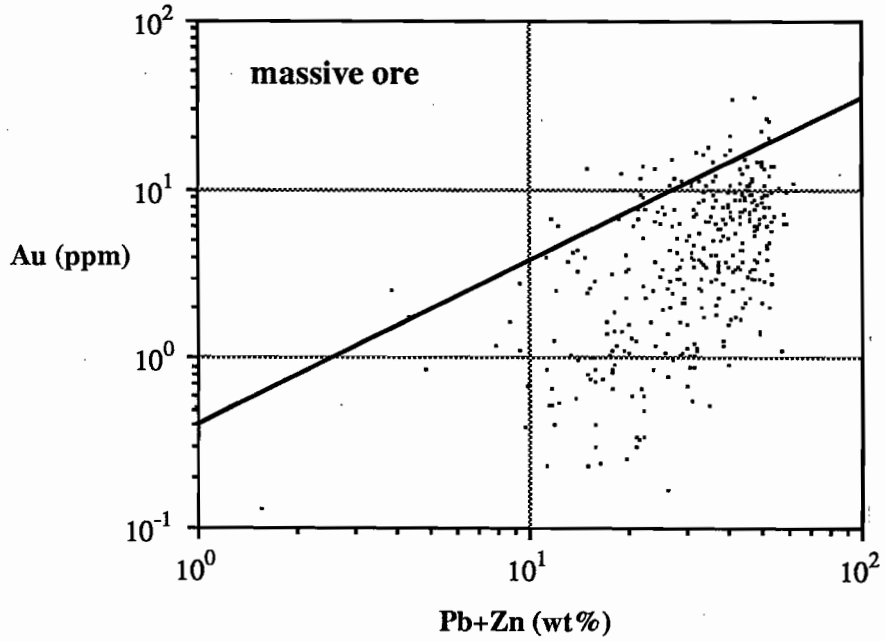

Fig. 5 Gold v Pb+Zn for Que River "normal" stringer, PMZ stringer and massive ores; the sloping line corresponds to a Pb + Zn : Au ratio of 25000 : 1.

Figure 6 depicts bar charts of frequency percent versus grade for Pb, Zn, Cu, Au, Ag, As, Sb and Ba for QR 417 and QR 631 stringer samples. The following observations can be made:

1. Higher Pb and Zn grades are observed in QR 417 stringer samples than in the PMZ stringer in QR 631.
2. A larger proportion of samples from QR 631 have low Cu (<2 wt %) and low Ag (<50 ppm) levels than from QR 417.
3. In contrast, higher levels of Au, Ba, Sb and As are present in stringer samples from the PMZ.

Further evidence for a relative enrichment of Ba and volatile metals (Sb and As) compared to base metals in the PMZ is provided by differences in metal ratios (notably Au, Ba, Sb and As: total Pb+Zn) in individual samples from QR 417 and QR 631. Although Au/(Pb+Zn) displays the largest differences between PMZ and "normal" stringer the majority of QR 631 samples have higher metal/(Pb+Zn) ratios than QR417 samples (Fig. 7).

-discussion

The association of the metals Au, Sb and As is well documented from epithermal systems (eg., Ewers and Keays, 1977; Weissberg et al.,1979) where the character of the metal-transporting solutions and the physico-chemical processes responsible for metal deposition result in effective separation of base metals (early paragenesis) from Au, As and Sb (later paragenesis). Ewers and Keays (1977) argued that separation of these metals in a drill hole from Broadlands, N.Z., occurred because the base metals were chloro-complexed and could not remain in solution on cooling while Au (and possibly As and Sb) were transported as bisulfide that remained stable as solution temperatures dropped. Ultimately Au precipitated in response to any or all of the following processes: solution pH change, H_2S loss or oxidation (Hedinquist and Reid,

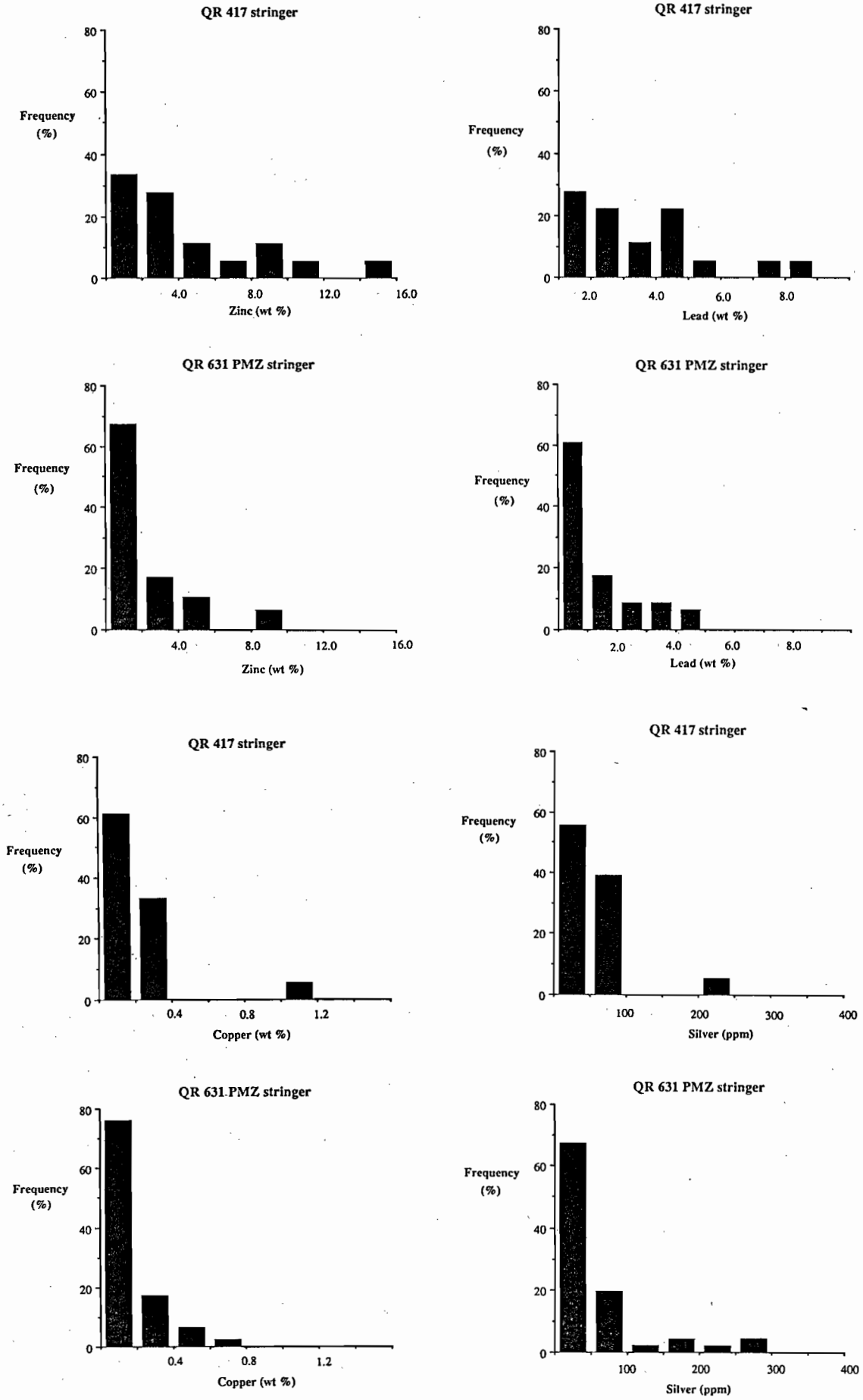

Fig. 6 a) histograms for Zn, Pb, Cu, and Ag for 18 samples of "normal" stringer (QR 417) and 46 samples of PMZ stringer (QR 631).

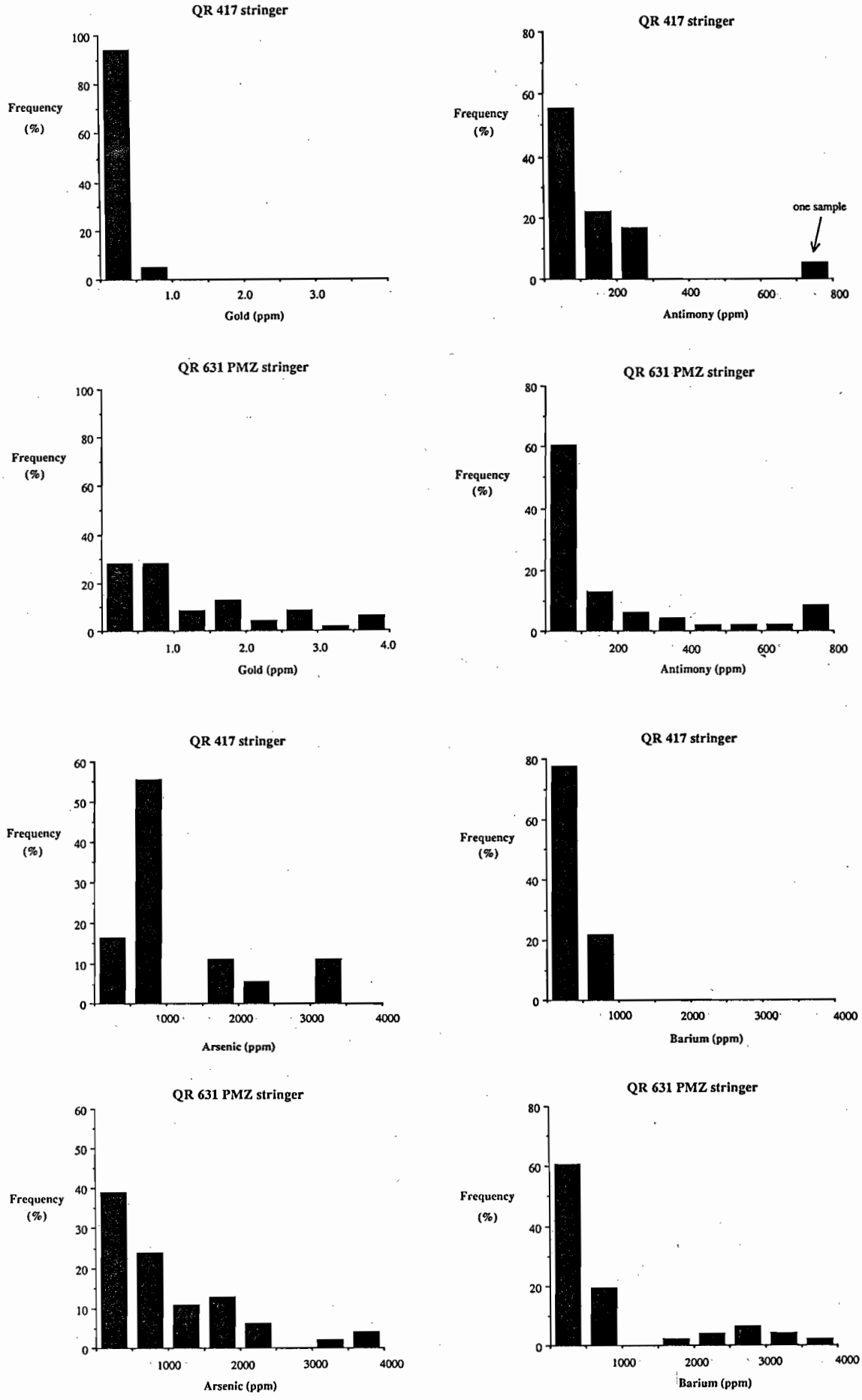

Fig. 6 b) histograms for Au, Sb, As and Ba for 18 samples of "normal" stringer (QR 417) and 46 samples of PMZ stringer (QR 631).

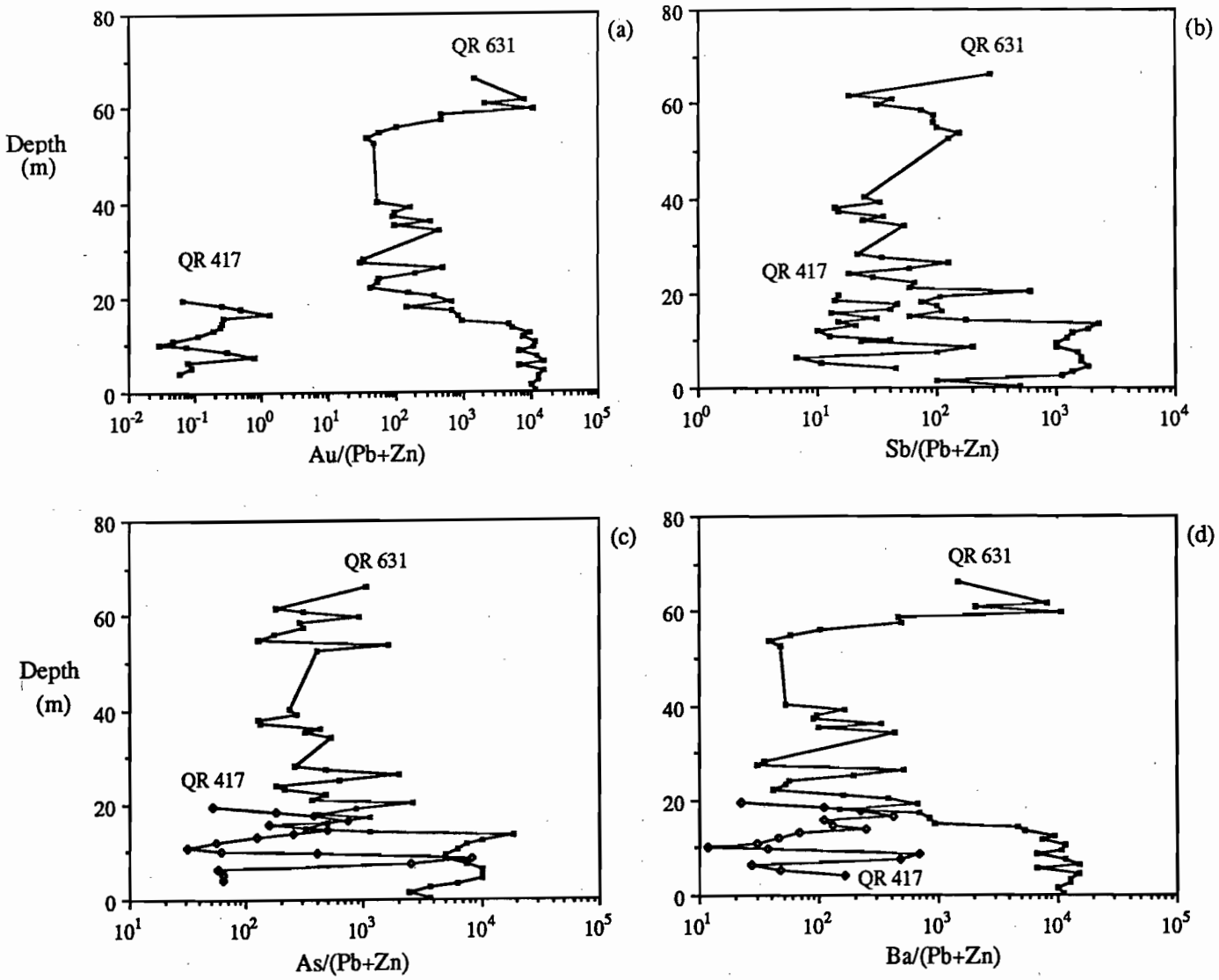

Fig. 7 a) Downhole variations in Au/(Pb+Zn) in QR 417 and QR 631.
b) Downhole variations in Ba/(Pb+Zn) in QR 417 and QR 631.
c) Downhole variations in Sb/(Pb+Zn) in QR 417 and QR 631.
d) Downhole variations in As/(Pb+Zn) in QR 417 and QR 631.

1985). Physical processes such as boiling or mixing with ground waters may be the cause of these changes.

Pyrite is ubiquitous throughout the Que River stringer as disseminations and discrete veins, and evidence of some mineralogical zoning is provided by chalcopyrite-pyrite stringers occurring in the area of most intense stringer development beneath the thickest massive ore (eg., 7550 N section). Variable amounts of sphalerite and galena are observed in other parts of the stringer system.The Cu-rich central core surrounded by high Zn and Pb grades and the occurrence of anomalous Au,Ba, As and Sb in more distal parts of the stringer (eg., 7700 N), indicates that the Que River stringer system has a gross chemical zonation. The central core of the stringer zone is Cu-rich but passes rapidly into a Zn-Pb-Ag stringer (eg.,7550 N section) and ultimately (in places) to a Zn-Pb-Ag-Au-Sb-As stringer (eg., 7700 N).

Some of the Ba in the PMZ samples must be present in K feldspar (0.5 to 2 wt % BaO). However, this mineral is seldom present at levels more than ten modal percent, hence, the elevated Ba levels (up to 4600 ppm) in some samples would suggest that some barite occurs in this part of the stringer.

-S isotopes

Some preliminary S isotope data for sulphide mineral separates from PQ lens, "normal" footwall stringer and PMZ samples are presented on Figure 8. Samples of pyrite from the PMZ have the heaviest S and show a wide range of values (+7.8 to +17.1 permil), while most samples from "normal" stringer and massive ore have somewhat lighter S and cluster together. On average stringer pyrite (range 5.6 to 10.3 permil for all but two samples) is heavier than the massive ore sulphides (range 5.0 to 8.5 permil for all but one sample). This trend from heavy S in parts of the footwall stringer to lighter S in the massive ores is similar to that observed at Hellyer (D. Jack pers comm., 1987),

but is the opposite of the stratigraphic variation inferred for samples from Rosebery (Green et al., 1981).

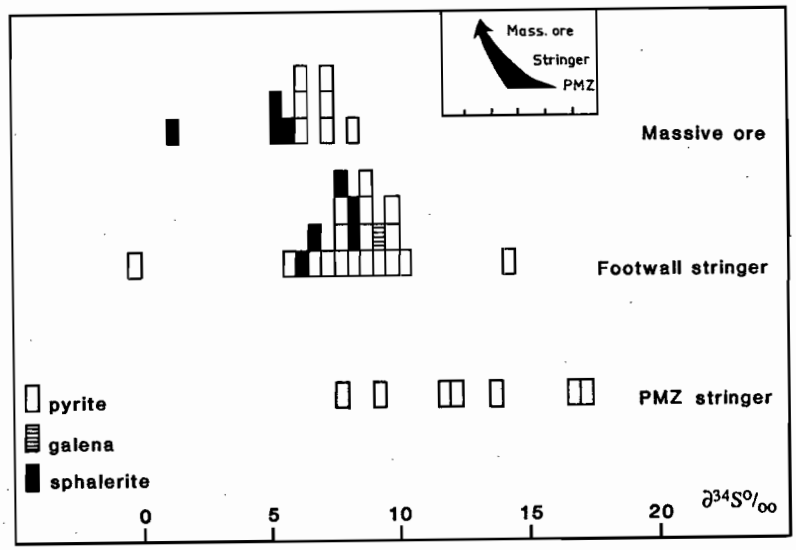

Fig. 8 Sulphur isotope data for individual mineral separates from Que River (the inset summarises t to massive ore).

-discussion

The isotopically heavy S in the massive ore and stringer zone at Que River indicates an important seawater S component in the mineralisation (Solomon et al., in press). Variations in S isotope ratios can be produced by changing physico-chemical conditons during sulphide deposition, in particular the oxidation state of the mineralising solutions. Alternatively, the increase in $\partial^{34}S$ from massive ore to "normal" stringer to PMZ stringer can be interpreted as indicating more extensive mixing of seawater and hydrothermal fluid taking place in parts of the stringer zone away from the main hydrothermal fluid input.

Discussion

-Zoning in massive ores

Previous work has documented a zonation in western Tasmanian Zn-rich massive sulphide ores in which highest Cu grades occur at their bases nearest the postulated site

of maximumum fluid input (and highest fluid temperatures). Zinc and Pb sulphides occur throughout the massive ore, but Au tends to be concentrated toward the stratigraphic tops of the massive sulphides (eg., Que River - see April 86 progress report, Rosebery - Huston and Large; 1987). At Hellyer both Au and As are enriched toward the hanging wall of the massive sulphide (McArthur, 1986).

Huston and Large (1987) have produced a chemical model to account for the distribution of Au in volcanogenic massive sulphide deposits. The main features of this model are summarised as follows:

1. The solutions responsible for forming the massive ores and their related stringer systems transport the base metals (Cu, Pb, Zn) as chloro-complexes, but Au may be carried as either chloro- or bisulfide- complexes.
2. For solutions with geologically reasonable salinities and S contents under high temperature(275°C to 350°C), low pH conditions, Au-chloride complexes dominate Au transport. However, at lower temperatures (150°C to 275°C) and weakly acid to near neutral pH Au-bisulfide transport is more important .
3. Although changes in solution pH and fO_2 will affect base metal solubilities, cooling of the mineralising fluids as they reach the sea floor is probably the most important single cause of base metal sulphide precipitation in the massive sulphide body and the stringer zone.
4. In contrast, Au-bisulphide complexes are not strongly affected by temperature changes, but will be affected by processes which change solution pH, fO_2 or total S content (eg., boiling - which releases H_2S and CO_2 gas; mixing with seawater - which will increase solution fO_2; precipitation of sulphide minerals - this may cause local gradients in solution S contents).
5. Because of these differences between Au and base metal solution chemistry Huston and Large (1987) argue that some Au is deposited from bisulfide complexes during the first (low temperature) stages of massive sulphide mound development. With time, as the hydrothermal system builds up and solution temperatures increase, new Au will be

introduced by the hydrothermal solutions and Au fixed during early stages of mound growth will be mobilised as chloride and/or bisulfide complexes. As this solution moves through the growing mound its temperature drops and bisulfide complexing dominates Au transport. This Au is ultimately deposited in the upper and more distal parts of the sulphide mound or in related oxide facies deposits (eg., barite-hematite-silica cap).

6. Gold-rich Cu stringer in these deposits and massive sulphide deposits of the Cu-Au association (Huston and Large, 1987) formed from solutions in which Au was chloro complexed and solution conditions never evolved to favour Au bisulphide complexing (Fig. 9) i.e., high temperature and low pH and/or high fO_2 solutions.

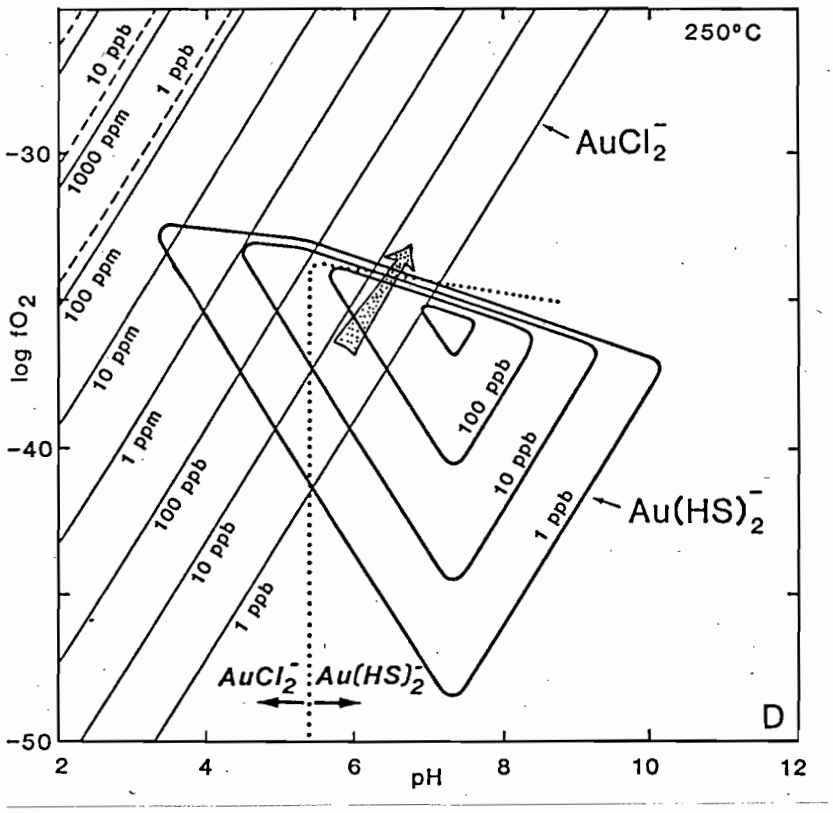

Fig. 9 fO_2 - pH diagram at 250° C ($a_{\text{total S}} = 10^{-2.5}$, $a_{Cl^-} = 1$) with Au solubility contours and possible fluid evolution path for stringer solutions (modified from Huston and Large, 1987).

-Zoning in the Que River stringer/PMZ system

The Que River footwall stringer system is interpreted here as an irregularly and asymmetrically zoned body and an idealised N-S section is presented on Figure 10. The stringer is dominated by a pyrite -sericite -silica ± carbonate ± K feldspar ± base metal sulfide assemblage superimposed onto a variety of andesitic volcaniclastic rock types. It has a Cu-rich core, best developed near 7550 N section, interpreted to represent the main focus of mineralising fluids. To the south, although pyrite disseminations and stringers are common for tens of meters into the footwall, high Pb and Zn grades do not extend much more than a few meters into the footwall of the massive ore (eg., 7400 N). To the north (eg., 7700 N, 7725 N) good Zn and Pb grades extend more than 50 meters into the footwall and beneath the massive sulphide mineralisation.

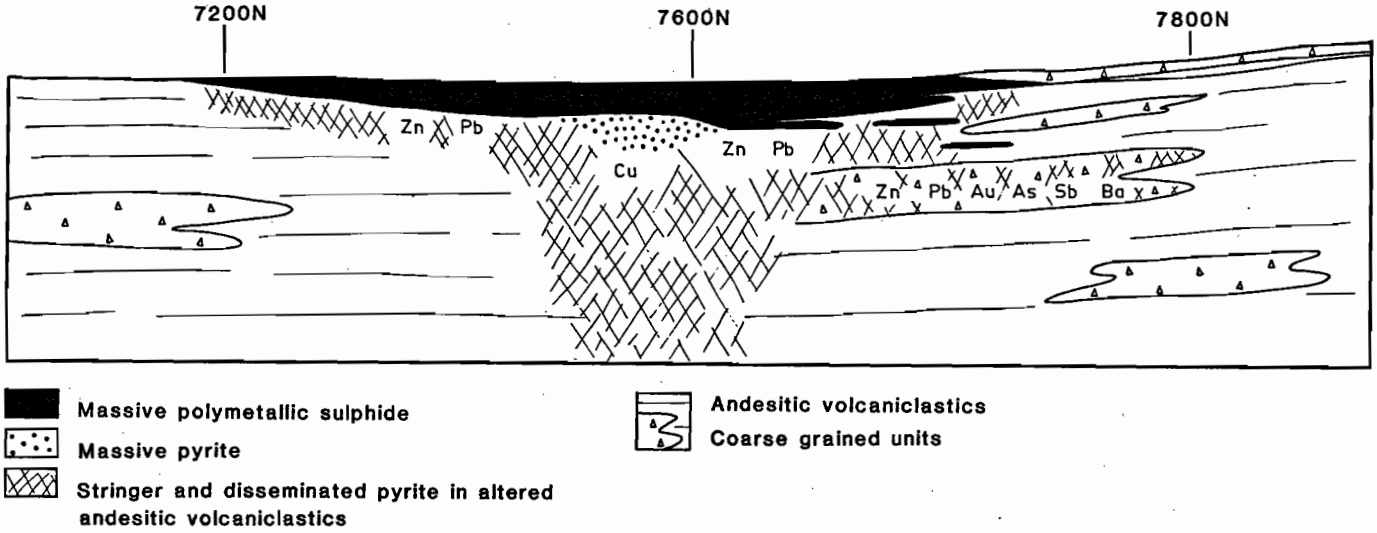

Fig. 10 Idealised north - south section through Que River massive ore and footwall stringer depicting metal zonation in the stringer.

There are two possible explanations for the broader metal distribution in northern parts of the stringer zone. The volcaniclastics comprising the footwall rocks in this area may have been more porous and permeable to the ore-forming solutions than footwall rocks to the south. Alternatively, epiclastic processes may have continued to dump clastic material into, and onto, actively forming massive sulfide mineralisation in the northern parts of the system. The former explanation is supported by the observation that the PMZ occurs in a distinctive coarse grained facies of the northern stringer, however, the existence of thin massive sulphide horizons in footwall rocks (including the PMZ) indicates that the seafloor position changed with time in the northern parts of the system and lends support to the latter explanation. In reality both processes may have been important reasons for the difference between the northern and southern stringer.

Model for the PMZ

The observations important for constraining the model proposed here for the footwall PMZ at Que River are summarised on Table 10.

During formation of the PQ - P north massive sulphide bodies the porous and permeable nature of much of the underlying volcaniclastics allowed the metalliferous solutions easy passage and lead to the development of an unusually extensive stringer system. The solutions formed massive Fe-Zn-Pb-Cu-Ag-Au sulphide ores at the seafloor but within the footwall rocks they have formed several types of stringer. All the stringer contains pyrite and the host volcaniclastics have been variably silicified, sericitised and K-feldspar altered. Copper-bearing stringer formed beneath the thickest parts of the massive sulphide during the hottest phase of fluid activity. As this Cu stringer is Au-poor, solution conditions in this part of the stringer must have favoured Au transport (A on Fig. 11). Cooling as they moved away from the main focus of hydrothermal activity these solution precipitated Zn-Pb-bearing stringers containing

TABLE 10: Important features of the Que River footwall precious metal zone

OBSERVATION:	INFERENCE
K feldspar is prominent in the PMZ	- mineralising fluids in the PMZ were only weakly acid or neutral
There is no direct association of Au with the characteristic "white alteration" observed in the PMZ	- Au is in stringers or disseminated sulfides in the matrix of the PMZ host rock
Isotopically heavy sulphur occurs in pyrite from PMZ stringers; sulphur in "normal" stringers and massive ore is lighter than PMZ sulphur	- a larger component of seawater S is present in the PMZ sulphides than elsewhere in the Que River mineralisation
The Au : base metal ratios in PMZ stringer samples are indistinguishable to those in some (Au-rich?) parts of the massive ores	- the same physico-chemical controls on Au distribution in the massive ores could have controlled Au distribution in the footwall stringer and PMZ
The PMZ contains higher Sb and As levels (as well as Au) than other parts of the stringer zone but the best Cu (and Pb-Zn?) grades occur in stringer proximal to the proposed vent	- the northern half of the stringer zone at Que River is coarsely zoned from a Cu-rich core to Zn-Pb rich stringer to a distal Zn-Pb-Au-Sb-As (Ba) zone
Higher Ba levels are observed in the PMZ than in other parts of the stringer zone	- conditions were somewhat more oxidising in the PMZ than in "normal" stringer
The host rock for much of the PMZ is a distinctive coarse polymictic andesitic volcaniclastic unit	- the "best" development of PMZ style stringer has been in more porous and permeable footwall rocks, hence, favourable footwall lithologies and/or facies changes may have controlled the extent of the PMZ

only minor amounts of Au.(i.e., Au remained in solution as a bisulphide complex). In the southern part of the system these stringers are close to the massive ore and presumably fed their metal load (including Au) directly to the growing sulphide mound. In contrast, in the north these solutions moved through a larger volume of rock in the sub-seafloor and in so doing the resultant gradual changes in physico-chemical conditions caused a much more extensive Zn-Pb stringer development. While Pb and Zn sulphides were be precipitated more or less continuously down the temperature gradient in this zone, Au and other bisulfide complexed species (As, Sb?) were not, but precipitated only when the solution was oxidised(B on Fig 11). Mixing of mineralising fluids and seawater in the more permeable epiclastics of the PMZ would have been an excellent mechanism for increasing solution fO_2.

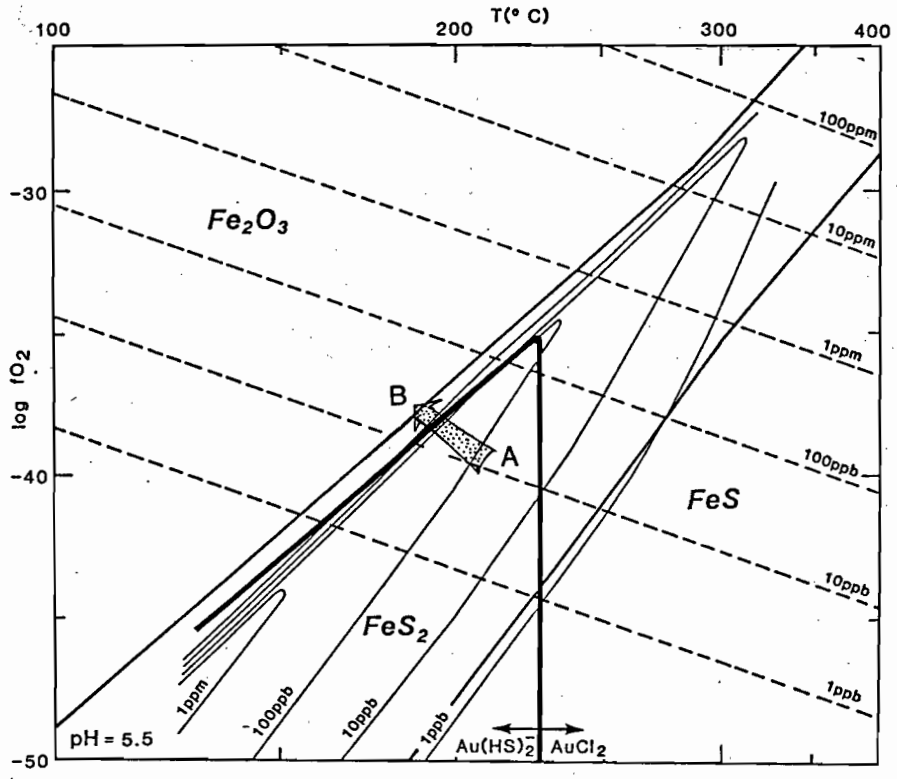

Fig. 11 fO_2 - temperature diagram with Au solubility contours and mineral stability fields at a pH of 5.5 ($a_{\text{total S}} = 10^{-2.5}$, $a_{Cl^-} = 1$); Au solubility is high at point A and actually increases as the fluid cools and oxidises until the pyrite - hematite boundary is approached (point B) where Au solubility as bisulphide complexes drops by several orders of magnitude (modified from Huston and Large, 1987).

- **Discussion**

Facies variations within the footwall volcaniclastics must have been important controls on the ultimate geometry of the Que River stringer system.It is possible to speculate that the Que River PMZ occurs as a discrete zone or zones within the stringer system because the Que River stringer zone is so extensive. In other deposits in which the feeder system is more pipe-like, and the transition from altered stringer to "normal" footwall rocks occurs over a short distance, distinct PMZ type stringer would not form because physico-chemical gradients were too steep.

- **Boiling in the PMZ**

Changes in fluid physico-chemical conditions caused by cooling and oxidation within the stringer system at Que River can adequately account for the observed metal zoning. Hence, it is not neccessary to invoke boiling as a process involved in formation of the PMZ mineralization. However, at this stage of our work boiling cannot be definitely eliminated as a process in the Que River stringer, and it is hoped that planned fluid inclusion studies will elucidate this problem. Solution boiling is an excellent process for de-stabilising metal bi-sulphide complexes because H_2S is lost to the gas phase, hence, boiling the mineralising solutions would cause Au precipitation.

However, several points should be made, firstly, if boiling had occurred in distal parts of the stringer to form the PMZ (where solutions presumably were colder than in the central core of the stringer), then boiling should have occurred in the proximal stringer and possibly at the sea floor. Recent modelling (Drummond and Ohmoto, 1985) suggests that boiling would cause a mineral paragenetic sequence starting with Fe oxides then sphalerite / galena followed by pyrite / chalcopyrite and finally Au. Hence, had boiling occurred in the Que River stringer or massive ore zone then a very different mineralogical zonation to that observed would result. Furthermore, the observed metal zoning in Que River massive ore and its proximal stringer is identical to metal zoning

observed in many Kuroko deposits - systems which demonstrably have not boiled (Pisutha-Arnond and Ohmoto, 1983).

Exploration Implications

This explanation for the Que River PMZ has important implications for exploration.

1. The PMZ is an unusual type of stringer zone genetically related to the Que River massive ore / "normal" stringer system; hence, similar Au-anomalous zones may occur in the footwall alteration systems of other "Au-Zn-Pb-Ag association" massive sulphides.

2. A broad dispersed stringer is more prospective for PMZ style mineralisation than (more typical?) pipe-like zones

3. Porous and permeable volcaniclastic successions are more favourable footwall lithologies for developing the extensive stringer zones required for PMZ development.

4. PMZ style mineralisation should always have an associated massive sulphide body unless it has been removed by subsequent erosion or weathering. However, hydrothermal systems operating in an actively depositing (pyroclastic / epiclastic) setting may continue operating as clastic material accumulates and large dispersed stringer-like zones may form with little or no massive ore. A large extended stringer / PMZ type body may be a low grade - high tonnage Au prospect in its own right.

5. Penecontemporaneous erosion and re-deposition of massive ores is common in the Kuroko district and in some Canadian camps and the potential must exist in the MRV for massive ores without footwall alteration zones and conversely stringer zones that

have lost their overlying massive ores. This latter group may contain PMZ style mineralisation.

6. PMZ style mineralisation is likely to have an alteration mineralogy reflecting the moderate pH and lower temperatures of their mineralising fluids. For instance, K feldspar (Ba-bearing) and carbonate alteration may be a diagnostic feature of such zones. It is interesting to note that anomalous Au grades (over 3 ppm) were recorded from a K feldspar bearing epiclastic (?) unit about 50 meters into the footwall of the Red Hills massive sulfide mineralization in DDH RH 8 drilled by Goldfields in 1977.

Acknowledgements

The continuing support and encouragement of Aberfoyle personnel is warmly acknowledged. June Pongratz is thanked for assistance with the drafting. Typing and drafting was substantially aided by A. Macintosh.

References

Drummond, S.E. and Ohmoto, H., 1985. Chemical evolution and mineral deposition in boiling hydrothermal solutions. Econ. Geol., 80, 126 - 147.

Ewart, A., 1982. The mineralogy and petrology of Tertiary - Recent orogenic volcanic rocks: with special reference to the andesitic - basaltic compositional range; in Andesites: Orogenic Andesites and Related Rocks, edited by R.S. Thorpe, J. Wiley and Sons, 25 - 95.

Ewers, G.R. and Keays, R.R., 1977. Volatile and precious metal zoning in the Broadlands Geothermal Fiel, New Zealand. Econ. Geol., 72, 1337 - 1354.

Green, G.R., Solomon, M. and Walshe, J.L., 1981. The formation of the volcanic-hosted massive sulfide deposit at Rosebery, Tasmania. Econ. Geol.,76, 304 - 338.

Hedinquist, J. and Reid, F., 1985. Epithermal Gold, The Earth Resources Foundation, University of Sydney.

Huston, D.L.and Large, R.R., 1987. A chemical model for the concentration of gold in volcanogenic massive sulphide deposits. submitted to Ore Geology Reviews.

McArthur, G.J., 1986. The Hellyer massive sulphide deposit, in Large, R.R., (ed), The Mount Read Volcanics and Associated Ore Deposits, 11 - 20.

McGoldrick, P.J. and Large, R.R., 1986. Preliminary report on the footwall precious metal zone, Que River. AMIRA Project 84/P210, Controls on Gold and Silver Grades in Volcanogenic Sulphide Deposits, Progress Report, Nov., '86, 7 - 16.

Pisutha-Arnond,V. and Ohmoto, H., 1983. Thermal history, and chemical and isotopic compositions of the ore-fluids responsible for the Kuroko massive sulfide deposits in the Hokuroko district of Japan. Econ. Geol. Mono., 5, 523 - 558.

Solomon, M., Eastoe, C.J. and Walshe, J.L., 1987. Mineral deposits and sulfur isotope abundances in the Mount Read Volcanics between Que River and Mount Darwin, Tasmania. Econ. Geol. (in press).

Weissberg, B.G., Browne, P.R.L. and Seward, T.M., 1979. Ore metals in active geothermal systems, Ch. 15 in H.L. Barnes (ed); Geochemistry of Hydrothermal Ore Deposits, 2nd edition, 738 - 780.

PROGRESS REPORT ON F-LENS METAL ZONATION, ROSEBERY MINE

Khin Zaw

AMIRA Report

August 1987

INTRODUCTION

The author is presently carrying out a metal zonation study of the Fe-S-O replacement assemblages in the Rosebery south-end orebody, particularly F lens (Fig. 1). An outline of the research programme was presented in the previous AMIRA report (November, 1986).

Eight weeks field work have been completed at the Rosebery mine-site during December, 1986 to February, 1987. The field work included core logging, sample collection of DDHs on selected E-W X-sections and investigation of underground workings and exposures.

Background

Brathwaite (1974) initally reported pyrrhotite bearing assemblages replacing sulphide lenses at the south-end orebodies and attributed these assemblages to the Devonian metamorphism.

Later deep drilling has exposed an extensive zone of replacement and that in addition to pyrrhotite, a wide variety of replacement assemblages from magnetite (hematite)-biotite, pyrrhotite-pyrite to tourmaline-quartz and other minerals such as fluorite, garnet and helvite (Green, et. al., 1981; Solomon et. al., 1987; Lees, 1987).

Method

(1) The author selected eleven E-W X-sections through the F lens and logged the available drill holes on each section. The selected X-sections are 300mS, 280mS, 270mS, 250mS, 220mS, 200mS, 190mS, 145mS, 130mS, 100mS, and 20mS, and shown in Fig. 2.

(2) Underground exposures of the Fe-S-O assemblages were investigated and their structural, textural and spatial relationships sketched and observed in detail.

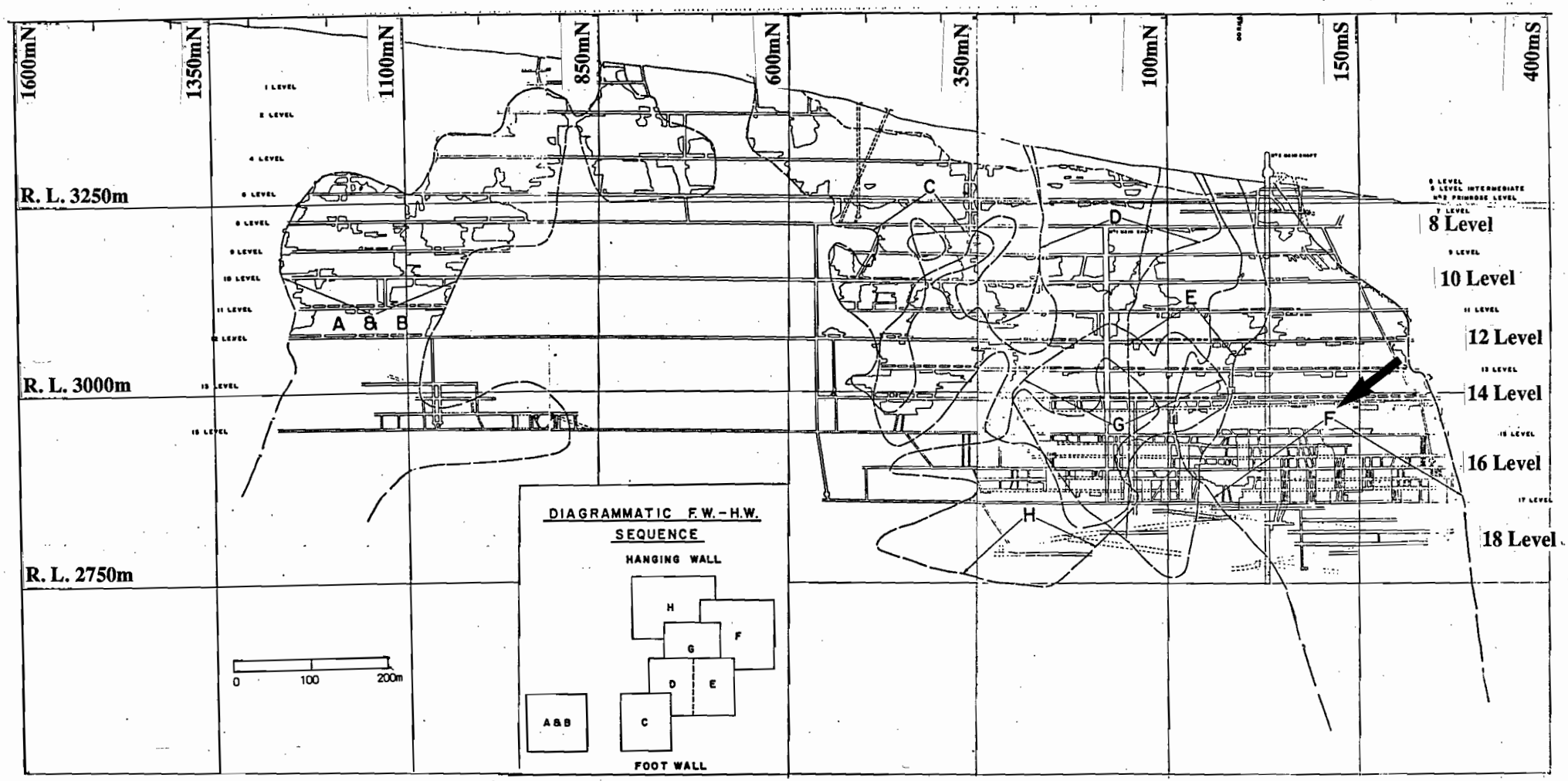

Fig. 1. Longitudinal projection of the Rosebery orebody showing relative position of ore lenses (insert). Note 'F' lens at southern-end of the orebody.

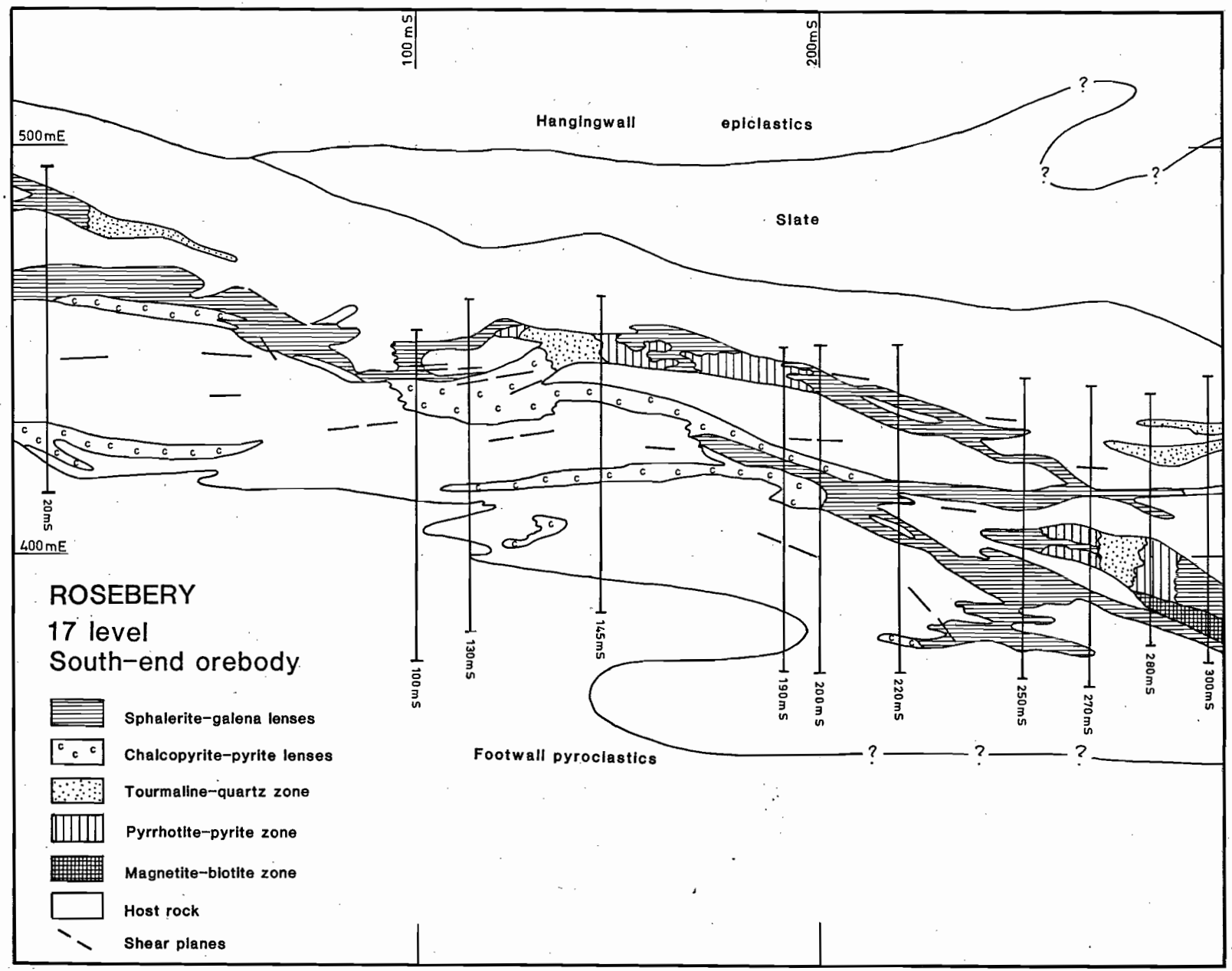

Fig. 2. Geology of 17 Level showing selected E-W cross-sections in this research programme, Rosebery Mine.

ZONATION OF FE-S-O REPLACEMENT ASSEMBLAGES

The present field investigation along different mine levels and logging of DDHs on the selected X-sections revealed a spatial distribution and zonation of Fe-S-O assemblages on an ore body scale as shown in Fig. 3. The following three major zones can be essentially distinguished;

(3) Tourmaline-quartz ± magnetite zone

(2) Pyrrhotite-pyrite zone

(1) Magnetite-biotite ± chalcopyrite zone

(1) Magnetite-biotite ± chalcopyrite zone

This zone (1) appears to be earliest and mostly confined to the lower levels of the mine particularly below 17 Level. Magnetite extensively replaces massive pyrite lenses and magnetite itself exists as massive bodies where replacement is complete. Pyrite occurs as cubes of various sizes in the magnetite host. Hematite is also noted in association with magnetite and in places hematite alone is found replacing pyrite.

The footwall chlorite appears to alter to biotite in this zone and recrystallised chalcopyrite is present in a high concentration in this zone. Unusual replacement assemblages such as garnet-biotite, garnet-helvite-tourmaline were noted.

(2) Pyrrhotite-pyrite zone

Major pyrrhotite-pyrite exposures replacing Pb-Zn sulphide lenses were recorded in the F lens along 16 No. 2 Sub-Level, 16 Level, 17 No. 2 Sub-level and 17 Level. In most cases this zone

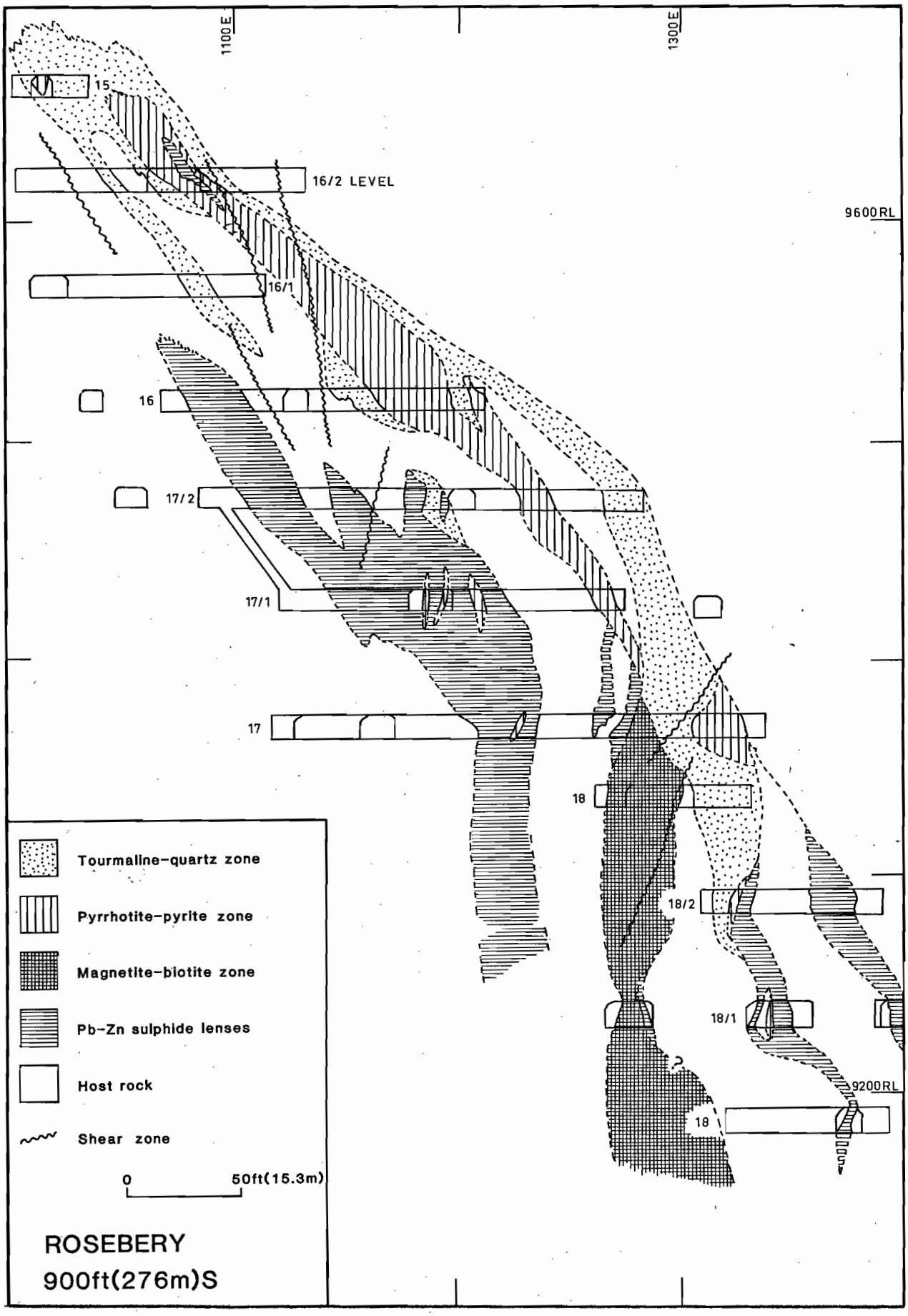

Fig. 3. Geological cross-section showing spatial distribution and zonation of Fe-S-O replacement assemblages at 'F' lens, south-end orebody, Rosebery Mine.

was enclosed by zone (3) assemblages of quartz and tourmaline with a variable amount of magnetite and chlorite (Fig. 3). The massive pyrrotite-pyrite bodies range from a lens of one meter to more than twenty meters across. A zone of dark brown, coarse-grained sphalerite was sometimes observed as a reaction rim between the replacing massive pyrrotite-pyrite and the original sphalerite-galena lenses (see Fig. 4).

As described by Solomon et. al., (1987) this replacement zone also varies from prrhotite-dominant to pyrite-dominant with or without tourmaline and magnetite. Below 17 Level no large bodies of pyrrhotite-pyrite was observed although thin lenses of pyrrhotite-pyrite with chalcopyrite was found in the massive magnetite-biotite assemblages of zone (1).

(3) Tourmaline-quartz ± magnetite zone

This zone (3) appears to have formed at a late-stage during the replacement process as evidenced by irregular and patchy quartz-tourmaline veins cross-cutting the host rock and other sulphide lenses (Fig. 4). Tourmaline in this zone sometimes form criss-crossing, banded, thin veinlets. Although this pseudo-banding of the tourmaline assemblages appears to ressemble tourmalinites of strabound origin (e.g. Taylor and Slack, 1984), the cross-cutting textural relationships and its iron-rich composition (see later) positively indicate that they are formed due to replacement (see Fig. 4).

This tourmaline-quartz zone (3) occurs mostly enveloping and immediately lying above the massive pyrrhotite-pyrite bodies of zone (2). It is well exposed at the southernmost end of F lens. Though tourmaline and quartz are the dominant minerals in this zone, patches of pyrrhotite, pyrite and magnetite (hematite) with chlorite, fluorite and carbonates were noted.

Chemistry of replacement mineralogy

Preliminary microprobe analyses of the Rosebery replacement assemblages have been completed.

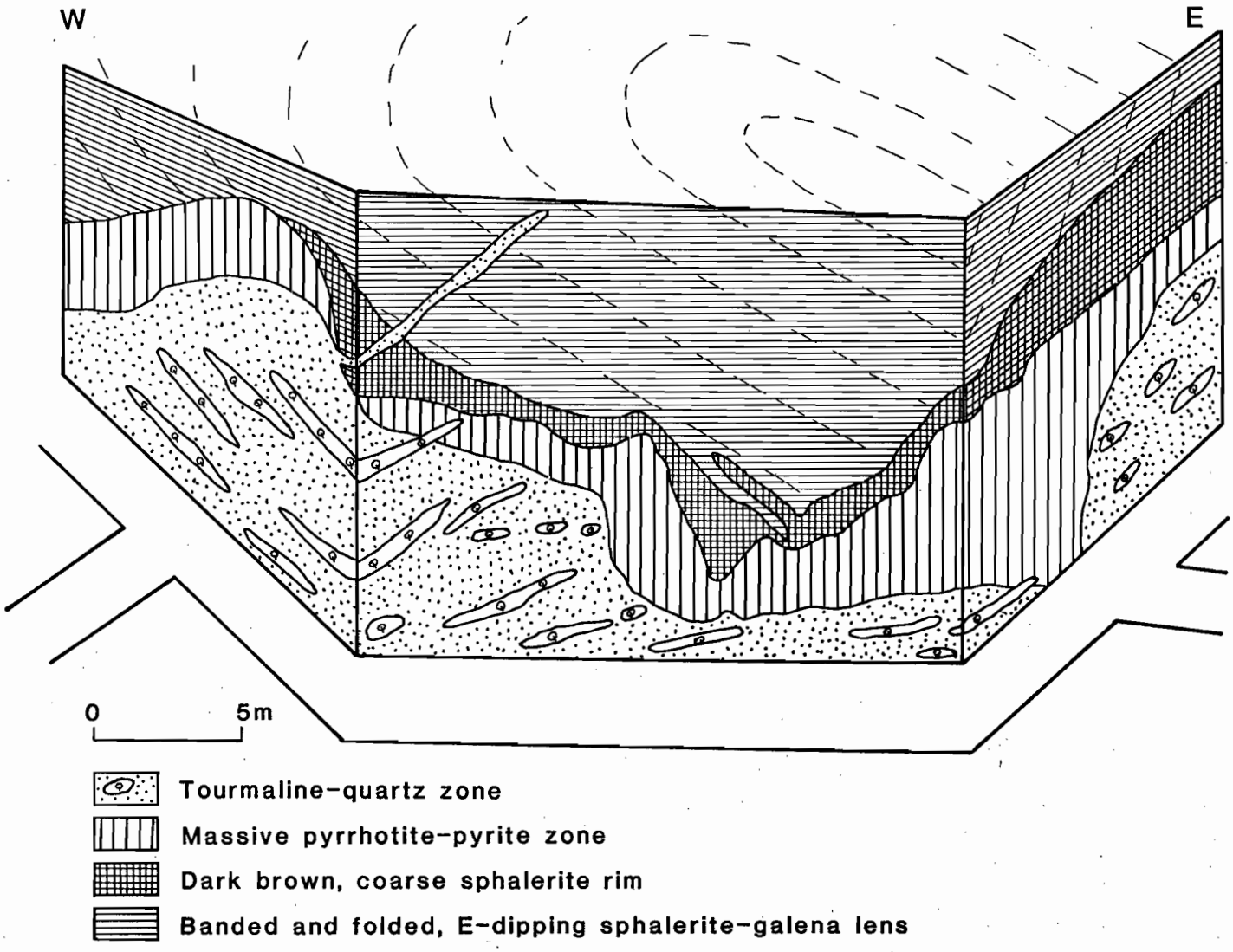

Fig. 4. A sketch showing pyrrhotite-pyrite and tourmaline-quartz assemblages replacing Pb-Zn lens. Note banded Pb-Zn lens is dipping to the east and apparently folded. Dark brown, coarse-grained sphalerite forms as reaction rim between Pb-Zn lens and phyrrotite-pyrite assemblage and cross-cut by patchy quartz-tourmaline veins. Location 16 No. 2 Sub-Level, 900' (276m) cross-cut.

Garnets

Stillwell (1934) first reported spessartine garnet at Rosebery Mine which was later confirmed by Green et. al., (1981) and Lees (1987) who attributed the garnet bearing assemblage to post-depositional metamorphism.

In this study, garnet samples collected from the DDH-88R were studied. Garnet was found to be mostly anhedral, creamy white and associated with phyrrotite, pyrite, magnetite, biotite, tourmaline and fluorite. Under the microscope, garnet is light orange, commonly anisotropic and very often zonned. In sample 88R-6, garnet altered to helvite and both minerals were cross-cut by tourmaline veinlets or rimmed by prismatic tourmaline grains. In other samples, the garnet bearing assemblage was cut by quartz-carbonate-fluorite veins.

Microprobe analyses of the garnet samples are shown in Fig. 5. The garnets from the Rosebery Mine consist predominantly of spessartine molecules from 76.38 to 91.28 %. In Figure 5 the composition of garnets from Rosebery Mine is shown in comparison with those of of typical, high temperature skarn garnets from CanTung Mine, NWT (Khin Zaw, 1976) and Cleveland replacement deposit, western Tasmania (Barth, 1986). It is noted that the composition of Rosebery garnets is different from those of high temperature skarn garnets, but the similar compositional range of garnets from Rosebery and Cleveland deposits suggests similar metamorphic-metasomatic conditions probably under relatively low to moderate temperature range.

Helvites

The general formula of the helvite group is $R_4Be_3(Si0_4)_3S$ (R=Mn, Fe^{2+}, Zn). The member with Mn preponderant is helvite, the Fe^{2+} end member is danalite, and the zinc end member is genthelvite.

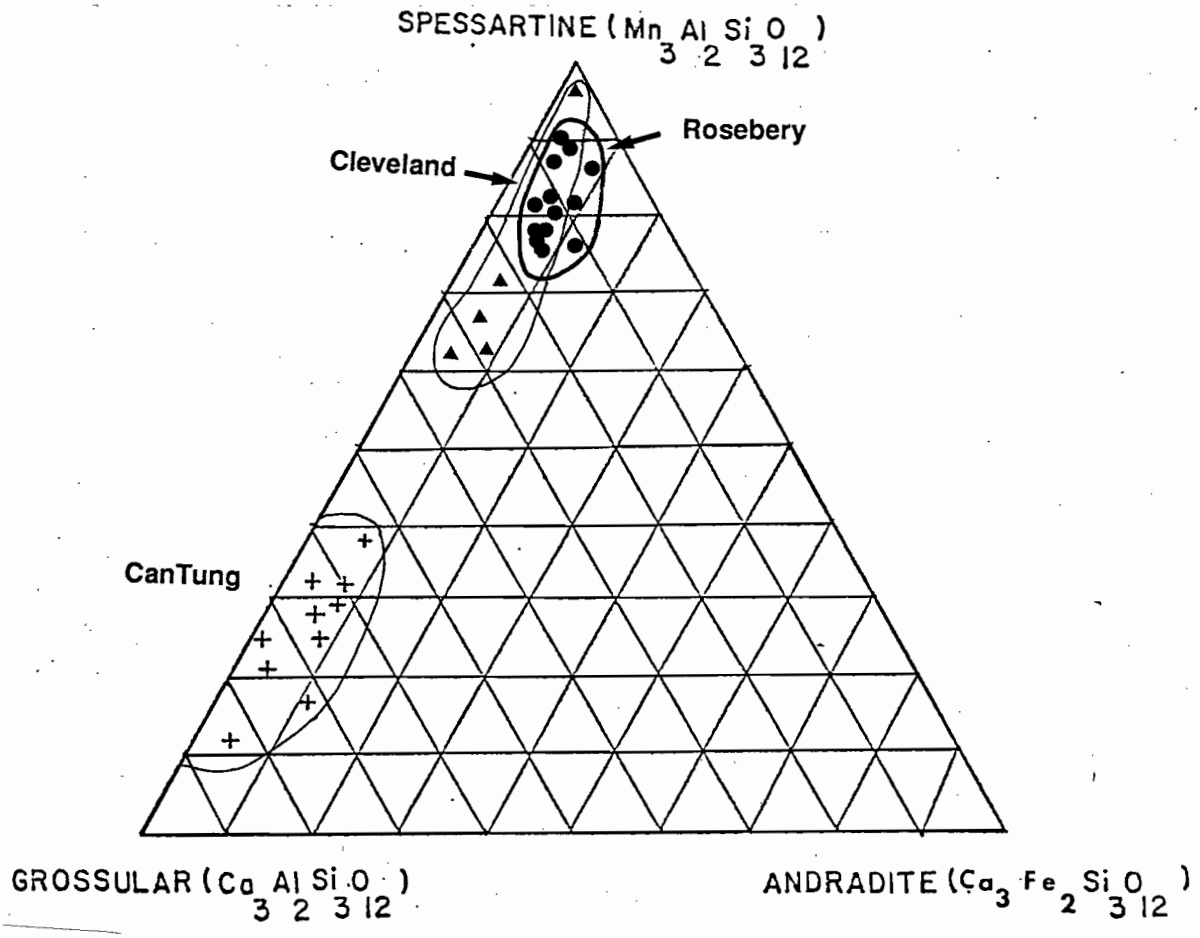

Fig. 5. Composition of garnets from 'F' lens, south-end orebody, Rosebery Mine together with compositional variation of garnets from Cleveland, western Tasmania (after Barth, 1986) and garnets from typical, high temperature skarn deposit, NWT, Canada (after Khin Zaw, 1976).

Under the microscope helvite from Rosebery is pink-coloured, rhombic in shape and found replacing garnet. Some helvite grains are distinctly zoned. The Rosebery helvite shows presence of a considerable amount of zinc up to (7) wt percent. A plot of Zn, Mn, Fe for analyses of the helvite minerals from Rosebery is shown in Fig. 6. Microprobe analyses of different zones of single helvite grain was attempted in this study. Mn content shows enrichment from core to rim whereas Fe^{+2} is decreased towards outer zones (Fig. 7).

Biotites

Biotite is commonly intergrown with magnetite in the deeper levels of the south-end orebodies. In hand specimen, biotite can be easily mistaken either with tourmaline or a dark green variety of chlorite. Microscopically, it forms as thin veinlets or flakes and sometimes it occurs as alteration products of garnets.

The composition of preliminary probe data for the Rosebery biotites are plotted in the Figure 8 (after Deer et. al., 1962) in terms of phlogopite $\{(K_2Mg_6\ [Si_6Al_2O_{20}]\ (OH)_4\}$, annite $\{(K_2Fe_6\ [Si_6Al_2O_{20}]\ (OH)_4$, eastonite $\{K_2Mg_5Al\ [Si_6Al_2O_{20}]\ (OH)_4\}$, and siderophyllite $\{K_2Fe_5Al\ [Si_6Al_2O_{20}]\ (OH)_4\}$ end-members.

The preliminary probe data indicate that the biotites are uniformly high in K_2O contents (7.48-9.04 wt %) and TiO_2 ranges from 0.27 to 1.19 wt %. The biotites display a range of octahedral Al^{vi} (2.35-2.61) and tetrahedral Al^{iv} (0.41-0.70) whereas $100Mg/Mg+Fe^{+2}$ values gave a restricted range of 27.2 to 35.00 and they are clearly biotites.

Compositional variation of biotites can be applied to distinguish different modes of its occurrence e.g. magmatic vs. metasomatic origins in porphyry copper and skarn environments (Bean, 1974; Jacobs and Parry, 1976; Khin Zaw and Clark, 1978).

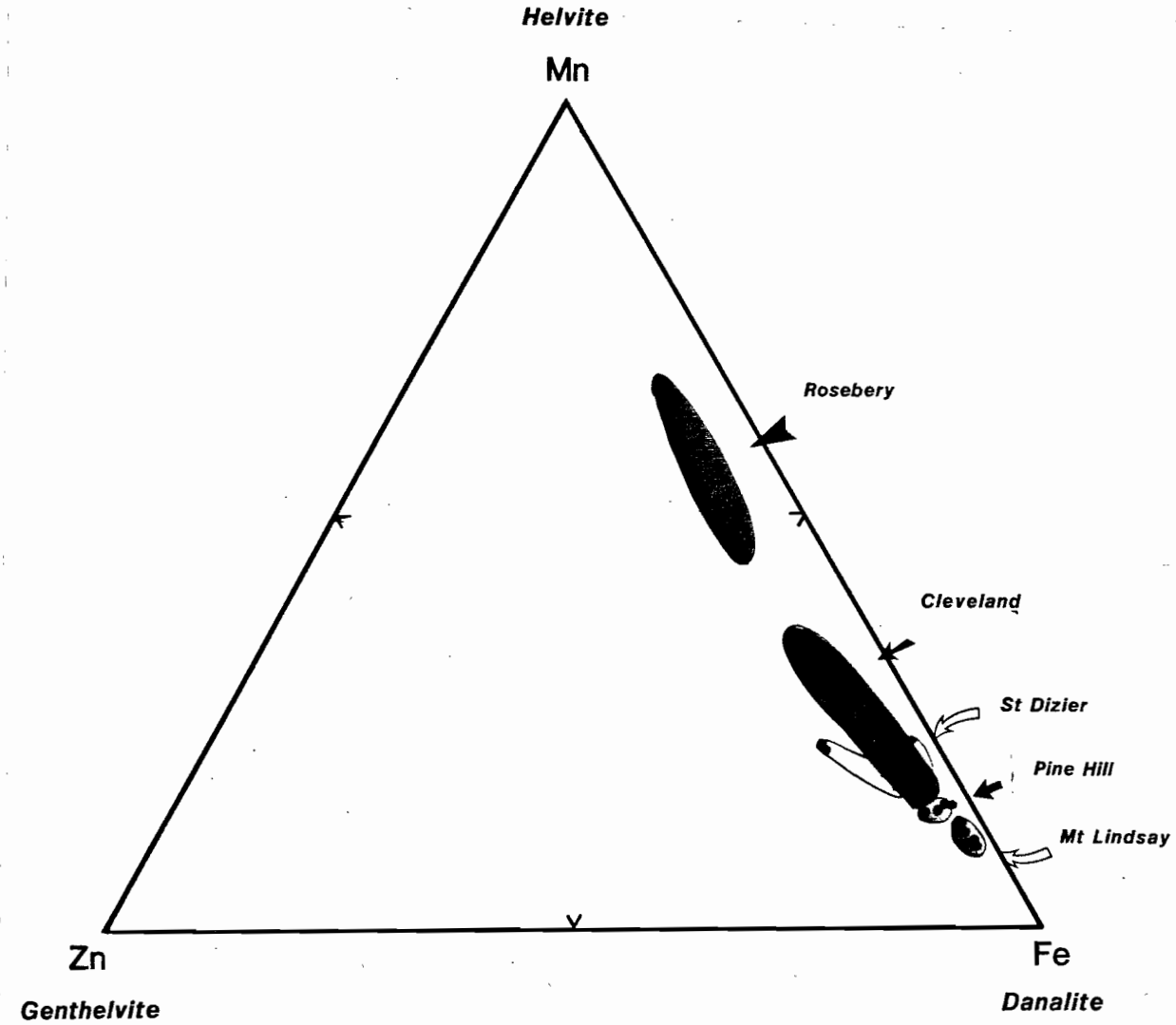

Fig. 6. Composition of helvites from 'F' lens, south-end orebody, Rosebery Mine together with compositional variation of helvites from Cleveland and other replacement deposits in western Tasmania (after Barth, 1986).

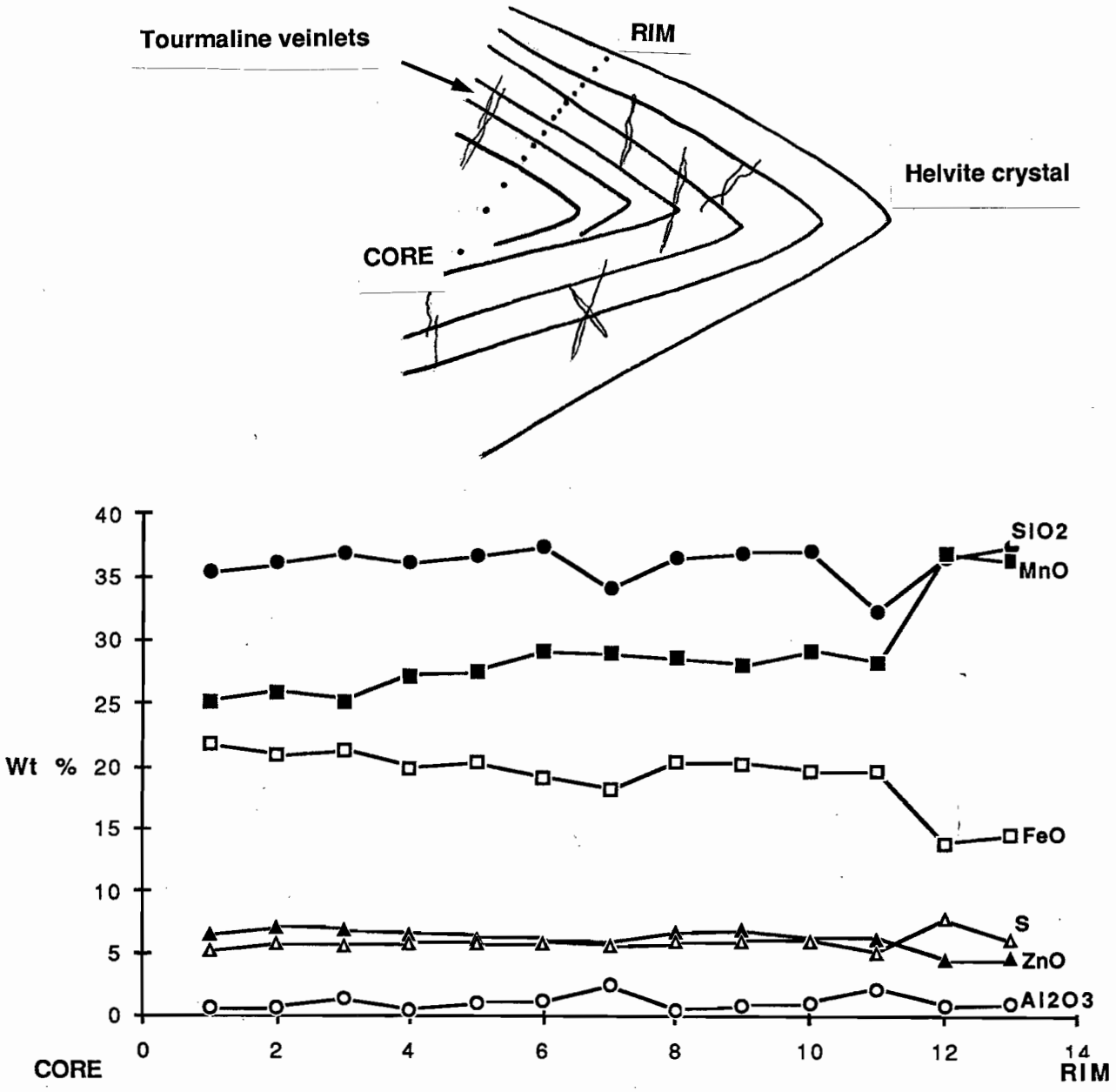

Fig. 7. A plot of compositional variation of a helvite grain from core to rim zones, 'F' lens, south-end orebody, Rosebery Mine. Note that Mn increases from core to rim whereas Fe^{+2} decreases towards rim.

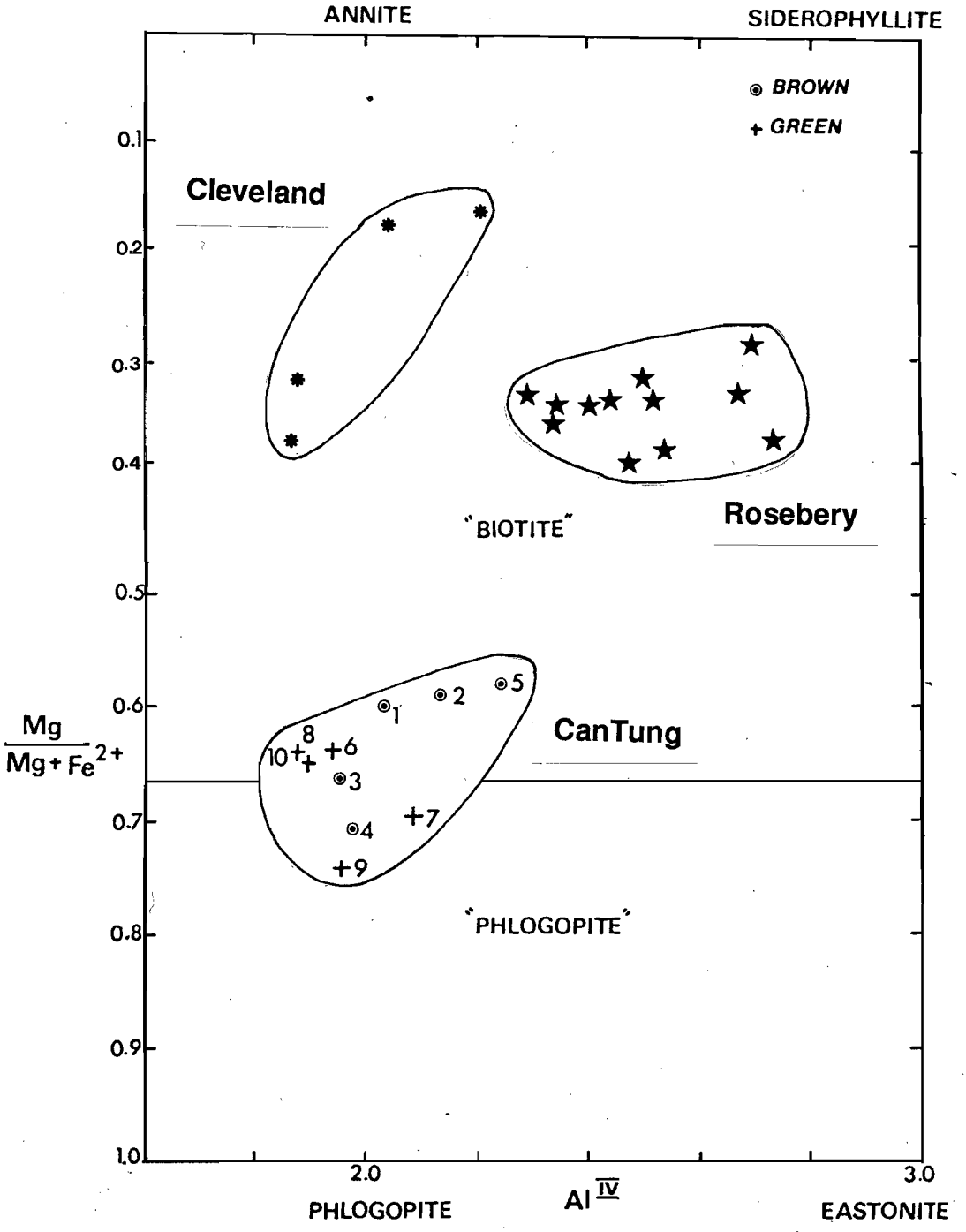

Fig. 8. A plot of $Mg/Mg+Fe^{+2}$ vs. Al^{iv} for biotites from 'F' lens, south-end orebody, Rosebery Mine together with composition of biotites from Cleveland, western Tasmania (after Barth, 1986) and biotite-phlogopites from typical, high temperature skarn deposit, NWT, Canada (after Khin Zaw, 1976).

Barth (1986) recently demonstrated that biotites from the Cleveland replacement deposit, western Tasmania gave a range of $100Mg/Mg+Fe^{+2}$ ratios 15.79 to 48.31. In Figure 8, the composition of Rosebery biotites are shown in comparison with those of Cleveland and of typical, high temperature W bearing biotite skarns from, CanTung Mine, NWT, Canada (Khin Zaw, 1976).

It is noteworthy that the Rosebery biotites are comparable with those of biotites from Cleveland replacement deposit, but its compositional difference from typical, high temperature skarn deposit suggest a different mode of occurrence probably low to moderate temperature.

Tourmalines

Tourmaline is a most ubiquitous mineral and found cross-cutting sulphide lenses and host rock in the south-end orebodies of the Rosebery Mine. Tourmaline occurs as thin veinlets or lenses and intimately associated with pyrite, pyrrhotite, magnetite and other silicate minerals such as garnet, helvite, biotite and chlorite. Under the microscope, tourmaline is found extensively replacing pyrite and locally garnet and helvite.

Tourmaline is a complex hydrous borosilicate mineral esstentially of Al, Ca, Fe, Mg and Na and occurs in a wide geological environment. As shown in the Figure 9 Rosebery tourmalines are predominantly of schorl $\{(Na\ Fe^{+2}_3\ Al_6B_3Si_6O_{27}\ (OH, F)_4\}$ rather than dravite $\{Na\ Mg_3Al_6B_3Si_6O_{27}\ (OH, F)_4\}$and elbaite $\{(Na\ (Li, Al)_3\ Al_6B_3Si_6O_{27}\ (OH, F)_4\}$. Preliminary microprobe data of tourmalines are also shown in Fig. (10) in comparison with other stratabound tourmalinites and it clearly indicates that Rosebery tourmalines are distinctly iron-rich than the tourmalines of stratabound origin as previously shown by Lees (1987).

PRECIOUS METALS DISTRIBUTION

It is interesting to note that precious metals precipitated during the formation of the Rosebery orebodies on the Cambrian sea-floor were redistributed and concentrated by the later replacement

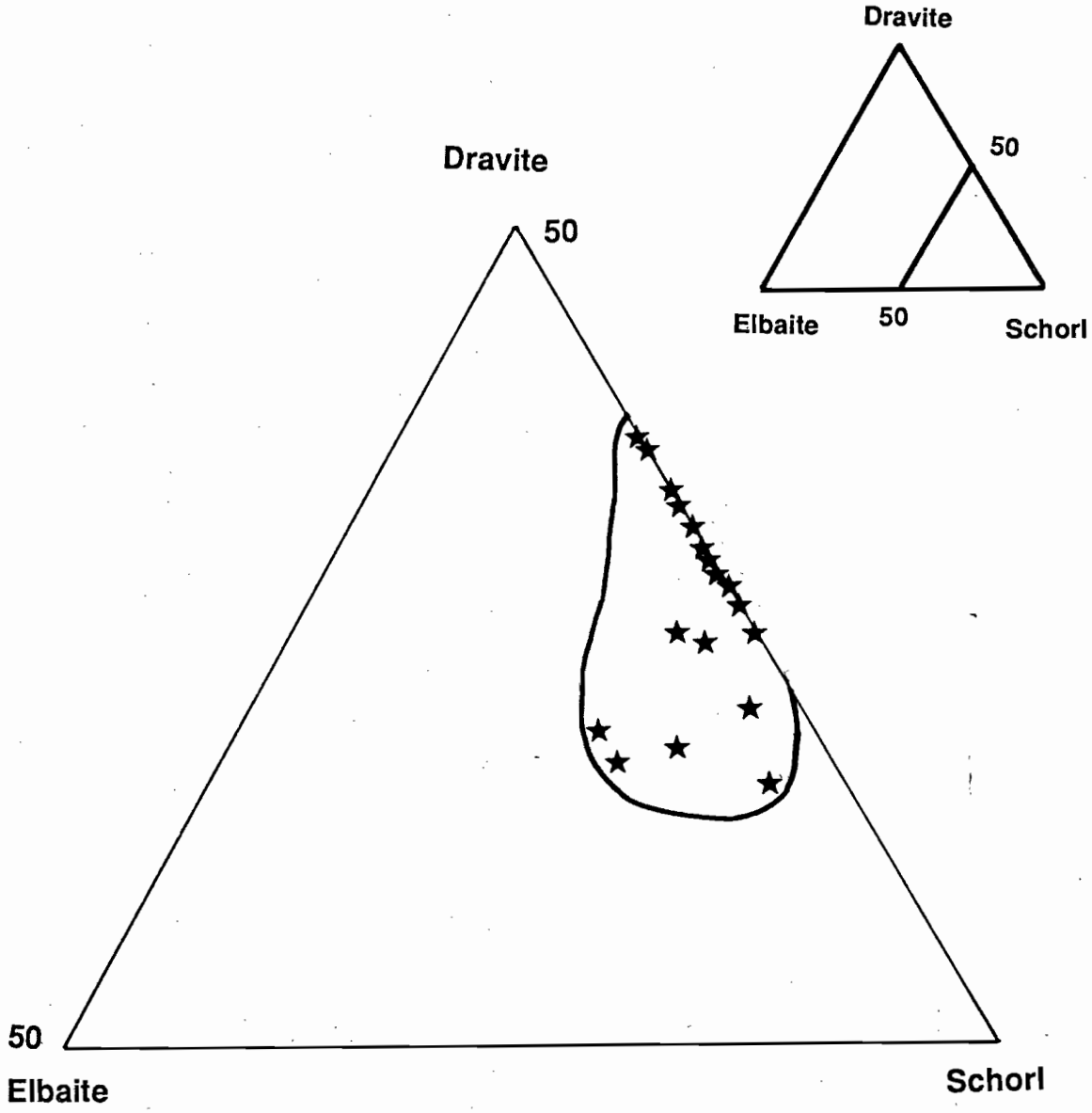

Fig. 9. compositional variation of tourmalines from 'F' lens, south-end orebody, Rosebery Mine

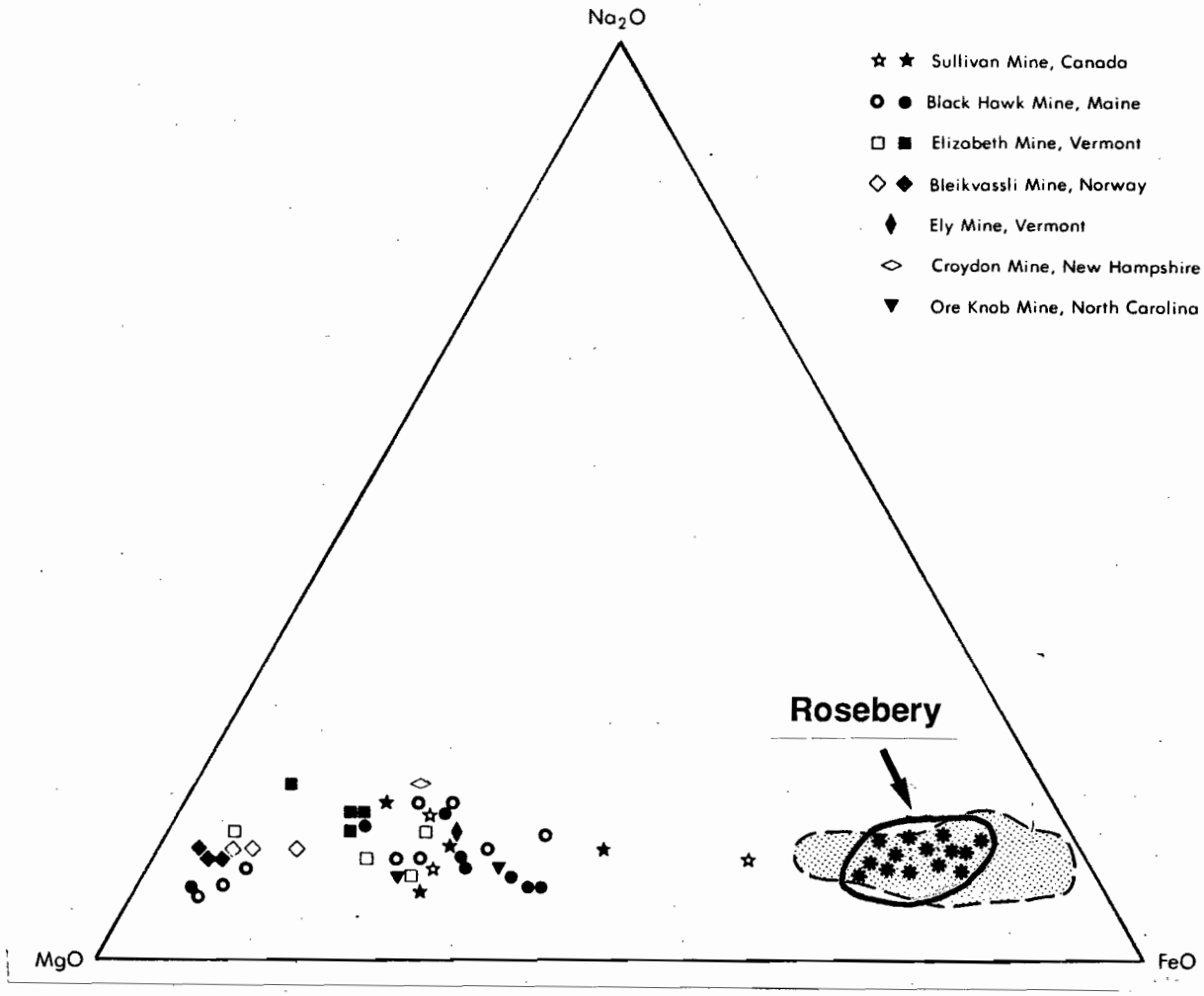

Fig. 10. Composition of tourmalines from 'F' lens, south-end orebody, Rosebery Mine together with average chemical compositions of tourmalinites from selected strata-bound sulfide deposits (solid and open symbols) and tourmalines from granites, pegmatites and aplites (shaded patterns). Data after Slack (1982).

event. Part of the main objectives of this research is to investigate the precious metal distribution in different replacement zones.

Present core logging and plotting of assay data indicate that gold was apparently dissolved out of Pb-Zn sulphide lenses and reprecipitated in the massive pyrrhotite-pyrite zone during replacement. Figure 11 shows the distribution of development assay gold grades on the 16 No. 1 Sub-Level plan and it can be seen that gold values are high in the replacement pyrrhotite-pyrite bodies.

Similarly, Figures 12-14 shows distribution of gold grades on E-W X-sections 300mS, 270mS, and 220mS. It is clearly indicated that gold is significantly low in the lower and deeper magnetite (hematite)-biotite zones (<5 g/t) whereas gold grades are visually increased in the pyrrhotite-pyrite zones (up to 29.4 g/t). The Pb-Zn sulphide lenses contain considerable gold values but generally less than (15) g/t.

Hence, it is apparent that Au has been dissolved out of primary Pb-Zn sulphide lenses and reprecipitated in the pyrrhotite-pyrite zones during the later replacement event. Tourmaline-quartz zones gave generally low gold grades (<3 g/t) but very erratic in places and sometimes up to (9.0) g/t gold grades are noted.

Future work

- further petrographic and mineragraphic studies of the collected samples to demonstrate precious mineral mineralogy and paragenesis.

- further electron microprobe analyses to determine the compositional variation of ore and gangue minerals.

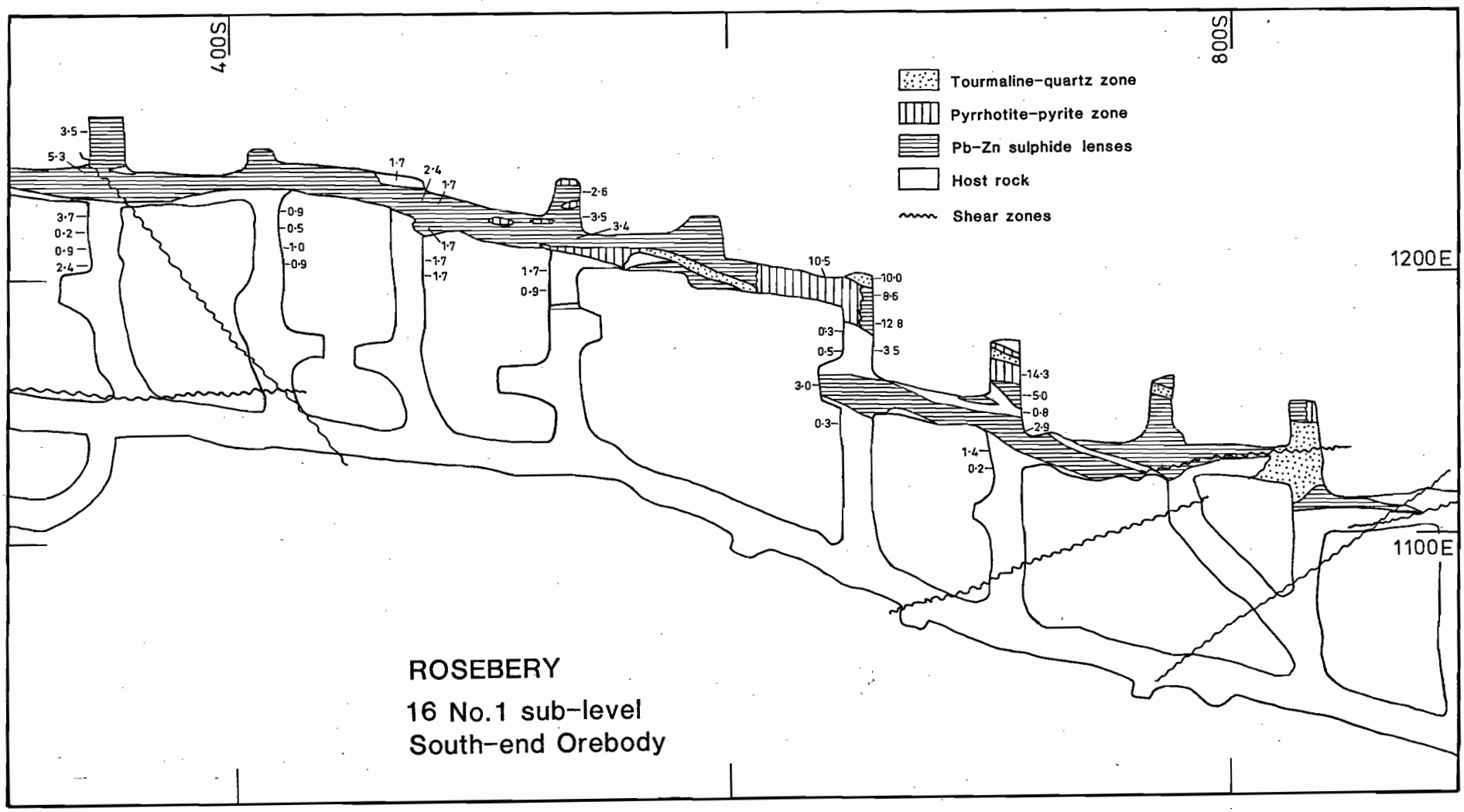

Fig. 11. Geological plan map of part of 16 No. 1 Sub-Level showing Fe-S-O assemblages replacing Pb-Zn sulfide lenses together with development assay data for gold (g/t). Note up to 14.3 g/t Au in po-py zone.

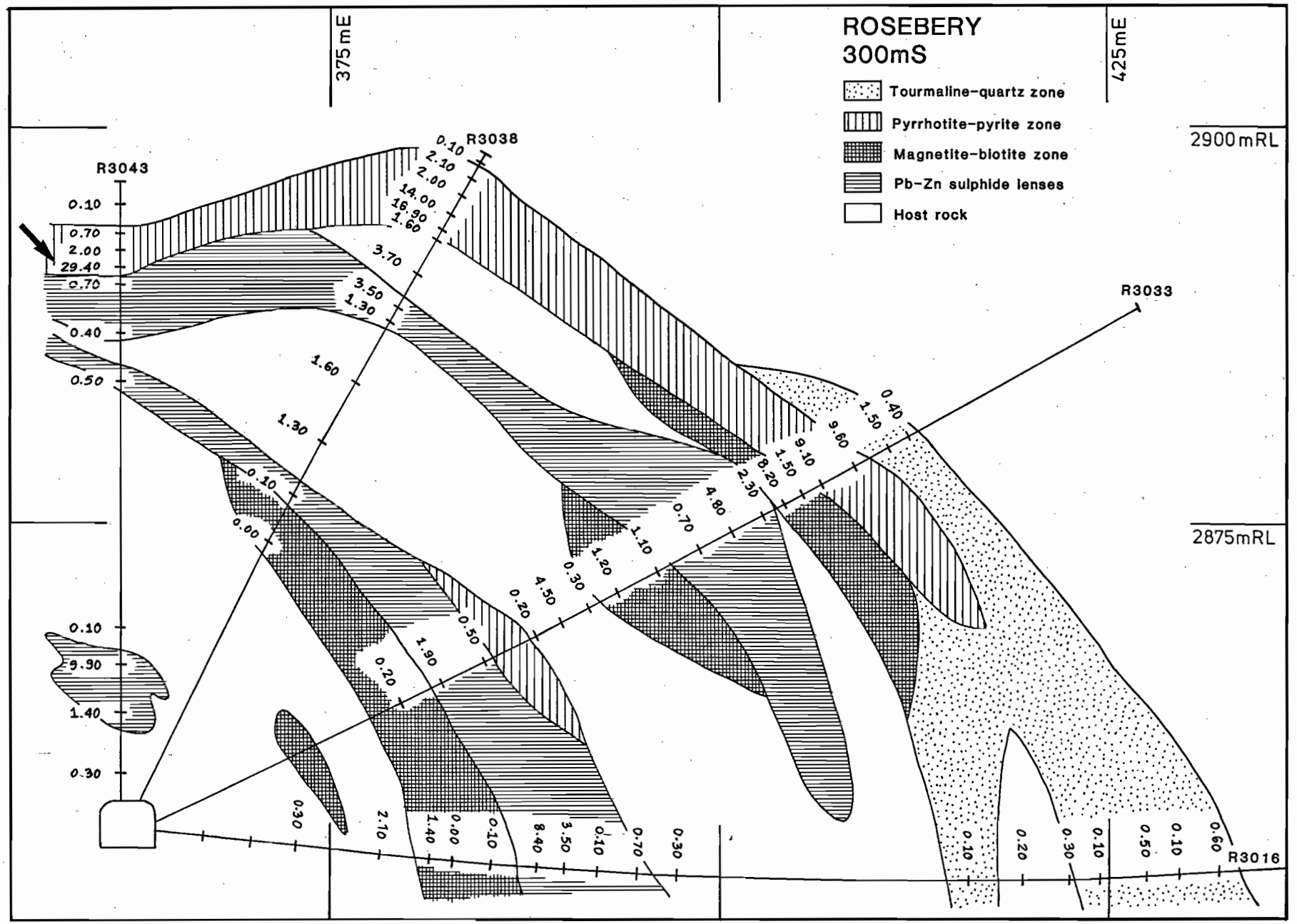

Fig. 12. Distribution of assay data for gold (g/t) in different replacement zones and Pb-Zn sulfide lenses. Note up to 29.40 g/t Au in po-py zone.

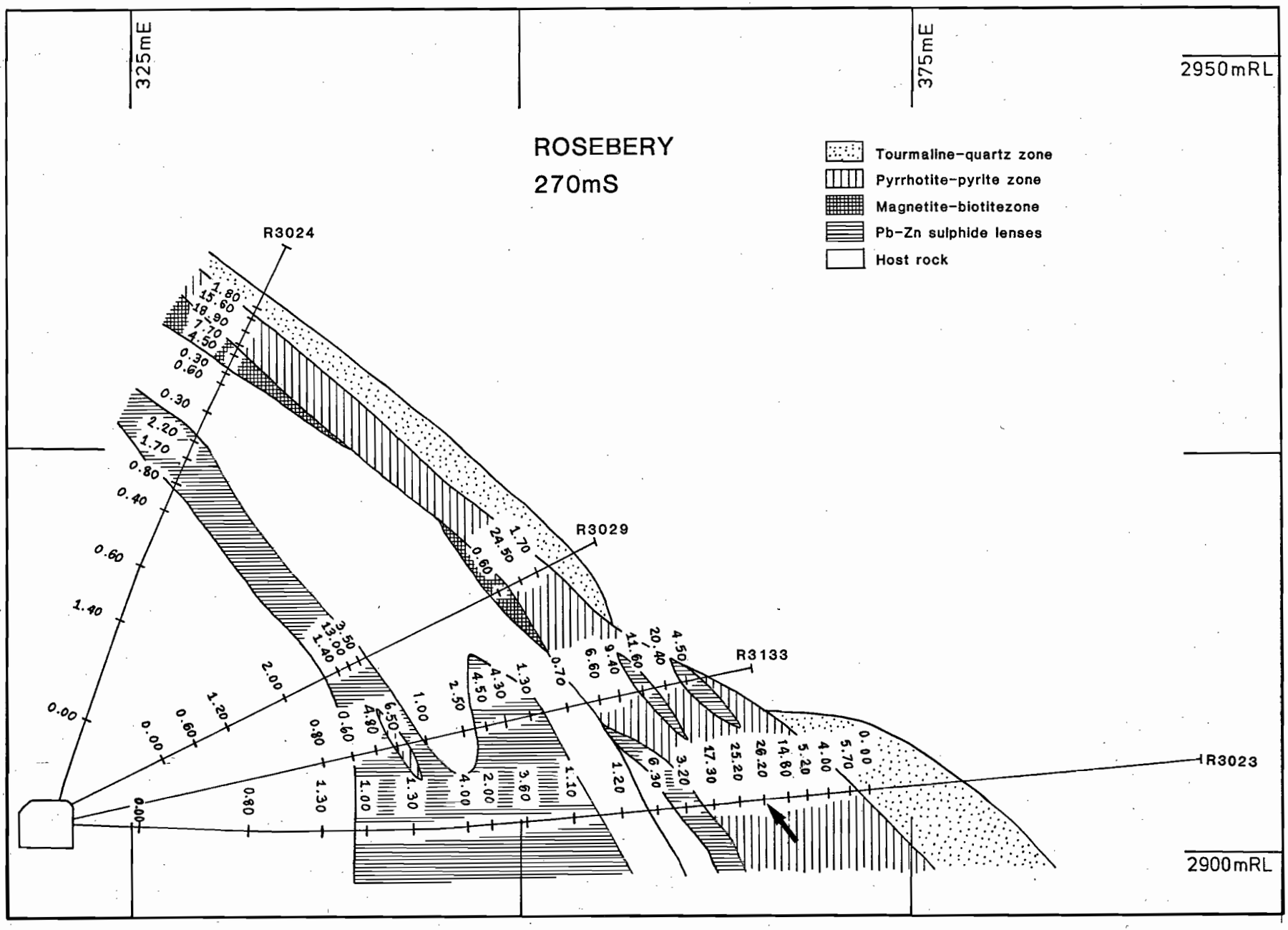

Fig. 13. Distribution of assay data for gold (g/t) in different replacement zones and Pb-Zn sulfide lenses. Note up to 26.20 g/t Au in po-py zone.

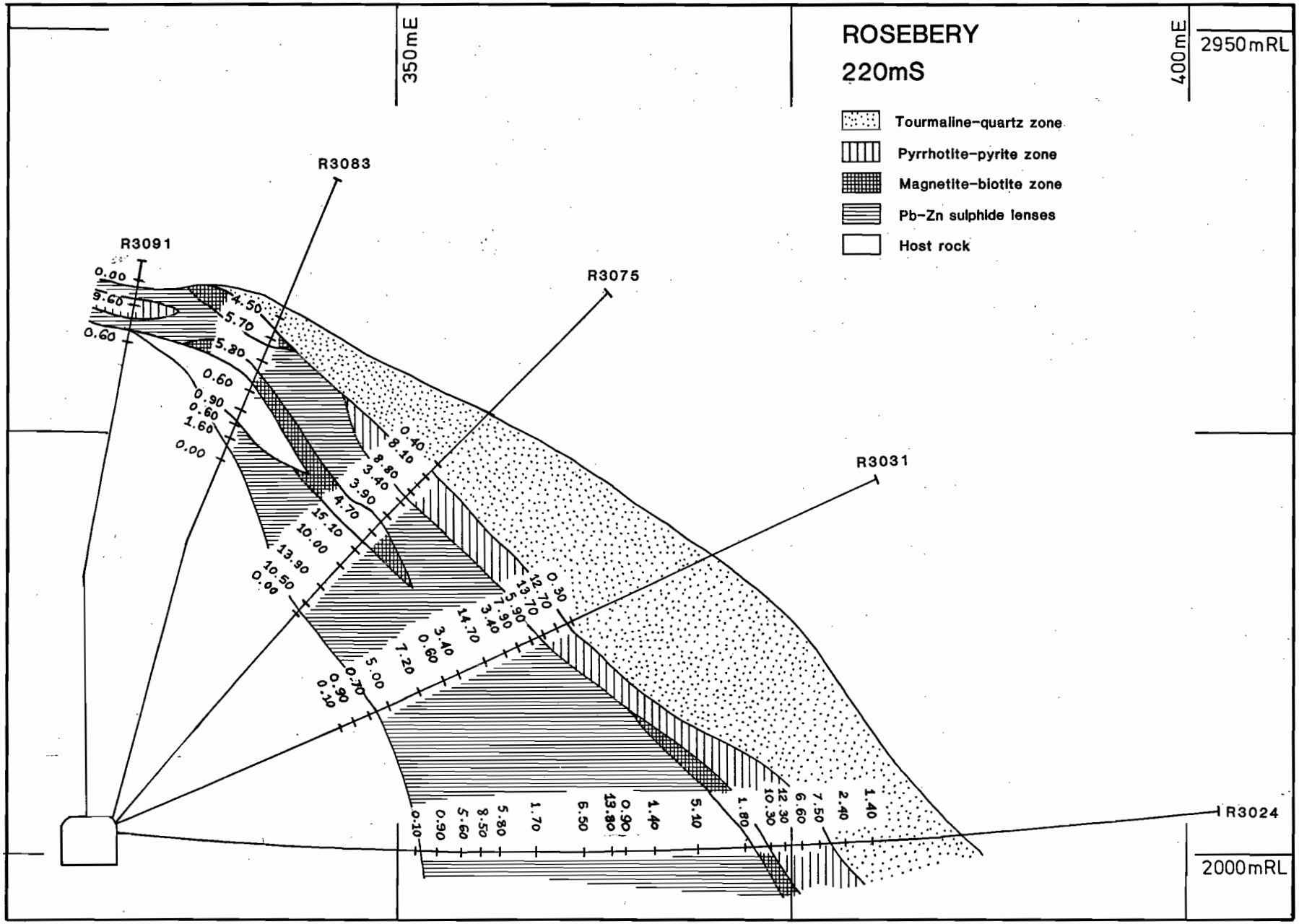

Fig. 14. Distribution of assay data for gold (g/t) in different replacement zones and Pb-Zn sulfide lenses.

- stable isotopes (O, H) and fluid inclusion studies together with Laser Raman and Infra Red Spectroscopy and Thermodecrepitation mass-spectrometry to deduce temperature, salinity, f_{O2}, pH, ΣS and gaseous composition of the ore-forming fluids during the replacement process and also to investigate the mechanism of precious metal mobilisation and precipitation.

ACKOWLEDGEMENTS

The author would like to thank Dr. Ross Large who introduced me to this project and for reading this report. The author is indebted to Dr. P. McGoldrick, Dr. P. Ruxton, D. Huston, Dr. W. Barth and S. Hunns for stimulating discussions. Special thanks are due to geologists at the Rosebery Mine: G. Iliff, J. Howarth, J. Farquar, T. Lees, I. Gordon, I. Matheson and P. Rice for logistical support and discussing the ideas presented in this report.

REFERENCES

Barth, H., 1986, Geology of the Cleveland Tin Mine, Tasmania, Australia with special reference to mineral chemistry and rare earth distribution: Unpub. Ph. D. thesis, University of Heidelberg.

Bean, R. E., 1974, Biotite stability in the porphyry copper environment: Econ. Geol., v. 69, p. 241-256.

Brathwaite, R. L., 1974, The geology and origin of the Rosebery ore delposits, Tasmania: Econ. Geol., v.69, p.1086-1101.

Deer, W. A.., Howie, R. A., and Zussman, J., 1962, Rock-Forming Minerals. 3. Sheet Silicates. Loongman, London.

Green, G., Solomon, M., and Walshe, J. L., 1981, The formation of volcanic-hosted massive sulphide ore deposit at Rosebery, Tasmania: Econ. Geol., v. 76, p. 304-338.

Jacobs, D. C., and Parry, W. T., 1976, A comparison of the geochemistry of biotite from some Basin and Range stocks, Econ. Geol., v. 71, p. 1029-1035.

Khin Zaw, 1976, The CanTung E-zone orebody, Tungsten, Northwest Territories: A major scheelite skarn deposit: Unpub. M.Sc. thesis, Queen's University, Kingston, Ontario.

Khin Zaw and Clark, A. H., 1978, Fluoride-hydroxyl ratios of skarn silicates, CanTung E-zone scheelite orebody, Tungsten, Northwest Territories: Canadian Mineralogist, v. 16, p. 207-221.

Lees, T., 1987, Geology and mineralization at Rosebery-Hercules area, Unpub. M.Sc. thesis, University of Tasmania.

Slack, J. F., 1982, Tourmaline in Appalachian-Caledonian massive sulphide deposits and its exploration significance: Inst. Mining Metallurgy Trans: v.91, sec B, p. B81-B89.

Stillwell, F. L., 1934, Observations on the Lead-zinc ore at Rosebery, Tasmania: Australian Inst. Mining Metallurgy Proc., No. 94, p. 43-67.

Solomon, M., Vokes, F. M., Walshe, J. L., 1987, Chemical remobilization of volcanic-hosted sulphide deposits at Rosebery and Mt. Lyell, Tasmania: Ore Geol. Review, No. 2, p. 173-190.

Taylor, B. E., and Slack, J. F., 1984, Tourmalines from Appalachian-Caledonian massive sulphide deposits: textural, chemical, and isotopic relationships: Econ. Geol., v. 79, p. 1703-1726.

SUMMARY OF WORK COMPLETED TO DATE ON THE MINERALIZATION IN THE TYNDALL GROUP - THE LAKE SELINA PROSPECT.

Steven R. Hunns

AMIRA Report
August 1987

SUMMARY OF WORK COMPLETED TO DATE ON THE MINERALIZATION IN THE TYNDALL GROUP - THE LAKE SELINA PROSPECT

By Steven R. Hunns

INTRODUCTION

The Lake Selina prospect is a large "'barren" pyrite mineralized hydrothermal system. Dispersed pyrite and magnetite with minor basemetal values occur throughout the Selina Volcanics, but are concentrated into two linear parallel zones; the 3.5 km long Eastern Pyrite Zone and the 4 km long Western Pyrite Zone. To date 13 diamond drill holes have intersected these two zones. The Selina Volcanic Belt extends for 10 km from the Murchison Granite in the north and to Lake Dora to the south and averages 1.5 km in width.

LOCAL GEOLOGY

The local geology is dominated by the Selina Volcanics. The Selina Volcanics are a sequence of steeply dipping broadly west facing epiclastics and or pyroclastics, crytstal tuffs, intrusive quartz, plagioclase, mafic rhyo-dacitic porphyries, minor lavas, and sediments. Conformably underlying the Selina Volcanics are the Sticht Range Beds, which are a sedimentary sequence of black shales, pebbly conglomerates, sandstones and siltstones. The Sticht Range Beds lie unconformably on the the Precambrian basement immediately to the east. Disconformably overlying the Selina Volcanics is the Dora Conglomerate. The

Selina Volcanics west of the Gold Fields exploration road are in faulted contact with the Ordovician Owen Conglomerate. South of Mount Selina the Selina Volcanics are covered by the Quarternary Rollerston Moraine up to 200m thick, and to the north by fluvio-glacials (Bowden 1974).

DIAMOND DRILL ASSAY INTERPRETATION

The diamond drill hole assays (Cu, Pb, and Zn) for Lake Selina have been plotted, both for the individual drill holes and also collectively. These illustrate the low levels of basemetal mineralization within the Lake Selina Prospect. Basemetal values fall within the following ranges. Cu has a range of between 10 - 7200ppm, Pb 10 - 1150ppm and Zn 10 - 10,600ppm.

The zinc number of Huston & Large (*in press*) was applied to the Lake Selina Sulphide System, in order to determine if there are any affinities between the Lake Selina Sulphide System and Tasmanian Volcanogenic Massive Sulphide Systems, or other deposit styles. For Lake Selina a cutoff of 150ppm Pb was used to determine the zinc number. This cutoff value was selected so as to eliminate any analytical errors and possible contamination. The volcanogenic massive sulphides of western Tasmania have a restricted zinc number mean values of between 64-77 and low standard deviations (<15), e.g. Rosebery 71.99 and 11.83 respectively. Whilst the Lake Selina Sulphide System has a mean zinc number of 55.5 and a standard deviation of 22.4.

STRUCTURE

The structure of the Lake Selina Prospect is poorly understood at this stage. There are two major contributing factors for this poor understanding. Firstly is the lack of outcrop, and the discontinuous nature of any outcrops, so that contact

relationships are not readily mappable in the field. Secondly, the Selina Volcanics have been extensivley altered and more importantly strongly deformed, so that any primary structures have almost been totally destroyed. Bedding was not noted in the Selina Volcanics in the field, but tenative observations in drill-core give a facing towards the west. Mapping by McKibben in 1972 and subsequently confirmed by the author recorded uniformly westerly dips and facings in the Sticht Range Beds to the east. Two dominant cleavages were noted in the field and trend approximately NNW and dip steeply to the west and east. These cleavages impart a strong schistosity to the volcaniclastics. Hutton (1982) inferred that the Dora Conglomerate on Mt. Selina occupies the core of a north plunging syncline based on stratigraphic evidence and E-W foliations to the east of Mt. Selina. It is now considered that the Dora Conglomerate occupies the core of an anticline based upon poles to cleavage contour plot for the Selina Volcanics . A major NNW trending fault "The Anthony Fault" (Hunns 1986), forms the contact between the Owen Conglomerate to the west and the the Selina Volcanics to the east. Also a number of later E-W trending faults were mapped and inferred in the Lake Selina Prospect. At least one and possibly two significant mylonites were mapped. The first being related to the Anthony Fault and the second to the east of the Eastern Pyrite Zone.

SULPHIDE and OXIDE MINERALOGY

Base metal sulphides within the Lake Selina Sulphide Zone are not present in significant amounts (i.e. economic importance). The most common sulphide is pyrite, followed by chalcopyrite, sphalerite and galena. Minor sulphides include molybdenite, covellite (after chalcopyrite), arsenopyrite and pyrrhotite. The most dominant oxide phase is magnetite, then haematite, (either as a primary assemblage or as an alteration product of magnetite) and rutile. For some samples

a paragenetic sequence of mineralization was difficult to obtain due to the strong deformation overprint of the rocks.

Four paragenetic sequences were deduced from thin sections:

1). Magnetite, pyrite ± chalcopyrite assemblages. This assemblage is probably reflecting high fluid temperatures, i.e. $T^{o} \geq 300^{o}C$.

2). Sphalerite, chalcopyrite and galena assemblages, reflecting lower fluid temperatures, i.e. $T^{o} \leq 250^{o}C$.

3). Sphalerite ±chalcopyrite ±galena mineralization associated with quartz, carbonate ±chlorite veins.

4). Remobilization and recrystallization of sphalerite, chalcopyrite and galena during the Tabberabberan Orogeny.

ALTERATION TYPES and RELATION to MINERALIZATION

The major alteration assemblages of the Lake Selina Sulphide System were discussed in Hunns (1986). Further work over the last year has reinforced these initial observations. These are summarised below. Two extra alteration assemblages can now be added.These are 1): silica-K-spar ±pyrite and 2): silica-pyrite assemblage. These two assemblages occur within the chlorite zone. In thin section the quartz is recrystallized and crypto-crystalline in nature and is apparently replacing the earlier fine grained K-spar. The pyrite apperas to have come in with the silica, but more detailed petrographic work needs to be done to either confirm this or not.

1). K-feldspar Zone:- dominated by very fine grained to coarse grained K-spar. This alteration assemblage is altered pervasively by later chlorite.

2). Chlorite Zone:- Occurs from total replacement of the host volcanic to more subtle pervasive alteration.

3). Sericite/Quartz Zone:- Largest of the alteration zones, and the sericite occurs throughout the groundmass of the epiclastics.

The major alteration minerals present at Lake Selina are chlorite, K-spar, sericite, quartz, magnetite, pyrite, haematite, rutile, calcite and/or dolomite, muscovite, epidote and apatite.

DISCUSSION and FUTURE WORK

The origin of the Lake Selina Sulphide System is still considered to be genetically related to the altered Murchison Granite equivalent that outcrops through the volcanics. As the granite is exposed tens of metres below the base of the Dora Conglomerate it is considered to be a high level intrusive granite. A speculative model for the origin of the Lake Selina Sulphide System is now proposed.

1). Sedimentary basin "Selina Basin", bounded to east by the Precambrian Tyennan Nucleus. Starts to be infilled by the alluvial to shallow marine Sticht Range Beds, with material being derived from the Precambian basement.

2). Input of epiclastics and minor lavas from a distant source i.e. outside the Selina Basin. The epiclastics may have overlapped onto the Precambrian basement. Possibly even with further reworking of the introduced epiclastics and lavas.

3). Intrusion of the core rhyo-dacitic porphyry into the epiclastic sequence. Possibly related to the initial activation of the Anthony Fault. Subsequent high level intrusion of the Murchison Granite equivalent. Related mineralization and alteration (K-spar-chlorite and later pyrite and sericite) was centered along the contact between the porphyry and the epiclastics. Associated with the granite intrusion were the intrusion of more quartz, feldspar, mafic rhyo-dacitic porphyries. Deeper level intrusive of the Murchison Granite caused hornfelsing, of the sediments and 'tuffs'.

4). Further uplift along the Anthony Fault and possibly the Precambrian basement, which produced a narrow basin, into which the Dora Conglomerate was deposited as a mass flow unit. Possibly with contributions of material from the northwest and the eroded epiclastics and pyroclastics initially deposited onto the Precambrian.

5). Deposition of the Ordovician Owen Conglomerate over the Selina Volcanics.

6). Re-activation of the Anthony Fault during the Tabberabberan Orogeny and the subsequent intense deformation and folding of the Selina Volcanics, and the remobilization of chalcopyrite, sphalerite and galena into pressure shadows growing off pyrite grains. Possible fault induced shear in the pyritic epiclastics and sediments of DDH LS10.

Future Work

Future work that is planned for the Lake Selina Sulphide System is listed below.

1). Sulphur isotopes on pyrite and other suphide phases if possible. Solomon *et.al* . (in prep) have four analyses from Lake Selina, and these give a magmatic signature. Four samples are not considered to statistically significant, and further analyses are required.

2). Oxygen and hydrogen isotopes on carbonates, quartz and chlorites, and possibly some geochemistry on the chlorites. These will help to give an idea on the origin and temperature of the mineralizing and alteration fluids.

3). On going petrography, whole rock, trace element and rare earth geochemistry, to better define the origin of the Selina Volcanics, and the nature of the alteration.

References

Bowden A. R. (1974). The Glacial Geomorphology of the Tyndall Mountains, Western Tasmania: Unpubl B.Sc(Hons) Thesis, Dept. of Geog. Univ. of Tas.

Hunns S. R. (1986). Lake Selina Prospect : AMIRA Progress Report, November 1986.

Hutton M. J. (1982). Annual eport. E.L.9/66 : The Mt. Lyell Mining and Railway Co. Ltd.

Huston D. & Large R. R. (in press). Genetic and Exploration Significance of the Zinc Number in Massive Sulfide Systems : Econ. Geol.

McKibben (1972); in Purvis *et.al.* (1983): A Geological Review of the Tyndall Exploration Licence 9/66. Western Tasmania. Unpubl. Internal Rept. to Gold Fields Exploration Pty. Ltd.

PROGRESS REPORT ON THE PETROLOGY, GEOCHEMISTRY AND TECTONIC IMPLICATIONS OF THE MOUNT READ VOLCANICS

Anthony J. Crawford

AMIRA Report
August 1987

Introduction

In the April 1986 AMIRA Progress Report for this research group (84/P210), I reported preliminary results of a detailed geochemical study of the Mount Read Volcanics (MRV). The core of that report was the presentation of approximately 100 analyses of least-altered lavas and shallow intrusives, carefully selected to represent the petrographic (basalt to ryholite), stratigraphic and geographic range of the MRV. A further twenty analyses have been added to the suite studied; these are mainly of lavas from the Tyndall Group, which was poorly represented in the original data set.

The primary aims of this study are four-fold:

1: to determine the primary geochemical range and magmatic affinities of the MRV,

2: to determine their tectonic setting of eruption,

3: to use detailed geochemical studies of lavas, especially trace element "fingerprinting", to aid in stratigraphic correlation of lavas and intrusives within the MRV, and

4: to use these 'best estimates' of the primary geochemistry of the MRV to assess directions and amounts of element mobility accompanying mineralization-related alteration.

Here, I address the first three of these aims. To aid the discussion and interpretation of data, the analyses presented 'en masse' in the April 1986 AMIRA Report are herein listed according to their stratigraphic occurrence (Central Volcanic Complex, Western Volcanic Sequence or Tyndall Group). In addition, approximately 40 representative lavas have been analyzed for rare earth elements (REE) using a method developed in this Department (Robinson et al. 1986). These REE data have been very useful in interpreting the petrogenesis and tectonic significance of the MRV, as well as in aiding regional correlation within the MRV. All trace element ratios used in this report are based on data determined in the Geology Department XRF Laboratory.

The Mount Read Volcanics: Geological Considerations

The MRV form a continuous belt along the western and northern margins of the Tyennan Block, eventually disappearing beneath post-Palaeozoic sedimentary rocks and dolerite sheets in the vicinity of Quamby Brook. It is important to note, however, occurrences of volcanics petrographically and chemically closely similar to typical MRV at localities away from this main belt, specifically:-

1. as a fault-bounded slice several kilometers wide on Sorell Peninsula, where these lavas are known as the Noddy Creek Volcanics. Included in this belt are several little-known hornblende diorite-granodiorite plutons;
2. in the Beaconsfield area, where andesites, mafic-ultramafic complexes and possible Crimson Creek Formation correlates occur in adjacent fault slices;
3. in the Dial Range Trough, where the Lobster Creek Volcanics occupy a fault slice within a sequence which contains Rocky Cape Group, and Crimson Creek Formation and Dundas Group correlates (Burns 1964);
4. near Hobart, where cleaved high-Al basalts in a drillhole are chemically and petrographically like those in the main MRV belt in western Tasmania (Solomon & Griffiths 1974).

The MRV are an orogenic basalt-andesite-dacite-rhyolite suite with abundant interbedded pyroclastics, epiclastics and shale horizons. Recent systematic detailed mapping (Corbett 1979; Corbett 1986; Komyshan 1986; McNeil 1986; Corbett & Lees 1987) has clarified important geological relationships within the belt. While the Tyndall and Dundas Groups both clearly overlie volcanics of the Central Volcanic Complex, Corbett (1979) considered that since the Western Sequence apparently dips beneath the Central Volcanic Complex, it is likely to be older than the latter (Fig. 1). However, detailed geochemical studies of Western Sequence lavas, and a reconsideration of the regional geology of the area S and W of Queenstown, indicate that Corbett's Western Sequence is almost certainly equivalent to the basal Dundas Group of the Que-Hellyer-Boco district (see later). This suggests that the Central Volcanic Complex in the area south and west of Queenstown may have been thrust westward over flanking, younger Western Sequence rocks. This postulated fault may be a southern analogue of the east-dipping Rosebery Fault, which juxtaposes Dundas Group rocks with overthrust but older Central Volcanic Complex in the Rosebery area (Corbett & Lees 1987).

A significant finding of geological mapping of the MRV by Corbett and others has been the discovery of a belt of tholeiitic lavas outcropping in the core of an anticline within the Western Sequence at Miners Ridge, SW of Queenstown (Corbett 1979), and in the western part of the block sandwiched between the north and south Henty Faults (known as the Henty Fault wedge). These lavas are most unlike the high-K calc-alkaline MRV, and their nature and existence must be taken into account in any comprehensive attempt to model the tectonic development of western Tasmania. Geochemical data presented further on indicate that these tholeiitic lavas are compositionally closely similar to the uppermost lavas in the MUC at Serpentine Hill, which interdigitate with basal Dundas Group sediments (Brown 1986). On the basis of these observations, I suggest the following revision of the stratigraphy of the MRV, which is believed to be consistent with all available geological and geochemical constraints. The Western Volcanic Sequence NW and SW of Queenstown is a correlate of the Que-Hellyer sequence; at Miners Ridge the Western Volcanic Sequence appears to overlie depleted tholeiites like those in the upper levels of the Serpentine Hill MUC. Therefore, important points to note regarding the stratigraphy of the MRV are that :

1. the Central Volcanic Complex is nowhere seen in contact with older (basement) rocks;
2. tholeiitic lavas of the western Henty Fault wedge and Miners Ridge, which apparently form basement to the Western Volcanic Sequence, are correlates of the uppermost lavas in the Serpentine Hill Mafic-Ultramafic Complex (MUC) further northwest;
3. the Western Volcano-Sedimentary Sequence of Corbett (1979), formerly considered to dip beneath, and therefore be older than, the Central Volcanic Complex, is here shown to be a correlate of the Que-Hellyer sequence assigned by Corbett and Lees (1987) to the base of the Dundas Group. We refer to this lava-dominated sequence along the western margin of the MRV as the Western Volcanic Sequence, and reserve

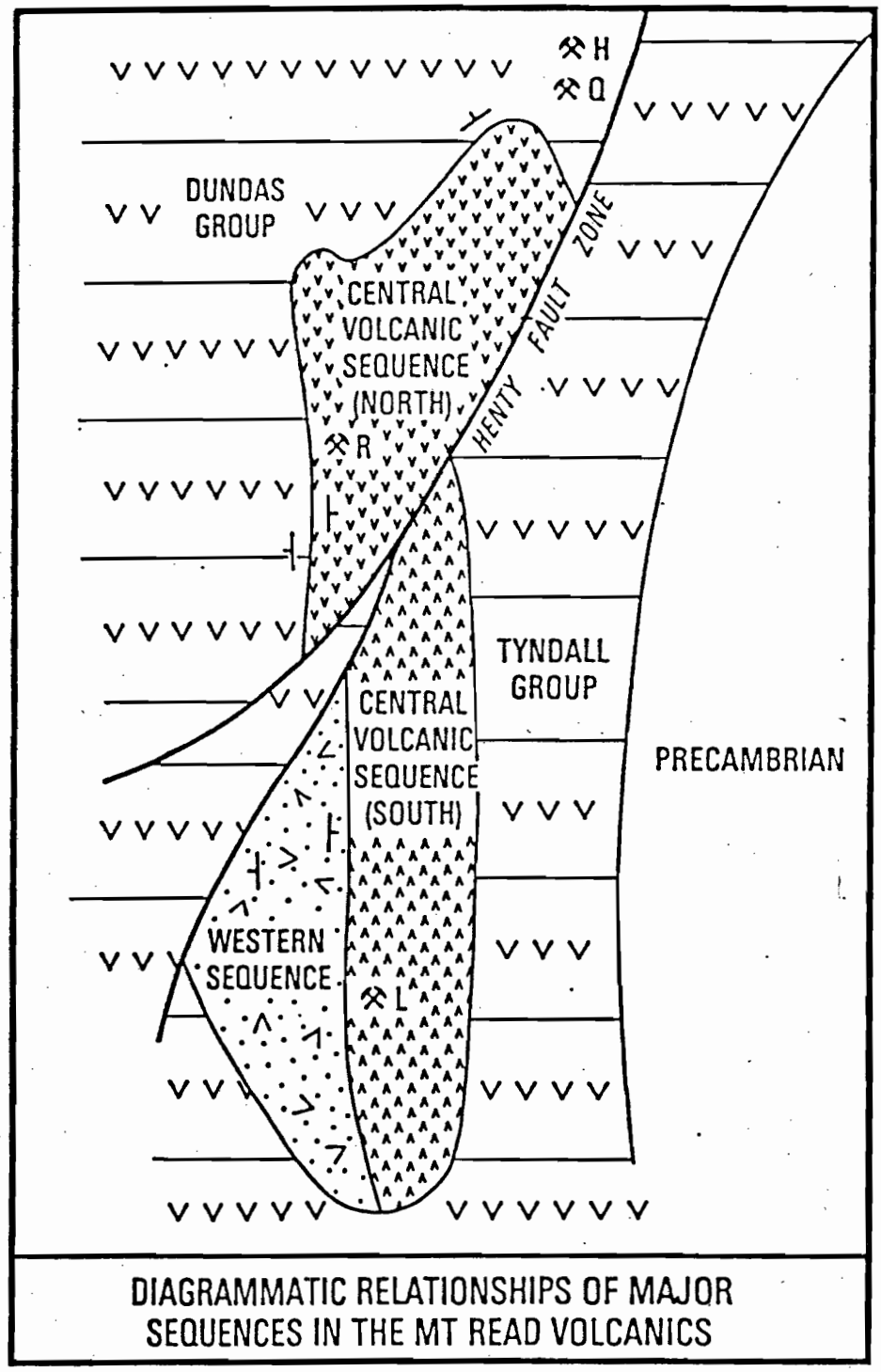

FIGURE 1: Diagrammatic representation of the geology of the Mount Read Volcanics south of the Henty Fault Zone (Area 2 of this report). From Corbett (1986).

the term Dundas Group for the sediment-dominated sequence stratigraphically above the Western Volcanic Sequence. Late Middle Cambrian fossils occur in the Que River Shale at the base of the Dundas Group.

4. the contact between the Western Volcanic Sequence and the Central Volcanic Complex is poorly known, but from evidence in the area north of Mount Charter, Corbett (1986) and Komyshan (1986) considered this contact to be a faulted unconformity at which the Western Volcanic Sequence overlies the Central Volcanic Complex.
5. the Tyndall Group (type formation is the Comstock Tuff) only occurs south and west of the Henty Fault system. It conformably overlies both the Western Volcanic Sequence and the Central Volcanic Complex in the Queenstown area (Corbett 1979), and contains late Middle Cambrian fossils in its lower part. It is mainly younger than the Western Volcanic Sequence, and overlaps onto the Tyennan Block in several places.

Geochemistry of the Mount Read Volcanics and Related Rocks

1. The Central Volcanic Complex.

South of the Henty Fault Zone the Central Volcanic Complex is dominated by plag-phyric dacitic and rhyolitic lavas and pyroclastics intruded by bodies of hbd+plag-phyric andesite (Crown Hill, Leech Hill) and pyx+plag-phyric andesite (Queenstown Reservoir, south of Little Owen); extrusive andesites are rare. The dacitic and rhyolitic lavas are extensively altered to pink Kfels- and sericite-rich lithologies and subordinate green chlorite-rich rocks. Although the intense alteration of the latter lavas precludes them from consideration amongst the "least-altered" MRV lavas on which this study is based, one pink K-rich rhyolite (JD6) has been analyzed for REE to compare with less altered rhyolites from elsewhere in the MRV.

North of the Henty Fault Zone, apparently extrusive andesites are more abundant than further south, but dacitic to rhyolitic lithologies still predominate. *Importantly, no basaltic lavas are known from the Central Volcanic Complex, either N or S of the Henty Fault Zone.*

Wholerock analyses of Central Volcanic Complex lavas are given in Tables 1 (andesites; 56-66% SiO_2), 2 (dacites; 66-70% SiO_2) and 3 (rhyolites; >70% SiO_2).

Andesites range from mafic pyx-phyric varieties to more evolved hbd+plag-phyric lavas which dominate exposures of the Central Volcanic Sequence in the belt between Queenstown and the Henty Fault just south of Mt. Read. The very similar Ti/Zr (16 - 21), Zr/Nb (17 - 21), V/Sc (6.3 - 7.6) and Zr/Y (4.8 - 7.0) ratios (Table 1) of these lavas suggest thet they are essentially comagmatic. REE data (Fig. 2) support this contention; the $(La/Sm)_N$ (chondrite-normalized) ratios normally increase with increasing fractionation in orogenic basalt-andesite-dacite suites. For MRV mafic pyx-phyric andesite 39233, $(La/Sm)_N$ is 3.00, while for the hbd-andesites this ratio ranges from 4.4 to 6.0. The K/Rb ratio for many of the andesites from south of the Henty Fault Zone fall between 269 and 321, almost certainly reflecting the range of primary values for the suite.

TABLE 1: Wholerock XRF analyses of andesites from the Central Volcanic Complex of the Mount Read Volcanics: M189 to 32522 are from south of the Henty Fault; the remaining samples are from north of the Henty Fault System. Mines Dept. analyses are marked by an asterisk. REE data for representative samples are given below.

SAMPLE	M189	32522	M235	HR71	Z632	AR6	3399	3402	39233	W93	39232	32522	MR396*	MR654*	44078
SiO2	58.8	58.9	63.3	63.8	60.9	58.45	59.5	63.1	58.5	58.7	58.8	58.9	60.1	63.88	61.4
TiO2	0.48	0.53	0.42	0.40	0.49	0.46	0.45	0.42	0.56	0.55	0.57	0.53	0.69	0.63	0.68
Al2O3	15.9	15	14.7	15	14.3	16.02	15.50	14.90	14.2	14.2	14.4	15	17.04	16.15	16.30
Fe2O3	7.65	8.99	7.42	6.38	7.29	7.41	7.26	6.79	8.11	7.9	7.83	8.99	5.97	5.96	7.37
MnO	0.21	0.14	0.16	0.07	0.13	0.11	0.13	0.11	0.13	0.12	0.12	0.14	0.12	0.11	0.13
MgO	4.37	4.62	3.45	3.2	4.84	4.37	4.53	3.39	6.75	6.19	5.24	4.62	1.57	2.59	3.35
CaO	6.35	6.62	4.51	4.96	6.29	6.26	5.45	5.75	5.18	5.05	5.62	6.62	9.58	3.86	4.61
Na2O	4.4	3.24	4.05	3.64	4.07	6.75	5.36	2.55	4.76	3.97	4.24	3.24	3.52	4.23	4.03
K2O	1.59	1.57	1.77	2.32	1.39	0.37	1.56	2.77	1.61	3.15	2.97	1.57	0.85	2.24	1.88
P2O5	0.21	0.34	0.19	0.2	0.32	0.33	0.25	0.17	0.2	0.2	0.22	0.34	0.15	0.15	0.15
TOTAL	100	100	100	100	100	100	100	100	100	100	100	100	100	100	100
LOI	1.81	1.81	2.96	1.72	1.94	1.65	2.03	3.62	2.11	1.65	1.85	1.81	2.06	3.42	2.42
Ni	15	47	25	24	39	40	38	32	53	52	49	47	10	3	22
Cr	68	321	40	59	130	142	139	72	224	157	160	321	145	60	81
V	181	198	172	157	175	206	184	155	196	188	201	198	145	140	161
Sc	27	28	24	22	25	27	29	22	30	30	31	28	13	13	22
Zr	144	157	150	138	169	160		133	159	181	167	157	210	220	133
Nb	8.4	9	7.8	7.6	8	8		7	8	10	9	9	11	10	10
Y	25	26	26	21	24	23		21	27	28.5	35	26	33	28	31
Sr	716	682	418	488	683	516		620	363	354	262	682	390	200	465
Rb	49	65	52	70	42	14		74	53	93	85	65	27	89	48
Ba	1403	1067	2720	773	1184	188	1143	1148	572	1160	1068	1067	200	530	664
Cu	40	67	70	14	77		144	18	16	18	60	67	10	13	40
Pb	6	11	17	6	3		5	5	19	6	10	11	23	8	8
Zn	277	90	62	22	69		66	31	86	48	71	90	1750	47	62
Ti/Zr	19.98	20.24	16.79	17.38	17.38	17.24		18.93	21.11	18.22	20.46	20.24	19.70	17.17	30.65
Zr/Y	5.76	6.04	5.77	6.57	7.04	6.96		6.33	5.89	6.35	4.77	6.04	6.36	7.86	4.29
Zr/Nb	17.14	17.44	19.23	18.16	21.13	20.00		19.00	19.88	18.10	18.56	17.44	19.09	22.00	13.30
V/Sc	6.70	7.07	7.17	7.14	7.00	7.63	6.34	7.05	6.53	6.27	6.48	7.07	11.15	10.77	7.32
Zr/Sc	5.33	5.61	6.25	6.27	6.76	5.93	0.00	6.05	5.30	6.03	5.39	5.61	16.15	16.92	6.05
K/Rb	269	201	283	275	275	219		311	252	281	290	201	261	209	325

SAMPLE	La	Ce	Pr	Nd	Sm	Eu	Gd	Dy	Er	Yb
39233	40.7	87	10.9	41.1	8.26	1.97	6.32	4.49	2.99	2.73
M189	88.8	162	16.5	57.2	9.06	2.08	6.07	4.19	2.71	2.56
Z632	63.7	131	14.1	52.5	8.87	2.34	6.67	4.32	2.25	2.13
AR6	71.7	149	15	55	8.79	1.41	6.11	4.07	2.28	1.85

TABLE 2: Wholerock analyses of dacites from the Central Volcanic Complex of the Mount Read Volcanics, and a Lobster Ck. Volcanics dacite (Lob. Ck.).

	36113	40140A	44063	40140	44041	30039A	44067	LDP11A	44045	30039B	30050	HR70	HR65	Lob. Ck.
SiO2	65	65.5	65.5	65.7	66.5	66.6	67	67.1	67.2	67.8	69.8	67.6	66.6	68.5
TiO2	0.67	0.62	0.68	0.66	0.68	0.62	0.67	0.68	0.67	0.60	0.46	0.44	0.36	0.41
Al2O3	15.3	15.8	15.4	15.4	14.9	15.5	15.1	15	15	14.5	15.6	16.9	14.6	16.23
Fe2O3	6	5.92	5.83	5.57	5.72	5.11	4.84	5.24	5.52	4.85	3.86	6.76	4.98	4.59
MnO	0.08	0.1	0.07	0.07	0.11	0.09	0.08	0.1	0.09	0.07	0.04	0.02	0.11	0.04
MgO	2.37	1.94	1.74	1.71	1.88	1.08	0.94	1.98	2.01	0.88	1.23	3.43	2.66	1.34
CaO	3.17	3.71	3.36	3.12	2.96	2.33	3.29	2.04	1.91	6.99	0.69	0.1	2.3	0.18
Na2O	4.25	3.74	4.5	4.2	4.31	4.43	4.04	3.33	4.35	3.34	2.87	1.44	5.53	6.28
K2O	3.05	2.53	2.78	3.43	2.83	4.18	3.97	4.45	2.92	0.82	5.36	3.02	2.74	2.34
P2O5	0.13	0.12	0.12	0.14	0.14	0.12	0.13	0.13	0.27	0.13	0.1	0.23	0.19	0.08
TOTAL	100	100	100	100	100	100	100	100	100	100	100	100	100	100
LOI	2.3	2.23	1.67	1.52	1.44	0.95	1.89	1.28	1.49	1.56	1.44	4.28	1.26	1.97
Ni	6	4	5	4	4	5	5	3	4	5	3	24	17	2
Cr	23	9	23	12	13	12	23	9	12	15	7	64	52	<2
V	111	92	107	91	92	88	104	92	94	269	55	177	140	75
Sc	15	11	13	12	11	13	15	11	11	13	11	26		10
Zr	227	228	231	228	231	221	226	216	209	213	227	155	132	164
Nb	13	14	13	13	13	12	12	14	12	12.5	15	7.1	6.8	8
Y	37	40	39	37	37	39	39	34	34	35	30	27	23	44
Sr	191	204	264	182	184	188	218	182	172	435	156	94	1004	68
Rb	75	101	58	88	119	118	105	155	89	25	218	105	116	60
Ba	658	696	620	882	764	927	819	1099	860	218	1463	747		416
Cu	2	2	9	5	9	8	23	5	7	8	1	6	23	<2
Pb	9	8	10	4	5	4	5	5	5	7	6	14	5	4
Zn	69	57	49	32	63	39	35	53	55	17	65	112	89	29
Ti/Zr	17.69	16.30	17.65	17.35	17.65	16.82	17.77	18.87	19.22	16.89	12.15	17.02	16.35	15.00
Zr/Nb	17.46	16.29	17.77	17.54	17.77	18.42	18.83	15.43	17.42	17.04	15.13	21.83	19.41	20.50
Zr/Y	6.14	5.70	5.92	6.16	6.24	5.67	5.79	6.35	6.15	6.09	7.57	5.74	5.74	3.72
Zr/Sc	15.13	20.73	17.77	19.00	21.00	17.00	15.07	19.64	19.00	16.38	20.64	5.96		16.40
K/Rb	338	208	398	324	197	294	314	238	272	272	204	239	196	315

SAMPLE	La	Ce	Pr	Nd	Sm	Eu	Gd	Dy	Er	Yb
HR65	51.7	97.7	9.96	35.8	6.07	1.38	4.17	3.23	2.05	2.19
HR70	68.4	124	12.1	42.5	6.97	1.63	5.38	4.17	2.5	2.73
30039A	34	74.1	8.27	32.6	6.64	1.37	6.21	5.87	4.05	4.04
LPD11A	29.8	69.5	7.86	31.6	6.86	1.66	5.89	5.56	3.7	3.8

TABLE 3: Wholerock analyses of rhyolites from the Central Volcanic Complex, Mt. Read Volcs.

	30051A	40136	36117	LPD6	42610	HCL	JD6	MRDDH	PD1
SiO2	70.3	73.5	75.1	75.4	76.3	73.09	75.5	73.1	78.1
TiO2	0.45	0.27	0.29	0.23	0.23	0.39	0.23	0.38	0.26
Al2O3	15.2	13.9	12.9	14.5	13.8	15.45	12.58	14.57	12.57
Fe2O3	3.67	2.73	2.8	2.37	1.82	2.68	4.13	2.84	1.35
MnO	0.07	0.04	0.05	0.02	0.04	0.04	0.01	0.07	0.07
MgO	1.16	0.46	0.32	0.76	0.3	1.4	0.26	0.8	0.56
CaO	1.54	1.39	0.64	0.03	0.1	0.64	0.02	1.28	1.34
Na2O	2.93	3.29	2.82	2.81	4.32	4.2	0.08	2.4	2.09
K2O	4.52	4.34	5.05	3.87	2.99	2.09	7.2	4.55	3.19
P2O5	0.1	0.06	0.04	0.01	0.01	0.04	0.03	0.06	0.03
TOTAL	100	100	100	100	100	100	100	100	100
LOI	1.22	1.66	0.83	1.74	1.35	1.99	1.35	2.5	2.83
Ni	3	2	2	2	<2	<2	2	<2	<2
Cr	9	5	4	6	3	<2	<2	<2	<2
V	51	11	12	6	10	10	11	18	13
Sc	9	5	8	7	7	4	7	5	3
Zr	216	205	225	256	165	280	261	259	223
Nb	15	15	13	17	11	16	13	15	13
Y	36	40	45	35	27	40	45	40	29
Sr	238	153	134	52	120	248	29	98	61
Rb	169	134	133	114	76	104	206	216	140
Ba	1033	1093	987	808	1189	840	1620	839	750
Cu	9	2	2	3	4	12	4	3	8
Pb	7	14	3	4	57	4	14	10	4
Zn	31	14	19	31	57	66	27	42	21
Ti/Zr	12.49	7.90	7.73	5.39	8.36	8.35	5.28	8.80	6.99
Zr/Nb	14.40	13.67	17.31	15.06	15.00	17.50	20.08	17.27	17.15
Zr/Y	6.00	5.13	5.00	7.31	6.11	7.00	5.80	6.48	7.69
Zr/Sc	24.00	41.00	28.13	36.57	23.57	70.00	37.29	51.80	74.33
K/Rb	222	269	315	282	327	167	290	175	189

JD6: Jukes-Darwin Ridge
HCL: footwall ignimbrite from Hercules
MRDDH: Mount Read
PD1: Pieman Dam Road Ignimbrite

SAMPLE	La	Ce	Pr	Nd	Sm	Eu	Gd	Dy	Er	Yb
42610	36.5	75.8	7.52	26.3	4.39	0.87	3.72	4.07	3.03	3.46
LPD6	20.2	47	4.99	19.4	4.11	0.85	3.87	5.11	3.8	4.58
JD6	45.8	98.9	10.6	41.3	7.23	0.82	6.55	7.03	4.42	4.04
HCL	51.8	111	12	45.8	7.53	0.92	5.98	6.03	4.11	4.03

Extrusive dacites from the Central Volcanic Complex (Table 2) have Ti/Zr, Zr/Nb, V/Sc and Zr/Y ratios which overlap with the ranges for these ratios in intrusive hbd-phyric dacites (eg. HR65, HR70) associated with hbd-andesites at Crown Hill and elsewhere along the Central Volcanic Complex belt north of Queenstown. However, the extrusive dacites have notably higher TiO_2, Nb, Y and Zr contents, and much lower Sc and Sr contents than the intrusive dacites at any SiO_2 or MgO content, and indicate that these two groups of dacites are most unlikely to be cogenetic. REE data emphasize the different origins for the intrusive and extrusive dacites (Fig. 3). At a similar level of differentiation, the $(La/Sm)_N$ ratio of an intrusive dacite (HR66) is 5.2, while that for an extrusive dacite from north of the Henty Fault Zone (LPD 11A) is only 2.6.

Least-altered rhyolites from the Central Volcanic Complex have up to 76.3% SiO_2 (Table 3). Up to around 73% SiO_2, the REE patterns (Fig. 4) for the rhyolites are very similar to those of the extrusive dacites, except for the expected slightly higher LREE levels, and more pronounced Eu anomalies due to extensive plagioclase fractionation during differentiation from dacite to rhyolite. However, the two analyzed Central Volcanic Complex rhyolites with >73% SiO_2 show unusual, broad V-shaped REE patterns with lower LREE abundances than even the dacites. These patterns are thought to be due to very late stage fractionation of LREE-enriched accessory minerals, dominantly apatite; separation of even very small amounts of apatite will dramatically decrease LREE and MREE abundances in residual liquids. As expected, the high-Si rhyolites with relatively depleted LREE and MREE levels are also depleted in P_2O_5 compared to other rhyolites from the MRV.

Affinities of the Central Volcanic Complex

The Central Volcanic Complex consists of andesites, dacites and rhyolites which include lavas and ignimbritic rocks and shallow, sub-volcanic intrusives. South of the Henty Fault System, andesites are mainly intrusive hbd-rich bodies, while north of the Henty Fault System extrusive andesites are more abundant (yet still subordinate in volume to more silicic lavas). I consider that the oldest rocks in the Central Volcanic Complex are the comagmatic, largely extrusive andesite-dacite-rhyolite suite lavas which dominate this belt north of the Henty Fault System. This same suite occurs along the length of the belt south of the Henty Fault System all the way down to the Jukes-Darwin area, but is frequently highly altered to pink, K-rich sericite- and K felspar-rich lithologies. It hosts common plug-like intrusions of notably more LREE-enriched pyx- and hbd-phyric andesites, of which no counterparts have been discovered to date in the Central Volcanic Complex north of the Henty Fault System.

The Central Volcanic Complex is a high-K calc-alkaline orogenic andesite- dacite-rhyolite suite (Figure 5a). These lavas are compositionally most similar to high-K calc-alkaline orogenic suites erupted through fairly thick continental crust, such as those erupted in Central America and the northern and central Andes. The MRV were probably erupted through Precambrian

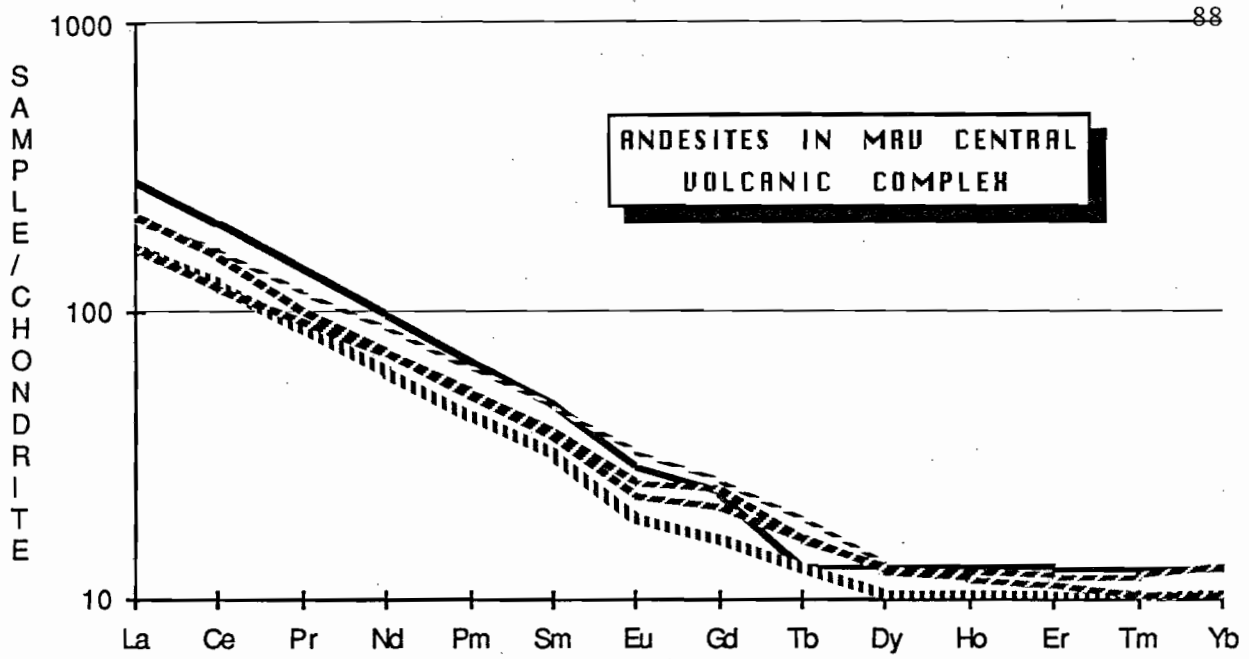

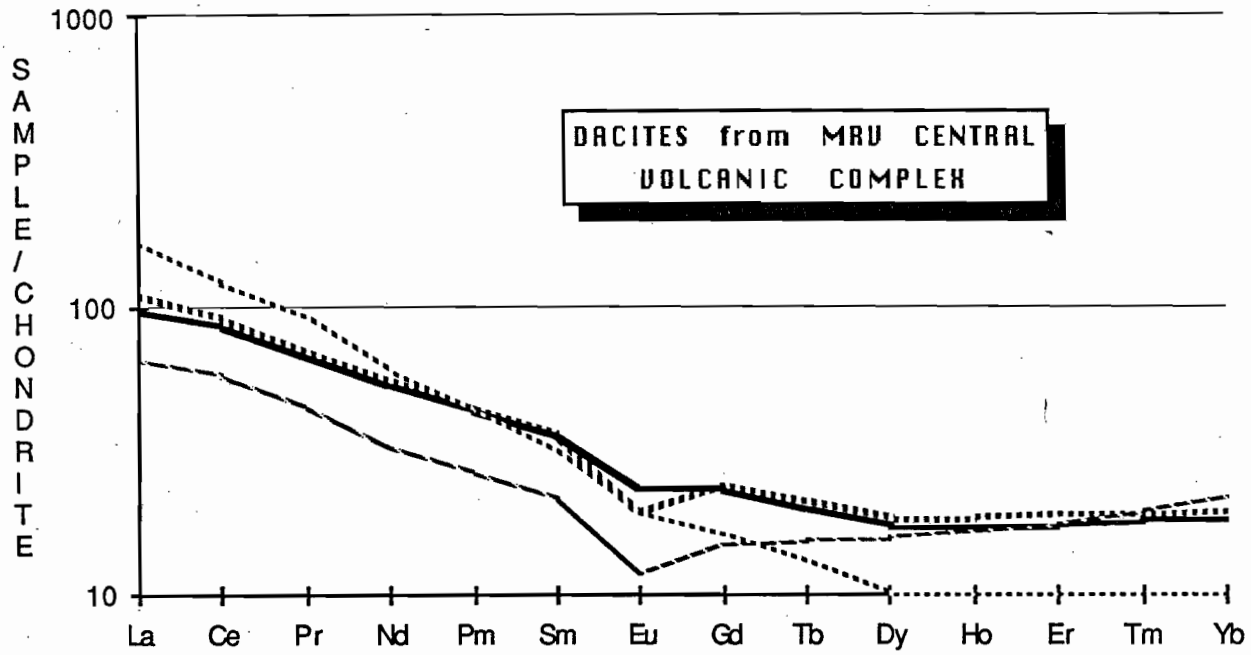

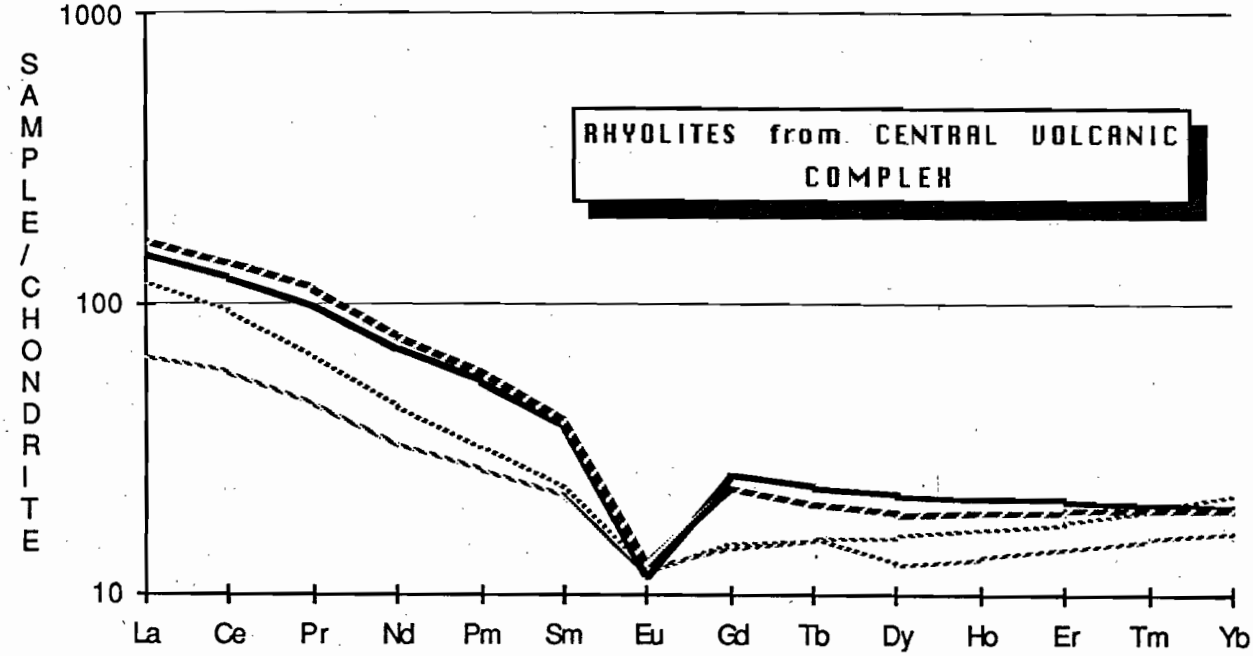

FIGURES 2 (top), 3 (middle) and 4 (bottom): Chondrite-normalized REE plots for lavas from the Central Volcanic Complex of the Mount Read Volcanics.

continental crust. Evidence supporting this interpretation includes:

1.the K_2O-SiO_2 diagram (Fig. 5a) shows the Central Volcanic Complex lavas (and other MRV) plotting largely in the field of high-K calc-alkaline orogenic suites. Importantly, even though K, Ba and Rb are mobile to some extent during pervasive, low-grade alteration, and are extremely mobile during mineralization-related hydrothermal alteration, careful sample selection can reduce considerably the elemental scatter resultant from variable alteration. This is emphasized by the scatter shown on the K_2O-SiO_2 diagram (Fig. 5b) by 25 MRV lavas selected for analysis without careful petrographic "filtering" and analyzed in the Geology Department in early 1986.

2. although Ba is even more mobile than K, a high proportion of least-altered MRV lavas contain from 500 - 3000 ppm Ba; such high Ba contents are virtually unknown in lavas from intra-oceanic arcs, but are common in arc suites erupted through continental crust (eg. Mexico, N. Andes, Roman Province). Regional, low-grade (burial) metamorphism usually results in a depletion of K-group elements, so the almost ubiquitous high Ba contents of the MRV lavas are considered to reflect scatter around a formerly (perhaps) more coherent high-Ba trend.
3. the abundance of hornblende in the Central Volcanic Complex andesites is characteristic of continental margin calc-alkaline andesite suites.
4. REE patterns and abundances are more typical of high-K Andean-type calc-alkaline lavas than low- or medium-K orogenic arc lava suites erupted in intra-oceanic arcs.
5. there is strong evidence from Sr and Pb isotopes (Whitford and Craven, 1986; Gulson et al., 1987), and the presence of inherited Precambrian zircons in some MRV lavas (Adams et al. 1985), that Precambrian continental crust underlay the MRV volcanoes when they were active in the early and mid- Cambrian.

2. The Western Volcanic Sequence.

An important difference between the Central Volcanic Complex and the rocks flanking it to the west is the occurrence of basaltic lavas in the latter sequence. Major basalt+andesite-dominated sequences occur at Que-Hellyer and at Lynch Creek (SW of Queenstown); both may represent individual volcanic edifices (see later). More restricted occurrences of basalt are in the Swan Creek-Madam Howards Plains areas NW of Queenstown.. Two distinct basalt-andesite suites (which also contain dacite and rhyolite) are represented (Table 4), a volumetrically dominant high-K suite (typified by the Que Rv. andesite-dacite association; Fig. 6d) with strong LREE-enrichment and other compositional features close to the andesitic intrusives in the Central Volcanic Complex south of the Henty Fault System (Fig. 6a), and an exceptionally P_2O_5- and LREE-enriched shoshonitic suite (Fig. 6b). In both the Que-Hellyer area (D. Jack, pers. comm. 1987), and 70km further south in the area SW and NW of Queenstown, these two suites appear to

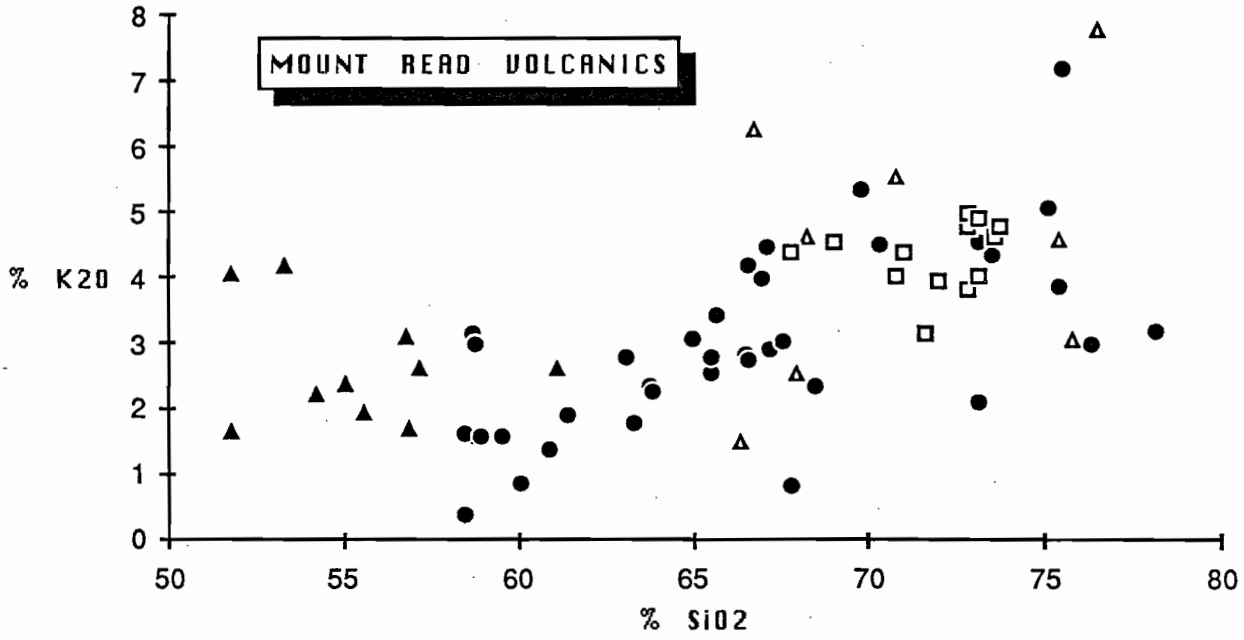

FIGURE 5a: K2O-SiO2 plot for Mount Read Volcanics. Filled triangles are basalts in the Western Volcanic Sequence, filled circles are Central Volcanic Complex lavas, hollow squares are intrusive dacitic-rhyolitic porphyrites in the Western Volcanic Sequence, and hollow triangles are Tyndall Group lavas ans intrusives.

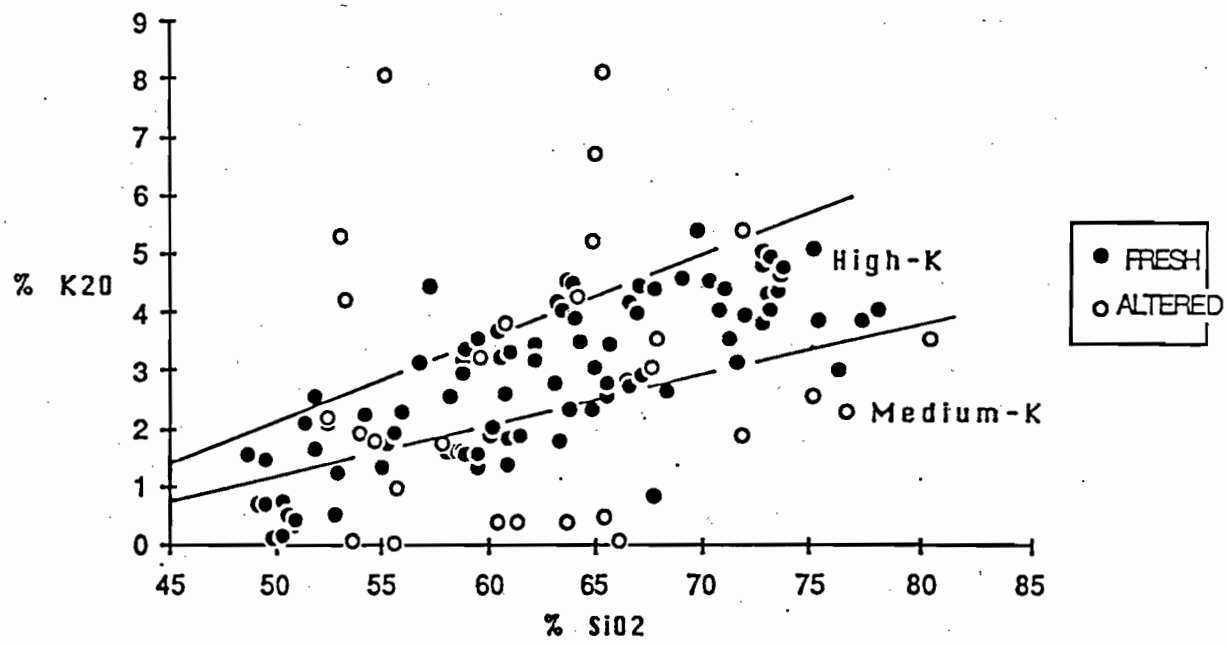

FIGURE 5b: K2O-SiO2 diagram showing carefully-selected least altered (filled symbols) Mount Read Volcanics, and randomly selected Mount Read Volcanics which were not put through the petrographic alteration filter (open symbols). Fields for high-K and medium-K orogenic lavas are indicated (from Gill, 1981).

TABLE 4: Wholerock analyses of lavas from the Western Volcanic Sequence. Samples Z627 to Z96 are from the area NW of Queenstown, RM49 to B6* are from Lynch Creek southwest of Queenstown, BBP253 is a dyke in Central Volcanic Complex rhyolites from an EZ DDH (BBP 253 at 290m), and 334162 is an andesite from Hellyer.

SAMPLE	Z627	Y408	Z102	Z96	RM49	C9*	C11*	C8*	B6*	BBP253	334162
SiO2	49.5	51.8	54.2	56.8	53.3	56.9	55.05	57.2	61.1	51.8	55.6
TiO2	0.32	0.41	0.38	0.47	0.60	0.55	0.57	0.47	0.52	0.89	0.77
Al2O3	8.9	12.5	12.0	13.7	16.6	17.5	18.2	15.9	15.0	12.5	18.6
Fe2O3	10.5	10.0	9.1	8.8	10.1	7.8	8.5	8.0	7.2	9.9	10.5
MnO	0.2	0.18	0.14	0.17	0.09	0.16	0.18	0.14	0.26	0.16	0.23
MgO	16.4	11.4	9.84	6.91	9.37	5.04	5.09	6.26	3.55	8.39	4.6
CaO	11.9	9.48	9.2	6.55	2.92	5.99	5.19	5.73	4.49	10.1	3.08
Na2O	1.35	2.02	2.92	3.23	2.50	3.99	4.36	3.41	4.70	1.12	4.12
K2O	0.70	1.66	2.21	3.11	4.19	1.68	2.39	2.61	2.61	4.07	1.93
P2O5	0.17	0.48	0.28	0.23	0.31	0.24	0.35	0.28	0.29	0.98	0.57
TOTAL	100	100	100	100	100	100	100	100	100	100	100
LOI	3.28	4.07	2.87	2.59	4.44	4.28	4.06	3.87	3	1.88	3.99
Ni	303	130	115		125	42	39	57	19	45	17
Cr	819	580	640		295	85	74	152	20	181	5
V	221	240	240		284	217	300	227	256	267	302
Sc	49	39	42		47	19	26	21	20	37	31
Zr	53	105	76			114	130	137	147	295	187
Nb	4	4	1.5			9	6	<5	6	14	11
Y	34	32	17			20	25	24	23	37	32
Sr	182	420	185			372	516	636	696	881	595
Rb	155	41	45			35	45	34	63	111	46
Ba	382	1300	1750		2599	825	1740	1650	1500	2500	3407
Cu	12	94	110		59	109	125	105	76	3	58
Pb	5	5	6		3	<6	7	<6	93	12	33
Zn	64	90	72		61	76	87	80	317	150	224
Ti/Zr	36.20	23.41	29.98			28.92	26.29	20.57	21.21	18.08	24.69
Zr/Y	1.56	3.28	4.47			5.70	5.20	5.71	6.39	7.97	5.84
Zr/Nb	13.25	26.25	50.67			12.67	21.67		24.50	21.07	17.00
Zr/Sc	1.08	2.69	1.81			6.00	5.00	6.52	7.35	7.97	6.03
K/Rb	37	336	408			398	441	637	344	304	348

SAMPLE	La	Ce	Pr	Nd	Sm	Eu	Gd	Dy	Er	Yb
Y408	112.5	209	26.2	103.4	18.8	4.49	13.2	7.51	3.67	2.87
Z102	54.3	99.9	11.4	43.6	7.65	1.96	6.09	3.84	2.18	1.78
Z96	63.3	117.1	12.85	47.8	8.18	1.69	6.03	4.41	2.75	2.14
C9	40.1	82.5	8.64	33.5	5.69	0.93	4.32	3.68	2.43	2.1
334162	93.5	193.8	21.4	84.1	15.1	3.8	10.7	6.93	3.32	2.93

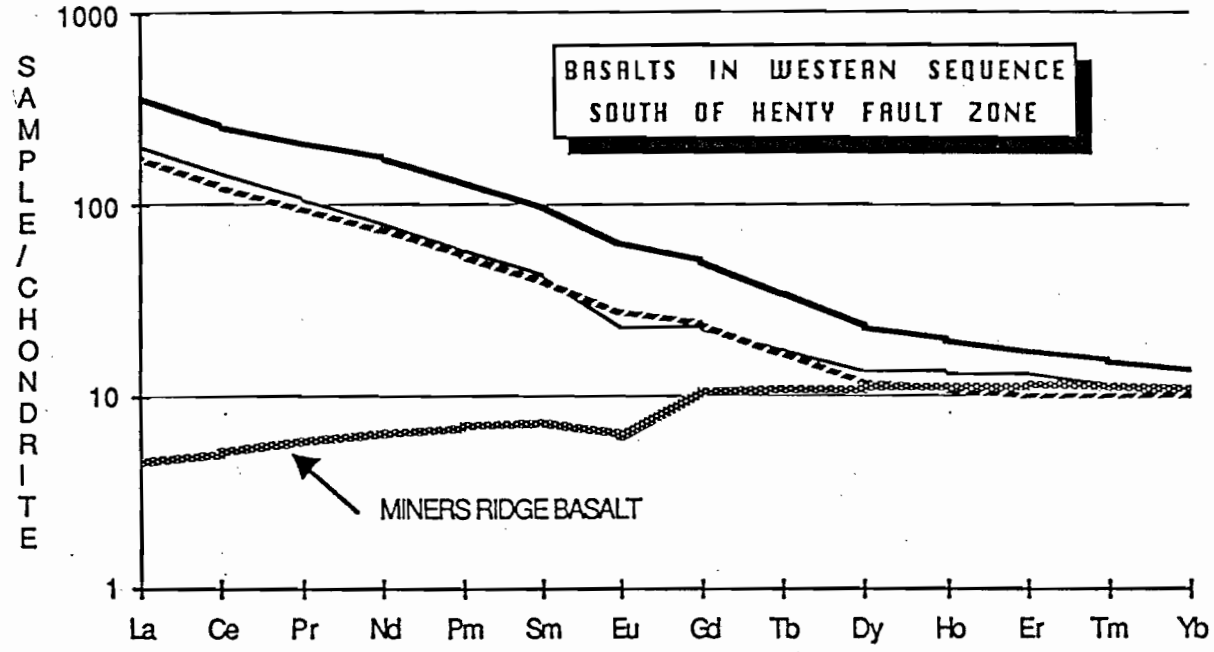

FIGURE 6a: Chondrite-normalized REE plots for basaltic lavas from the Western Volcanic Sequence south of the Henty Fault Zone, and for Miners Ridge tholeiitic lava W64.

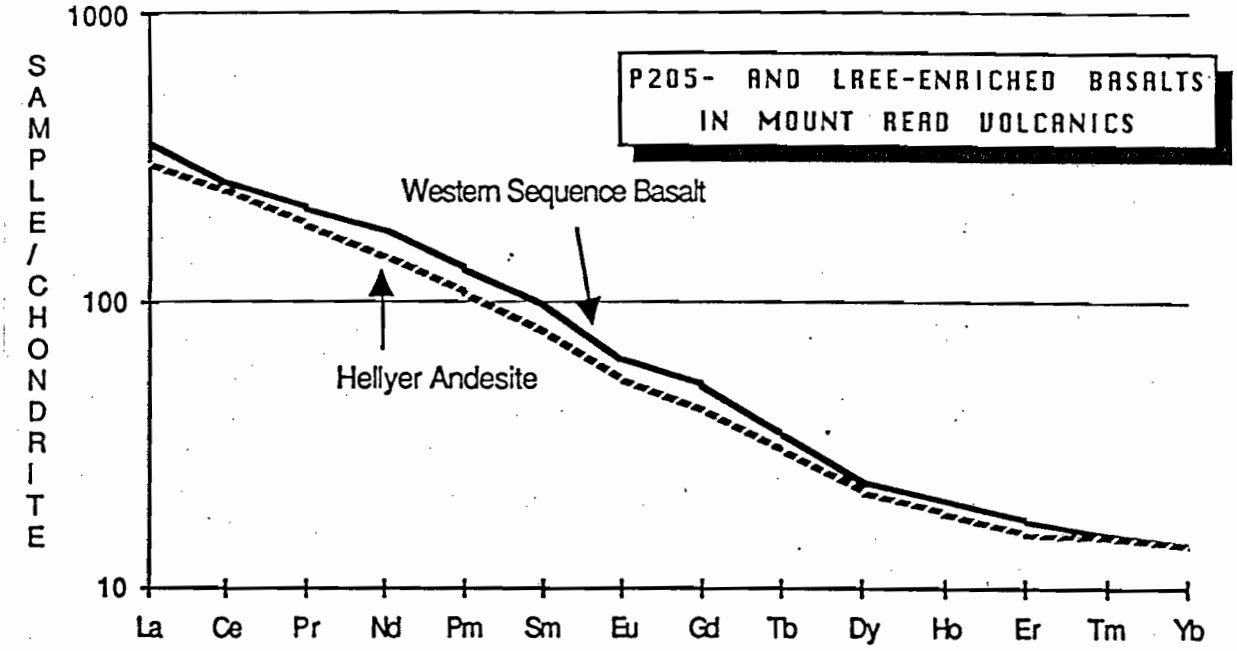

FIGURE 6b: Chondrite-normalized REE plots for exceptionally LREE-enriched basaltic lavas in the Western Volcanic Sequence near Queenstown (Y408) and at Hellyer.

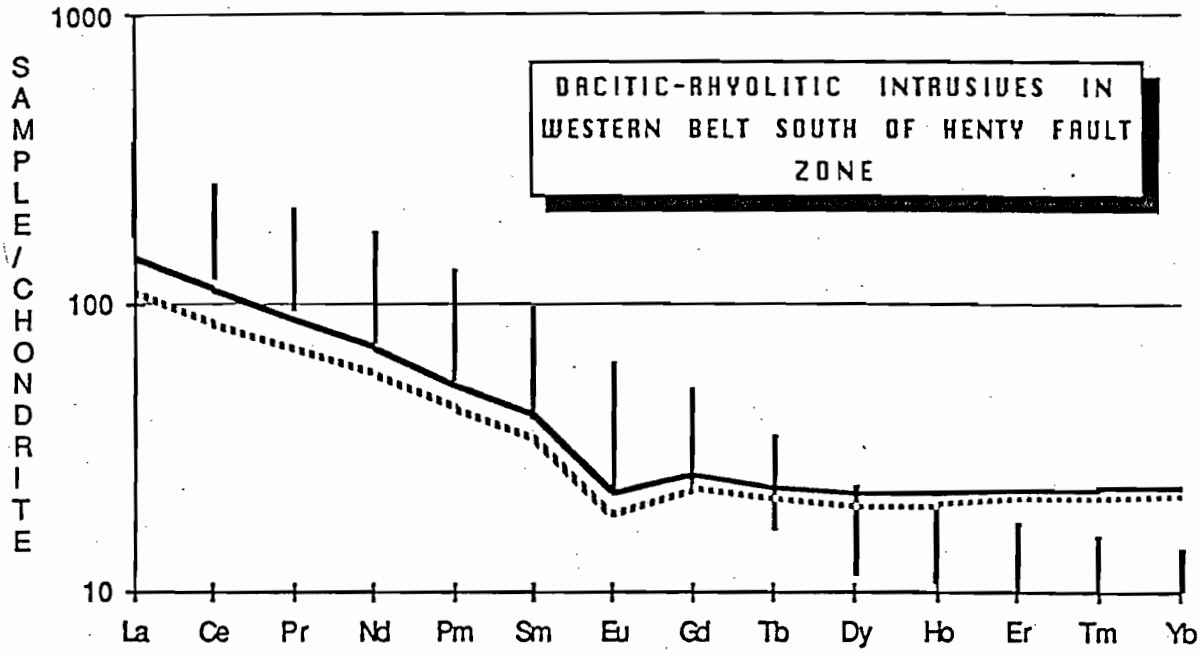

FIGURE 6c: Chondrite-normalized REE plots for dacitic to rhyolitic porphyrites intruding the Western Volcanic Sequence. Also shown is the range for basalts from within the Western Volcanic Sequence.

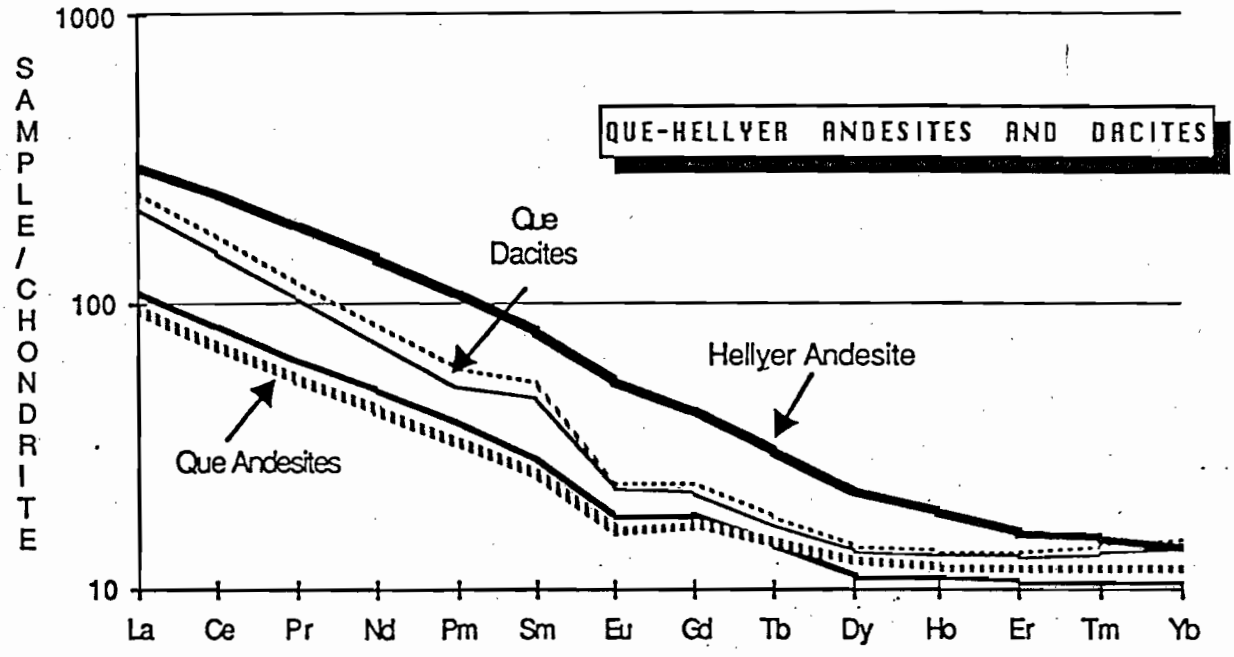

FIGURE 6d: Chondrite-normalized REE patterns for dacites and andesites from Que River (data from Whitford et al., 1987), and Hellyer andesite 334162 (AJC, unpubl. data).

be interbedded, while very P_2O_5-rich shoshonitic basalts have been encountered in drillholes in the Boco Siding area in a sequence generally considered to be Central Volcanic Complex. In addition, on the basis of their strongly LREE- enriched REE patterns (see later), I consider that the basalt-andesite-dacite-rhyolite sequence on Sorell Peninsula (the Noddy Creek Volcanics) is probably a southern continuation of the Western Volcanic Sequence.

Large feldspar-porphyrite intrusive bodies extend along the western side of the Western Volcanic Sequence from the Que River area to well south of Queenstown. Analyses of these dominantly rhyolitic rocks are listed in Table 5, and REE patterns are shown in Figure 6c. These rhyolites are compositionally distinct from extrusive rhyolites in either the Central Volcanic Complex or the Tyndall Group, especially in terms of the generally lower SiO_2 and higher Ti, V and FeO* of the former; REE patterns of these rhyolitic intrusives in the Western Volcanic Sequence are fairly similar to those in the Tyndall Group, but have less pronounced negative Eu anomalies. Further samples of these rocks are presently being analyzed for REE, and will provide more representative data on which to base a petrogenetic comparison of these Western Volcanic Sequence intrusives with other rhyolites within the MRV.

Affinities of the Western Volcanic Sequence

The closest modern analogues of the high-K and shoshonitic suites in the Western Volcanic Sequence are the high-K (including shoshonitic) mafic-intermediate lava series from E Papua (Jakes & Smith 1970; Jaques 1976) and the Papua-Niugini highlands (Mackenzie & Chappell 1972), the Roman Province (Peccerillo 1987) and the European Alps in northern Italy (Venturelli et al. 1984). In these areas, magmatism is post-collisional yet the lavas show evidence (eg. low Ti, Nb) of derivation from a subduction-modified upper mantle. Johnson et al. (1978) suggested that the E Papuan late Cainozoic high-K magmas were generated by partial melting of upper mantle which had been modified by LILE-enriched fluids derived from subducted ocean crust during earlier late Mesozoic, SW-directed subduction.. Varne (1985) argued that K-rich lavas in the Indonesian and other arcs may be derived from ancient, enriched subcontinental mantle dragged into the sub-arc subduction zone of magma generation during continent-arc collision.

Whatever the correct petrogenetic scenario for the high-K lavas in the Western Volcanic Sequence, I am impressed by the similarities in geological setting and composition of these lavas and those from E Papua. At the latter location, high-K and shoshonitic lavas overlie allochthonous, depleted 'ophiolitic' basement (that includes boninites; Jenner 1981) of the Papuan Ultramafic Belt, which had been emplaced during Mid-Tertiary arc-continent collision (Smith 1982). As shown in the Miners Ridge area S of Queenstown (see later), similar strongly LREE-enriched, high-K andesites and basalts (shoshonites) overlie LREE-depleted basalts identical to those in the low-Ti lava carapace of the Serpentine Hill MUC thrust slice.

TABLE 5: Wholerock, and 2 REE analyses of dacitic- rhyolitic porphyrites from the Western Volcanic Sequence south and west of Queenstown

SAMPLE	Z488	Y249	Y318	Y549	Y324	Y311	Y5	Y821	Z221	Y4	Y74	Y75	Y472
SiO2	67.8	69	70.8	71	71.6	72	72.8	72.8	72.8	73.1	73.1	73.6	73.7
TiO2	0.62	0.74	0.40	0.33	0.38	0.41	0.49	0.48	0.52	0.48	0.49	0.51	0.48
Al2O3	14.4	15.1	14.7	14.3	14.6	14.8	14.8	15.4	14.3	14.7	14.4	14.7	14.8
Fe2O3	4.99	5.37	4.06	4.51	4.89	3.64	3.44	3.1	3.07	3.51	3.83	3.42	2.83
MnO	0.19	0.11	0.06	0.09	0.05	0.06	0.05	0.02	0.01	0.04	0.03	0.03	0.03
MgO	2.76	2.52	0.56	0.73	0.66	0.38	1.42	1.16	0.96	1.36	1.21	0.89	1.19
CaO	1.89	1.11	0.5	1.1	0.19	0.88	0.03	0.06	0.07	0.03	0.06	0.04	0.06
Na2O	2.83	1.42	4.72	3.92	4.37	3.8	2.07	1.98	4.36	1.76	2.81	2.16	2.34
K2O	4.39	4.56	4.04	4.4	3.13	3.96	4.8	5	3.81	4.92	4.04	4.62	4.77
P2O5	0.13	0.13	0.17	0.11	0.07	0.06	0.05	0.04	0.05	0.07	0.05	0.05	0.03
TOTAL	100	100	100	100	100	100	100	100	100	100	100	100	100
LOI	1.82	3.88	1.14	1.72	1.34	2.02	2.58	3.51	1.49	2.52	2.45	2.86	2.5
Ni	31	30	2	2	2	2	9	1	10	0	8	8	10
Cr	113	118	2	5	4	2	33	2	39	0	30	33	34
V	115	121	24	29	26	21	69	46	84	24	75	70	69
Sc	19			8		11		14	16			0	0
Zr	245	260	254	230	240	257	240	251	251	225	283	256	266
Nb	14	17	13	8	13	13	13	18	14	17	17	17	17
Y	48	41	46	32	30	36	30	39	34	24	35	37	48
Sr	265	208	158	220	120	208	120	84	86	72	76	97	75
Rb	176	173	109	145	84	129	84	150	120	154	129	146	169
Ba	1614			1200		1032		1275	946			0	0
Cu	4			20		7			7			0	0
Pb	104			44		10		4	5			0	0
Zn	706			84		57			84			0	0
Ti/Zr	15.17	17.06	9.44	8.60	9.49	9.56	12.24	11.46	12.42	12.79	10.38	11.94	10.82
Zr/Nb	17.50	15.29	19.54	28.75	18.46	19.77	18.46	13.94	17.93	13.24	16.65	15.06	15.65
Zr/Y	5.10	6.34	5.52	7.19	8.00	7.14	8.00	6.44	7.38	9.38	8.09	6.92	5.54
Zr/Sc	12.89			28.75		23.36		17.93	15.69				
K/Rb	207	219	308	252	309	255	474	277	264	265	260	263	234

SAMPLE	La	Ce	Pr	Nd	Sm	Eu	Gd	Dy	Er	Yb
Y75	34.2	69.8	8.75	33.9	6.6	1.34	5.94	6.36	4.43	4.51
Y821	45.2	91.7	10.9	40.8	7.73	162	6.7	7.04	4.76	4.59

3. The Tyndall Group.

This is apparently restricted to the southern side of the Henty Fault System, and unconformably overlies both the Tyennan Block Precambrian and the Central Volcanic Sequence of the MRV. It is probably a lateral correlate of the upper Dundas Group and uppermost Western Volcanic Sequence. The latter correlation is strongly supported by the striking similarity noted by Corbett (1979) between the type Tyndall Group Comstock Tuff, and the Lynchford Tuff of the uppermost Western Volcanic Sequence. The Tyndall Group is dominated by felsic epiclastic and pyroclastic rocks, and includes the subvolcanic Murchison and Darwin Granites, and probably the diorite-granodiorite intrusions in the Noddy Creek Volcanics south of Macquarie Harbour.

Lavas which might be classified amongst the 'least-altered' MRV are scarce within the Tyndall Group; some of the least-altered Tyndall Group rocks are listed in Table 6. Their K_2O contents are highly variable due to the more intense K-metasomatism of these rocks (perhaps due to fluids deriving from Murchison-Darwin and related granites in the subsurface; R. Large, pers. comm.). However diagnostic trace element ratios (eg. Zr/Nb) and REE patterns (Fig. 7) indicate that the Tyndall Group andesites, dacites and rhyolites are closely similar to those in the Central Volcanic Complex, and are best classified as a high-K cal-alkaline suite.

4. The Henty Dyke Swarm

A basaltic dyke swarm occurs within the Central Volcanic Sequence north of the Henty Fault Zone (Corbett 1985). Compositions of five dykes are given in Table 7; they are low-K tholeiites with only slightly LREE-enriched REE patterns (Fig. 8), and Ti/Zr and Zr/Nb ratios around 90-100 and >30 respectively. They have no counterparts in the extrusive section of the MRV, and are chemically most similar to basalts erupted during the earliest phase of arc splitting and backarc basin opening (Saunders et al. 1980; Crawford & Keays 1987). They attest to a period of tension having affected at least this part of the Mount Read arc sometime before eruption of the Western Volcanic Sequence and Tyndall Group rocks, as no similar dykes are presently known from either of these sequences.

5. The Miners Ridge - Henty Fault Wedge Tholeiites

Basaltic lavas occurring at the base of the Western Volcanic Sequence at Miners Ridge are low-K, relatively low-Ti (Table 7), LREE-depleted (Fig. 6a) tholeiites chemically dissimilar to any basalts within the MRV (including the dyke swarm discussed above). We correlate the Miners Ridge basalts chemically and stratigraphically with the uppermost lavas of the low-Ti basalt sequence in the MUC at Serpentine Hill. The pronounced similarities of these two groups of lavas provides an important stratigraphic link between the MUC and the Mount Read Volcanics; I argue that the MUC and their carapace of low-Ti, LREE-depleted lavas form basement to the Western Volcanic Sequence. Support for this contention is found in the Henty Fault Wedge, where tholeiitic pillow basalts, gabbros and dolerites (Corbett and Lees 1987) occurs just west of basalts and andesites with compositional features typical of Western Volcanic Sequence lavas.

TABLE 6: Wholerock and REE analyses of Tyndall Gp. lavas and granite intrusives

SAMPLE	AR1	AR4	T04069	T04130	T04137	T04087	T04082	JD13
Unit	TG	TG	TG	TG	TG	TG	TG	
Lithology	pink qz-fsp pprtc rhyolite	Pink tuff banded	Andesite Lake Selina	Rhyolite Lake Selina	Murchison Granite	Dacite	Dacite	Darwin Granite
SiO2	75.81	66.35	66.77	76.48	67.93	70.8	68.23	75.37
TiO2	0.18	0.5	0.72	0.15	0.53	0.44	0.42	0.22
Al2O3	12.87	16.48	16.15	12.34	14.11	15.32	14.2	14.27
Fe2O3	2.69	4.58	7.7	2.5	4.6	6.34	6.37	1.71
MnO	0.02	0.11	0.09	0.03	0.24	0.19	0.35	0.02
MgO	0.81	1.73	2.15	0.32	1.93	0.98	2.39	0.37
CaO	0.03	0.88	0.01	0.05	3.47	0.23	3.21	0.28
Na2O	4.47	7.67	0.1	0.25	3.11	0.2	0.1	3.1
K2O	3.08	1.5	6.28	7.79	2.53	5.55	4.61	4.59
P2O5	0.03	0.19	0.11	0.02	0.13	0.09	0.15	0.03
TOTAL	100	100	100	100	100.26	100	100	99.73
LOI	1.34	1.18	3.42	0.82	1.68	2.54	6.33	1.56
Ni	<1	3	8	1	3	1	14	1
Cr	<2	6	15	1	16	5	7	1
V	5	63	168	14	104	52	90	21
Sc	6	15	28	4	18	14	9	3
Zr	200	314	195	140	218	272	183	132
Nb	19	13	10	13	13	16	11	14
Y	46	35	25	16	36	34	24	18
Sr	107	253	80	148	345	23	35	138
Rb	62	27	290	233	148	278	300	135
Ba	1560	574	1758	2637	604	1062	387	1385
Zn	41	71	311	66	198	867	624	
Cu	2	7	24	1	3	65	7	
Pb	3	44	36	19	32	116	145	
Ti/Zr	5.4	9.5	22.1	6.4	14.6	9.7	13.8	10.0
Zr/Nb	10.5	24.2	19.5	10.8	16.8	17.0	16.6	9.5
Zr/Y	4.35	8.97	7.80	8.75	6.06	8.00	7.63	7.33
Zr/Sc	33.33	20.93	6.96	35.00	12.11	19.43	20.33	44.00
K/Rb	412	461	180	278	142	166	128	282

SAMPLE	La	Ce	Pr	Nd	Sm	Eu	Gd	Dy	Er	Yb
AR1	63.2	143	15.9	63.7	11.4	1.14	9.63	8.27	4.49	3.53
AR4	37.1	84.8	9.27	36.9	7.07	1.55	5.76	5.52	3.87	3.37
JD13	44.7	89.5	8.21	26.5	4.15	0.87	2.68	2.38	1.85	1.85
T04130	35.1	74.9	6.86	23.6	3.45	0.36	2.22	2.22	1.69	2.16
T04137	32.8	73.7	8.31	32	5.51	0.83	4.87	5.36	3.73	3.48

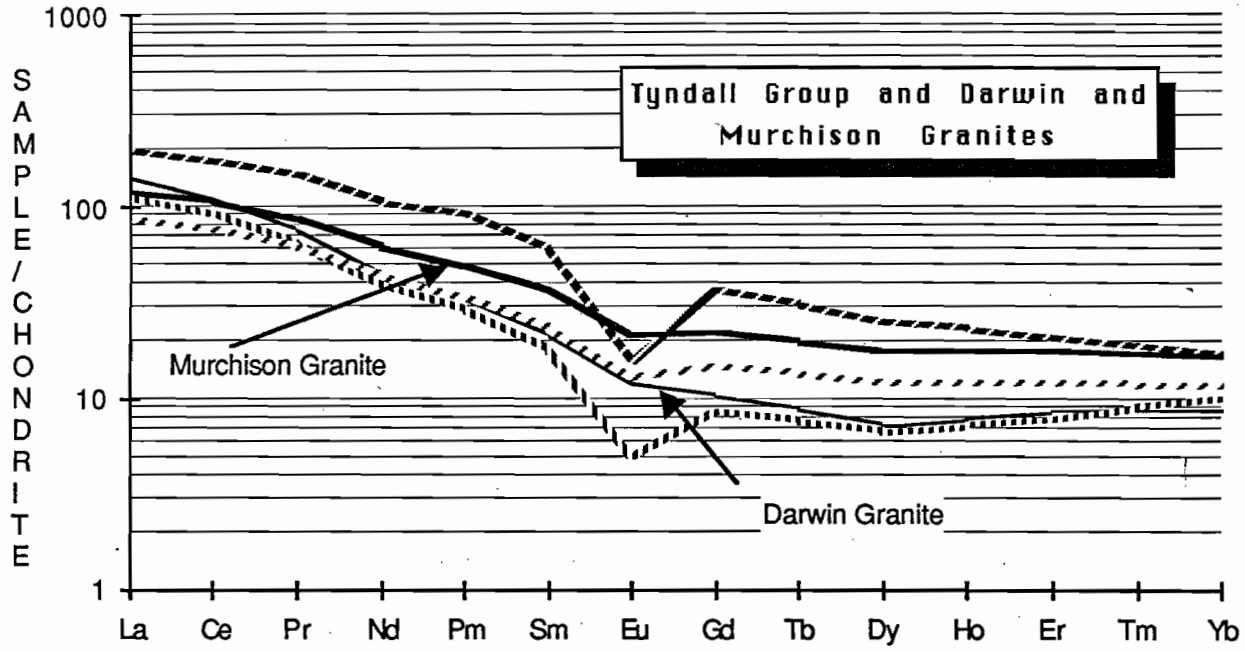

FIGURE 7: Chondrite-normalized REE plots for lavas from the Tyndall Group, and also for the Murchison and Darwin Granites.

TABLE 7: Wholerock analyses of basaltic dykes from the swarm in the Central Volcanic Complex N of the Henty Fault System (R8 to R227), of lavas from the Henty Fault wedge (HR23 to 1984/11) and Miners Ridge (W64 to C2*). Analyses marked by asterisks are Mines Dept. analyses (Corbett 1979).

SAMPLE	R8	R14	STP234	R195	R227	HR23	HR24	1984/9	1984/11	W64*	LE196*	C1*	C2*
SiO2	49.8	50.8	50.3	50.6	50.9	60.5	60.4	58.3	52.8	48.7	47.9	49.7	51.9
TiO2	1.02	1.32	1.13	0.99	0.88	0.76	0.75	1.59	1.59	0.71	0.40	0.51	0.52
Al2O3	16.7	15.9	17.1	17.0	17.7	14.7	14.7	18.0	14.8	15.3	16.5	15.7	15.1
Fe2O3	10.5	10.1	9.8	9.1	10.3	7.42	8.72	13.2	14.4	11.4	9.59	8.98	12.1
MnO	0.19	0.19	0.24	0.48	0.17	0.10	0.10	0.14	0.25	0.2	0.18	0.19	0.22
MgO	11.3	7.47	7.73	9.42	7.08	4.53	5.72	4.02	5.04	12.7	10.3	11.1	10.3
CaO	6.84	9.59	8.81	7.04	7.44	6.68	3.46	1.21	5.99	6.28	10.91	9.04	4.32
Na2O	4.09	4.16	3.94	4.76	4.93	1.95	2.36	4.13	3.52	3.07	3.26	3.53	4.00
K2O	0.1	0.33	0.73	0.5	0.43	3.24	3.67	0.37	1.30	1.56	0.34	0.88	1.16
P2O5	0.07	0.13	0.15	0.07	0.12	0.12	0.13	0.18	0.21	0.06	0.08	0.03	0.05
TOTAL	100	100	100	100	100	100	100	100	100	100	100	100	100
LOI	4.3	2.64	7.98	4.24	3.29	2.71	3.24	4.62	3.24	4.3	3.87	4.45	4.82
Ni	202	40	70	72	47	45	40	3	11	177	160	182	52
Cr	528	118	175	293	39	182	166	5	<5	365	470	376	21
V	218	241	223	205	233	184	183	200	380	254	290	253	279
Sc	42	32	30	47	33	27	26	28	29	78	43	33	41
Zr	61	84	71	66	73	183	194	89	105		27	19	19
Nb	<3	<3	<3	<3	0.9	12	11	<3	<3		<3	<5	<5
Y	22	32	25	30	33	30	38	48	35		12	18	18
Sr	415	255	184	495	320	375	192	220	290		150	356	66
Rb	2.5	9	30	13	13	100	93	17	34		41	36	37
Ba	132	188	173	960	185	901	1316	185	590	730	170	237	430
Cu	43	51	75	156	8	19	60			30	46	132	137
Pb	20	3	6	15	24	24	16			3	<4	<6	<6
Zn	105	118	148	375	131	115	260			60	80	54	96
Ti/Zr	100.24	94.21	95.41	89.93	72.27	24.90	23.18	107.10	90.78		88.81	160.92	164.07
Zr/Nb					81.11	15.25	17.64						
Zr/Y	2.77	2.63	2.84	2.20	2.21	6.10	5.11	1.85	3.00		2.25	1.06	1.06
Zr/Sc	1.45	2.63	2.37	1.40	2.21	6.78	7.46	3.18	3.62		0.63	0.58	0.46
K/Rb	332	304	202	319	275	269	328	181	317		69	203	260

SAMPLE	La	Ce	Pr	Nd	Sm	Eu	Gd	Dy	Er	Yb
HR23	30.9	67.5	7.71	29.2	5.98	1.39	5.73	5.34	3.47	3.54
R8	5.32	13.62	2.19	9.88	2.77	0.91	3.66	4.46	2.79	2.45
R195	7.39	13.4	2.27	11.93	3.43	1.30	4.86	5.2	3.33	2.85
STP234	9.78	24.3	3.23	15.5	3.95	1.43	4.73	4.93	2.74	2.45
W64	1.54	4.20	0.70	3.83	1.39	0.4	2.76	3.71	2.45	2.21

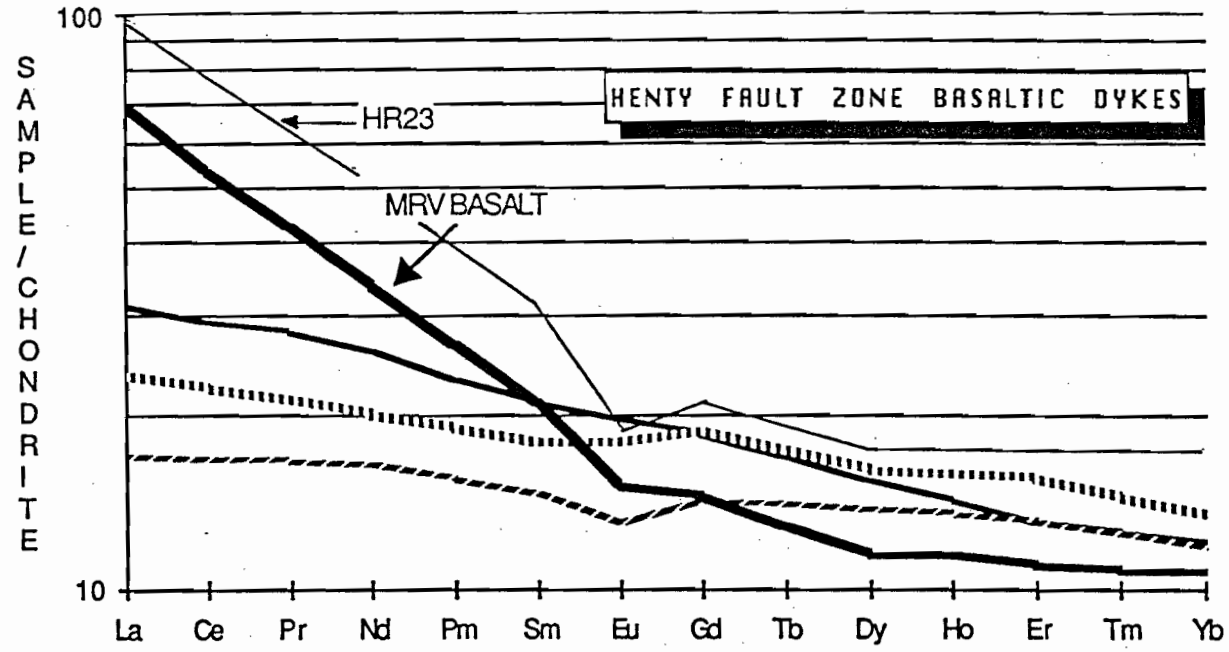

FIGURE 8: Chondrite-normalized REE patterns for three basalts from the Henty Fault Zone dyke swarm, and andesite from the Halls Rivulet sequence of the Henty Fault wedge (HR23), and a typical Mount Reid Volcanics basalt (462A) for comparison.

6. Sorell Peninsula

Details of the stratigraphy and structure of the MRV in this remote and largely inaccessible area are presently lacking. Analyzed samples were collected by AMOCO geologists during traverses across the area in summer 1985-86. As shown on the Queenstown 1: 250,000 sheet, a probably fault-bounded block of MRV-type volcanics, informally named the Noddy Creek Volcanics by White (1975), extends from Asbestos Point on the southern shore of Macquarie Harbour southward past the Timbertops area to the headwaters of the Hibbs River and beyond (Fig. 9). It is overlain, probably unconformably, by Owen Conglomerate and Gordon Limestone; these form a syncline which trends NNW, at a high angle to the regional strike of the Cambrian lavas and associated rocks. A second, complex belt of mafic and ultramafic rocks, with slivers of Owen Conglomerate and fossiliferous Dundas Group lithologies, occurs subparallel to the Noddy Creek belt only a few kilometers further west; on the Queenstown sheet, this belt appears to be pinched out by faulting before it reaches the southern shore of Macquarie Harbour.

Mapping by the author along the southern shore of Macquarie Harbour around Asbestos Point, where the Noddy Creek belt is supposed to outcrop, has shown that the sequence here is lava-poor and highly sheared. Cataclasized and serpentinized formerly opx-rich ultramafics contain boudins of dolerite, and dolerite dykes up to 10m thick occur immediately east of Asbestos Point. No MRV lithologies have been found along this coast, and I suggest that it is, in fact, the western mafic-ultramafic belt which reaches the southern shore of Macquarie Harbour at Asbestos Point, not the Noddy Creek belt. The former belt, which contains opx-rich ultramafics and gabbros, and also boninitic lavas inland from the coast, is interpreted to be a considerably more tectonized equivalent of the mafic-ultramafic complexes exposed further north in the Dundas Trough at Heazlewood River, Serpentine Hill and McIvor Hill. The extent of the Noddy Creek belt heading northward from the Timbertops area remains unknown, but it certainly does not intersect the shoreline of Macquarie Harbour.

MRV rocks collected in the Noddy Creek belt-Hibbs River area on the Sorell Peninsula include representatives of a basalt-andesite-dacite-rhyolite suite, and a range of hornblende-bearing dioritic to granodioritic shallow intrusives. A small hornblende-bearing granodiorite intrusion at the Timbertops (Fig. 9), and a newly-discovered larger pluton of diorite-granodiorite in the head-waters of the Hibbs River (boundaries presently unknown) are undoubtedly part of the MRV (ie. Cambrian) sequence in this area.

Wholerock analyses of 16 rocks from this belt (see Figure 9 for locations) are given in Table 8. Only the two most magnesian samples have been analyzed for REE to date; REE data for these samples is listed below.

SAMPLE	La	Ce	Pr	Nd	Sm	Eu	Gd	Dy	Er	Yb	
925	21.6	43.3	5.14	20.1	3.93	1.09	3.82	3.76	2.37	2.27	Hbd gabbro
462A	22.7	49.9	5.71	22.6	4.42	1.15	3.86	3.24	2.07	1.88	Basalt

The lavas range from basalt to rhyolite compositions, although compared to the Central Volcanic Sequence further north in the main outcrop area of the MRV, rhyolites appear to be volumetrically

TABLE 8: Wholerock, and two REE analyses of Mt Read Volcanics, Noddy Creek Belt, Sorell Peninsula

	462A	925	462	385A	123	385	52	977	47	X	58	85	413	150	65	98
SiO2	51.8	52.9	55.2	55.9	57.2	58.1	58.2	59.4	60.1	60.7	62.1	62.2	63.2	63.4	64	64.2
TiO2	0.59	0.56	0.55	0.61	0.67	0.61	0.57	0.48	0.68	0.62	0.66	0.66	0.72	0.55	0.54	0.53
Al2O3	13.9	14.4	15.5	14.9	16.4	16.4	14.6	14.1	14.7	14.9	16.6	16.9	16.5	15.6	15.8	16.2
Fe2O3	10	10.3	9.06	10	9.03	9.14	9.44	7.35	9.72	7.44	6.5	6.2	6.41	8.03	5.78	5.18
MnO	0.28	0.18	0.21	0.07	0.13	0.12	0.27	0.08	0.1	0.1	0.08	0.11	0.11	0.07	0.06	0.07
MgO	8.9	9.78	5.05	6.06	3.5	5.1	7.27	6.27	3.27	3.3	2.45	2.1	1.94	2.71	1.9	1.97
CaO	9.24	6.01	7.58	5.97	5.13	5.43	3.66	4.26	3.73	7.91	4.86	5.54	3.89	1.89	4.47	4.87
Na2O	2.64	4.58	4.93	2.79	3.21	3.36	3.11	6.67	5.53	2.37	3.21	2.94	2.87	3.6	3.38	3.35
K2O	2.56	1.24	1.72	2.26	4.45	1.59	2.56	1.33	1.99	2.59	3.43	3.15	4.16	4.04	3.9	3.48
P2O5	0.1	0.08	0.11	0.11	0.24	0.16	0.14	0.07	0.14	0.13	0.15	0.16	0.17	0.12	0.16	0.13
TOTAL	100	100	100	100	100	100	100	100	100	100	100	100	100	100	100	100
LOI	2.37	3.79	1.15	1.45	2.1	2.96	3.27	1.73	1.33	2.93	1.7	2.44	1.6	2.56	1.49	1.6
Ni	198	291	91	81	26		61	112	38	16	11	11	13	16	10	9
Cr	342	638	70	213	82		250	134	151	116	29	30	20	39	19	16
V	211	196	225	185	195		218	182	186	182	152	132	135	169	125	130
Sc	32	28	25	29	24		33	30	28	29	19	18	15	20	16	15
Zr	55	81	74	145			145		107		199	184	228	161	204	199
Nb	3.2	3.4	4.1	7.3			8		7		14	13	13	8	13	14
Y	18	21	20	28			26		24		34	28	38	37	29	29
Sr	262	177	350	271			200		243		292	247	371	123	281	285
Rb	101	15	104	116			76		61		135	117	148	136	161	148
Ba	919	310	403	288	1019		1032	226	695	702	667	793	927	839	721	692
Cu	44	84	39	4	139		12	75	12	16	0	4	5	65	13	2
Pb	4	11	4	1.7	4		11	3	8	5	3	5	8	5	3	4
Zn	122	115	76	13	66		214	16	48	58	24	29	23	55	12	17
Nb	3.2	3.4	4.1	7.3			8		7		14	13	13	8	13	14
Ti/Zr	64.31	41.45	44.56	25.22			23.57		38.10		19.88	21.50	18.93	20.48	15.87	15.97
Zr/Nb	17.19	23.82	18.05	19.86			18.13		15.29		14.21	14.15	17.54	20.13	15.69	14.21
Zr/Y	3.06	3.86	3.70	5.18			5.58		4.46		5.85	6.57	6.00	4.35	7.03	6.86
K/Rb	210	686	137	162			280		271		211	223	233	247	201	195
Zr/Sc	1.72	2.89	2.96	5.00			4.39		3.82		10.47	10.22	15.20	8.05	12.75	13.27

SAMPLE	La	Ce	Pr	Nd	Sm	Eu	Gd	Dy	Er	Yb
925	21.6	43.3	5.14	20.1	3.93	1.09	3.82	3.76	2.37	2.27
462A	22.7	49.9	5.71	22.6	4.42	1.15	3.86	3.24	2.07	1.88

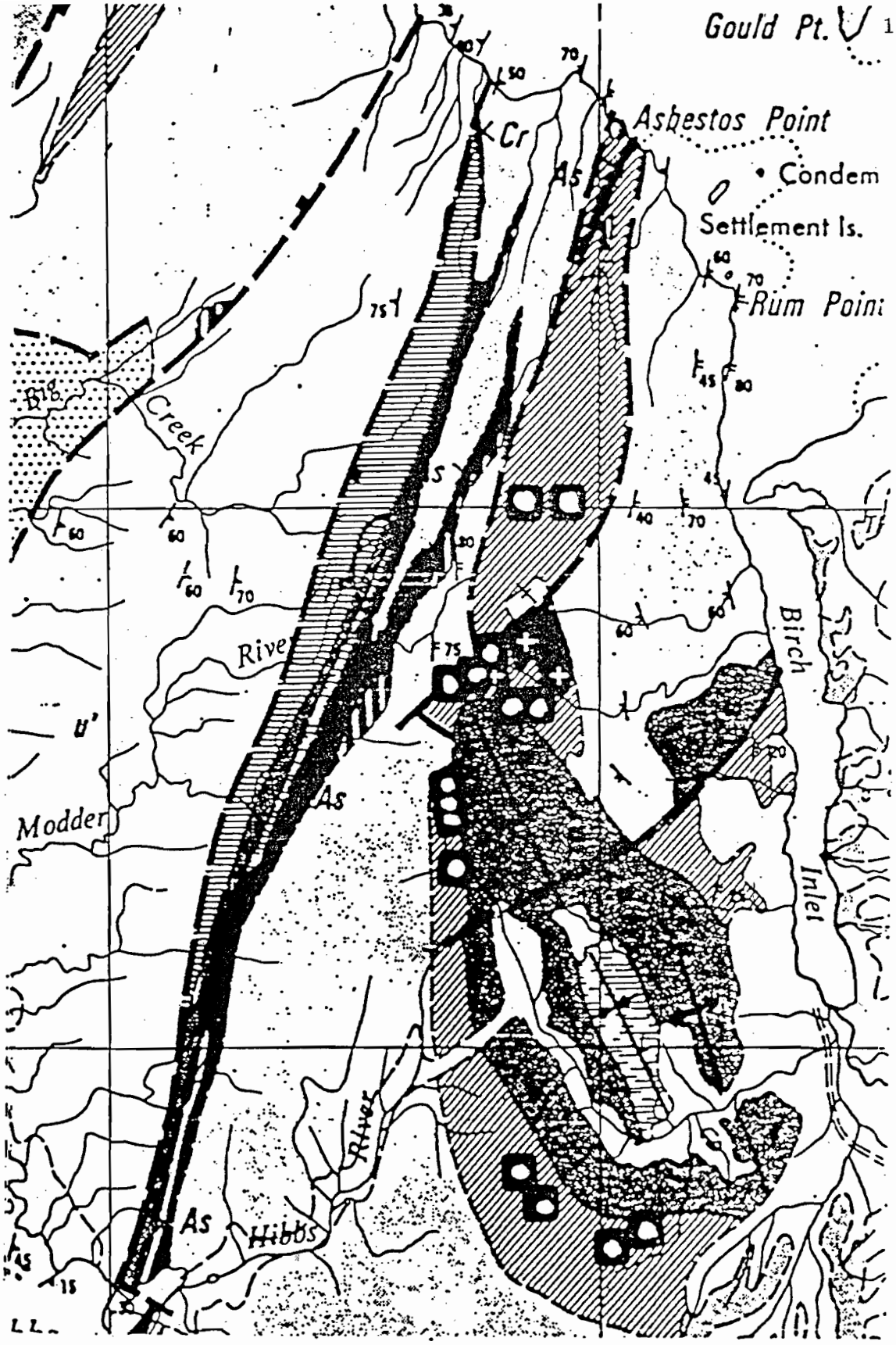

FIGURE 9: Part of the Queenstown 1 : 250,000 geological sheet showing the geology of the eastern Sorell Peninsula south of Macquarie Harbour, with locations of analyzed samples marked. The Noddy Creek belt of the Mount Read Volcanics is marked by diagonal hachuring, the mafic-ultramafic belt by horizontal hachuring, and Owen Conglomerate correlates are dark grey to black shading. A Cambrian granite is marked by two crosses on a black background in the central part of the Noddy Creek belt, at an area known as the Timbertops.

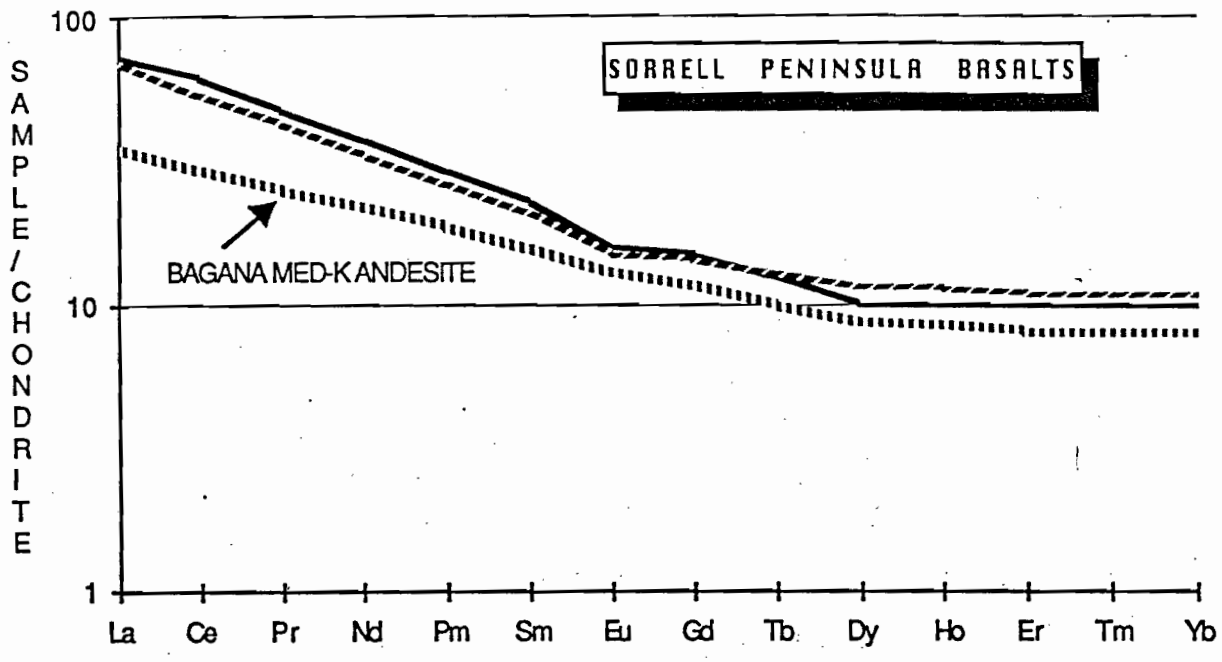

FIGURE10: Chondrite-normalized REE patterns for a basalt and a hornblende gabbro from the Sorell Peninsula extension of the Mount Reid Volcanics. A typical medium-K calc-alkaline andesite from Bagana Volcano, New Britain arc, is shown to emphasize the strong LREE-enrichment of the Mount Read rocks. REE data are in text.

subordinate. The 'dioritic' intrusives cover a similar SiO_2 range as the lavas, and diagnostic trace element ratios and REE patterns (Fig. 10) indicate that the intrusives and lavas in this area are likely to have been comagmatic. In Figure 10, REE patterns for the most primitive basalt and hornblende-bearing intrusive from the Sorrell Peninsula show both to be quite strongly LREE-enriched, with flat HREE patterns. The Sorell Peninsula MRV lavas are also a high-K calc-alkaline suite enriched in LREE and Ba; in this respect, and from the presence of relatively abundant basalts and basaltic andesites in the Noddy Creek sequence, it is considered to be a fault-bounded southern continuation of the Western Volcanic Sequence.

7. Other Areas of the Mount Read Volcanics

Petrological-geochemical investigations, including REE studies, of MRV from other areas in western Tasmania are in progress. Samples from the Lobster Creek Volcanics in the Dial Range Trough, from the MRV north of the Tyennan Block, and from Elliot Bay and Beaconsfield have been analyzed for major and trace elements. A list of samples for which REE analyses will be performed (for AMIRA and the Mines Department) during the next 6 months is appended (Table 9).

SUMMARY

The Central Volcanic Complex of the Mount Read Volcanics contains at least three geochemically distinct magma series. An older sequence of high-K andesites, dacites and rhyolites is intruded in the belt south of the Henty Fault Zone by notably more K_2O- and LREE-enriched pyx- and hbd-phyric andesites and dacites. These more K-rich intrusives appear to have no geochemical intrusive analogues north of the Henty Fault Zone, but their diagnostic chemical features overlap with those from the Que Rv. andesite-dacite extrusive sequence of the Western Volcanic Belt. A basaltic dyke swarm unrelated to any MRV lithologies intrudes the Central Volcanic Complex north of the Henty Fault System, and has no extrusive correlates within the MRV; these basaltic dykes are compositionally similar to basalts formed during incipient rifting (backarc basin opening) of modern island arcs.

The Western Volcanic Sequence extends along the length of the MRV belt from Hellyer in the north, to the Noddy Creek belt south of Macquarie Harbour. Unlike the Central Volcanic Complex, it contains relatively abundant basalts. Two major magma series are represented in the Western Volcanic Sequence, a high-K basalt-andesite-dacite-rhyolite association with strong LREE-enrichment, and compositionally similar to the hbd-bearing intrusive andesites and dacites intruding the Central Volcanic Complex south of the Henty Fault System. Apparently interbedded in this association are flows of exceptionally LREE-enriched high-K basalts with P_2O_5 contents at least three times greater than any other basalts in the MRV. These unusual and compositionally distinctive lavas are compositionally closely similar to shoshonitic lavas occurring in zones of post-collisional orogenic magmatism, such as the Roman Province and the Papua-Niugini highlands - Eastern Papua region.

Sparse least-altered lavas in the Tyndall Group are comagmatic with the Murchison and Darwin granites. Further study of the Tyndall Group, especially of relatively unaltered lavas and intrusives, is required before a thorough synthesis of the compositional range and affinities of this suite can be done. Based on available data, however, they constitute a high-K andesite-dacite-rhyolite suite compositionally overlapping with lavas of the Central Volcanic Complex from north of the Henty Fault System. This implies that petrogenetic conditions (source, P, T, depth of fractional crystallization) during the production of Tyndall Group lavas were very close to those pertaining during generation of the underlying Central Volcanic Complex.

Finally, the strongly LREE-depleted tholeiitic lavas sequences at Miners Ridge and in the western part of the Henty Fault wedge are compositionally distinctive, being unlike any MRV lavas, but closely similar to the uppermost basalts in the Serpentine Hill Mafic-Ultramafic Complex further northwest. On this basis, I conclude that the Western Volcanic Sequence high-K lavas were erupted through and onto a basement of mafic-ultramafic rocks, which outcrops along the western margins of the Dundas Trough along the length of W Tasmania. This has profound implications for the tectonic development of the region during the Lower Palaeozoic, and is discussed below.

Tectonic Implications of the Geochemistry of the Mount Read Volcanics

Based on extensive petrological-geochemical studies of Late Precambrian and Lower Palaeozoic igneous rock associations (Crawford and Berry, in prep.), and a re-interpretation of the structural and tectonic significance of the extensive mafic-ultramafic complexes in W Tasmania (Berry and Crawford, in prep.), a new, actualistic tectonic model for the evolution of this region has been put forward (Crawford and Berry, in prep.). This model is summarized below, and some comments are made on its implications for mineralization in W Tasmania.

The Rocky Cape Block represents an attenuated Late Precambrian passive continental margin transected by localized rifts containing continental tholeiites (Crimson Creek Formation and correlates) and basal shallow-water carbonate sequences (Smithton Trough, Dundas Trough, Sorrel Peninsula). In the Middle Cambrian, this passive margin approached and collided with an intra-oceanic arc above an east-dipping subduction zone. Extensive allochthonous sheets of mafic-ultramafic rocks from the forearc region of this arc were emplaced across the passive margin during this continent-arc collision, which jammed the subduction zone. Continued regional plate convergence resulted in a reversal of subduction direction, so that subduction commenced beneath the attenuated passive continental margin, and high-K orogenic lavas of the Central Volcanic Complex were erupted through and onto the mafic-ultramafic allochthon. Continued penetration of the subducted slab into the sub-continental upper mantle generated unusual shoshonitic lavas of the Western Volcanic Sequence, which erupted further west of mainly slightly younger Tyndall Group high-K andesites, dacites and rhyolites. This short-lived period of subduction polarity reversal ceased with eruption of the uppermost Tyndall Group lavas, and the plate boundary locked, leading to backthrusting, and uplift of the region east of the MRV. Resulting erosion of the extensive

mafic-ultramafic sheet from this region led to exposure of the Tyennan basement, which provided the source for the Owen Conglomerate that shed mainly west of the uplifted region.

This model is not ad hoc for the Late Proterozoic and Lower Palaeozoic of W Tasmania, but is based on several modern examples of arc-continent collision, notably those exposed in Oman, and in the Papua-Niugini Highlands and E Papua. Especially in the latter example, the timing, sequence and nature of volcanism before and after collision are remarkably similar to those in W Tasmania. Details of this model and modern analogues are discussed in Crawford and Berry (in prep.) and Berry and Crawford (in prep).

Some implications of the above model for exploration are noted below. Firstly, the recognition that the Western Volcanic Sequence extends from the Que-Hellyer area all the way south to the Sorrel Peninsula offers significant potential for locating more Que-Hellyer style VMS mineralization further south in the belt. One area of particular potential interest is around Lynchford (Corbett 1979), where a 1km by 3km sized body of basaltic lavas compositionally identical to those at Hellyer probably represents a volcanic edidifice, as does the Que-Hellyer sequence. The bimodality of lava compositions noted for the latter area by Komyshan (1986), Corbett (pers. comm.) and this AMIRA group is typical of large caldera volcanoes in arcs, typified by Rabaul, Krakatoa and Batur (Bali), and has been discussed by Wheller et al. (1986). It is possible that conditions for the generation of VMS in the MRV were best developed in the proximity of these large caldera volcanoes, following massive caldera-forming eruptions and marine invasion of the calderas. If this hypothesis is correct, it emphasizes that a detailed study of the volcanology and geochemistry of belts of arc lavas are important aids in the prediction of potential target areas for VMS deposits.

The model proposed above may offer an explanation as to why the gold tenor of W Tasmanian volcanogenic massive sulphide (VMS) deposits are so high relative to other VMS in the Lachlan Foldbelt and elsewhere. The mafic-ultramafic complexes exposed in W Tasmania are parts of a formerly extensive allochthon in which the dominant lavas represented are depleted low-Ti lavas, including boninites. Work by the AMIRA Group at the Geology Dept. University of Melbourne (Hamlyn et al. 1985; Hamlyn and Keays 1986) has shown that these 'second-stage melt' magmas are significantly enriched in precious metals relative to 'normal' basalts or andesites. I propose that the hydrothermal cells which generated the VMS deposits in the Mount Read Volcanics reached well down into the mafic-ultramafic basement allochthon (and probably into the underlying Precambrian continental crust; see also Large, this volume), from which they scavenged gold and probably other metals for later deposition in VMS bodies in MRV higher in the pile.

ACKNOWLEDGEMENTS

I am particularly grateful to Ross Large and Keith Corbett for sharing their extensive knowledge of the Mount Read Volcanics, and these guys and Ron Berry for many stimulating discussions. Rod Williams and Peter Ellis (CSR), Phil Jones (AMOCO), Doug Jack (Aberfoyle) and Rod Sainty (formerly EZ) assisted with sample provision and information.

REFERENCES

Adams, C.J., Black, L.P., Corbett, K.D. and Green, G.R., 1985. Reconnaissance isotopic studies bearing on the tectonothermal history of the Early Palaeozoic and Late Proterozoic sequences in western Tasmania. Austr. J. Earth Sci. 32, 7-36.

Brown, A.V., 1986. Geology of the Dundas-Mount Lindsay-Mount Youngbuck region. Tasmanian Geol. Surv. Bull. 62, 221pp.

Burns, K.I., 1964. One Mile Geological Map Series K/55-6-29, Devonport. Explanatory Rept. Geol. Surv. Tasmania.

Corbett, K.D. 1986. The geological setting of mineralization in the Mt. Read Volcanics. In: Large, R.R. (Ed.)., The Mount Read Volcanics and Associated Ore Deposits. Geol. Soc. Austr., Tas. Div. Symposium, 1-10.

Corbett, K.D., 1979. Stratigraphy, correlation and evolution of the Mount Read Volcanics in the Queenstown, Jukes-Darwin and Mount Sedgwick areas. Tasmanian Geol. Surv. Bull. 58, 75pp.

Corbett, K.D. and Lees, T.C., 1987. Stratigraphic and structural relationships and evidence for Cambrian deformation at the western margin of the Mt. Read Volcanics, Tasmania. Austr. J. Earth Sci. 34, 45-67.

Crawford, A.J. and Keays, R.R., 1987. Petrogenesis of Victorian Cambrian tholeiites and implications for the origin of associated boninites. J. Petrol. (in press).

Gulson, B.L., Large, R.R. and Porritt, P.M., 1987. Base metal exploration of the Mount Read Volcanics, western Tasmania. Part 111. Application of lead isotopes at Elliott Bay. Econ. Geol. 82, 308-327.

Hamlyn, P.R. and Keays, R.R., 1986. Sulfur saturation and second-stage melts: application to the Bushveld platinum metal deposits. Econ. Geol. 82, 123-145.

Hamlyn, P.R., Keays, R.R., Cameron, W.E., Crawford, A.J. and Waldron, H., 1985. Precious metal contents of low-Ti lavas. Geochem. Cosmochem. Acta 49, 1797-1811.

Jakes, P. and Smith, I.E.M., 1970. High-K calc-alkaline rocks from Cape Nelson, Eastern Papua. Contrib. Mineral. Petrol. 28, 259-271.

Jaques, A.L., 1976. High-K island arc volcanic rocks from the Finisterre and Adelbert Ranges, northern Papua New Guinea. Geol. Soc. Amer. Bull. 87, 861-867.

Jenner, G.A., 1981. Geochemistry of high-Mg andesites from Cape Vogel, Papua New Guinea. Chem. Geol. 33, 307-332.

Johnson, R.W., Mackenzie, D.E. and Smith, I.E.M. 1978. Delayed partial melting of subduction-modified mantle in Papua New Guinea. Tectonophysics 46, 197-216.

Komyshan, P. 1986. Geology of the Hellyer-Mt. Charter area. In: Large, R.R. (Ed.)., The Mount Read Volcanics and Associated Ore Deposits. Geol. Soc. Austr., Tas. Div. Symposium, 53-56.

Mackenzie, D.E. and Chappell, B.W., 1972. Shoshonitic and calc-alkaline lavas from the Highlands of Papua New Guinea. Contribs. Mineral. Petrol. 35, 50-62.

Macneil, A.W. 1986. The geology of the Tullah-Mount Block area. In: Large, R.R. (Ed.)., The Mount Read Volcanics and Associated Ore Deposits. Geol. Soc. Austr., Tas. Div. Symposium, 71-72.

Robinson, P. Higgins, N.C. and Fryer, B.J., 1986. A combined ion-extraction XRF procedure for the analysis of rare earth elements in rocks and minerals. Chem. Geol. 81, 121-139.

Saunders, A.D., Tarney, J., Marsh, N.G. and Wood, D.A., 1980. Ophiolites as oceanic crust or marginal basin crust: a geochemiccal approach. Proc. Int. Ophiolite Symposium, Nicosia, Cyprus, 193-204.

Smith, I.E.M., 1982. Volcanic evolution in Eastern Papua. Tectonophys. 87, 315-333.

Solomon, M. and Griffiths, J.R., 1974. Aspects of the early history of the Tasman Orogenic Zone. In: Denmead, A.K., Tweedale, G.W. and Wilson, A.F. (Eds.) The Tasman Geosyncline- A Symposium. Geol. Soc. Aust. Qld. Divn., 19-44.

Varne, R., 1985. Ancient subcontinental mantle: a source for K-rich orogenic volcanics. Geology 13, 405-408.

Wheller, G.E. and Varne, R. (1986). Genesis of dacitic magmatism at Batur Volcano (Bali) Indonesia: implications for the origins of stratovolcano calderas. J. Volc. Geotherm. Res. 28, 363-378.

White, N. 1975. Cambrian volcanism and mineralization, SW Tasmania. Ph.D. thesis, Univ. of Tasmania (unpubl.).

Whitford, D.J. and Craven, S.J. 1986. Strontium isotope studies at Que River and Hellyer. In: Large, R.R. (Ed.)., The Mount Read Volcanics and Associated Ore Deposits. Geol. Soc. Austr., Tas. Div. Symposium, 87-88.

PROGRESS REPORT ON THE ALTERATION GEOCHEMISTRY OF THE MOUNT READ VOLCANICS

Peter J. McGoldrick, Stewart C. Capp and Ross.R. Large

AMIRA Report

August 1987

Progress Report on the Alteration Geochemistry of the Mount Read Volcanics

Peter J. McGoldrick, Stewart C. Capp and Ross.R. Large

Summary

This report briefly discusses important alteration processes that have affected the MRV. Analytical data for all the important host rock types at Que River are presented and summarised. These include "fresh" andesites, highly altered footwall volcaniclastic rocks and less altered hanging wall dacites and the fuchsite - carbonate altered "breccia". Data for samples of MRV from Lake Selina, the Sterling Valley and Mt. Jukes - Mt. Darwin areas are presented. Proposed future directions for this study are briefly discussed

Introduction

A major aim of the project to date has been to document the primary geochemical variation in fresh Mount Read Volcanics (MRV) as an aid to elucidating stratigraphic problems and to help constrain tectonic reconstructions (Crawford and Large, this report; Large, Crawford and Adrichem, 1986; Crawford, 1986). A second important reason for accumulating a large data base of fresh and altered whole rock analyses is to provide representative data of hydrothermally altered MRV in order to characterise the chemical signature of massive sulphide alteration systems and to discriminate VMS related alteration from other alteration types. This report summarises progress to date on the second aspect of this work and outlines possible future directions.

Alteration styles in the MRV

All the submarine units of the MRV will have suffered initial reaction between hot rock and seawater followed by low temperature rock - seawater interaction (halmyrolysis) to a lesser

or greater extent. The effects of such processes will vary considerably depending on a number of factors (eg., massive cf fragmental volcanics, glassy cf crystalline rocks, burial rates etc). For crystalline rocks the chemical effects of the former process should not be great. Halmyrolysis will involve some addition of alkalis (Hart, 1969) and oxidation of ferrous iron bearing mineral phases,and, if rocks are exposed for long enough on the sea floor, ultimately degrade the rocks to a clay mineral - Fe oxy hydroxide assemblage.

In contrast, in volcanic succession where burial rates are moderate to rapid (most of the MRV?), these sea floor weathering effects will be minimised and low grade burial metamorphic effects involving heated seawater - rock interactions will dominate. Experimental work on ocean floor basalt - seawater interaction (eg., Mottl and Seyfried, 1980) indicates that the effective rock : water ratio is a critical control on the alteration assemblages produced. Under rock dominant conditions (water : rock ratios < 50:1) the rocks gain Mg and alkalis and typical greenschist facies mineral assemblages are produced (eg., chlorite, albite, quartz, epidote) and good textural preservation could be expected. Under seawater dominant conditions (> 50 : 1 water : rock ratios for experimental conditions, but possibly only > 5 : 1 for natural systems) acid solutions are generated and much more intense alteration assemblages result. Alkalis and base metals are leached from the rocks and primary igneous textures are often destroyed. The transition between rock - and seawater - dominated conditions is abrupt (Mottl and Seyfried, 1980).

Similar processes would have acted to varying degrees in the MRV, as well as a third intense granite - related alteration that produced chlorite / pink K feldspar / pyrite assemblages (eg., Selina area, S. Hunns; 1986 and this report; and Red Hills). While overprinting by later alteration processes (eg., Devonian low grade regional metamorphism) may have been important locally in remobilising mineralisation (eg., Mount Lyell; Solomon et al., 1987), the massive polymetallic sulphide deposits of the MRV must have formed from hydrothermal solutions generated during Cambrian water dominated rock - water

interaction. Hence, unambiguous recognition of MRV altered in high water : rock ratio systems should be a useful guide to massive sulphide mineralization.

Detailed mineralogic studies can distinguish several alteration styles in the MRV (Eastoe et al., 1987), but their interpretation is difficult because an overlapping spectrum of alteration mineral assemblages seems to be present. The data base of fresh MRV rocks provides an excellent opportunity to compare the chemistry of altered samples from known massive sulphide systems with other altered MRV. In the following sections the alteration effects at Que River are discussed in some detail and whole rock geochemical data from variably altered samples from three other areas (Lake Selina, Sterling Valley and Mt. Jukes - Mt. Darwin) are presented.

Que River

-Andesites

Major and trace element data Ti/Zr variation diagrams are presented on Figure 1 for a set of 13 least altered andesites (and one andesitic volcaniclastic) from stratigraphically below the mineralised horizon at Que River (tabulation of all the Que River analytical data is presented in McGoldrick and Large, this report). The rationale behind the use of Ti/Zr diagrams has been discussed previously by Large et al., (1986). Briefly, Ti and Zr should be conserved under all but the most intense alteration processes, hence, if the primary variation of individual elements with respect to Ti/Zr is known then samples lying outside the range must indicate addition or subtraction of that component by alteration processes.

For major elements most of the andesite samples fall into coherent groups lying within the MRV "differentiation trend" defined by Large et al., (1986). A few samples appear to have lost some silica and Na_2O, and gained CaO and a small amount of Al_2O_3. Trace elements show somewhat more scatter, but most probably reflect primary values (except for loss of Sr and slight gain of Rb. It is concluded that these rocks have only suffered low grade

Fig. 1. Ti/Zr element variation diagrams for "fresh" andesites and altered footwall andesitic volcaniclastics.

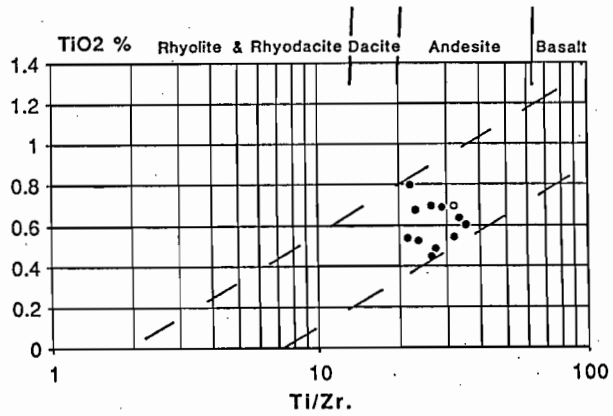

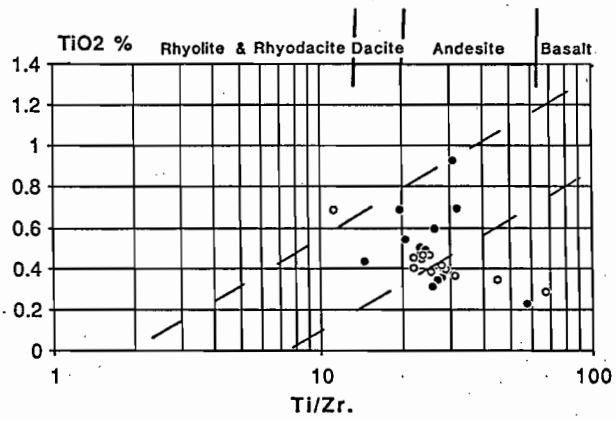

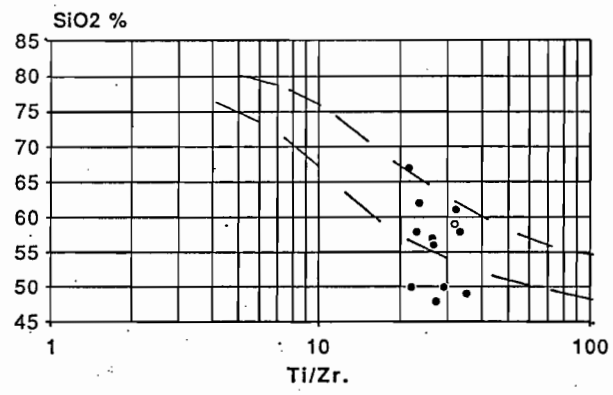

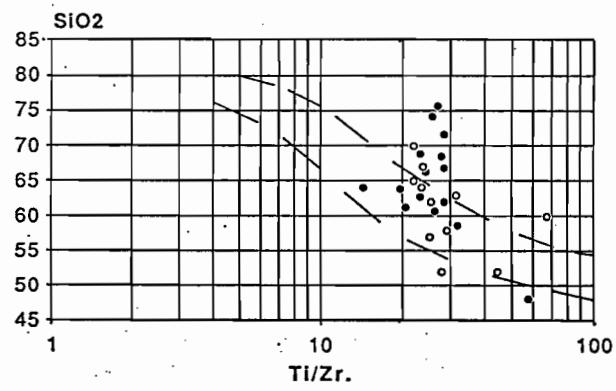

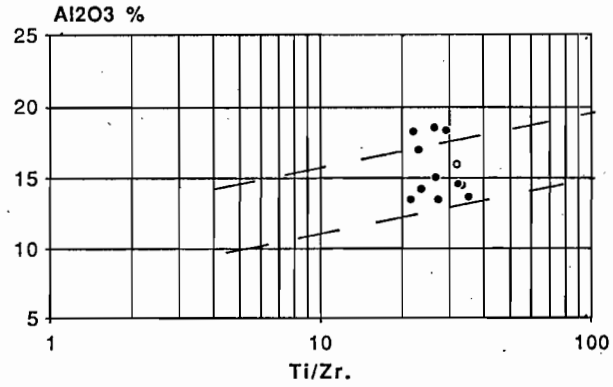

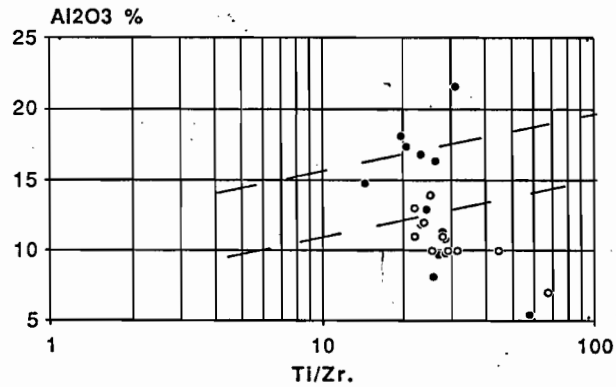

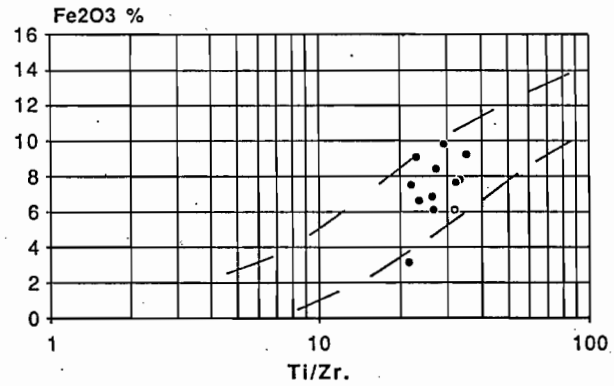

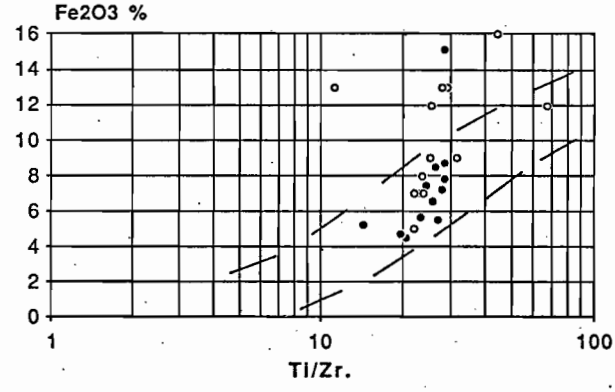

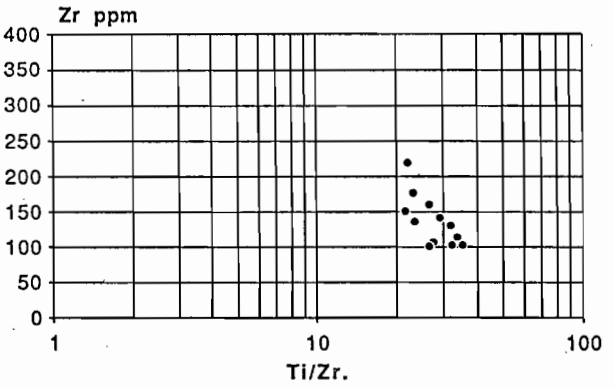

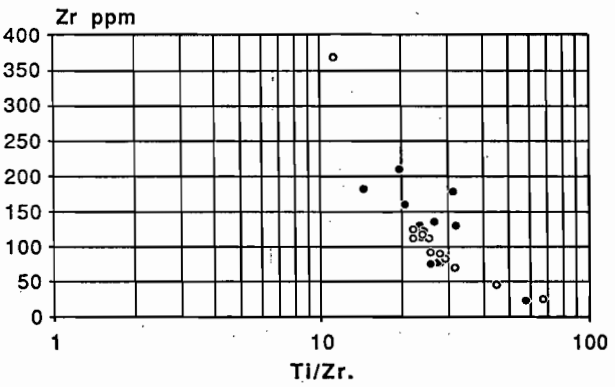

FRESH ANDESITES

FOOTWALL VOLCANICLASTICS

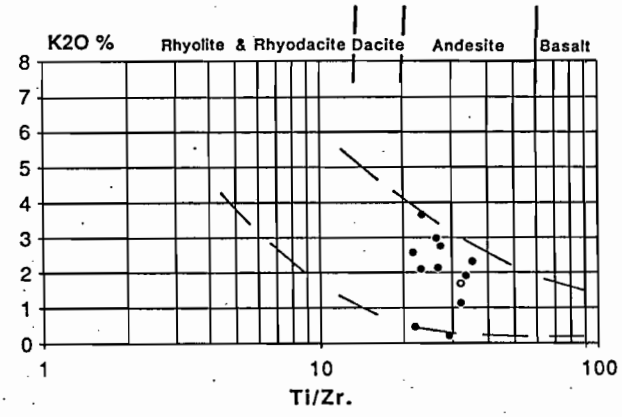

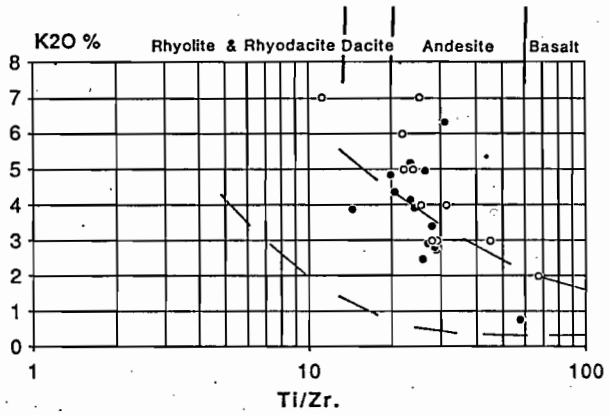

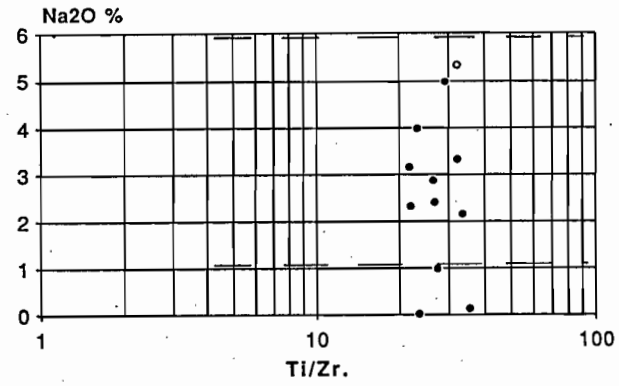

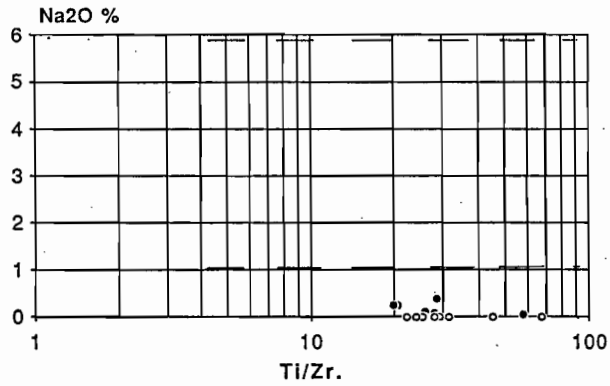

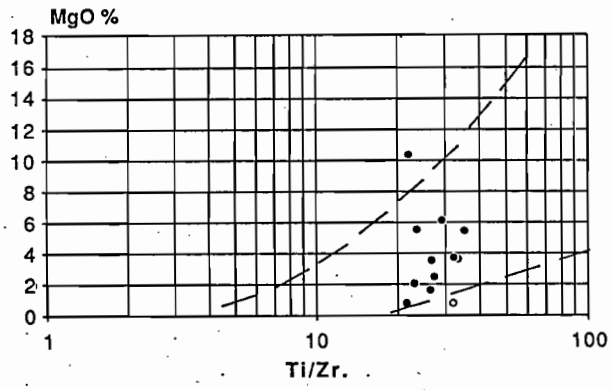

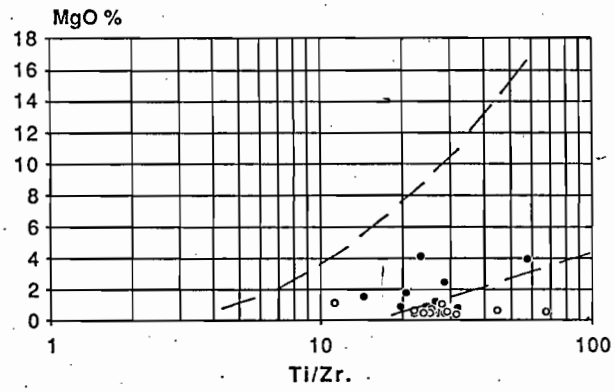

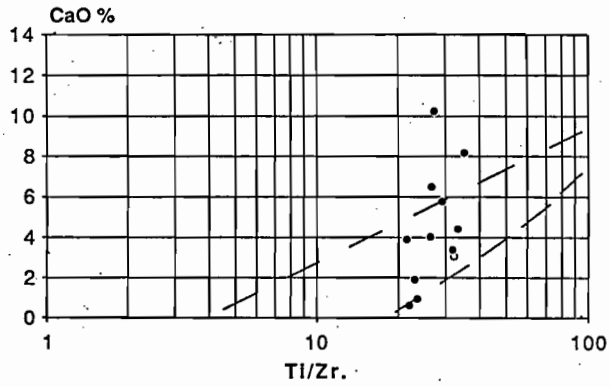

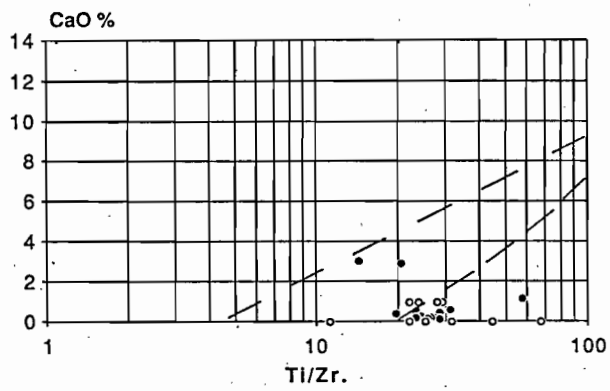

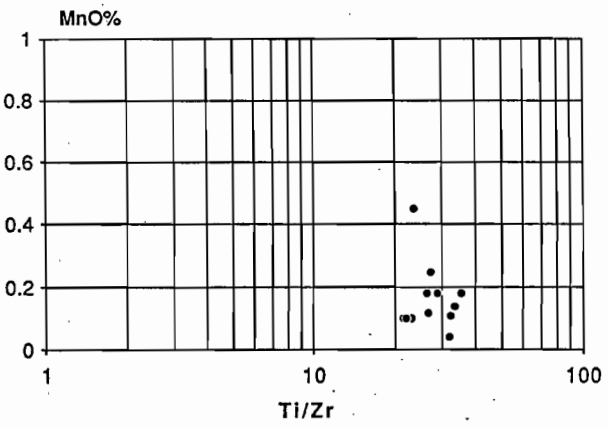

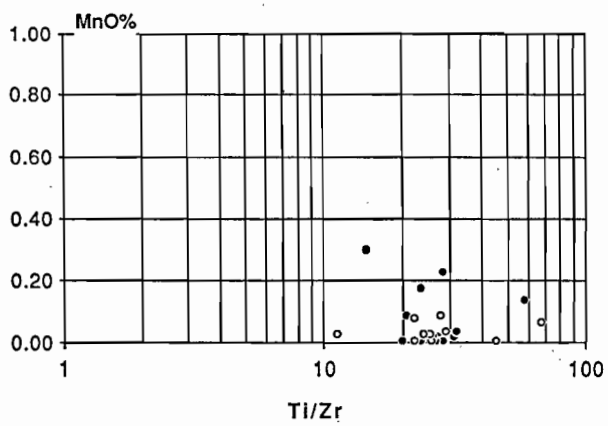

FRESH ANDESITES

Fig. 1. (con.).

FOOTWALL VOLCANICLASTICS

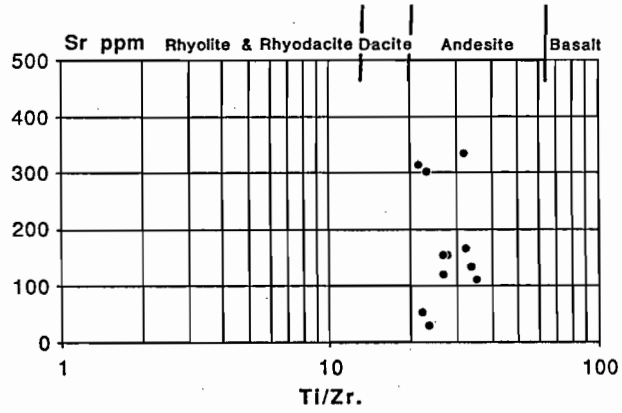

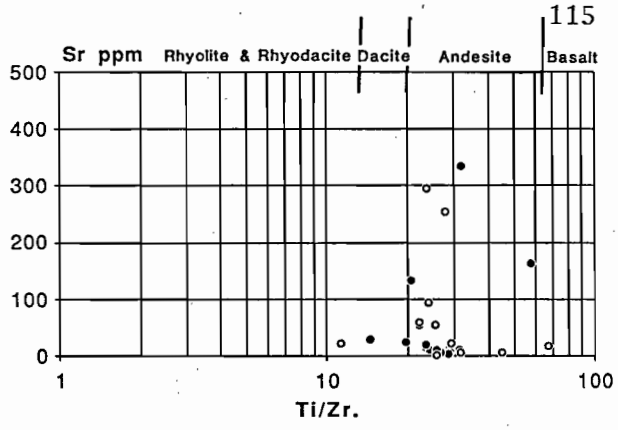

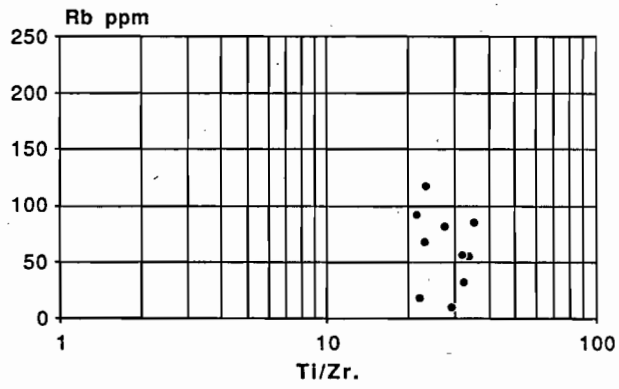

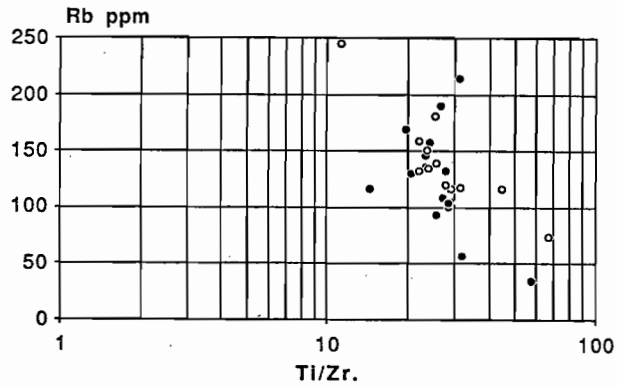

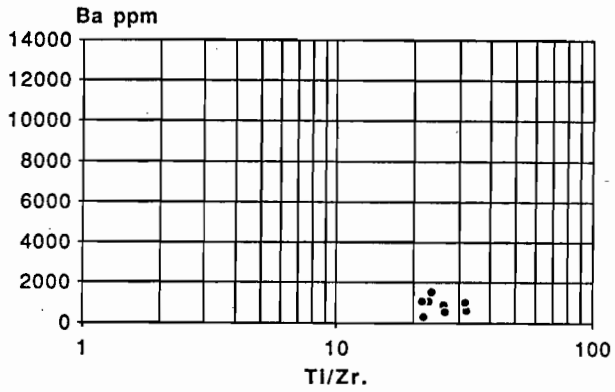

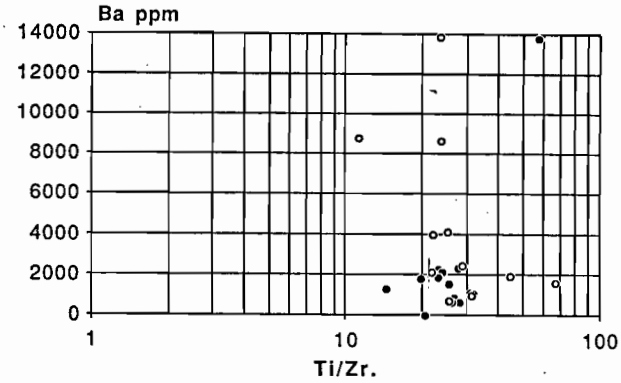

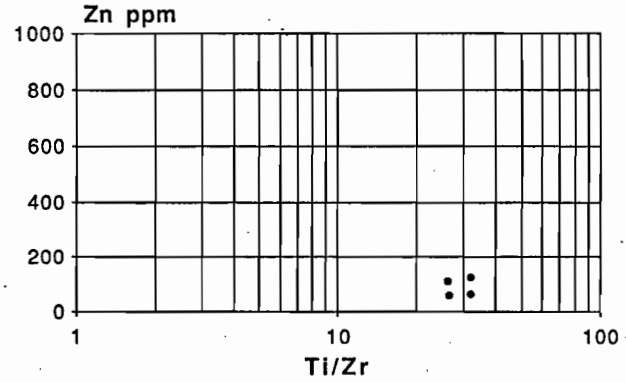

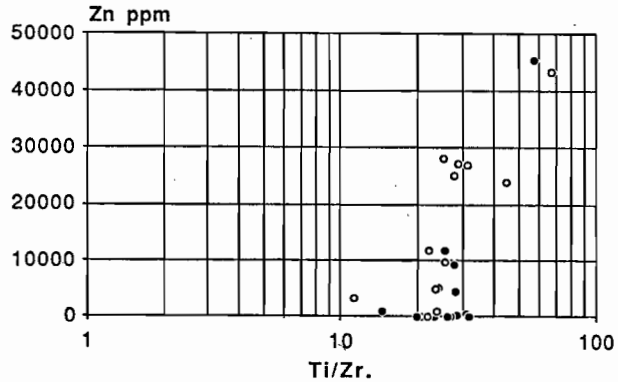

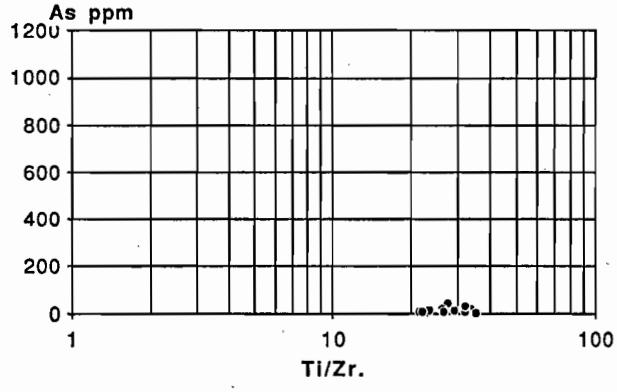

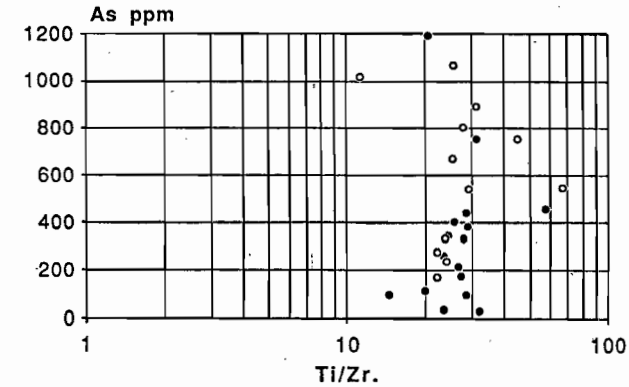

FRESH ANDESITES

Fig. 1. (con.).

FOOTWALL VOLCANICLASTICS

metamorphism or seawater interaction under rock - dominant conditions. The low - Na_2O samples may have experienced more intense alteration.

-Hydrothermally altered andesitic volcaniclastics

These are fragmental rocks of andesitic composition forming the immediate footwall of the PQ - Pnorth massive sulphide lens system at Que River. They are intensely altered and their major and trace element variations are compared to the "fresh" andesites on Figure 1.

The samples show losses of Na_2O, MgO, CaO, Sr and some MnO, gains of K_2O, SiO_2, Rb, Ba, Zn, Pb, As and Cu. Zirconium, TiO_2, Al_2O_3, Y, Sc, Ni, Nb and Cr are conserved.

-Chlorite-pyrite altered footwall rocks

These fine grained black pyritic rocks occur in the footwall of the massive sulphide lenses. No relict primary textures are preserved and their origin is problematical. It is possible that they represent chemical sediments formed from the spent mineralising fluids, but their Ti/Zr ratios would indicate that they are alteration products of an original andesitic composition rock type. Their position in the footwall of the mineralisation supports the latter interpretation, and they may derive from intense alteration of fine grained andesitic epiclastics. Element variation diagrams are presented on Figure 2 and indicate that significant amounts of Sr, SiO_2, Na_2O have been lost from these rocks, while Fe_2O_3, MgO and some MnO have been added.

-Fuchsite-carbonate altered volcaniclastic breccia

Immediately overlying the massive sulphide lenses at Que River is a polymictic fuchsite - carbonate altered volcaniclastic unit ("fuchsite - carbonate breccia"). Geochemical data for a number of samples of this unit are plotted on Figure 2. For most elements the samples lie within the fields for the "fresh" footwall andesites, however, K_2O, Rb, CaO, MnO,and Ba are significantly enriched, and Na_2O has been lost. These patterns would suggest that ore

Fig. 2. Zr/Ti element variation digrams for fuchsite-carbonate altered breccia (solid circles), chlorite-pyrite altered rocks (open circles), western dacites (open circle) and dacite wedge (solid circles) samples.

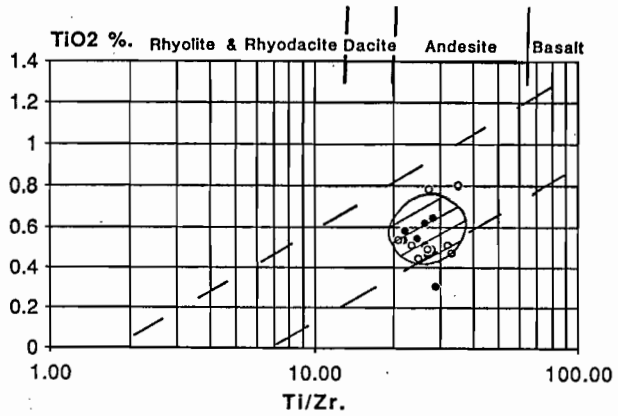

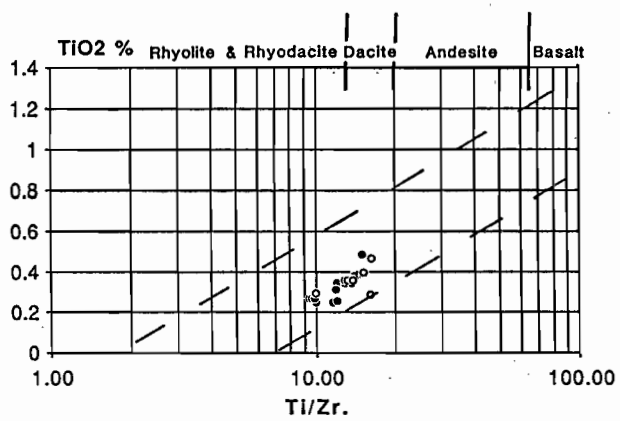

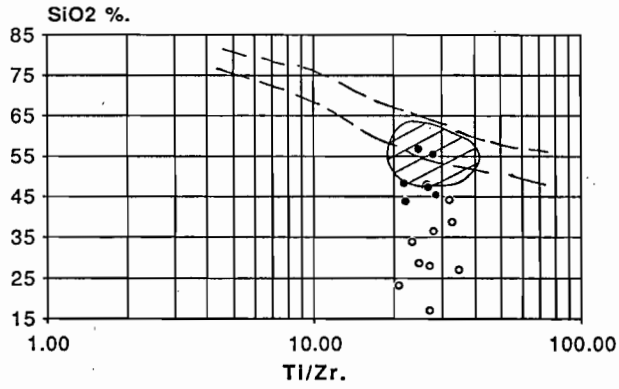

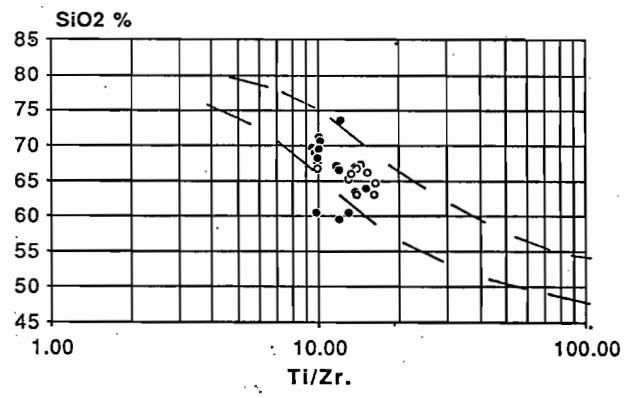

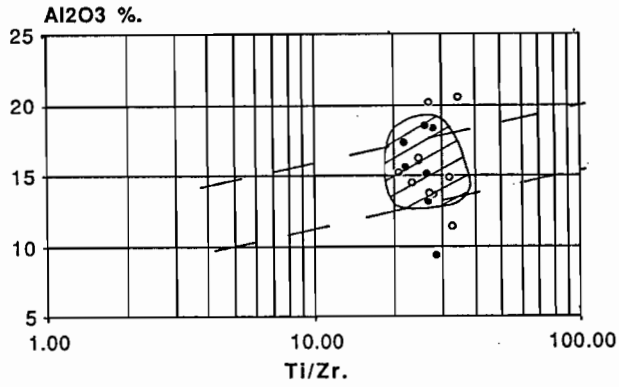

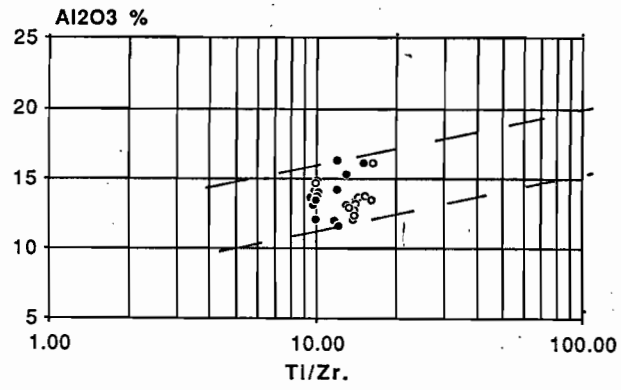

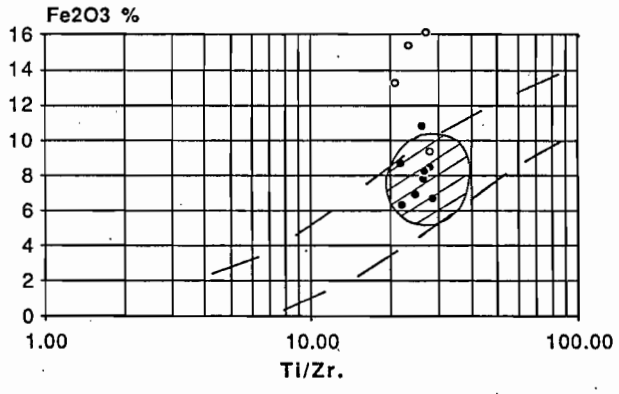

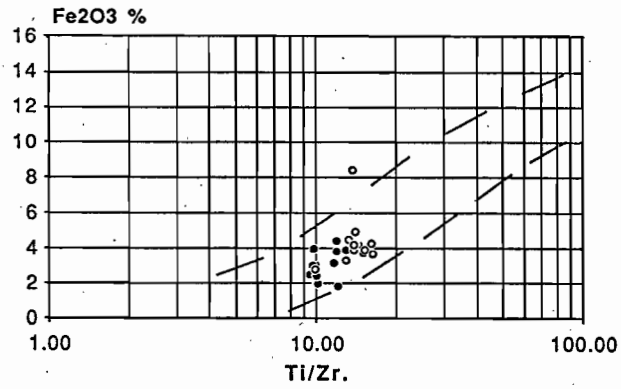

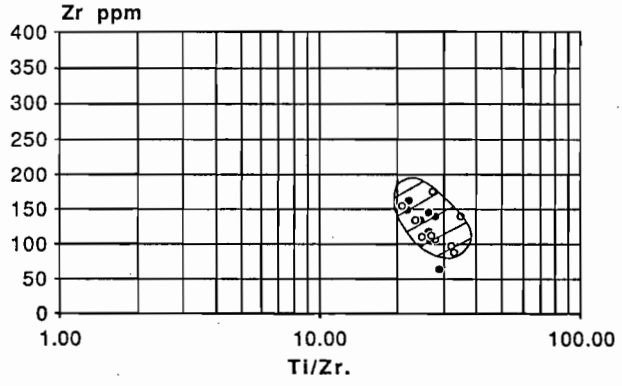

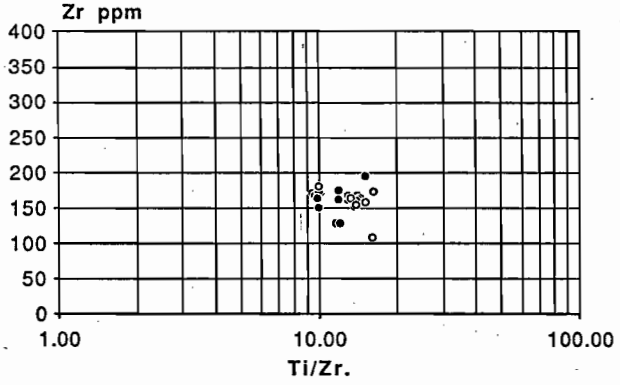

FUCHSITE-CARBONATE BRECCIA
& CHLORITE-PYRITE ALTERED ROCKS

DACITES

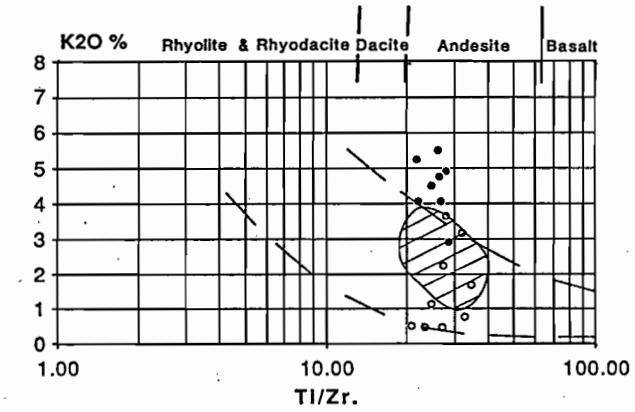

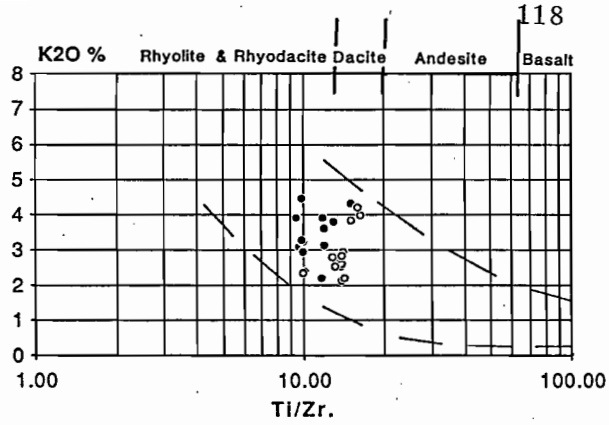

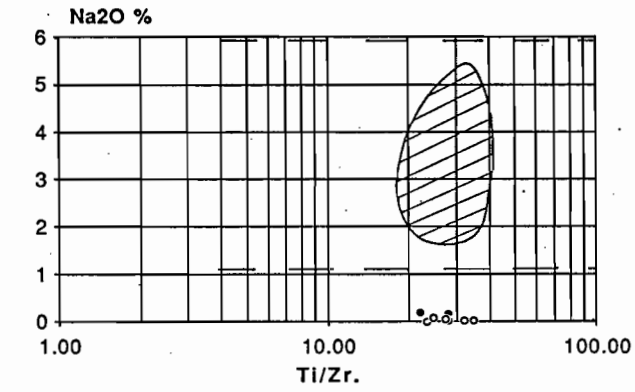

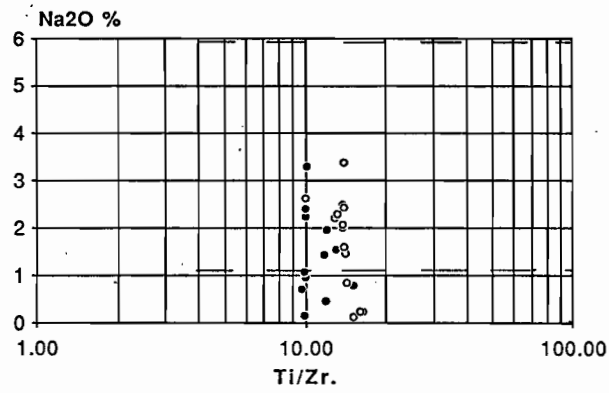

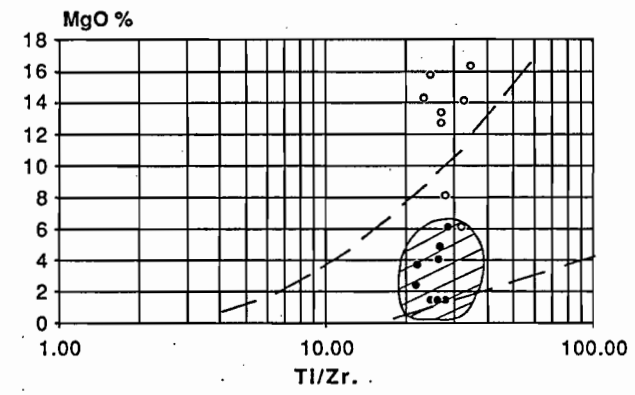

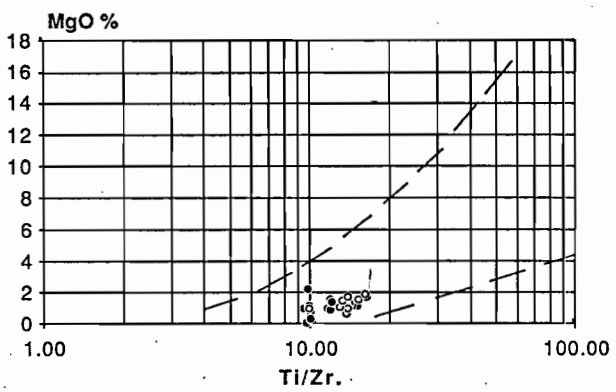

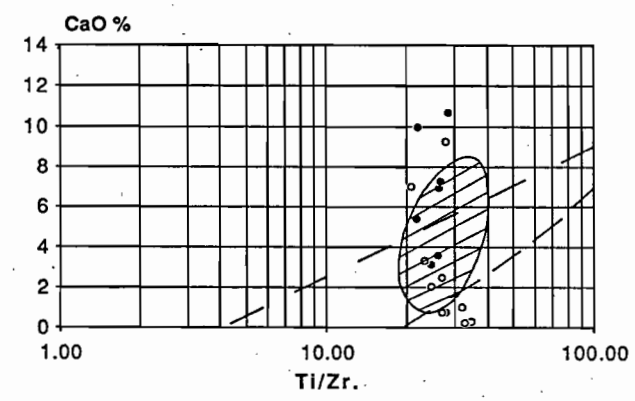

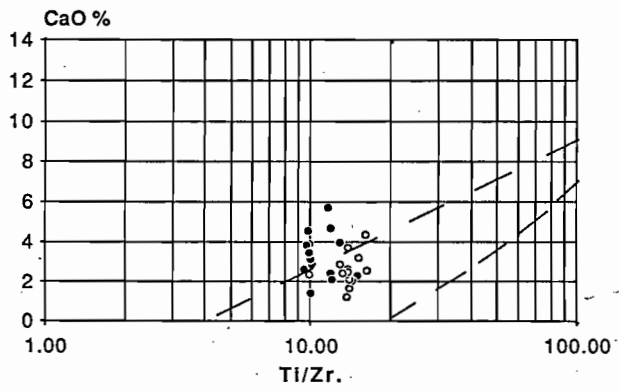

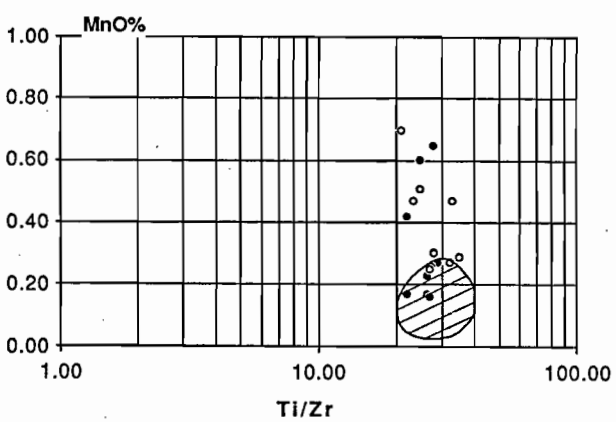

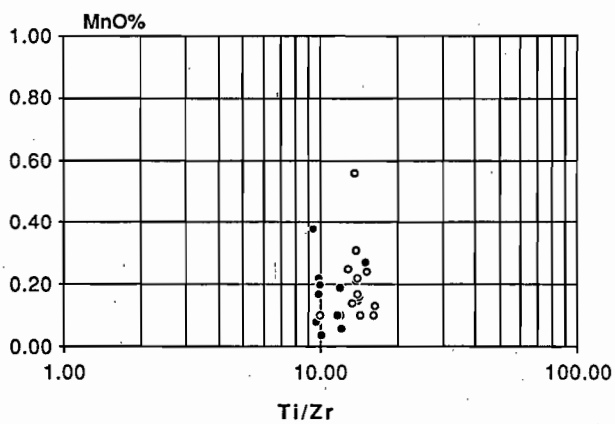

FUCHSITE-CARBONATE BRECCIA & CHLORITE-PYRITE ALTERED ROCKS

Fig. 2 (con.).

DACITES

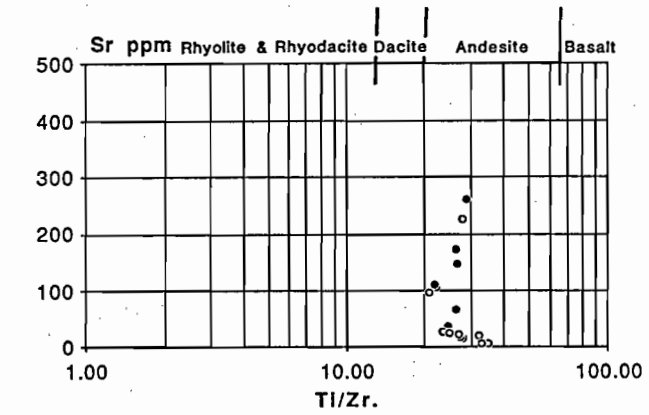

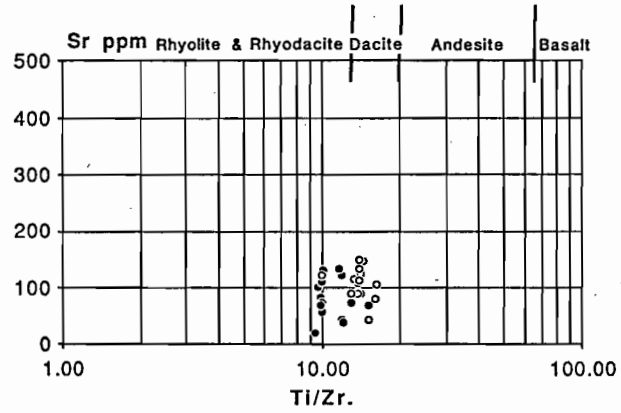

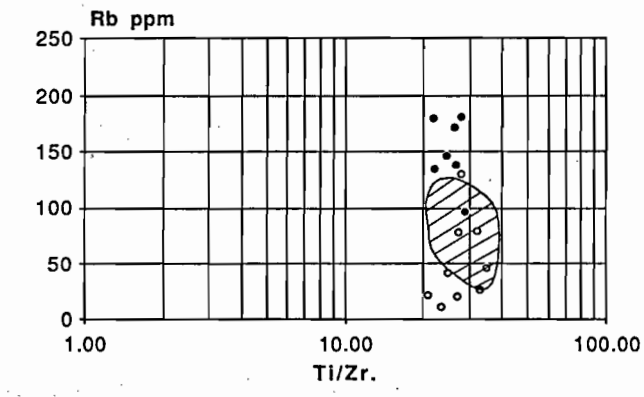

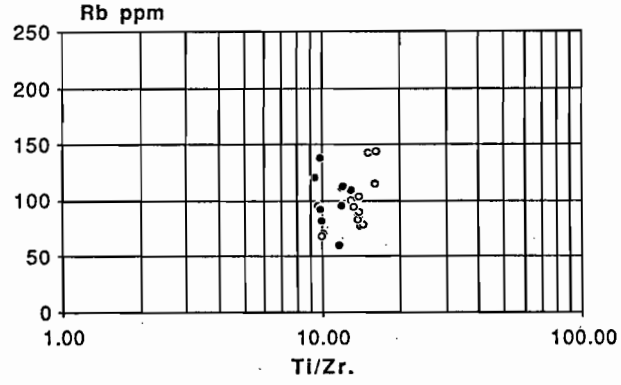

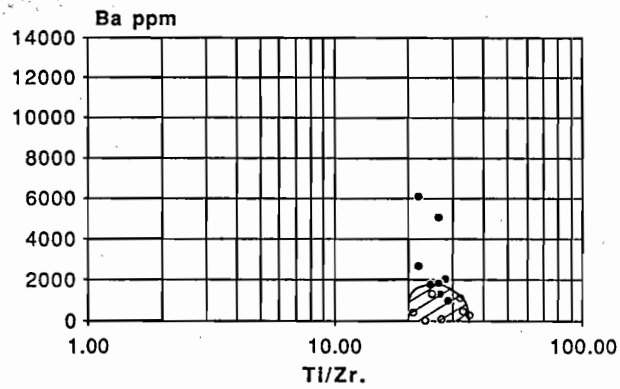

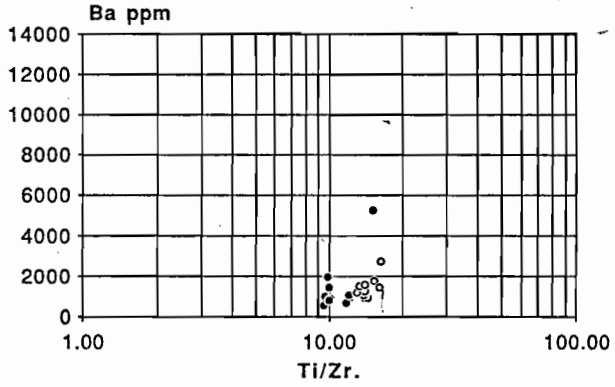

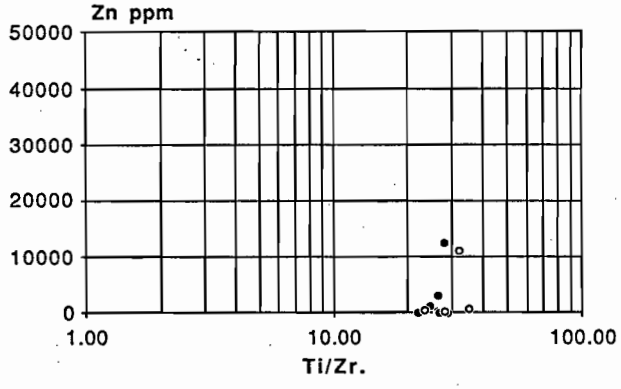

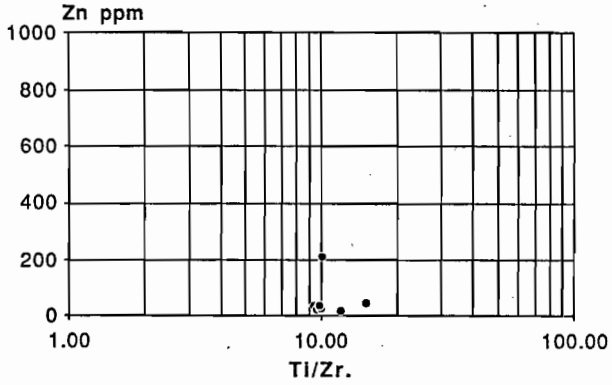

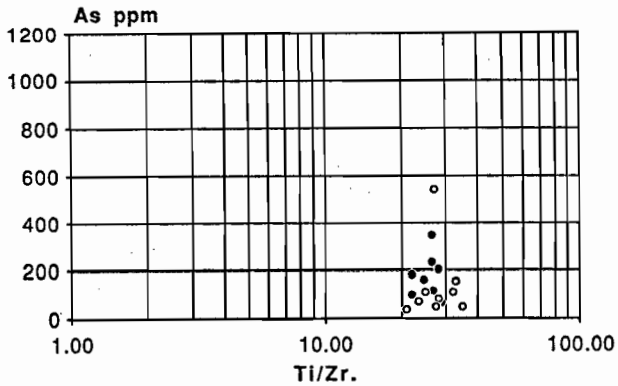

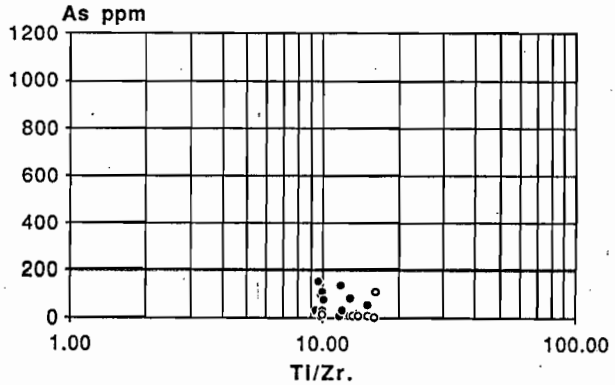

FUCHSITE-CARBONATE BRECCIA & CHLORITE-PYRITE ALTERED ROCKS

DACITES

Fig. 2 (con.).

forming solutions continued to interact with some of the (more permeable ?) overlying rocks after formation of the massive sulphides.

-Dacites

Subsequent to massive sulphide formation the volcaniclastic footwall rocks at Que River were intruded by rocks of dacitic composition (the "western dacites") and similar massive lavas covered the northern part of the massive sulphide body ("the dacite wedge"). These rocks are not mineralised and do not display obvious hydrothermal alteration effects in hand specimen. In thin section the dacites comprise fine grain granular quartz - carbonate - sericite(?) - albite assemblage with minor disseminated pyrite. Although no "fresh" Que River dacites were available for comparative purposes most samples lie within the boundaries defined by the MRV "differentiation" trend and the typical Na_2O depletion and K_2O enrichment exhibited by hydrothermal altered footwall rocks is absent. Furthermore, these dacites are remakably similar chemically to "average" young dacites from western North America of Ewart (1979), only CaO (higher) and Sr (much lower) are different.

Lake Selina, Sterling Valley and Mount Jukes - Mount Darwin Area

Three further data sets are presented here.These comprise MRV samples (Central Volcanic Sequence) from the Mount Jukes - Mount Darwin area collected by Peter Ruxton; Tyndall Group volcanics and volcanogenic sediments from the Lake Selina prospect diamond drill core (S. Hunns) and mixed Tyndall Group and CVS samples from the Sterling Valley (I. Gordon). The major and trace element data for these samples are presented in Table 1, and variation diagrams for major elementst are presented on Fig 3. Geological similarities exist between two areas where the volcanics show granite related alteration effects (Lake Selina and the Jukes - Darwin ridge area). Many samples plot within the MRV "differentation" trend but some have gained K_2O and some have lost Na_2O. Extreme Fe_2O_3 enrichment is observed in many Selina samples and a few from Jukes - Darwin. Alkali mobility and Fe

Fig. 3. Ti/Zr element variation diagrams for Lake Selina samples , Jukes -Darwin samples (open circles) and Sterling Valley samples (solid circles).

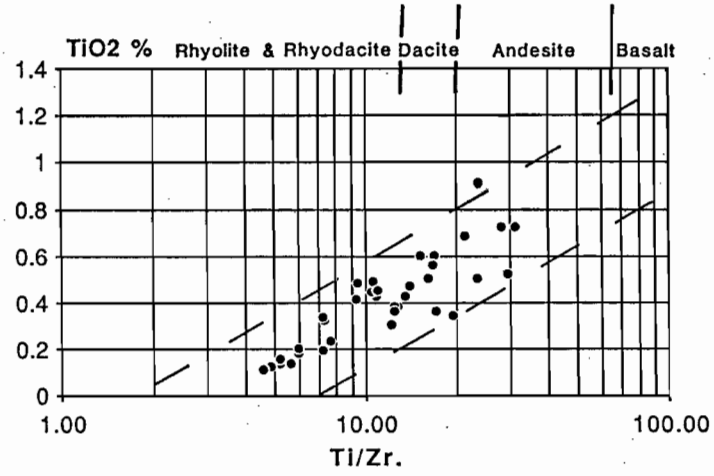

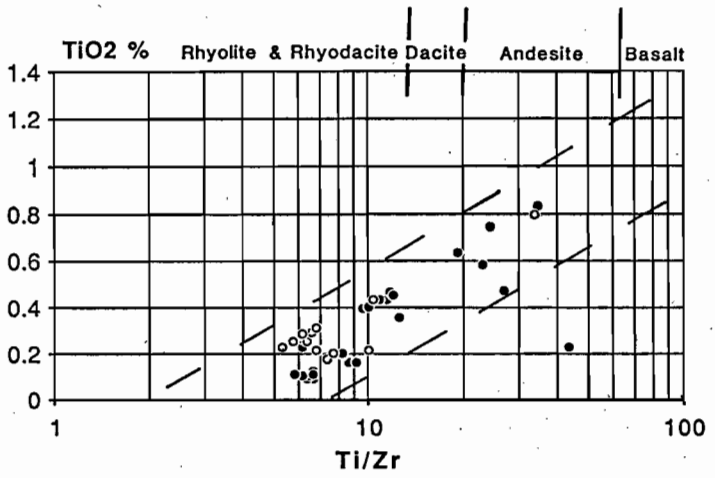

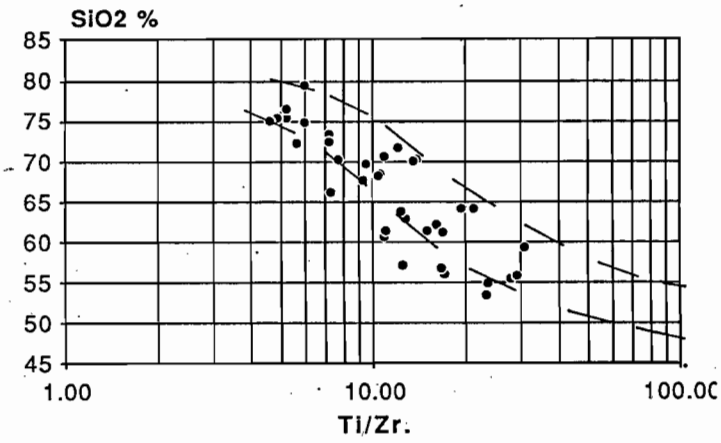

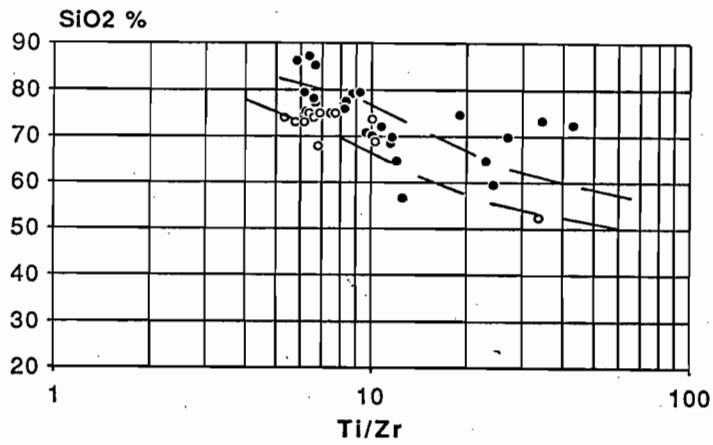

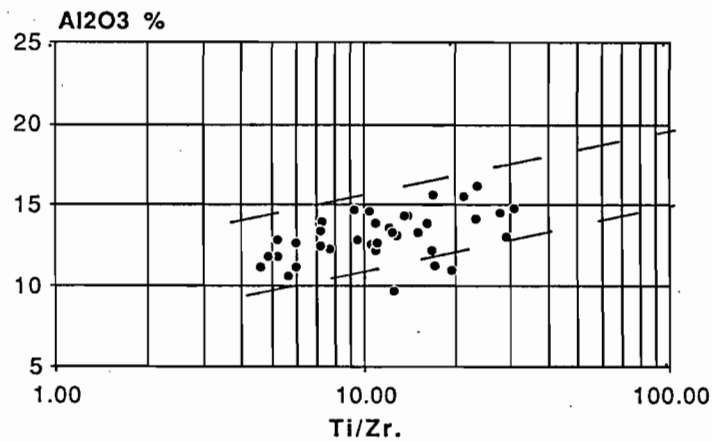

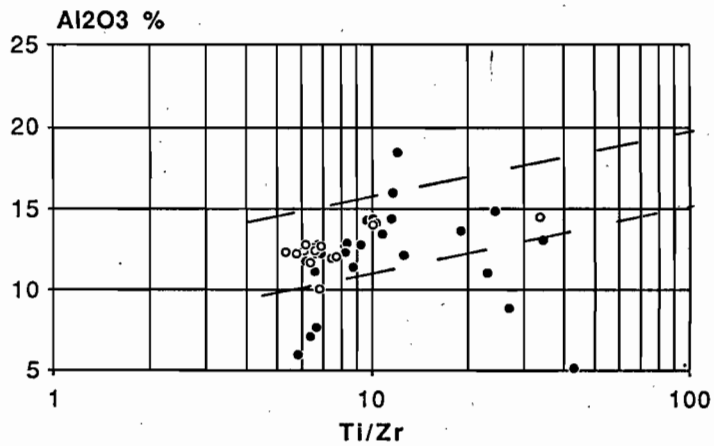

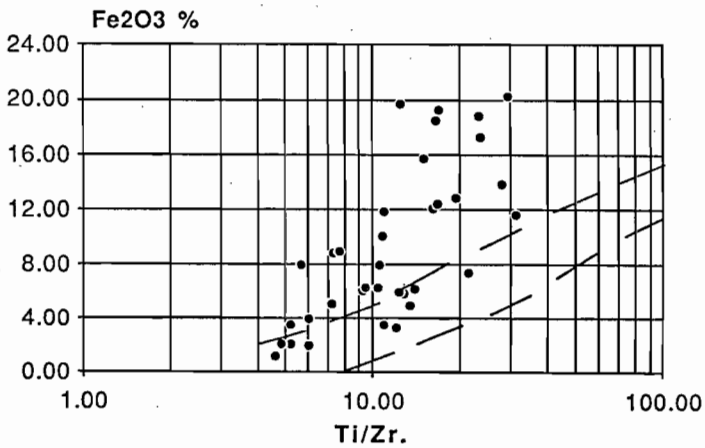

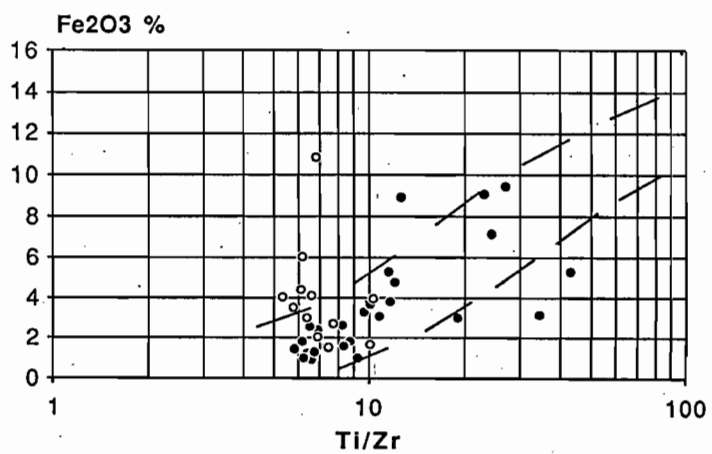

SELINA

JUKES-DARWIN & STERLING VALLEY

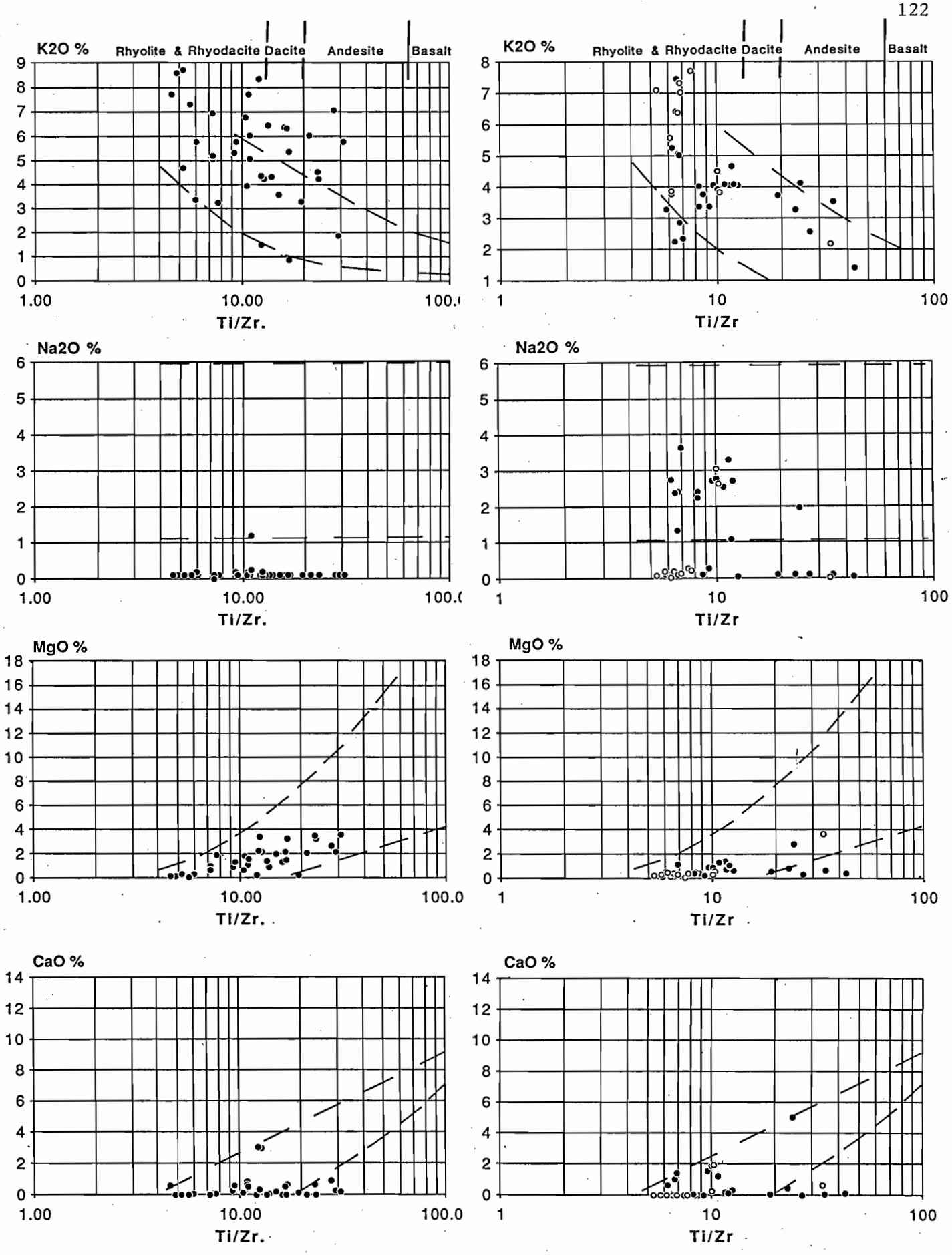

SELINA

JUKES-DARWIN & STERLING VALLEY

Fig. 3.(con.).

enrichment are also features of massive sulphide alteration systems so it appears the major element data displayed here cannot be used to discriminate barren from mineralised systems.

Future Work

Trace and minor element data may be more useful for distinguishing the different alteration styles, and it is planned to use the availble data from Selina and Jukes - Darwin to make a preliminary assessment of possible discriminant elements before proceeding with further analytical work.

Rare earth elements have been used as indicators of massive sulphide alteration systems (Campbell et al., 1984) report on a study of rare earth elements (REE) in altered rocks from Que River. In the light of the newly available REE data base for fresh MRV (Crawford,this report), and the revised geological interpretation at Que River (Large and McGoldrick, 1986), a study of REE in the altered Que River rocks (Whitford et al., 1987) will be re-assessed. Further REE work may be warranted for Que River, and the Selina and Jukes - Darwin samples.

References

Campbell,I.H., Lesher, C.M., Coad, P, Franklin, J.M.,Gorton, M.P. and Thurston, P.C., 1984. Rare-earth element mobility in alteration pipes below massive Cu-Zn sulfide deposits, Chem. Geol., 45, 181 - 202.

Crawford, A.J., 1986. Chemistry of volcanics in the Mount Read Arc - a preliminary report, AMIRA report, April, 1986.

Eastoe, C.J., Solomon, M. and Walshe, J.L., 1987. District scale alteration associated with massive sulfide deposits in the Mt Read Volcanics, Western Tasmania, Econ. Geol. (in press).

Ewart, A., 1979. A review of the mineralogy and chemistry of Tertiay-Recent dacitic, latitic, rhyolitic and related salic volcanic rocks, In: "Trondjhemites, dacites and related rocks", F. Barker (ed), 12 - 121.

Hart, S.R., 1969. K, Rb, Cs contents and K/Rb, K/Cs ratios of fresh and altered submarine basalts, E.P.S.L., 6, 295 - 303.

Hunns, S., 1986. Lake Selina Prospect, AMIRA report, Nov., 1986.

Large, R.R. and McGoldrick, P.J., 1986. Structure and metal distribution in the PQ -P north lens system, Que River Mine, western Tasmania, AMIRA report, April, 1986.

Large, R.R., Crawford, A.J. and Adrichem,S., 1986. Primary and alteration chemistry of the Mount Read Volcanics, AMIRA report, Nov., 1986.

Mottl., m.j. and Seyfried, W.E., 1980. Sub-seafloor hydrothermal systems rock vs seawater dominated, Benchmark Papers in Geology, 56, 66 - 82.

Whitford, D,J., Korsch, M.J., Porritt, P.M. and Craven, S.J., 1987. Rare earth element distribution around the volcanogenic polymetallic sulfide deposit at Que River, Tasmania, Australian Jour. Earth Sci., (in press).

TABLE 1(a): Selina Data.

SAMPLE FIELD NUMBER	T03667	T03673	T03677	T03686	T03689	T03691	T03697	T03699	T04005	T04009	T04011	T04017
SiO2	62.26	54.91	66.25	70.25	73.44	70.34	61.39	56.79	68.52	57.23	60.66	55.59
TiO2	0.51	0.92	0.33	0.24	0.20	0.48	0.61	0.57	0.50	0.37	0.45	0.73
Al2O3	13.85	16.21	13.99	12.31	12.47	14.32	13.34	12.20	12.59	9.71	12.18	14.53
Fe2O3	12.06	17.23	8.83	8.93	5.24	6.22	15.70	18.51	8.02	19.78	10.05	13.80
MnO	0.05	0.19	0.03	0.14	0.12	0.04	0.14	0.12	0.12	0.20	0.18	0.11
MgO	1.31	3.23	0.98	1.95	1.00	0.93	2.01	2.13	1.82	3.44	1.09	2.62
CaO	0.01	0.02	0.02	0.04	0.05	0.08	0.19	0.55	0.18	0.33	0.82	0.93
Na2O	0.10	0.10	0.10	0.10	0.10	0.10	0.10	0.10	0.20	0.20	0.10	0.10
K2O	6.36	4.22	6.95	3.25	5.08	4.31	3.59	6.30	3.94	1.49	7.74	7.07
P2O5	0.04	0.04	0.03	0.04	0.04	0.08	0.15	0.15	0.09	0.08	0.07	0.32
L.O.I.	2.55	3.88	2.02	2.87	2.30	3.45	3.13	2.11	2.52	7.08	5.03	3.22
TOTAL	99.00	100.90	99.59	100.02	100.06	100.35	100.25	99.48	98.30	99.72	98.45	99.02
Ni	11	8	7	9	4	13	8	6	8	14	13	10
Co	34	89	21	29	10	39	43	29	21	336	220	66
Cr	9	14	4	3	1	46	3	6	22	5	18	4
V	107	159	51	33	13	55	82	71	79	51	32	123
Sc	17	21	9	10	6	10	13	11	13	7	4	
Zr	191	236	273	188	167	208	243	207	285	179	249	157
Nb	11	11	12	13	12	18	10	14	16	9	36	13
Y	56	25	27	19	18	58	28	18	26	23	19	19
Sr	121	11	76	8	41	14	11	106	27	17	146	142
Rb	243	240	353	166	217	183	177	227	189	100	175	241
Ba	2699	975	1818	589	1669	605	707	3394	986	201	4976	
As	8	8	10	12	12	44	19	14	21	51	47	37
Sb	7	14	11	<3	<3	<3	<3	5	<3	<3	<3	7
Cu	35	5	7	267	6	393	56	91	5	10	3	21
Pb	19	62	13	100	5	24	10	10	6	10	11	10
Zn	355	600	133	263	168	169	200	158	186	391	79	263

SAMPLE FIELD NUMBER	T04024	T04028	T04067	T04067 DP	T04068	T04069	T04070	T04071	T04071 DP	T04072	T04073	T04076
SiO2	61.47	70.61	61.20	60.67	72.50	64.21	70.14	75.43	75.56	71.80	59.37	53.59
TiO2	0.46	0.43	0.61	0.59	0.34	0.69	0.43	0.14	0.13	0.31	0.73	0.51
Al2O3	12.67	13.88	15.62	15.50	13.41	15.53	14.31	11.88	11.85	13.61	14.78	14.12
Fe2O3	11.90	3.56	12.38	12.27	5.15	7.41	4.94	2.14	2.15	3.28	11.68	18.86
MnO	0.07	0.08	0.05	0.05	0.01	0.09	0.05	0.01	0.02	0.01	0.11	0.22
MgO	1.60	1.05	1.53	1.60	0.68	2.07	1.38	0.22	0.19	0.29	3.60	3.45
CaO	0.52	0.65	0.01	0.00	0.01	0.01	0.02	0.01	0.02	0.01	0.18	0.68
Na2O	0.26	1.20	0.10	0.10	0.01	0.10	0.10	0.10	0.10	0.10	0.10	0.10
K2O	5.08	6.02	5.37	5.25	5.21	6.04	6.46	8.72	8.61	8.37	5.77	4.52
P2O5	0.11	0.10	0.09	0.08	0.08	0.11	0.04	0.04	0.03	0.04	0.14	0.15
L.O.I.	5.53	2.09	3.40	3.40	2.21	3.42	2.42	0.51	0.49	1.53	3.35	3.64
TOTAL	99.67	99.67	100.26	99.41	99.71	99.58	100.19	99.10	99.20	99.25	99.71	99.75
Ni	8	1	14		6	8	8	4	4	4	9	31
Co	83	4	43		14	52	44	10		18	37	101
Cr	21	6	15		7	15	7	1	1	10	45	12
V	76	48	181		51	169	107	4	6	28	238	202
Sc	10	10	24		11	28	14	4	4	9	30	18
Zr	252	238	218		283	195	192	161	161	154	141	132
Nb	14	18	13		15	10	11	15	15	15	8	10
Y	10	22	30		37	25	22	44	43	63	15	21
Sr	72	115	33		53	80	46	166	165	110	69	38
Rb	224	260	312		229	290	331	192	192	235	246	214
Ba	2699	1258	1837		2061	1758	1609	5729	5729	3744	1631	1071
As	41	7	6		4	29	26	11	10	17	6	29
Sb	13	<3	10		3			<3	<3		6	10
Cu	667	6	163		21	24	0	14	17	434	30	533
Pb	26	18	42		4	36	16	12	12	84	42	48
Zn	145	80	416		132	311	209	40	43	84	440	564

TABLE 1(a): Selina Data.

SAMPLE FIELD NUMBER	T04072	T04073	T04076	T04076 DP	T04078	T04082	T04082 DP	T04083	T04084	T04084 DP	T04085	T04086
SiO2	71.80	59.37	53.59	54.22	69.80	62.90	63.89	74.87	72.28	72.21	76.57	68.20
TiO2	0.31	0.73	0.51	0.51	0.49	0.39	0.39	0.19	0.14	0.11	0.16	0.45
Al2O3	13.61	14.78	14.12	14.34	12.89	13.10	13.35	12.70	10.66	10.62	12.87	14.62
Fe2O3	3.28	11.68	18.86	18.81	6.35	5.88	6.01	3.94	8.01	8.11	3.53	6.27
MnO	0.01	0.11	0.22	0.22	0.09	0.35	0.36	0.03	0.01	0.01	0.06	0.20
MgO	0.29	3.60	3.45	3.49	1.37	2.20	2.25	0.31	0.06	0.06	0.35	0.63
CaO	0.01	0.18	0.68	0.70	0.56	2.96	3.04	0.01	0.01	0.01	0.02	0.11
Na2O	0.10	0.10	0.10	0.10	0.10	0.10	0.10	0.10	0.10	0.01	0.10	0.10
K2O	8.37	5.77	4.52	4.51	5.76	4.25	4.37	5.78	7.30	7.30	4.68	6.77
P2O5	0.04	0.14	0.15	0.16	0.11	0.15	0.18	0.02	0.05	0.03	0.02	0.08
L.O.I.	1.53	3.35	3.64	3.73	2.48	6.33	6.43	1.59	0.57	0.56	1.94	2.26
TOTAL	99.25	99.71	99.75	100.72	99.90	98.51	100.27	99.45	99.73	99.06	100.20	99.59
Ni	4	9	31		6	14	13	2	2		1	3
Co	18	37	101		89	14		3	6			13
Cr	10	45	12		20	7	5	1	1		1	3
V	28	238	202		78	90	86	8	10		9	47
Sc	9	30	18		14	9	9	7	4		7	13
Zr	154	141	132		313	183	189	190	149		186	260
Nb	15	8	10		14	11	11	17	10		17	15
Y	63	15	21		23	24	23	37	40		41	39
Sr	110	69	38		64	35	35	54	107		12	57
Rb	235	246	214		271	300	309	269	210		262	289
Ba	3744	1631	1071		1415	387	388	1479	3882		589	2006
As	17	6	29		7	6	4	12	21		12	14
Sb		6	10					7	15		<3	5
Cu	434	30	533		2	7	2	6	41		9	3
Pb	84	42	48		11	145	145	29	44		7	8
Zn	84	440	564		182	624	608	186	38		181	503

SAMPLE FIELD NUMBER	T04087	T04088	T04089	T04091	T04092	T04092 DP	T04093	T04094	T04095	T04123	T04124
SiO2	67.78	75.17	55.87	56.14	79.44	79.42	64.19	52.94	67.92	59.33	62.10
TiO2	0.42	0.12	0.53	0.37	0.21	0.21	0.35	0.53	0.32	0.45	0.45
Al2O3	14.66	11.23	13.05	11.31	11.18	11.06	10.99	13.22	12.78	13.07	13.49
Fe2O3	6.07	1.17	20.27	19.29	2.01	2.02	12.84	18.69	9.33	15.54	15.90
MnO	0.19	0.13	0.57	0.31	0.17	0.16	0.01	0.30	0.01	0.05	0.05
MgO	0.94	0.20	2.18	3.21	0.30	0.83	0.26	1.85	0.19	1.09	1.13
CaO	0.23	0.60	0.27	0.67	0.09	0.10	0.13	0.24	0.06	0.14	0.14
Na2O	0.20	0.10	0.10	0.10	0.20	0.10	0.10	0.10	0.10	0.10	0.10
K2O	5.31	7.73	1.86	0.89	3.36	3.35	3.27	3.08	3.77	8.07	4.36
P2O5	0.09	0.03	0.12	0.53	0.07	0.08	0.12	0.12	0.04	0.14	0.12
L.O.I.	2.54	1.27	6.13	6.26	2.34	2.33	7.70	8.60	6.02	1.60	2.81
TOTAL	98.23	97.77	100.85	99.02	99.17	99.56	99.86	99.57	100.45	99.55	100.55
Ni	1	1	3	69	3		42			8	8
Co	9	3	39	24	1		20	20		18	8
Cr	5	1	1	90	9		70			24	15
V	52	1	182	93	25		112			128	128
Sc	14	6	20	10	10		13			14	17
Zr	273	157	109	131	211		109			172	285
Nb	16	15	6	10	11		8			8	14
Y	34	28	25	40	35		38			23	22
Sr	23	159	6	8	4		6			117	34
Rb	278	180	81	37	121		118			227	449
Ba	1062	5117	320	175	484		424			4162	961
As	9	11	60	219	15		35			93	16
Sb	<3	<3	<3	7	<3		<3			39	10
Cu	56	13	512	312	35		34			25	3
Pb	116	177	148	513	4		6			33	8
Zn	867	320	1354	9800	10		332			580	309

TABLE 1(a): Selina Data.

SAMPLE FIELD NUMBER	T04125	T04126	T04127	T04128	T04129	T04130	T04131	T04135	T04135 DP	T04136	T04137	T04137 DP
SiO2	64.30	67.30	76.09	65.80	63.54	75.34	77.13	71.20	71.76	64.53	67.93	66.83
TiO2	0.56	0.40	0.09	0.12	0.57	0.15	0.13	0.48	0.48	0.61	0.53	0.53
Al2O3	15.77	13.47	11.80	11.34	15.66	12.15	11.29	13.42	13.59	14.33	14.11	13.83
Fe2O3	7.32	7.25	2.74	15.54	11.82	2.48	1.31	4.29	4.27	5.81	4.60	4.54
MnO	0.07	0.04	0.01	0.11	0.14	0.03	0.05	0.07	0.08	0.23	0.24	0.24
MgO	2.35	0.93	0.21	0.95	1.66	0.32	0.40	0.93	0.96	2.42	1.93	1.88
CaO	0.30	0.34	0.02	0.06	0.20	0.05	0.69	0.51	0.53	4.31	3.47	3.42
Na2O	0.10	0.10	0.10	0.10	0.10	0.25	0.82	0.60	0.46	2.65	3.11	2.89
K2O	6.54	9.25	7.39	2.41	4.61	7.67	6.43	6.05	6.04	2.42	2.53	2.46
P2O5	0.19	0.24	0.02	0.03	0.14	0.02	0.02	0.10	0.10	0.13	0.13	0.12
L.O.I.	2.18	0.97	0.89	3.28	2.81	0.82	1.31	1.93	1.92	2.16	1.68	1.67
TOTAL	99.58	100.19	99.26	99.64	101.25	99.28	99.58	99.58	100.19	99.60	100.26	98.41
Ni	6	3	2	8	5	1	1	2	2	4	3	3
Co	23	11	4	45	21	9		3		9	9	
Cr	19	13	19	1	25	1	1	1	2	21	16	15
V	125	83	125	251	181	14	8	42	50	135	104	95
Sc	9	15	3	1	19	4	3	17	17	21	18	
Zr	190	225	104	108	201	140		377	373	131	218	209
Nb	11	12	13	9	11	13		17	16	14	13	12
Y	12	26	15	16	23	16		31	32	40	36	36
Sr	5	166	132	11	21	148		57	56	352	345	336
Rb	197	196	166	111	243	233		290	287	153	148	143
Ba	425	5014	3042	246	595	2637	2371	1105	1110	434	604	
As	13	12	8	32	9	12	14	10	11	9	6	6
Sb	5		<3	5	5	<3	<3	8	9	4	<3	<3
Cu	263	1	263	728	1	1	3	1	2	2	3	1
Pb	6	26	8	124	32	19	15	10	10	31	32	35
Zn	216	233	77	1754	456	66	52	121	129	221	198	190

TABLE 1(b): Jukes - Darwin Data.

SAMPLE #	JD1	JD2	JD3	JD4	JD5	JD6	JD7	JD8	JD9
SiO2	73.5	73.17	75.34	68.25	75.33	74.41	75.1	74.15	52.78
TiO2	0.27	0.26	0.26	0.22	0.18	0.23	0.21	0.3	0.8
Al2O3	12.48	12.26	11.7	10.07	12.02	12.41	12.1	12.53	14.48
Fe2O3	4.4	3.51	3	10.83	1.55	4.07	2.7	4.16	20.22
MnO	0.03	0.01	0.01	0.01	/,.01	<.01	0.01	0.02	0.11
MgO	0.61	0.3	0.19	0.29	0.09	0.26	0.39	0.41	3.62
CaO	<.02	<.02	<.02	<.02	0.02	<.02	<.02	<.02	0.63
Na2O	0.12	0.19	0.2	0.15	0.29	0.08	0.22	0.1	0.02
K2O	5.6	8.65	8.23	7.32	8.94	7.1	7.73	6.41	2.21
P2O5	0.05	<.03	<.03	0.14	0.04	<.03	0.03	<.03	0.54
TOTAL	99.21	99.52	99.78	99.37	99.4	99.96	99.92	99.97	99.78
LOI	2.15	1.17	1.05	2.11	0.94	1.35	1.43	1.89	4.37
Nb	14	11	12	11	13	13	12	14	6
Zr	266	272	245	195	146	3	164	273	143
Y	30	20	32	172	34	45	15	34	32
Sr	16	63	69	55	74	29	83	33	11
Rb	203	187	182	173	208	206	188	213	129
Zn	108	35	34	96	10	27	44	62	405
Cu	0	42	96	182	11	4	17	11	94
Ni	3	2	2	4	2	2	2	2	56
Cr	4	3	3	6	2	<2	4	4	770
V	10	8	7	7	4	11	20	6	322
As	<3	<3	<3	<3	9	<3	<3	3	<3
Pb	107	9	5	6	15	14	15	14	7
Ba	1080	2830	2680	2280	3710	1620	2425	1500	150
Sc	8	8	8	7	6	7	7	8	32
Bi	7	<2	<2	<2	<2	<2	<2	<2	<2

SAMPLE #	JD10	JD11	JD12	JD13
SiO2	73.46	75.34	69.07	74.02
TiO2	0.29	0.32	0.44	0.22
Al2O3	12.83	12.77	14.14	14.01
Fe2O3	6.05	2.06	3.96	1.68
MnO	0.05	0.01	0.15	0.02
MgO	0.54	0.35	0.59	0.36
CaO	<.02	<.02	1.97	0.28
Na2O	0.04	0.14	2.64	3.04
K2O	3.86	7.03	3.85	4.51
P2O5	0.04	<.03	0.08	0.03
TOTAL	99.99	99.53	99.97	99.73
LOI	2.83	1.51	3.08	1.56
Nb	15	15	14	14
Zr	284	281	256	132
Y	44	27	39	18
Sr	5	26	93	138
Rb	220	217	161	135
Zn	127	20	94	41
Cu	53	3	3	<2
Ni	3	2	1	1
Cr	2	5	2	<2
V	10	10	41	21
As	10	<3	<3	<3
Pb	303	8	10	6
Ba	510	1960	1200	1395
Sc	7	7	12	3
Bi	<2	<2	<2	<2

TABLE 1(c): Sterling Valley Data.

Sample #	STV 232	STV 234	STV 236	STV 237	STV 238	STV 239	STV 240	STV 241	STV 242
SiO2	79.55	85.74	77.95	76.13	68.69	79.94	87.47	77.52	78.44
TiO2	0.17	0.1	0.2	0.21	0.44	0.23	0.1	0.13	0.11
Al2O3	11.5	7.68	12.94	12.41	14.39	11.82	7.08	12.26	11.2
Fe2O3	1.85	1.14	1.63	2.64	5.3	1.83	1.29	1.2	0.95
MnO	0.02	0.01	0.01	0.06	0.07	0.01	0.02	0.02	0.01
MgO	0.38	0.43	0.53	0.42	1.39	0.36	0.2	0.36	0.13
CaO	<0.02	<0.02	0.03	0.05	0.11	<0.02	<0.02	0.02	0.02
Na2O	<0.2	<0.2	2.4	2.25	3.3	<0.2	<0.2	1.33	<0.2
K2O	3.77	2.86	3.4	4.05	4.07	3.79	2.27	5.07	7.47
P2O5	<0.03	<0.03	<0.03	<.03	0.08	0.04	<0.03	0.02	<0.03
LOI	1.92	1.51	1.62	1.68	1.82	1.87	1.55	1.4	0.84
Sum	99.16	99.47	100.71	99.9	99.66	99.89	99.98	99.33	99.17
Nb	12	12	14	13	11	16	10	14	12
Zr	118	90	145	153	231	225	95	118	101
Y	16	16	28	25	29	30	10	21	25
Sr	3	5	36	47	68	3	3	36	66
Rb	290	138	178	189	120	256	256	242	280
Zn	17	15	25	21	112	21	34	26	368
Cu	5	3	8	9	10	<2	<2	5	13
Ni	2	<1	<1	2	4	<1	<1	1	1
Cr	7	3	6	9	13	<2	5	8	2
V	14	6	17	16	86	7	9	10	7
As	147	<3	4	9	6	<3	3	4	124
Pb	203	2	11	42	24	<2	15	17	226
Ba	347	508	732	1087	1803	1242	210	935	2129
Sc	2	4	5	3	11	9	2	4	5

Sample #	STV 244	STV 245	STV 247	STV 248	STV 249	STV 251	STV 252	STV 255	STV 256A
SiO2	56.9	70.21	64.75	72.61	70.02	75.09	79.81	65.07	71
TiO2	0.36	0.47	0.59	0.23	0.48	0.64	0.17	0.46	0.4
Al2O3	12.18	15.99	11.1	5.17	8.92	13.71	12.88	18.46	14.32
Fe2O3	8.94	3.87	9.08	5.33	9.48	3.05	1.01	4.8	3.36
MnO	5.56	0.07	1.38	1.4	0.02	0.04	<0.01	0.04	0.1
MgO	0.66	0.77	0.8	0.4	0.35	0.59	0.24	1.07	0.89
CaO	0.33	0.17	0.46	0.15	0.01	0.05	<0.02	0.1	1.57
Na2O	0.06	1.07	<0.2	0.05	<0.2	<0.2	0.29	2.71	2.72
K2O	4.08	4.67	3.31	1.43	2.59	3.76	3.39	4.11	4.07
P2O5	0.1	0.14	0.26	0.07	0.11	0.05	0.03	0.08	0.07
LOI	8.58	2.38	7.5	5.45	7.15	2.83	1.99	2.87	1.67
Sum	99.39	99.81	99.86	99.51	100.03	99.81	99.81	99.77	100.17
Nb	9	13	11	4	10	10	13	12	17
Zr	173	242	154	32	107	201	111	230	251
Y	24	30	86	5	12	39	23	35	40
Sr	4	17	15	7	13	6	76	95	217
Rb	280	212	309	123	173	186	168	285	206
Zn	9082	118	4610	0	203	60	14	152	98
Cu	239	10	1399	127	74	9	6	19	4
Ni	8	5	39	46	34	1	1	2	<1
Cr	14	11	141	64	88	5	10	7	4
V	82	103	142	144	124	37	18	45	38
As	7	<3	91	88	449	4	7	8	<3
Pb	3018	69	619	0	0	17	22	643	22
Ba	764	1050	397	256	330	647	750	2358	1082
Sc	10	13	15	7	11	17	3	10	10

TABLE 1(c): Sterling Valley Data.

Sample #	STV 256B	STV 257	STV 258	STV 259	STV 261	STV 263	STV 264	STV 267	STV 268
SiO2	70.3	75.51	74.6	59.75	75.3	86.73	73.93	72.35	73.68
TiO2	0.41	0.11	0.12	0.75	0.22	0.12	0.3	0.44	0.84
Al2O3	14.38	12.84	12.88	14.89	12.32	6.06	12.66	13.47	13.12
Fe2O3	3.72	1.05	1.37	7.16	2.45	1.51	2.61	3.08	3.21
MnO	0.1	0.05	0.07	0.21	0.09	0.01	0.02	0.09	0.04
MgO	0.92	0.29	0.42	2.86	1.17	0.14	0.36	1.36	0.65
CaO	1.88	0.67	1.04	5.06	1.41	0.03	0.04	1.25	0.09
Na2O	2.76	2.73	2.41	1.97	3.64	<0.2	2.38	2.55	<0.2
K2O	3.93	5.28	5.05	4.14	2.37	3.29	6.44	4.11	3.55
P2O5	0.08	<0.03	0.03	0.18	0.04	<0.03	0.03	0.09	0.13
LOI	1.76	0.86	1.48	1.81	1.77	1.24	0.73	1.54	4.15
Sum	100.24	99.39	99.47	98.78	100.78	99.13	99.5	100.33	99.46
Nb	16	21	17	14	14	6	14	15	15
Zr	246	107	108	184	192	124	277	245	147
Y	38	34	36	30	43	14	41	40	27
Sr	246	121	108	423	114	16	78	125	28
Rb	182	230	233	208	146	266	159	146	203
Zn	93	28	55	483	73	26	76	213	181
Cu	4	4	7	31	6	6	<1	9	54
Ni	<1	1	1	9	10	2	2	9	29
Cr	8	5	6	34	9	6	<2	29	139
V	42	10	13	168	38	8	7	62	149
As	<3	<3	<3	5	3	<3	<3	17	74
Pb	18	11	20	80	20	13	24	72	887
Ba	1063	571	516	1252	425	538	2267	1000	599
Sc	11	3	3	23	8	3	6	13	18

GOLDEN GROVE - SCUDDLES DEPOSIT

P.A. RUXTON

11.8.87

1.0 INTRODUCTION

Three aspects of the Scuddles Deposit were further investigated:-

1. Down hole metal distribution,
2. Metal v Gold plots, and
3. Ore Mineralogy and Texture

2.0 DOWN HOLE METAL DISTRIBUTION

Four down hole metal plots are presented to illustrate the relationships between metal distribution, massive sulphide lithology and magnetic susceptibility. The four drillholes were chosen to incorporate all major aspects of the deposit. Drillhole locations are presented on Figure 1.

a) SC 124 Drillhole intersects the main Massive Zinc ore zone in an area with high zinc, lead, silver and gold concentrations (Plan 1 - B, C, E and F - Ruxton, 1986). The hole intersects copper-rich stringer material which forms part of the major hydrothermal fluid locus (Plan 3 - D) - Figure 2.

b) SC 200 Drillhole passes through a zone of medium zinc grade in the Massive Zinc Ore and then into copper-rich Stringer Ore (Plan 1 - B and Plan 3 - D, Ruxton, 1986) - Figure 3.

c) SC 113A Drillhole crosscuts the copper-rich Massive Pyrite Ore where pyrite and chalcopyrite have overprinted original zinc-rich massive sulphide (Plan 2 - D) - Figure 4.

d) SC 21 II Wedge Drillhole intersects a peripheral zinc and gold-rich portion of the massive sulphide. This is located on the southern end of the `inverted - V' structure (Plan 1 - B and F) - Figure 5.

Conclusions

Within the Massive Sphalerite and Massive Pyrite Ores there is a direct relationship of zinc to lead to silver grade. These metals are generally concentrated towards the top of the massive sulphide body (Figs. 2 and 3).

In contrast copper is concentrated towards the base of the massive sulphide and in the stringer zone, spatially distint from the zinc-rich ore (Figs. 2 and 3).

Gold is evenly distributed throughout the massive sulphide lens generally at 1ppm or larger levels (Figs. 2, 3 and 5). The highest grades of gold do not correspond to zinc, lead, silver or copper highs (Fig. 2). Despite the concentration of copper in the stringer zone and gold in the massive sulphide zone where copper kicks gold does also (Figs. 2 and 3). This may represent a fundamental association between the two metals.

The copper-rich portion of the massive sulphide illustrated by SC 113A (Fig. 4) is distinct from the general trends of the Scuddles Deposit. The concentration of copper towards the top of the massive sulphide is unusual. There is also no clear correlation between zinc, lead or silver. A very general relationship between copper, silver and gold is suggested. Ore textures in this zone suggest overprinting of sphalerite, magnetite ore assemblages by pyrite, chalcopyrite and pyrrhotite. This overprinting of copper and iron and corresponding depletion of zinc, lead and possibly silver may account for the anomalous metal distribution in this area.

Magnetic susceptibility data on Figures 2, 3 and 4 indicates high values associated with the massive sulphide lithology. More erratic but often high readings occur in the stringer zone. High values in the stringer zone and in SC 113A (Fig. 4) are related to pyrrhotite which closely follows the distribution of chalcopyrite. High magnetic susceptibilities in the copper-poor massive sulphide are related to disseminated magnetite.

3.0 METAL V GOLD PLOTS

Drillhole assay data stored on computer tape was plotted. To reduce the large quantity of data and to establish some data control, information on three principle sections was separated and plotted, Sections 22240N, 22140N and 22040N. On each section the data was divided into four different ore types:-

1. Massive Sphalerite (>15% Zn) corresponding to visible massive sphalerite ore (>50% Zn sphalerite).

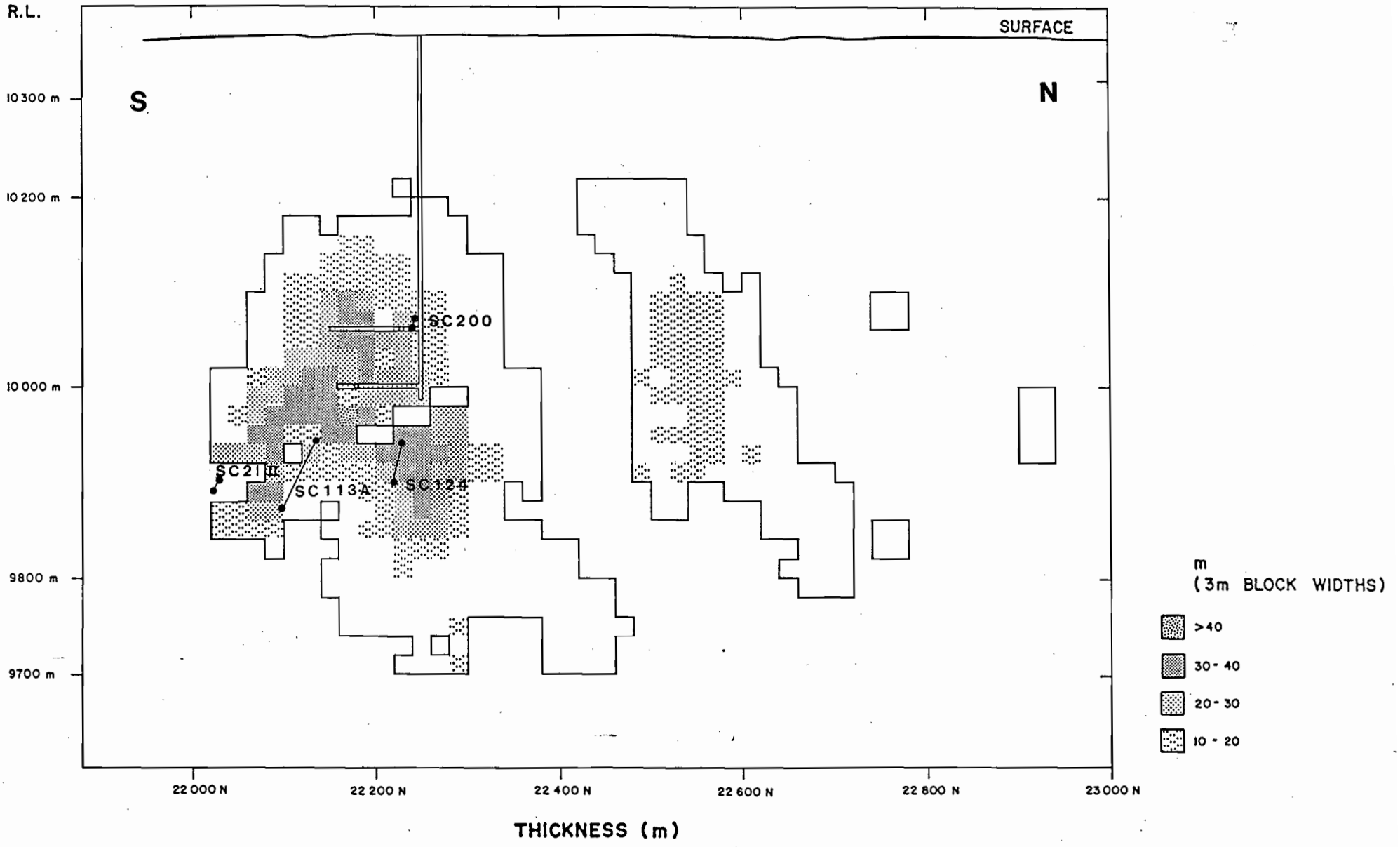

FIG. 1 POSITION OF DETAILED DRILLHOLE LOGS

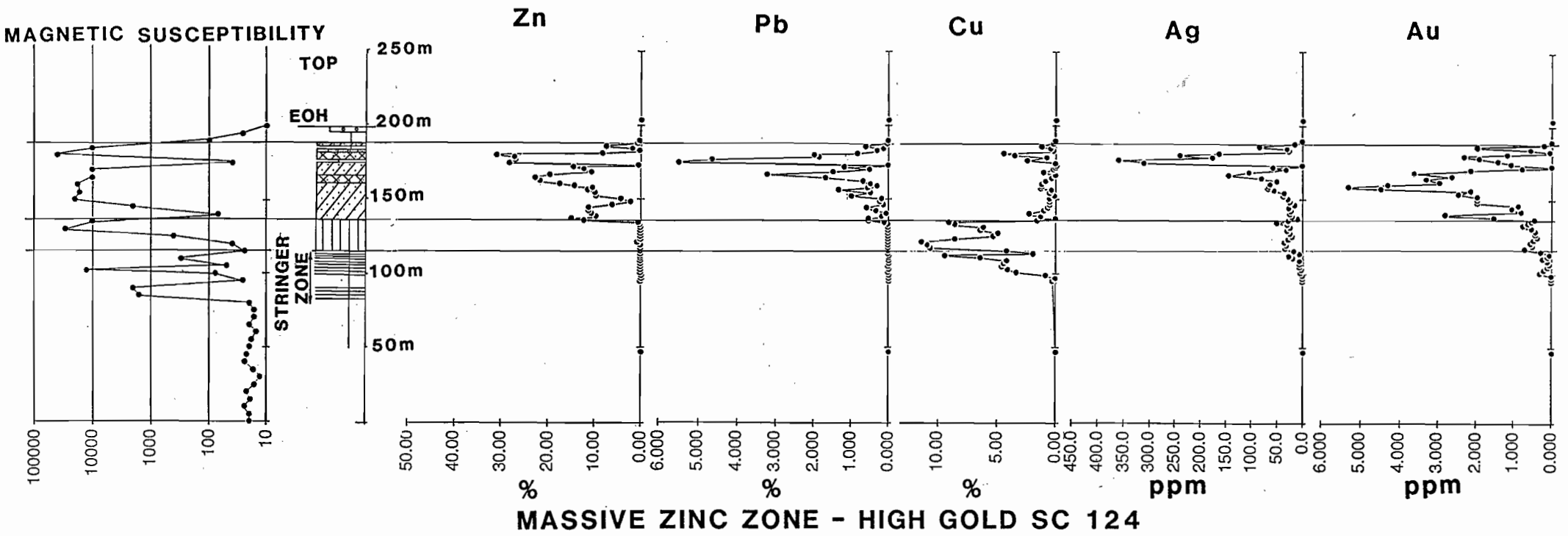

MASSIVE ZINC ZONE - HIGH GOLD SC 124

Massive Pyrite

Massive Sphalerite

Copper-rich Massive Pyrite

Disseminated magnetite

FIG. 2 DRILLHOLE SC 124 - SECTION 2224ON - MASSIVE ZINC ZONE - HIGH GOLD:

Zinc concentration correlates closely with lead and silver. Highest copper grades occur at the base of the massive sulphide and in the stringer zone. Gold is preferrentially concentrated in the massive sulphide. Note that the highest gold grades do not correlate with the maximum zinc grade. Despite the fact that copper concentrates in the stringer zone and lower massive sulphide, and gold in the massive sulphide itself; where copper peaks so does gold. High magnetic susceptibilities in the stringer zone are related to the occurrence of pyrrhotite which is typically associated with copper.

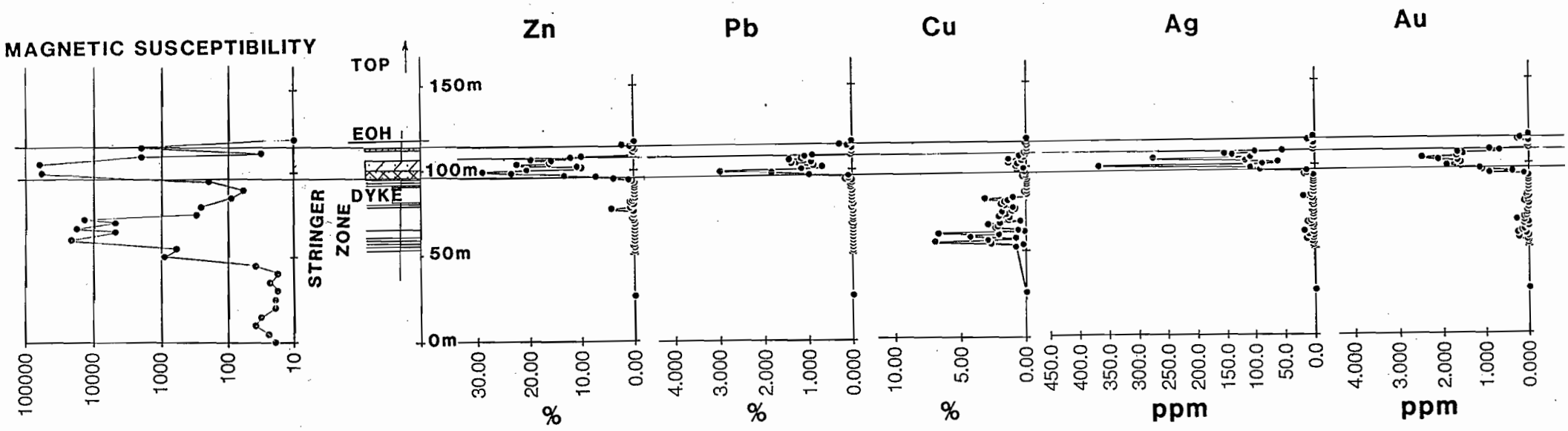

MARGINAL MASSIVE ZINC ZONE - COPPER-RICH STRINGER SC 200

/// Massive Pyrite

Massive Sphalerite

Disseminated magnetite

FIG. 3 DRILLHOLE SC 200 - SECTION 22240N - MARGINAL MASSIVE ZINC ZONE - COPPER-RICH STRINGER

A close correlation between zinc, lead and silver concentration is evident on this section. Copper is almost totally related to the stringer zone. Gold is elevated in the massive sulphide but doesn't peak with zinc, lead or silver. Despite the obvious distinction between copper and gold concentrations, where copper shows a peak, so does gold. High magnetic susceptibilities in the stringer zone are related to pyrrhotite.

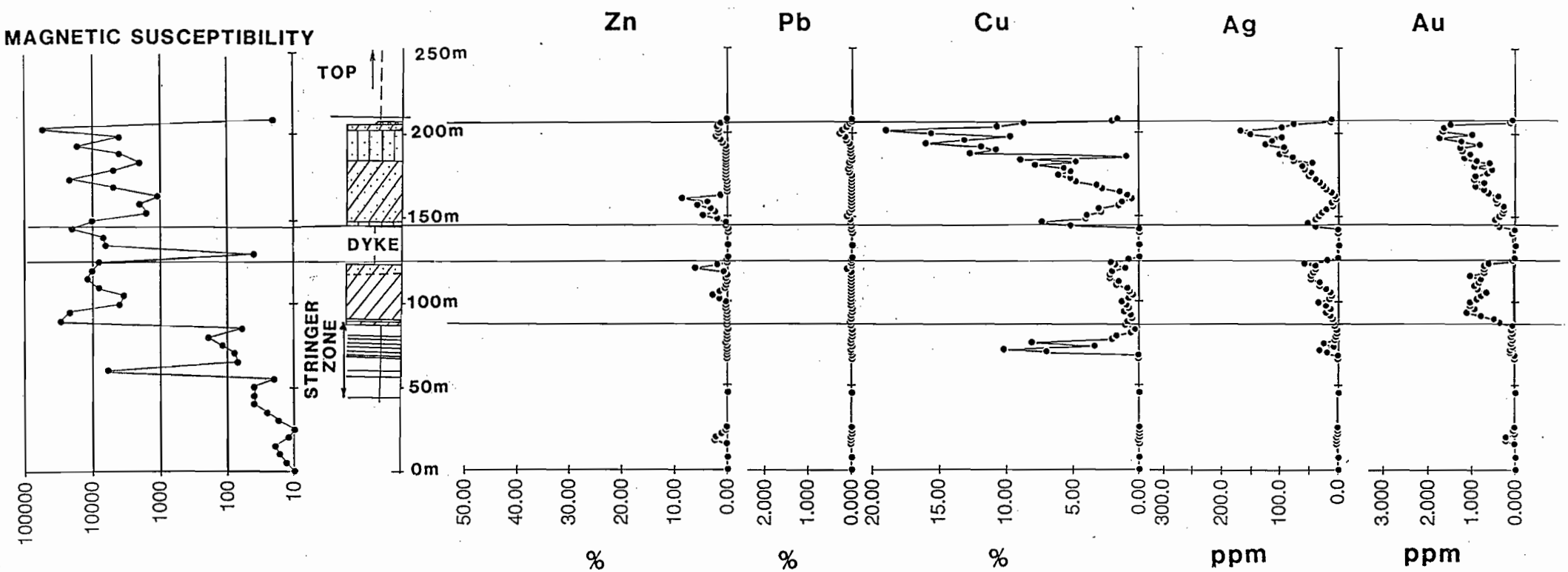

FIG. 4 DRILLHOLE SC 113A - SECTION 2214ON - COPPER-RICH ZONE

This section is unusual with copper concentrated towards the top of the massive sulphide unit. There is no clear correlation between zinc, lead and silver, as seen on the other drill sections. A rough correlation between copper, silver and gold exists. Textural evidence indicates significant replacement of existing sphalerite-rich massive sulphide by pyrite and chalcopyrite.

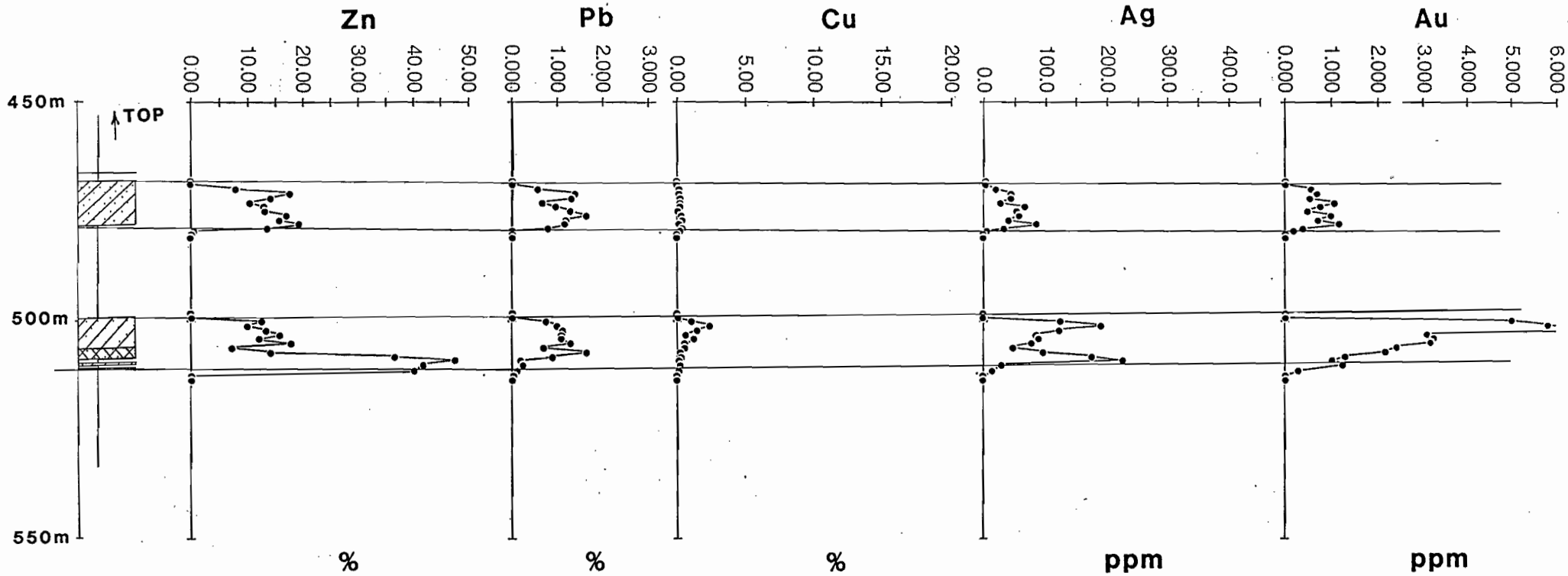

MARGINAL HIGH ZINC - FOLD ZONE SC 21 II

/// Massive Pyrite

Massive Sphalerite

Disseminated magnetite

FIG. 5 DRILLHOLE SC 21II - SECTION 22040N - MARGINAL HIGH ZINC - GOLD ZONE

Two bands of massive sulphide on this section pass laterally into the main ore zone to the south. In the top band a correlation between zinc, lead, silver and gold is not represented in the lower unit.

2. Massive Pyrite (<15% Zn and <2.5% Cu) corresponding to logged massive pyrite ore (<50% sphalerite and <2% chalcopyrite).

3. Copper-rich Massive Pyrite (>2.5% Cu) corresponding to massive pyrite with >2% chalcopyrite, and

4. Stringer Ore

Results are presented in Figures 6-22240N, 7-22140N and 8-22040N.

Conclusions

Gold - Gold is preferentially concentrated in the massive sulphide ore types, peaking towards the Massive Sphalerite/Massive Pyrite boundary. The highest gold values correspond to zinc grades of 10 to 12%.

Zinc - The massive sulphide ore is significantly enhanced in zinc relative to the Stringer zone.

Lead - Follows zinc.

Silver - Silver is enriched in the Massive Sphalerite Ore and basically follows zinc and lead.

Copper - The highest copper grades are localised to the copper-rich Massive Pyrite Ore and the Stringer zone.

In the gold-rich part of the Scuddles deposit (Section 22040N - Drillhole SC21 IIW) a strong peaking of gold occurs at 10 to 12% Zn (Fig. 8). On log:log plots linear correlations between copper and gold, and silver and gold are evident. A suggestion that a linear relationship between zinc and gold, and lead and gold, beneath grades of 8% Zn and 0.8% Pb respectively exists. These linear correlations strongly suggest a similar transport mechanism for all metals.

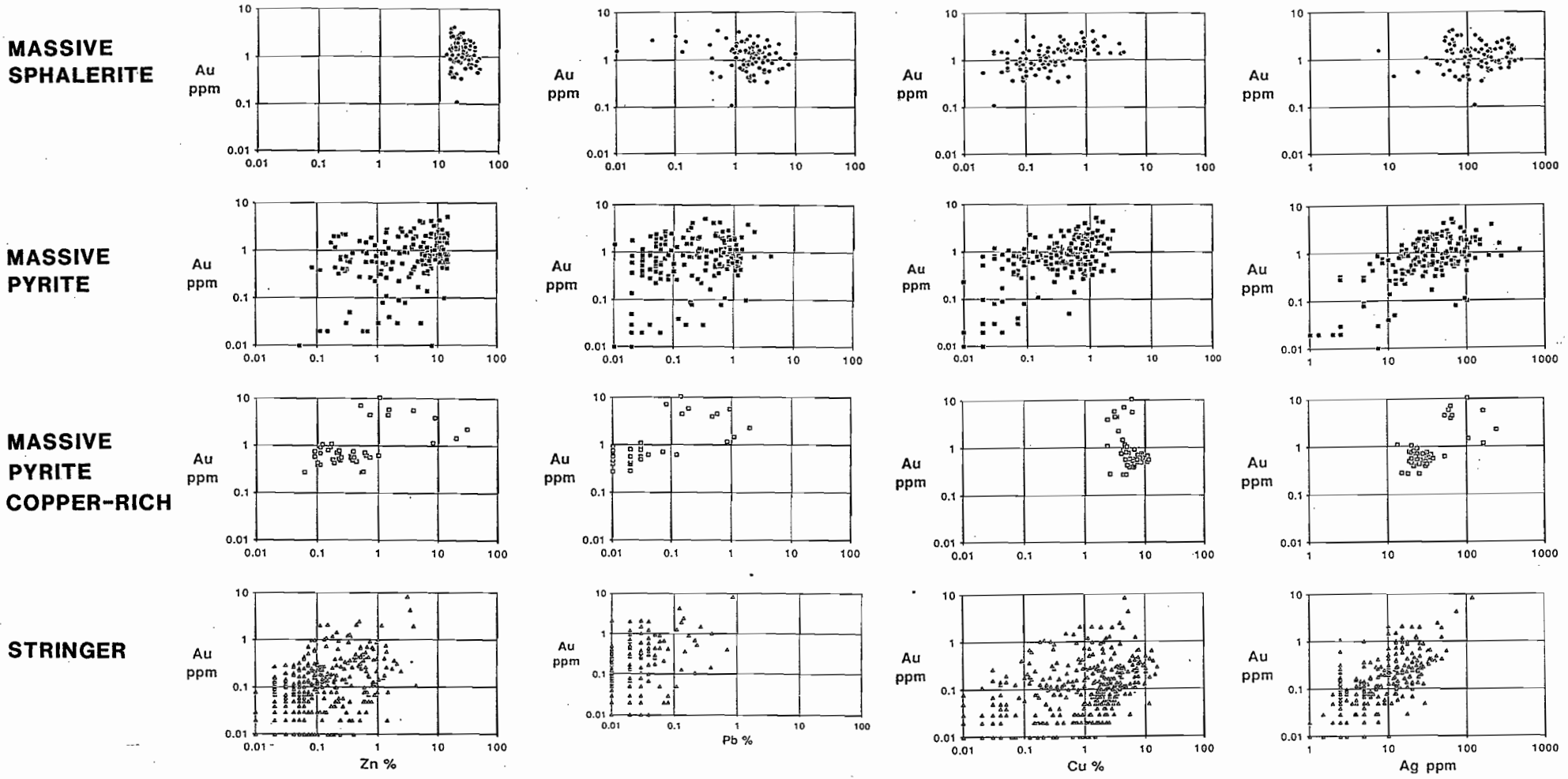

FIG. 6 METALS V. GOLD PLOTS FOR 2224ON SECTION

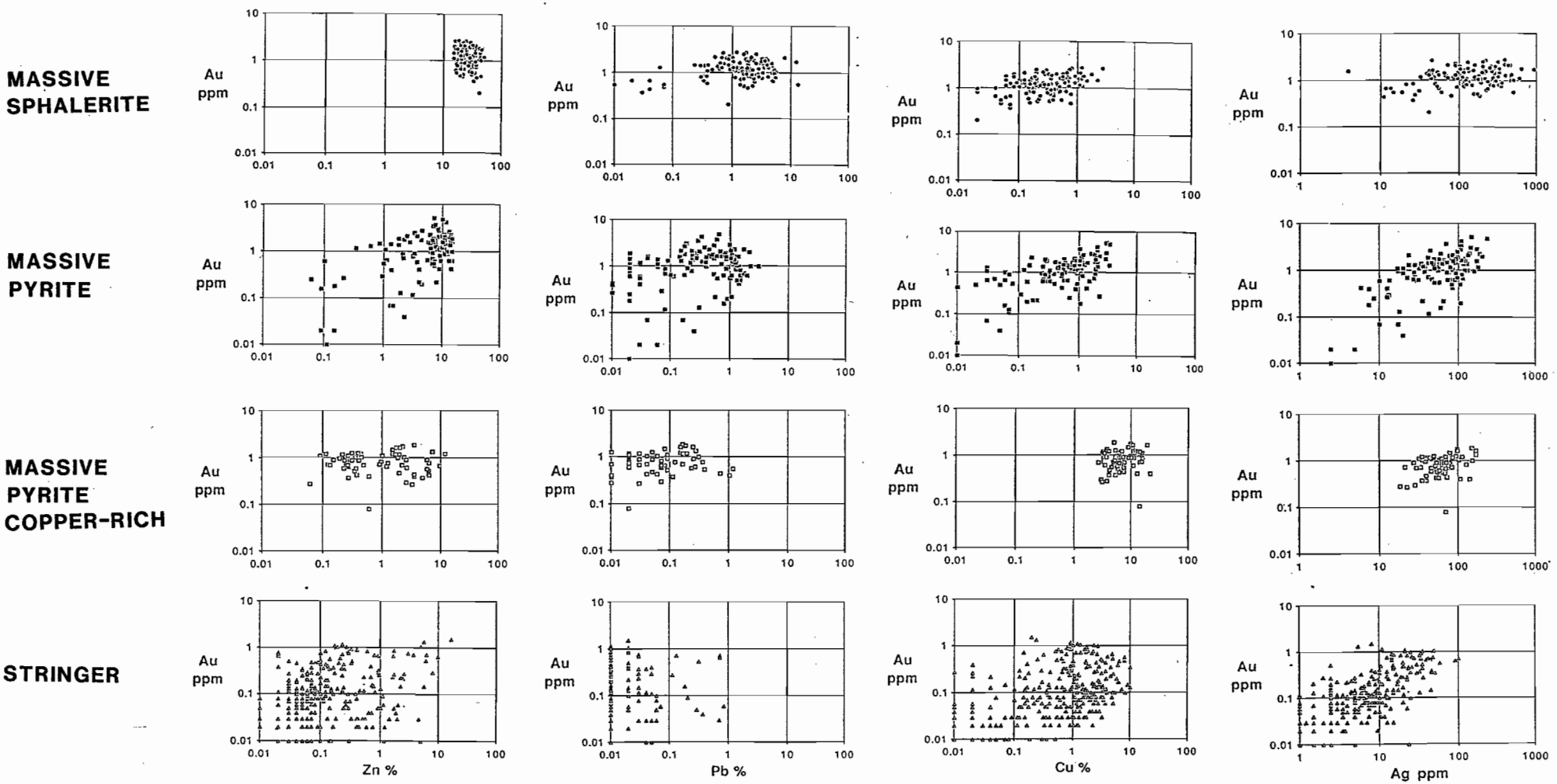

FIG. 7 METAL V. GOLD PLOTS FOR 2214ON SECTION

MASSIVE SPHALERITE

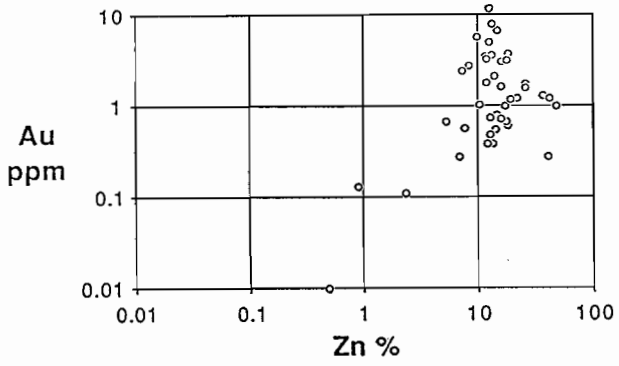

MASSIVE PYRITE

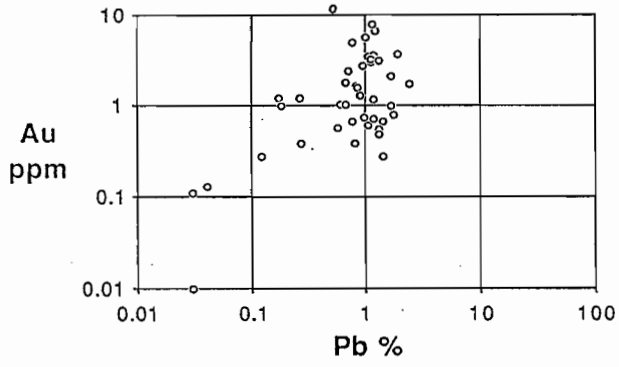

MASSIVE PYRITE COPPER-RICH

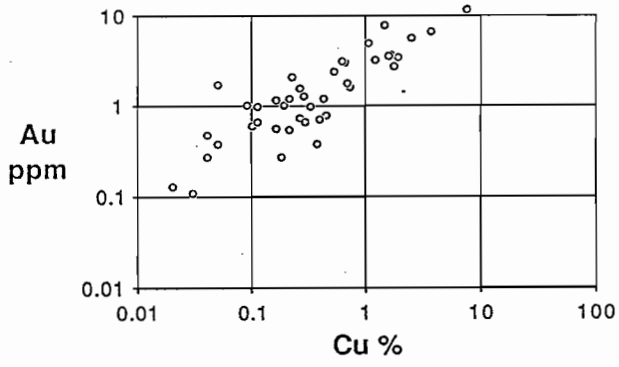

STRINGER

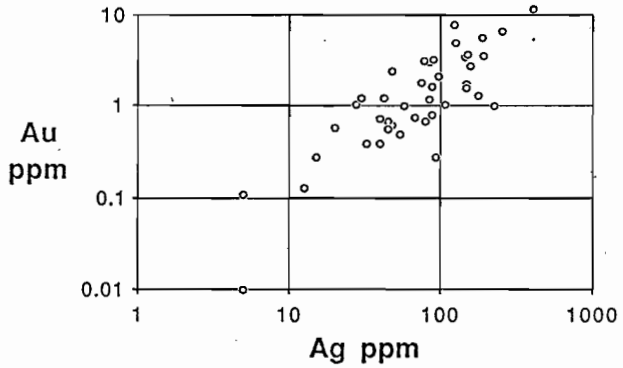

FIG. 8 METAL V. GOLD PLOTS FOR 2204ON SECTION

4.0 ORE MINERALOGY AND TEXTURE

Preliminary textural and mineralogical studies of the Scuddles deposit have been made. A recent paper by Ashley et al. (In Press - Economic Geology) describes the mineralogy and microtextures at Scuddles in detail. Poignant aspects of Ashley et al.'s work are summarised below.

4.1 Gross Structures/Textures

The top part of the Scuddles massive sulphide is generally highly laminated. Sphalerite + magnetite and pyrite + magnetite layers are present on fine (1 to 2mm) and large (0.5m) scales. This layering is probably a primary feature.

Sphalerite-rich areas (i.e. sphalerite > pyrite) show a strong mylonitic fabric. More pyritic sections (pyrite > sphalerite) display a more brittle deformation, with massive pyrite blocks in a sheared sphalerite matrix. Pre-deformational textures are destroyed in the ductile sphalerite zones but often preserved in the more competent pyritic sections.

4.2 Summary of Mineralogy

This work is based on detailed descriptions by Ashley et al. (In Press) and embellished with the authors observations from limited polished thin section studies.

4.2.1 Hanging-wall (MI Marker - Ashley et al.; Frater, 1986)

Finely laminated chert with chlorite-rich epiclastic:

- exhalative cherts,
- exhalative magnetite layers - now nodules/euhedra,
- exhalative sulphides in layers.

Quartz, chlorite, granular magnetite, carbonate, amphiboles, ilmenite + pyrrhotite, sphalerite, pyrite minor chalcopyrite.

Equivalent to the Key Tuffite at the Mattagame deposit, Canada.

Passes vertically and laterally into massive sulphide.

4.2.2 Massive Sphalerite Zone (Zn Zone - Ashley et al.)

- Mineralogical lamination on scale of mms to cms,
- Sulphide grain boundaries annealed,
- Intergrown sulphides with silicates.

Pyrite

a) Euhedral

b) Porphyroblasts corroded and fractured (5mm across) - fractures filled with chalcopyrite.

c) Fine to medium grained annealed pyrite in other sulphides - associated colloform, crustiform, skeletal, radial structures.

d) Intergrown with fine grained galena/sphalerite and tetrahedrite.

Sphalerite

a) Annealed, twinned sphalerites with curvilinear boundaries.

b) Interlocking mosaics - lined by exsolution chalcopyrite and pyrrhotite.

c) With scattered inclusions of sulphides and silicates, magnetite and fine grained cassiterite.

Magnetite

Trace amounts up to 25% by volume -

a) Sieved anhedral to subhedral porphyroblasts (2mm across) with inclusions of sulphides and silicates.

b) Inclusion-free subhedral granular grains (2mm across).

No magnetite pseudomorphs after hematite observed in contrast to Frater's (1986) work at Gossan Hill.

Pyrrhotite

a) Isolated grains associated with chalcopyrite anhedral.

b) Large bladed texture with inclusions of sulphides and silicates plus magnetite. Blades up to 1cm long.

Galena

a) Small anhedral grains concentrated in the Massive Sphalerite Ore, associated with sphalerite and pyrite.

Inclusions of argentian tetrahedrite exclusive to galena.

Chalcopyrite

a) Anhedral in sphalerite-rich areas.

b) Fracture filling in pyrite porphyroblasts.

4.2.3. Massive Pyrite Zone (Pyrite Zone - Ashley et al.)

A zone of greater than 80% sulphide. Dominated by interlocking fine to medium grained pyrite grains. Scattered and layered subhedral, magnetite grains are fairly common. Towards the base of the unit veins of cross-cutting pyrite and granular recrystallised pyrite are more common.

Minor amounts of chalcopyrite/pyrrhotite, sphalerite, chlorite, quartz and calcite.

4.2.4. Massive Pyrite Copper-rich

Similar to the massive pyrite zone with significantly more chalcopyrite and pyrrhotite as discrete grains, as veins or as interstitial fills between grain boundaries.

4.2.5. Stringer Zone (Copper Zone - Ashley et al.)

Semi-massive sulphide in host rocks of tuff, sandstone, mudstone and cherts. Sulphides occur in veins associated with chlorite and calcite with minor magnetite.

Pyrite

a) Fine to coarse grained (up to 1cm) in anhedral or subhedral form.

b) Crustiform pyrite.

4.3 Textural Characteristics

Detailed examination of drillcore with supportive thin section studies has enabled a rough paragenetic sequence to be determined. This work is a re-evaluation of data presented in the November 1986 progress report.

4.3.1. Early Textures/Minerals

a) Fine grained sphalerite and galena. Sphalerite is pink in colour. Shows high degree of fine layering.

b) Colloform, crustiform, radial and skeletal pyrite in places replaced by chalcopyrite.

c) Layered granular magnetite. Probably recrystallised from its original form to give it a sieved granular habit. Relic layering of magnetite visible in massive pyrite.

4.3.2. Nodular Pyrite

Bulbous nodules of pyrite which may be sieved or unsieved are common. Sieved nodules include magnetite and silicates.

Unsieved nodular pyrite may contain rims of granular or coalesced granules of magnetite. This texture is thought to represent the growth of pyrite nodules in a matrix containing magnetite. In some areas nodular pyrite 'growths' coalesce and residual triangular magnetite-rich matrices are preserved.

Pyrite nodules are generally composed of mosaic pyrite grains or one single form. However some nodules show concentric ring structures whilst others contain stellate growth patterns.

The matrix to nodular pyrite generally consists of subhedral magnetite grains, fine or coarse grained sphalerite, minor galena with silcates + chalcopyrite and pyrrhotite.

4.3.3. Pyrite Overprint

Pyrite overprinting of earlier massive sulphide is suggested by a number of textures:

a) Layered subhedral pyrite grains in massive pyrite.

b) Relic triangular interstices cemented by pyrite. These are the result of growing pyrite nodules followed by pyrite overprinting.

c) A texture involving nodular inclusion - free pyrite which is fractured. Fractures are filled with chalcopyrite. These nodules and chalcopyrite are surrounded by massive pyrite with inclusions of subhedral magnetite and disseminated chalcopyrite. Massive pyrite has effectively overprinted the pre-existing sphalerite in this texture.

4.3.4. Chalcopyrite - Pyrrhotite

A variety of forms of chalcopyrite are noted, always associated with pyrrhotite:-

a) In fractures at the margins of nodular pyrite.

b) Disseminated in the sphalerite - magnetite matrix.

c) Found at the margins of medium grained mosaic sphalerite. This may be the metamorphosed/annealed equivalent of chalcopyrite disease. This texture has also been recognised in the Archaean Canadian deposits (Sangster, 1972).

d) Pyrite nodules with numerous inclusions of chalcopyrite. Pyrite is being replaced by copper sulphide on the introduction of high temperature copper-rich fluids.

4.4. Metamorphic (?) Recrystallization

a) Fine grained pink sphalerite recrystallizes to a medium to coarse grained red/brown sphalerite. The latter contains annealed grain boundaries and twinning.

b) Galena occurs as anhedral grains with recrystallized sphalerite. Argentian tetrahedral occurs exclusively in galena grains.

c) Pyrite recrystallizes to form euhedral rhombs and cubes and also a fine grained granular pyrite.

4.5. Deformation

a) Sphalerite-rich areas are deformed in a ductile manner to produce mylonitic fabrics.

b) Chalcopyrite and pyrrhotite-rich areas are sheared to form banded chalcopyrite/pyrrhotite layers in a sphalerite, magnetite and pyrite matrix.

c) Boudinage textures form around more brittle pyrite blocks. Granular pyrite grains may contain pressure shadows of quartz.

4.6. Conclusions

The Scuddles massive sulphide is highly deformed although sphalerite/pyrite laminations probably reflect origional layering.

Early structures/textures can be recognised in brittle massive pyrite sections of the ore.

Early colloform/crustiform/skeletal pyrite is preserved within nodular pyritic zones. A significant pyrite overprinting is recognised subsequent to the major introduction of chalcopyrite and pyrrhotite.

Silver occurring as electrum, native silver, pyrargyrite, friebergite and in solid solution in galena occurs in the sphalerite-rich sections commonly closely associated with galena (Townsend, 1985).

Gold occurs as electrum and is distributed throughout the massive sulphide.

ACKNOWLEDGEMENTS

Thanks to John Mill of E.Z. Perth for organising the computer tape of Scuddles data and to ESSO Melbourne for supplying it.

Thanks also to Kate Dunn for typing this report and Adrienne Carrett for drafting the diagrams.

REFERENCES

ASHLEY, P.M., DUDLEY, R.J., LESH, R.H., MARR, J.M., RYALL, A.W., (IN PRESS) The Scuddles Cu-Zn Prospect, an Archaen Volcanogenic Massive Sulphide Deposit, Golden Grove District, Western Australia. Submitted to Economic Geology.

FRATER, K.M., 1983. Geology of the Golden Grove prospect, Western Australia;a volcanogenic massive sulphide-magnetite deposit. Economic Geology v. 78, p. 875-919.

RUXTON, P.A., 1986. Golden Grove, Western Australia. AMIRA Report on controlon gold and silver grades in volcanogenic sulphide deposits. Progress Report - November, 1986.

TOWNSEND, R., 1985. Golden Grove Joint Venture, Scuddles Project. Mineragraphic study of 26 polished sections from SC 200 and SC 205. Unpublished report to the E.Z. Company.

BALCOOMA PROSPECT, NORTHERN QUEENSLAND

David L. Huston

AMIRA Report

August 1987

BALCOOMA PROSPECT, NORTHERN QUEENSLAND

By David L. Huston

This section details the final interpretation of the structural and stratigraphic relationships of the Balcooma prospect, briefly describes the mineralization, and reports the initial results of studies relating the distribution of precious metals to base metals.

STRATIGRAPHY

The Balcooma prospect lies in a pelitic lens within a sequence of multiply deformed interbedded metagreywackes and metapelites. Stratigraphically, the basal unit in the prospect area is a fine grained quartz-biotite-feldspar±muscovite schist with minor interbeds of crenulated muscovite-biotite-quartz (hereafter termed the 'Footwall metagreywacke'). Above this unit lies a fine grained quartz-muscovite-biotite schist with interbedded staurolite-bearing schist (the 'hanging wall metagreywacke'). These two metagreywacke sequences are distinguished most readily by the presence or lack of staurolite porphyroblasts.

The mineralization lies within a lens of pelitic sediments (the 'Balcooma host rocks') that occurs at the contact between the two metagreywacke sequences. The pelitic sediments are characterized by an abundance of staurolite with lesser andalusite and cordierite. Kyanite and sillimanite may be present locally. Several lenses of volcaniclastics occur through the Balcooma stratigraphic sequence. Figure 1a illustrates this stratigraphic sequence in the relatively undeformed section 8600 mN.

The sequence has been intruded by later quartz-feldspar sills which cut stratigraphy only obliquely and have been used to define fold structures (Fig. 1b). This intrusion was followed by the intrusion of a biotite microgranite which crops out in the eastern part of the prospect area as shown in Figure 2.

LEGEND

Cenozoic laterite


Biotite microgranite


Quartz-feldspar porphyry


Exhalite


Lead gossan

Massive sphalerite-galena-pyrite mineralization


Iron gossan

Massive pyrite-chalcopyrite mineralization


Sulfidic muscovite-quartzite or quartz-muscovite± biotite schist


Chloritic schist


Quartz-muscovite-biotite schist


Staurolite-bearing schists


Quartz-feldspar-muscovite-biotite schist


Volcanoclastics

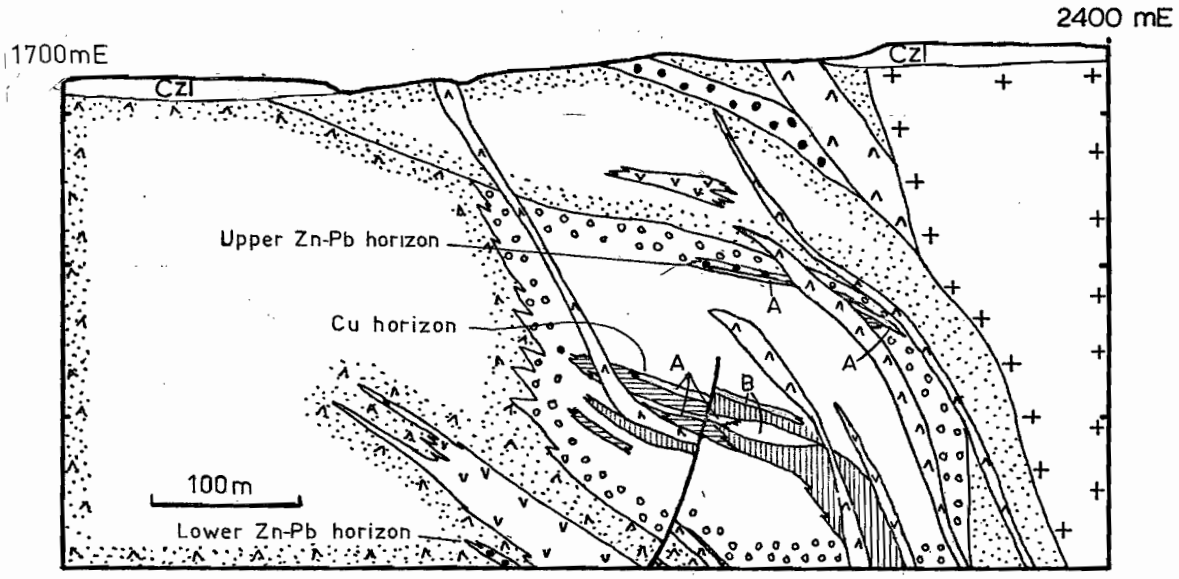

Figure 1a: Section 8600mN, Balcooma prospect.
Legend as for Figure 2.

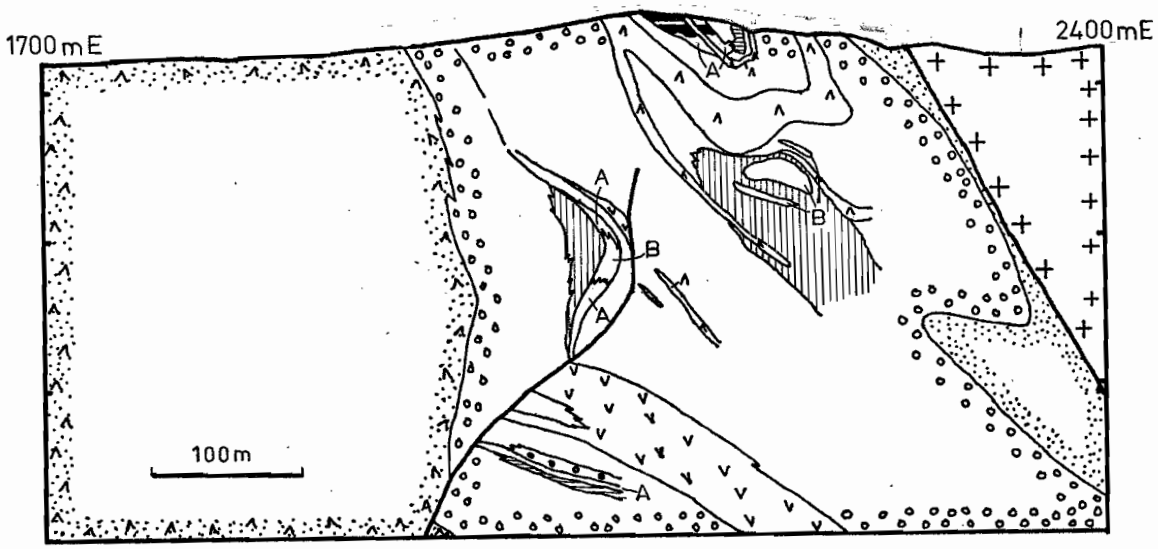

Figure 1b: Section 9000mN, Balcooma prospect.
Legend as for Figure 2.

LEGEND

Cenozoic laterite


Biotite microgranite


Quartz-feldspar porphyry


Exhalite


Lead gossan

Massive sphalerite-galena-pyrite mineralization


Iron gossan

Massive pyrite-chalcopyrite mineralization


Sulfidic muscovite-quartzite or quartz-muscovite± biotite schist


Chloritic schist


Quartz-muscovite-biotite schist


Staurolite-bearing schists


Quartz-feldspar-muscovite-biotite schist


Volcanoclastics

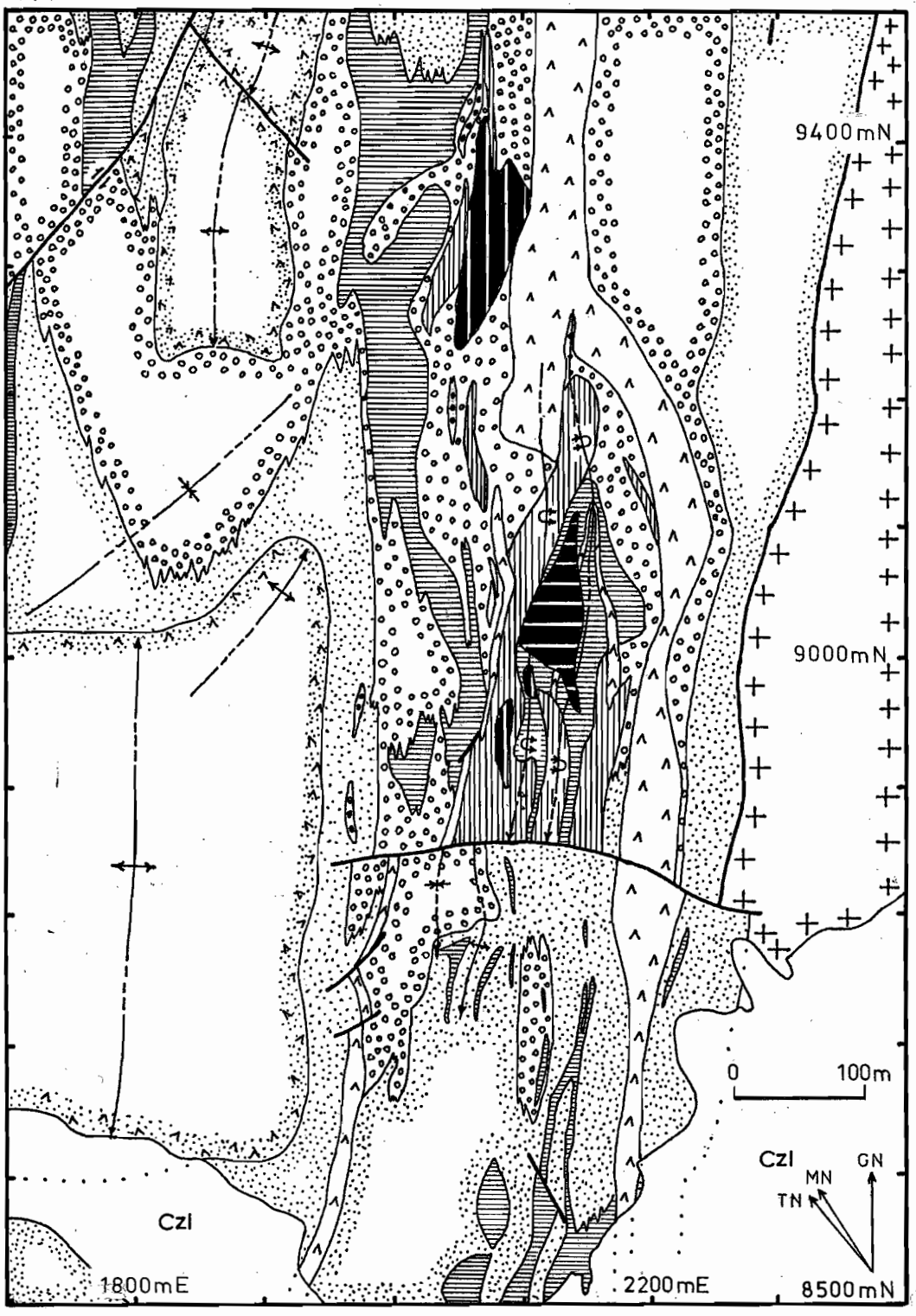

Figure 2: Interpretive geology of the Balcooma prospect.

Figure 2 illustrates the surficial geology of the prospect. The footwall metagreywacke crops out in the west at the core of a D_3 (see below) anticline while the hanging wall metagreywacke crops out in the eastern part of the prospect area next to the microgranite. The Balcooma host rocks occupy the centre of the prospect area.

STRUCTURE

As described in the previous AMIRA report, the Balcooma prospect has undergone four phases of deformation involving folding. Only two of these (D_2 and D_3) have affected the geometry of the prospect significantly. Three structural entities control the geometry of the deposit.

An overturned D_2 syncline-anticline pair occurs in the Balcooma host rocks north of 8850 mN. In plan (Fig. 2) and section (Fig. 1b), a quartz-feldspar porphyry sill defines the shape of these folds. Balcooma copper mineralization has been remobilized into the core of the antiformal syncline and plunges at 20° to the south-southwest (Harvey, 1984).

At 8850 mN, the D_2 syncline-anticline pair is truncated by an east-west trending cross fault. The fault is interpreted to have formed during D_2 as a tear. To the south, the sequence lacks intense folding and dips gently to the east (Fig. 1a).

The third major structure in the prospect area is an open D_3 anticline cored by the footwall metagreywacke which is present to the west of the prospect. The prospect occurs on the eastern limb of this fold while the Surveyor prospect (Noranda, Jones Mining and Lachlan Resources) lies at the nose of the fold.

MINERALIZATION

Four separate stratigraphic horizons are thought to contain significant mineralization at the Balcooma prospect. Table 1 summarizes the characteristics of each horizon in stratigraphic order from top to bottom:

Table 1: Characteristics of mineralized horizons, Balcooma prospect

Horizon	Metal assemblage	Stratigraphic position
Upper Zn-Pb	Zn-Pb-Ag-(Cu-Au)	Occurs 10-20 m stratigraphically below the contact between the hanging wall metagreywacke and the Balcooma host rocks.
Cu	Cu-(Ag-Au)	Occurs in the centre of the Balcooma host rocks.
Central Zn-Pb	Zn-Pb-Ag-(Cu-Au)	Occurs in the centre of the Balcooma host rocks below the copper horizon.
Lower Zn-Pb	Zn-Pb-Ag-(Cu-Au)	Occurs at the base of the Balcooma host rocks 10-30 m below a thick volcaniclastic lens.

A case can be made to include the copper and central zinc-lead horizons as a single horizon. This possibility is being investigated. Section 8600 mN, which is relatively undeformed, illustrates the relative positions of the upper Zn-Pb, Cu and lower Zn-Pb horizons (Fig. 1a). Section 9000 mN, which is strongly deformed, illustrates the relative positions of the Cu, central Zn-Pb and lower Zn-Pb horizons as well as the remobilization of the copper horizon into the hinge of the D_2 antiformal syncline (Fig. 1b). Figure 3 illustrates the surface projections of the various horizons.

Of the mineralized positions, the copper horizon contains most mineralization. Harvey (1984) estimates that it contains 3.5 m.t. of 3.0% Cu. Ted lower zinc-lead horizon contains lesser but still significant tonnages and is open down dip. The central and upper zinc-lead horizons

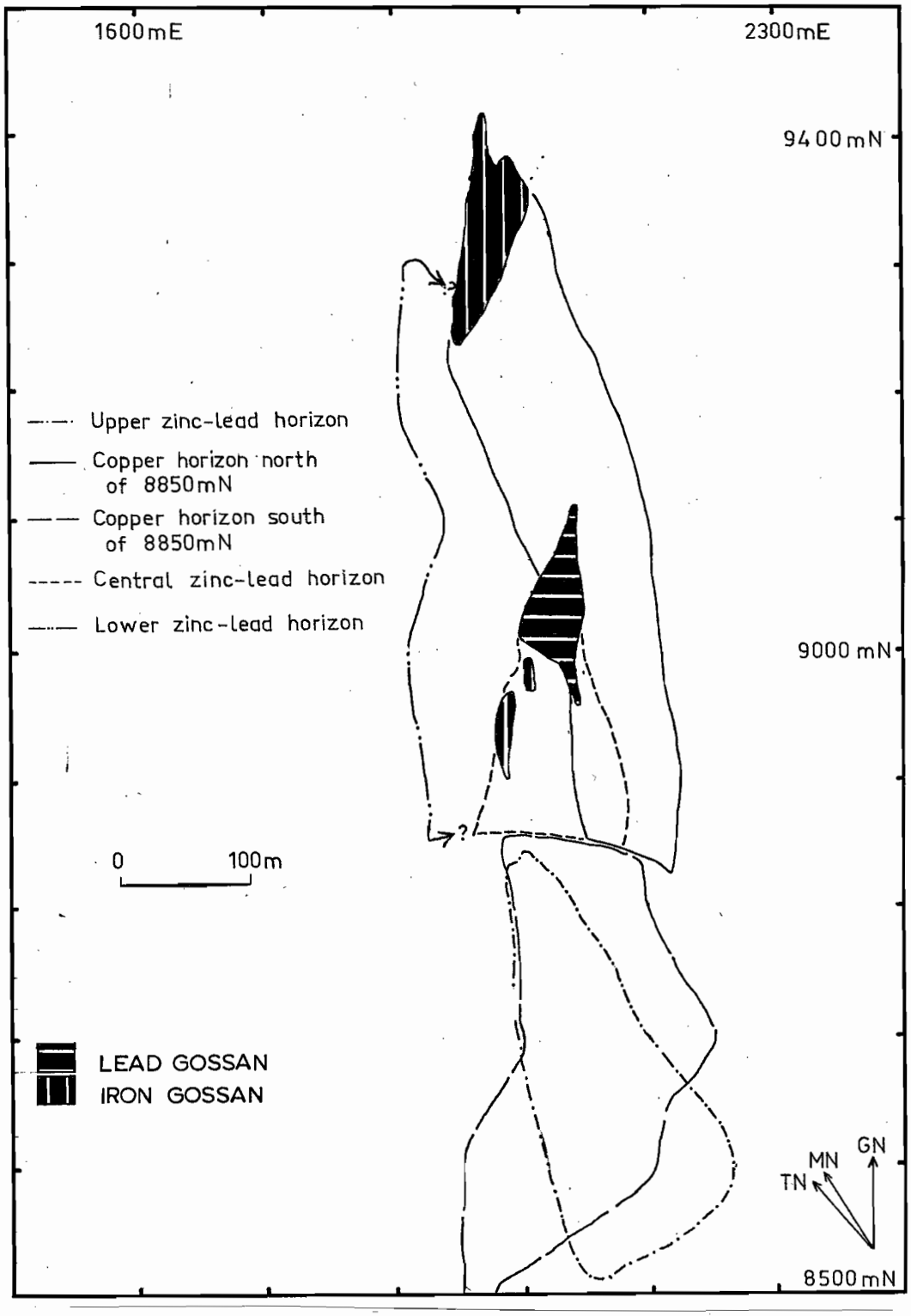

Figure 3: Location of ore shoots and lenses.

contain relatively small tonnages. Tonnage and grade figures for horizons other than the copper horizon have not been calculated.

Massive mineralization

Three distinct types of massive mineralization occur in the Balcooma prospect: (1) massive magnetite, (2) massive pyrite-chalcopyrite, and (3) massive sphalerite-galena-pyrite. The first two occur principally in the copper horizon while the last occurs principally in the zinc-lead horizons.

Massive magnetite

Massive magnetite mineralization usually consists of > 95% magnetite with accessory pyrite, chalcopyrite, pyrrhotite and chlorite gangue. Often the sulfides and chlorite occupy thin veinlets in the magnetite. This type of mineralization increases in amount to the south (Harvey, 1984).

Massive pyrite-chalcopyrite

This mineralization comprises the majority of the metal resources at Balcooma. The dominant mineral is pyrite with accessory chalcopyrite, pyrrhotite and magnetite. Patterson (1981) has reported the occurrence of gold, bismuth, bismuthinite and bismuth sulfosalts in association with chalcopyrite. Texturally, chalcopyrite usually occurs interstial to pyrite grains, and in strongly deformed areas (e.g. the antiformal syncline) may form an infill to a pyrite breccia.

Massive sphalerite-galena-pyrite

Massive sphalerite-galera-pyrite consists mainly of sphalerite, galena and pyrite, with minor to trace arsenopyrite, pyrrhotite and tetrahedrite. Only a few grains of tetrahedrite have been noted to date. This mineralization usually consists of subhedral to euhedral pyrite with interstitial or matrix sphalerite and galena. The sphalerite and galena are strongly annealed.

Alteration

Two types of alteration have been observed at Balcooma: (1) chlorite schist, and (2) quartz-muscovite schist. Both types usually contain disseminated pyrite, while the former may contain chalcopyrite, pyrrhotite and magnetite. Chlorite schists are usually related to massive pyrite-chalcopyrite and magnetite, while quartz-muscovite schists are related to sphalerite-galena-pyrite mineralization.

Chlorite schists

Chlorite schists occur both stratagraphically above and below the copper horizon although most occur below the horizon. Two distinct chloritic schists are present: (1) fine grained quartz-chlorite±biotite±staurolite±cordierite±andalusite±magnetite±garnet±sulfide schist, and (2) medium-grained chlorite-biotite±garnet±sulfide schist. The quartz-free chloritic schists occur usually as crosscutting veins in the quartz-rich chloritic schists. The quartz-free chloritic schists may carry significant sulfide, usually more than the quartz-rich chloritic schists.

Based on microstructural studies of the chloritic alteration zones relative to the enclosing metapelites, Van der Hor (1986) has suggested that the original chloritic alteration zone has been remodified and extended during both progressive and retrogressive metamorphism. Observations made by this author concur with Van der Hor's (1986) hypotheses. An additional implication of the model is that the sulfides may become mobile during metamorphism as suggested by quartz-free, sulfide-rich, crosscutting chloritic schists.

Quartz-muscovite schists

Quartz-muscovite schists occur largely in the footwall of massive sphalerite-galena-pyrite mineralization. Usually pyrite occurs as disseminations, and thin sheared out stringers. Gahnite, sphalerite, galena, chalcopyrite and staurolite also occur patchily in these schists.

Relationships between precious and base metals

Geologic information has been encoded onto the University computer and assay results from mineralized intersections have been separated into five groups:

1. Quartz-chlorite schist and chlorite-biotite schist with disseminated and stringer mineralization (1285 samples; interpreted as metamorphically modified chloritic footwall alteration);

2. Quartz-muscovite schist and quartzite with disseminated sulfide (462 samples; interpreted as metamorphosed sericitic footwall alteration and/or exhalite);

3. Massive magnetite (99 samples);

4. Massive pyrite-chalcopyrite (547 samples); and

5. Massive sphalerite-galena-pyrite (164 samples).

Only assay results for cut core were used, and samples showing oxidation or supergene mineralization were excluded. Sample lengths vary between 0.1 m and 3 m, but most lengths fall between 0.5 m and 1.5 m.

Table 2 indicates the average grades and variation within the differing styles of mineralization. Massive sphalerite-galena-pyrite and quartz-muscovite schist are enriched in lead, zinc, and silver. Massive pyrite-chalcopyrite and quartz-chlorite schist are enriched in copper. Massive sulfide mineralization is enriched in gold relative to massive magnetite and footwall alteration, but both types have approximately the same levels

Table 2: Average grades for different styles of mineralization.

Mineralization style	Pb(%)		Zn(%)		Cu(%)		Ag(g/t)		Au(g/t)	
	$\bar{x}$	s	$\bar{x}$	s	$\bar{x}$	s	$\bar{x}$	s	$\bar{x}$	s
Quartz-chlorite schist	0.06	0.40	0.13	0.71	0.88	1.85	6	10	0.14	0.57
Quartz-muscovite schist	0.72	1.77	1.21	3.00	0.23	0.45	11	24	0.12	0.20
Massive magnetite	0.10	0.48	0.23	0.66	0.68	1.40	9	17	0.20	0.39
Massive pyrite-chalcopyrite	0.08	0.11	0.26	0.72	3.67	3.53	21	16	0.43	0.38
Massive sphalerite-galena-pyrite	4.01	4.43	8.60	7.07	0.95	1.37	55	48	0.58	1.55

(massive sphalerite-galena-pyrite is slightly enriched due to several erratic high assays).

Relationships between gold, copper and zinc

Figures 4 through 8 illustrate the frequency distributions of silver and gold, and the relationships between precious and base metals for each of the 5 mineralization styles.

The Balcooma prospect contains very little gold - typical of some volcanogenic massive sulfides. In all styles of mineralization except quartz-chlorite schist gold has a moderate to good correlation with copper. None of the mineralization styles show correlations between zinc and gold. Consequently, the Balcooma deposit falls into the Cu-Au association for volcanogenic massive sulfides and gold transport probably occurred as a chloride complex (Huston and Large, 1987).

Huston and Large (1987) noted that in volcanogenic massive sulfide deposits gold may have two associations: (1) Au-Zn-Pb-Ag (e.g. Rosebery) and (2) Au-Cu (e.g. Mt Chalmers). Based on thermochemical modelling they suggest that deposits showing the Au-Zn-Pb-Ag association have enhanced gold grades in the mineralizing fluids, have a near neutral pH as evidenced by the presence of significant carbonate or feldspar gangue. On the other hand enhanced gold grades in the Cu-Au association occur if the mineralizing

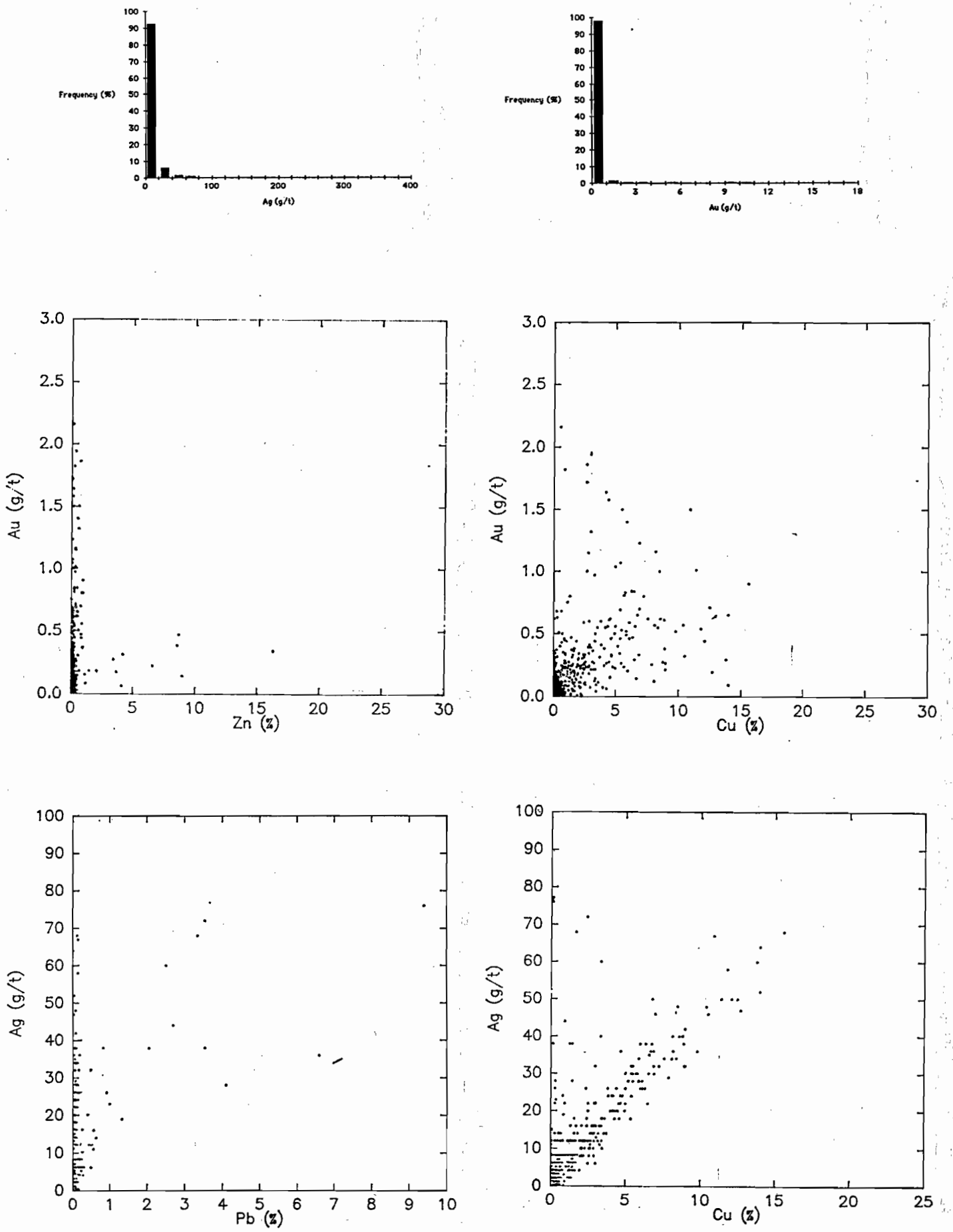

Fig. 4: Relationships between precious and base metals in sulfide-bearing quartz-chlorite schist from the Balcooma prospect.

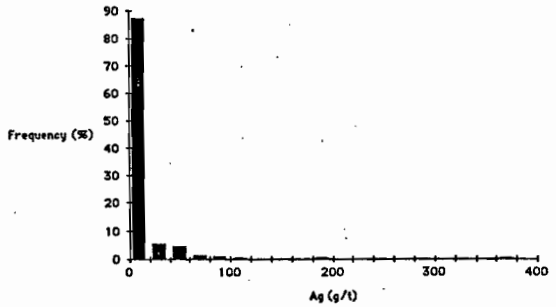

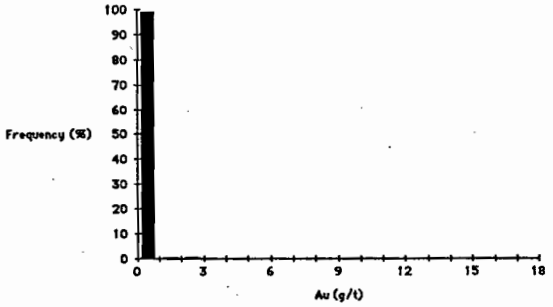

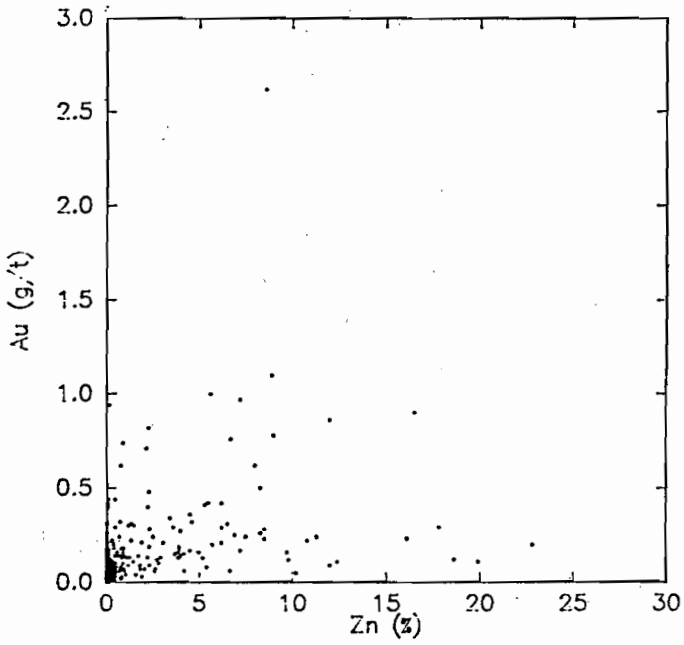

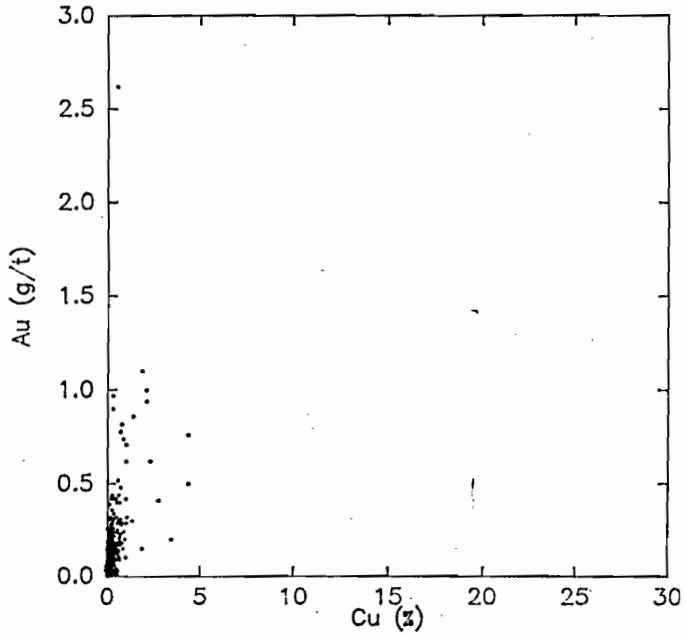

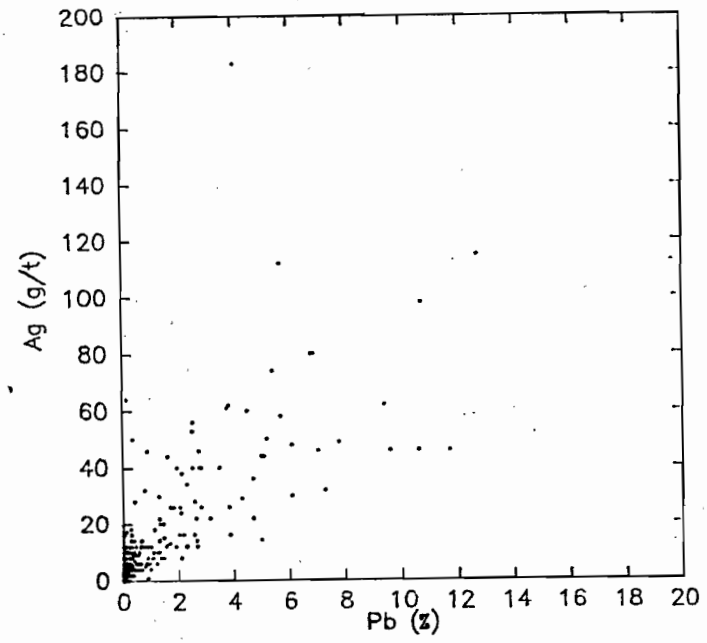

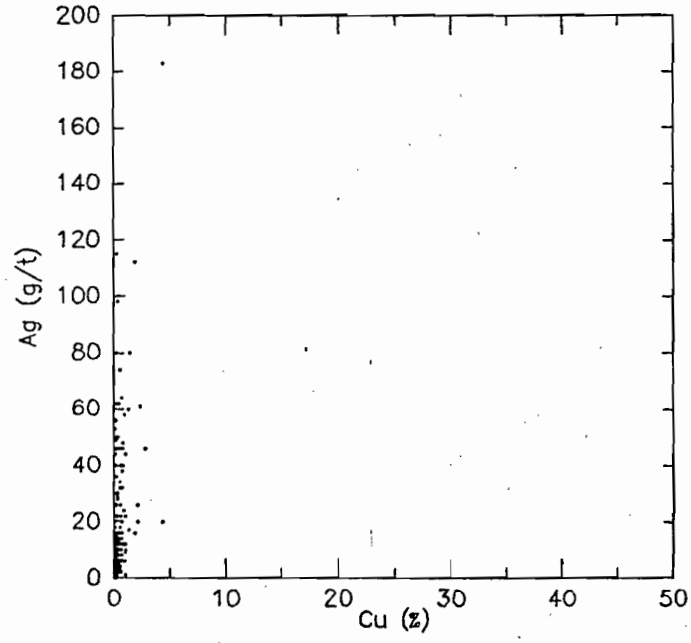

Fig. 5: Relationships between precious and base metals in sulfide-bearing quartz-muscovite schists from the Balcooma prospect.

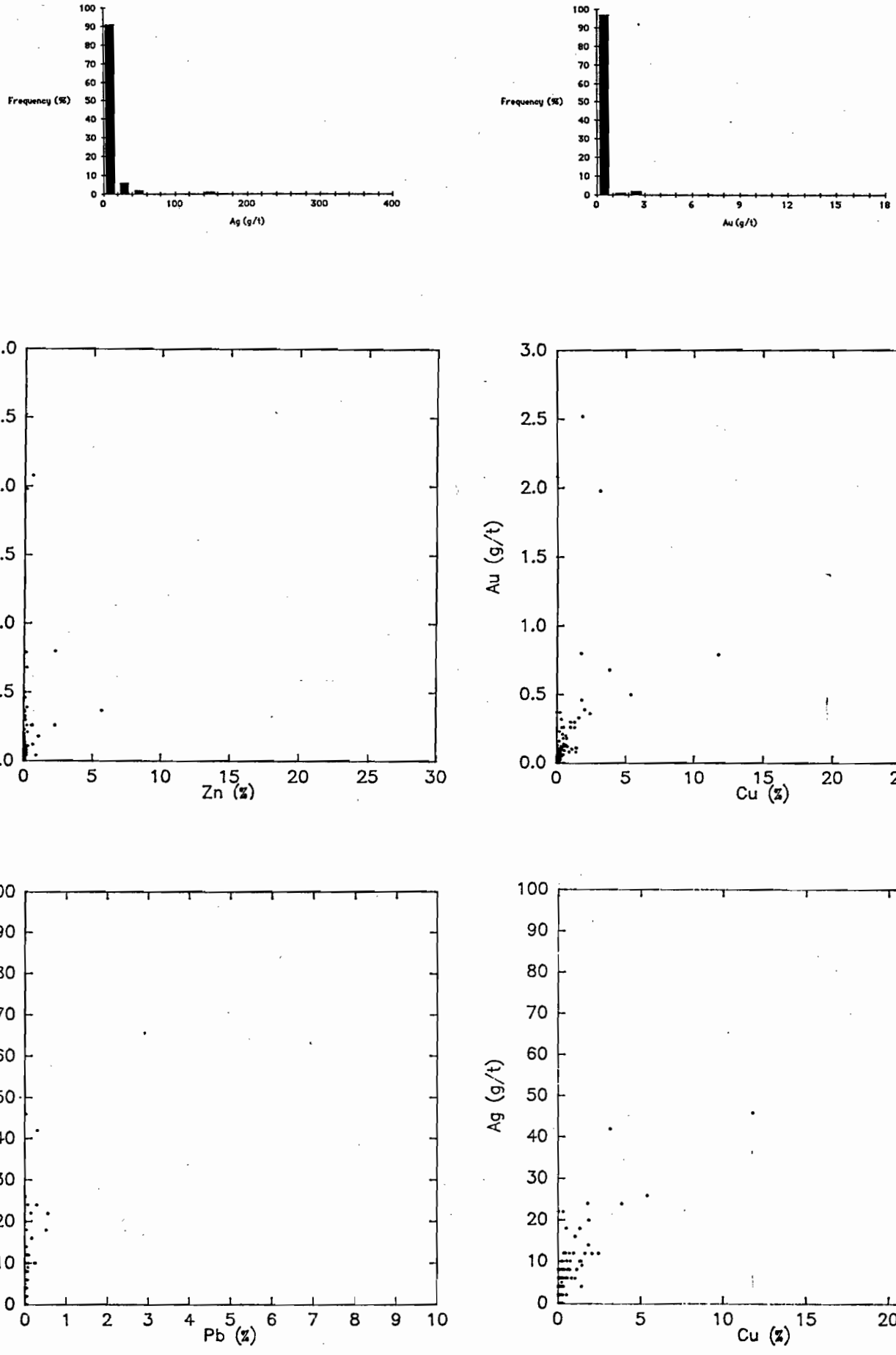

Fig. 6: Relationships between precious and base metals in massive magnetite from the Balcooma prospect.

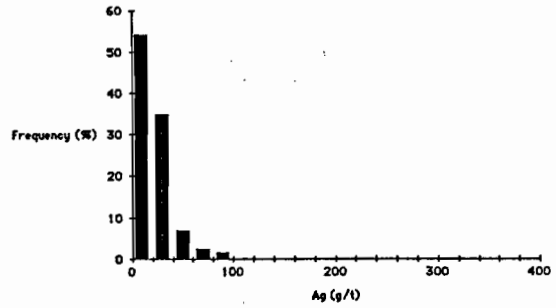

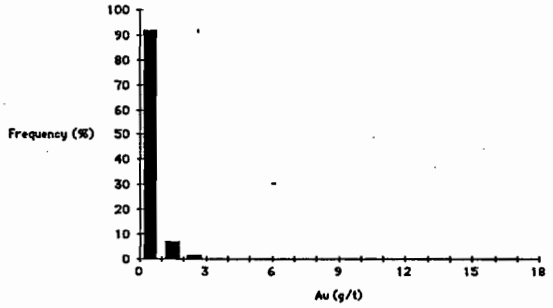

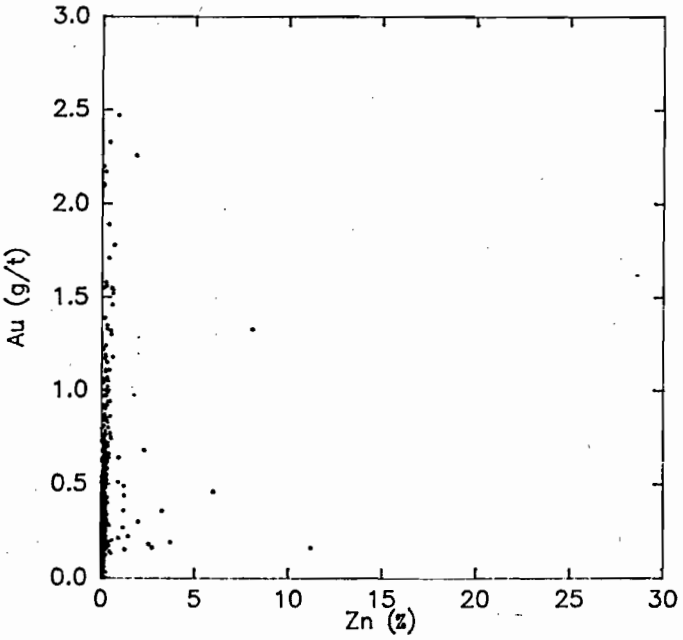

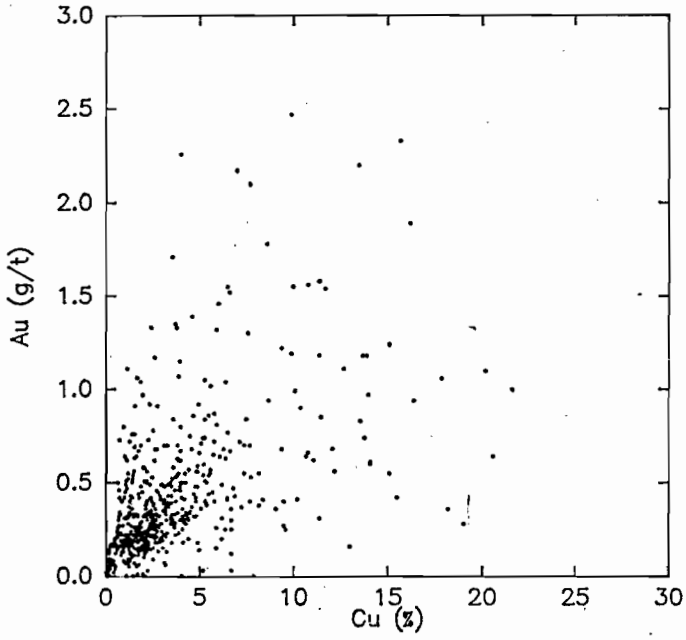

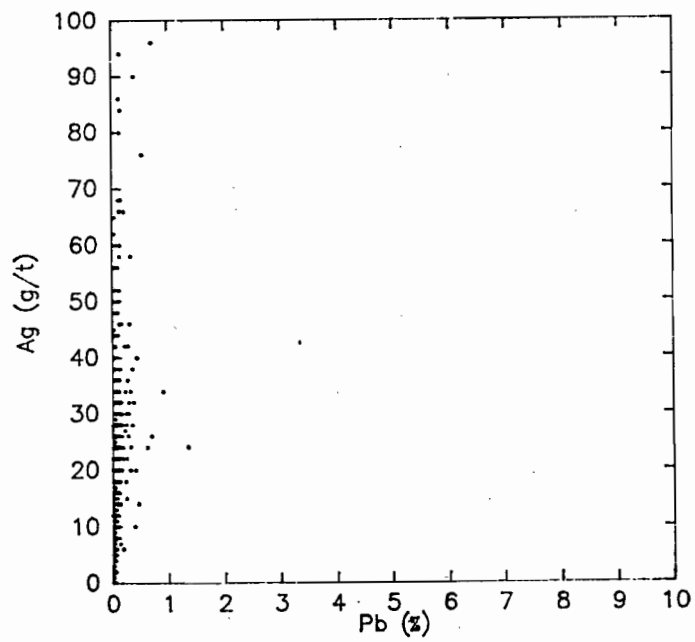

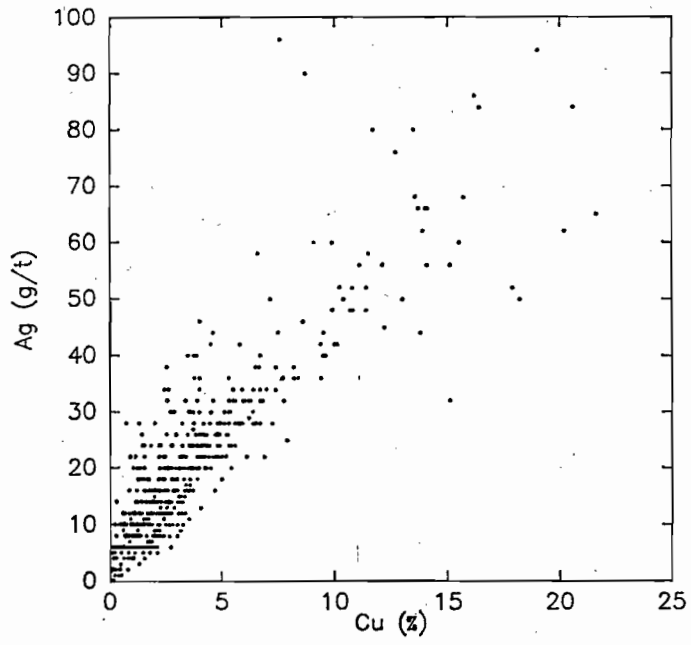

Fig. 7: Relationships between precious and base metals in massive pyrite-chalcopyrite from the Balcooma prospect.

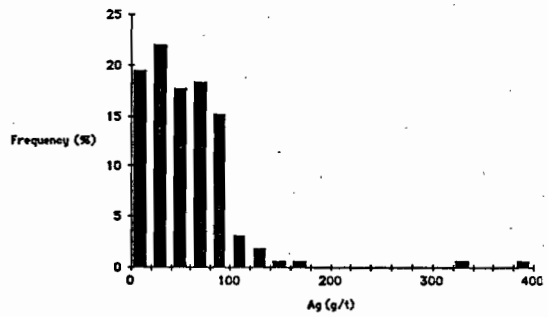

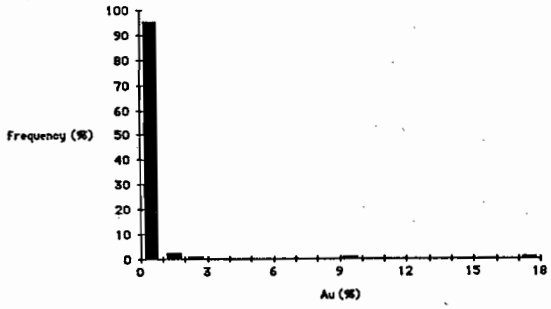

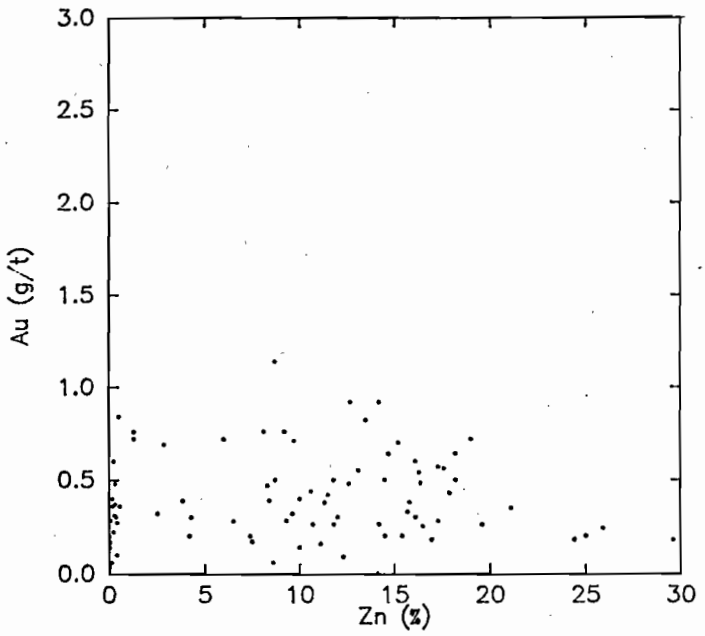

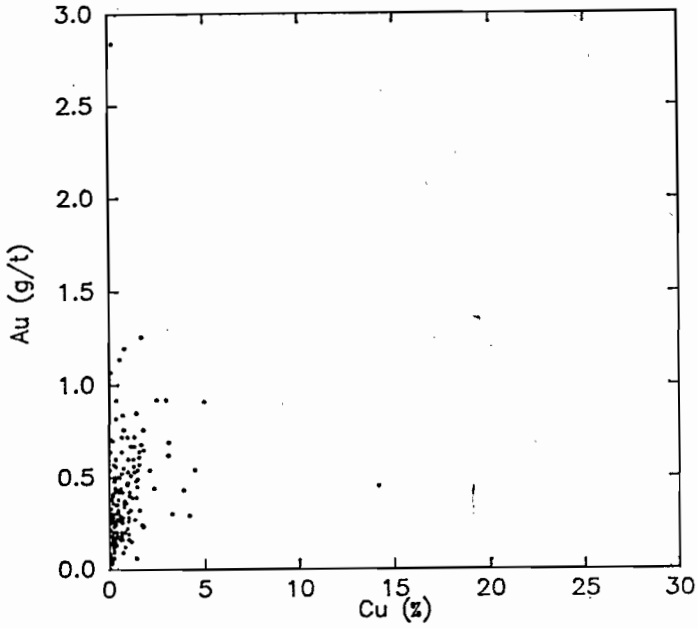

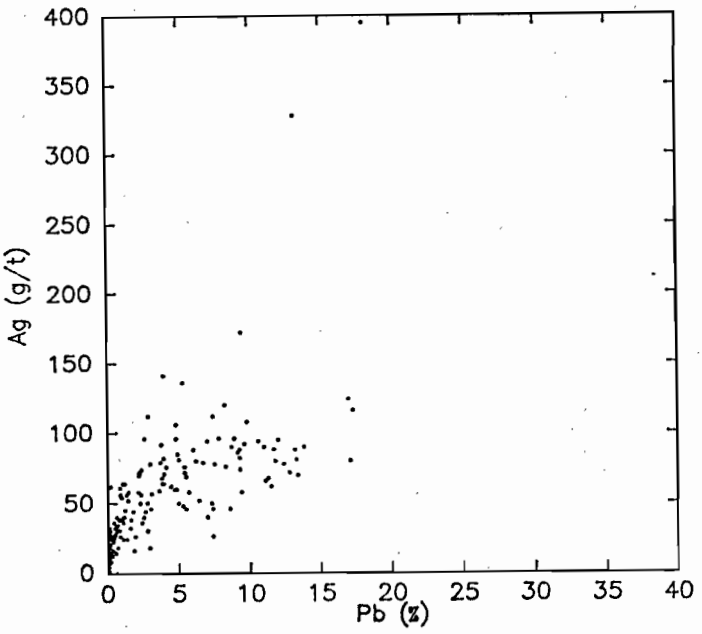

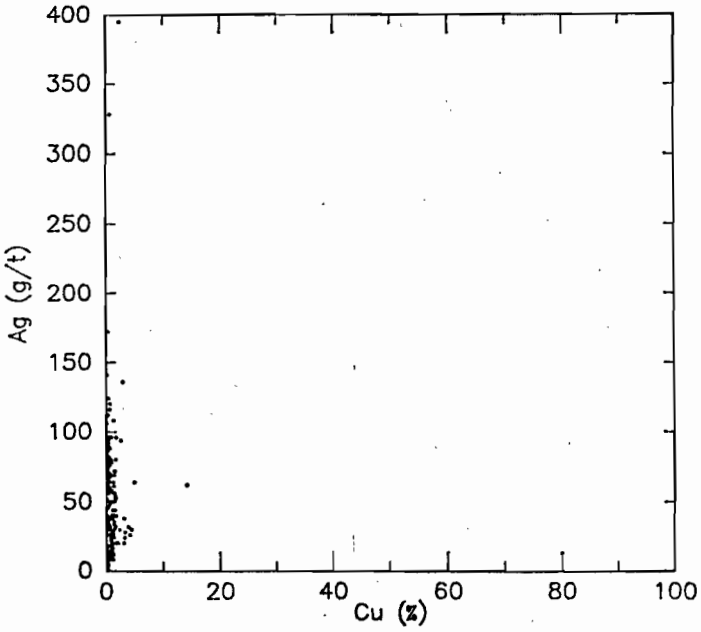

Fig. 8: Relationships between precious and base metals in massive sphalerite-galena-pyrite from the Balcooma prospect.

fluids were acid and relatively oxidized as indicated by the presence of barite, hematite or bornite. Unfortunately the fluids that deposited Balcooma probably had the wrong chemistry for enhanced gold grades. The fluids were too acid for the Au-Zn-Pb-Ag association as carbonate (or calc-silicate minerals) have not been observed at Balcooma. The fluids were too reduced to produce enhanced gold values of the Cu-Au association as pyrrhotite and magnetite are common constituents of the mineralization (assuming that this is not a metamorphic assemblage).

Relationships between silver, copper and lead

Silver has a quite different relationship to base metals. Massive sphalerite-galena-pyrite contains significantly more silver than massive magnetite or massive pyrite-chalcopyrite, and quartz-muscovite schist contains more silver than quartz-chlorite schist. Zinc-lead mineralization contains more than copper mineralization in general.

At Balcooma, silver has a good correlation to lead in zinc-lead-rich mineralization (quartz-muscovite schist (Fig. 5) and massive sphalerite-galena-pyrite (Fig. 8)). This association has been observed at Rosebery (Huston and Large, 1986) and other massive sulfide deposits in general (Amcoff, 1984). On the other hand, in copper-rich mineralization (quartz-chlorite schist (Fig. 4), massive magnetite (Fig. 6) and massive pyrite-chalcopyrite (Fig. 7)), the lead-silver relationship is replaced by an excxellent correlation of silver to copper.

Because tetrahedrite and other silver-bearing minerals are rare at Balcooma, galena is the likely host mineral for silver in zinc-lead mineralization. In copper-rich mineralization the strong linear correlation between silver and copper suggests that chalcopyrite contains silver as a trace element at a level of about 140 ppm. On the other hand, the 'fan-like' correlation between silver and galena in zinc-lead mineralization indicates that the silver content of galena varies significantly.

These observations may be modelled geochemically assuming the applicability of the Kuroko model (Eldridge and others, 1983) to Balcooma: (1) as hot

copper-rich fluids replace pre-existing zinc-lead mineralization to form copper-rich mineralization, enough silver drops out of solution to saturate chalcopyrite with respect to silver; and (2) the silver remaining in solution moves up through the massive sulfide lens to precipitate with zinc and lead at the top when the hydrothermal solutions mix with seawater.

Consequently, two parameters may control the concentration of silver in volcanogenic massive sulfide deposits. The silver content of zinc-lead-poor, copper-rich ore may be controlled by the solubility of silver in chalcopyrite (which should be dependent only on temperature), while the silver content of zinc-lead-rich mineralization may be controlled by the solubility of silver in the hydrothermal fluid (which is dependent on temperature and pH).

DIRECTION OF FUTURE RESEARCH

As suggested earlier, significant sulfide remobilization has probably occurred in the Balcooma prospect. This remobilization may occur either through fluid migration or through sulfide flowage. Precious metals movement may have also occurred. The main thrust of research will be to evaluate this possibility through metal contouring, mineragraphy and geochemical analyses (trace elements and stable isotopes).

REFERENCES

Amcoff, O. 1984. Distribution of silver in massive sulfide ores. Mineralium Deposita, v.19, p.63-69.

Eldridge, C.S., Burton, P.B. and Ohmoto, H. 1983. Mineral textures and their bearing on the formation of the Kuroko orebodies. Econ. Geol. Mon. 5, p.241-281.

Harvey, K.J. 1984. The geology of the Balcooma massive sulfide deposit, north-east Queensland. Unpub. M.Sc. thesis, James Cook Univ., 92 p.

Huston, D.L. and Large, R.R. 1986. The distribution, mineralogy and geochemistry of precious metals in the north-end orebody, Rosebery Mine, Tasmania: Final report to E.Z. Co., April 1986, 132 p.

Huston, D.L. and Large, R.R. 1987. A chemical model for the concentration of gold in volcanogenic massive sulphides deposit. Submitted to Ore Geology Reviews, June, 1987.

Patterson, D.J. 1981. Mineralogical reconnaissance of diamond drill core, Balcooma DDH-16, QA15432-15489(RA8003-8060). Unpub. Mt Isa Mines Mineral Services Report No. 4440, 4 p.

Van der Hor, F. 1986. Metamorphic hydrothermal alteration at the Balcooma massive sulfide deposit. Unpub. report to Carpentaria Exploration Company Pty Ltd. 46 p.

SOURCE AND MOVEMENT OF GOLD AND BASE METALS IN SUBMARINE VOLCANIC SYSTEMS: A DISCUSSION PAPER

Ross.R. Large

AMIRA Report

August 1987

SOURCE AND MOVEMENT OF GOLD AND BASE METALS IN SUBMARINE VOLCANIC SYSTEMS : A DISCUSSION PAPER

Ross R. Large

This is a preliminary paper designed to present an alternative viewpoint, and provoke discussion, on the subject of gold and base metal mobilisation and deposition in volcanic hydrothermal systems.

SUMMARY

Preliminary calculations suggest that gold, silver and base metals have been leached from a volume of about 60 km^3 of footwall source rocks to provide the quantity of metals in deposits such as Hellyer and Rosebery. The zone of leaching is approximated by an inverted cone with the deposit at the apex of the cone. Convective seawater leaching probably penetrated 4-6 km into the footwall sequence and leached metal from the Central Volcanic Sequence and Underlying early Cambrian(?) and Precambrian basement rocks. Calculated amounts of metals required to be leached are 0.25 ppm Cu, 4.3 ppm Pb, 8 ppm Zn, 18 ppm S, 0.01 ppm Ag and 0.2 ppb. Trace element data suggests that rhyolite-andesite volcanics within the CVS are an adequate source of all metals including the gold and silver.

Solubility calculations suggest that gold, silver and base metal are mobilised as chlorite complexes, deep in the high temperature part of the convection cone. In response to dropping temperature and buffering by the volcanics, gold transport switches from $AuCl_2^-$ to $Au(HS)_2^-$ in the upper part of the volcanic pile. The level of gold saturation and the elevation of the switchover of gold complexes in the convective cone has a major control on the ultimate gold content of the seafloor massive sulphide deposits.

INTRODUCTION

Our work to date on gold and base metal concentration in massive sulphides has revealed:

- The average gold content of VMS deposits varies from about 0.5 ppm to 5 ppm.

- Deposits in a given district (e.g. Mount Read Volcanics, Noranda area) may show a variety of gold concentrations.

- There are commonly two associations:

  - gold-copper association in the lower part of the deposit, and/or

  - gold-zinc-lead-silver association in the upper part of the deposit.

- These two associations are controlled by the method of gold transport. The gold-copper association indicates transport as $AuCl_2^-$, whilst the gold-zinc-lead-silver association indicates transport as $Au(HS)_2^-$.

- $AuCl_2^-$ transport is most likely in high temperature, low pH systems with high a_{Cl^-}/a_{H_2S} ratios. $Au(HS_2)^-$ transport is most likely in moderate to low temperature, moderate pH systems with low a_{Cl^-}/a_{H_2S} ratios.

In detail the suggested chemical criteria controlling gold grades are:

<u>In Zinc Ores</u> - low temperature (< 250 °C), high a_{H_2S}/a_{Cl^-}
- $Au(HS_2)^-$ transport.

- High gold ores (3-20 g/t) - high fO_2 (py-barite ± hematite), and moderate pH (carbonate stable).

- Moderate gold grades (1-4 g/t) - moderate fO_2 (pyrite only) and low pH (sericite-chlorite).

- Low gold grades (< 2 g/t) - low fO_2 (pyrite ± pyrrhotite) and low pH (sericite-chlorite).

<u>In Copper Ores</u> - high temperature (> 250 °C), high a_{Cl}/a_{H_2O}
- $AuCl_2^-$ transport.

- Bonanza gold ore (5-50 g/t) - high fO_2 (magnetite-pyrite), high temperature (> 300 °C) and low pH (sericite-chlorite).

- Variable gold ore (1-5 g/t) - moderate fO_2 (pyrite dominant) and temperatures 250-300°C.

- Low gold ore (< 2 g/t) - low fO_2 (pyrite ± pyrrhotite) and high pH (carbonate).

Source Rock Controls

Up to this point our research programme has concentrated on documenting gold distribution in VMS deposits and then relating the distribution to the chemistry of gold transport/deposition process. We now need to address the following questions:

- What are the source rocks for the gold, silver and base metals?

- Does the gold content of the source rocks affect their concentration in the ores?

Keays (1987) considers that high magnesium high temperature basalts are the best source of gold in volcanogenic systems, and that low temperature basalts or calc-alkaline rhyolite-andesite sequences are an unlikely source of gold. Hutchinson (1986) suggests that tholeiitic basalts are the best source rocks for high grade gold in VMS deposits.

SOURCE ROCK CALCULATIONS

Preliminary calculations have been undertaken to determine the likely volume of the source rocks and amount of metal leached to form an orebody of the tonnage and grade of the Hellyer deposit.

The results are presented in Table 1. The following assumptions were made in this calculation:

- The total tonnage of the deposit is 19 million tonnes.

- No significant mineralisation occurs outside the 19 million tonne massive sulphide.

- The system was 100% efficient, i.e. all metals transported were deposited in the orebody.

- The ore fluid was saturated with zinc at 250°C (based on our previous zinc number studies - Huston and Large, in press), and all zinc was precipitated in the massive sulphide. This results in a value of 9 ppm Zn in the ore fluid. Other metal values were calculated with respect to zinc, based on the grades in the ore deposit.

- All the metals were leached from the footwall volcanic pile by circulating hot seawater. The volcanics in the Mt Read arc average 80 ppm Zn. It was assumed that 10% of the zinc (i.e. 8 ppm) was leached from the source rocks. Other quantities of leached metal were based on this zinc value.

It is significant that the calculated copper, lead, zinc and silver content of the ore fluid (Table 1) correspond roughly to saturation values at 250°C. The gold content of 0.2 ppb appears to be well below saturation (see Huston and Large, 1987), although this depends on which solubility data for $AuCl_2^-$ is accepted as the most accurate. If Helgeson's (1969) data is used, then 0.2 ppb Au is equivalent to a saturated fluid. This is a very important problem which requires resolution. If on the one hand, 0.2 ppb Au represents an undersaturated fluid, then the leachable gold content of the source rocks will have an important control on the gold in the resultant VMS deposit. However, if 0.2 ppb Au represents saturation, then this places a control on the amount of gold that can be carried in solution, and chemical factors (fO_2, pH, T, a_{Cl}/a_{H_2S}) will control the grade of the ores.

Example of calculations for zinc

1. Amount of zinc in the orebody = 1.3×10^{12} gms.

2. Amount of zinc in the ore fluid based on saturation at 250°C = 9 ppm
   = 9×10^{-3} gms/litre.

3. Amount of ore fluid required to form Hellyer = $\frac{1.3 \times 10^{12}}{9 \times 10^{3}} = 1.4 \times 10^{14}$ litres.

4. Average amount of zinc in the source rocks = 80 ppm.

TABLE 1 : Calculated metal content of ores, ore fluid and source rocks for the Hellyer VMS.

	Cu %	Pb %	Zn %	S %	Ag ppm	Au ppm
Grade of ore (19 mt)	0.4	7	13	30	160	2.3
Tonnes of contained metal	7.6×10^4	1.3×10^6	2.5×10^6	5.7×10^6	2.8×10^3	40
Calculated metal content of ore fluid*	0.3ppm	5ppm	9ppm	20ppm	0.01ppm	0.0002ppm
Calculated amount of metal leached from source rocks**	0.25ppm	4.3ppm	8ppm	18ppm	0.01ppm	0.2ppb

* based on zinc saturation in the ore fluid at the point of ore deposition - 9 ppm Zn at 250°C.

** based on leaching of 10% of the available zinc from the source rocks.

5. Calculated mass of source rock (assuming 10% of zinc leached) $= \frac{1.3 \times 10^{12}}{8}$ tonnes.

$= 1.6 \times 10^{11}$ tonnes.

6. Volume of source rock $V = \frac{m}{\rho} = \frac{1.6 \times 10^{11} \times 10^6}{2.7}$

$= 6 \times 10^{16}$ c.c.

Volume $= 60$ km^3.

In a seawater convective circulating system the area of source rock leached will depend on the shape of the geotherms (see fig. 1) but it is likely to have an inverted cone shape with the orebody at the apex of the cone. Possible dimensions of a cone of 60 km^3 of rock are shown in fig. 2.

The thickness of the andesite dacite sequence below Hellyer is about 700 m (Komyshan, 1986) and the Central Volcanic Sequence below that may be 2-4 km

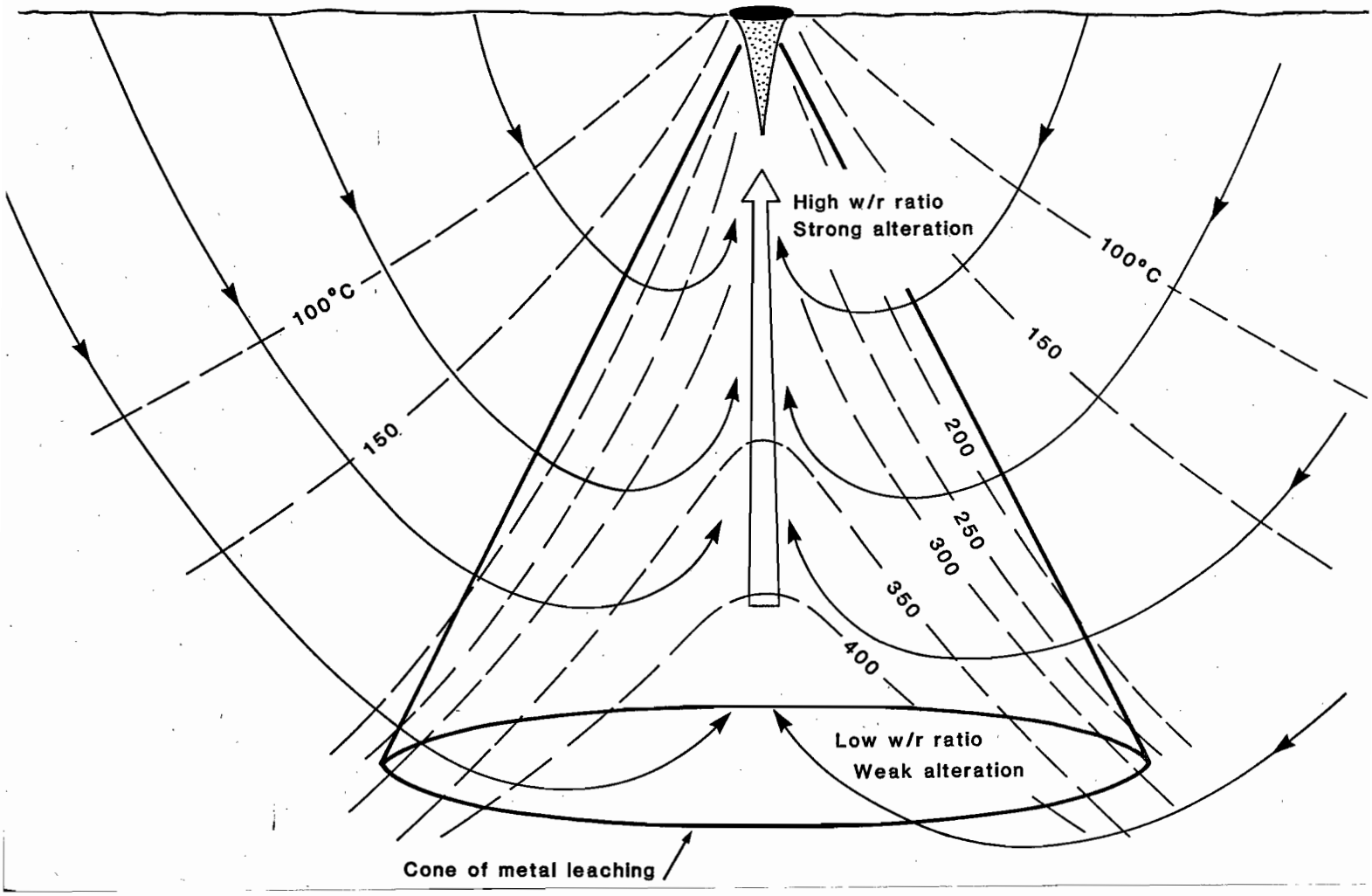

Figure 1 : Hypothetical sea water convection system in a homogeneous volcanic rock pile below a massive sulphide deposit. The cone of metal leaching is constrained by the 200^{0}C geotherm.

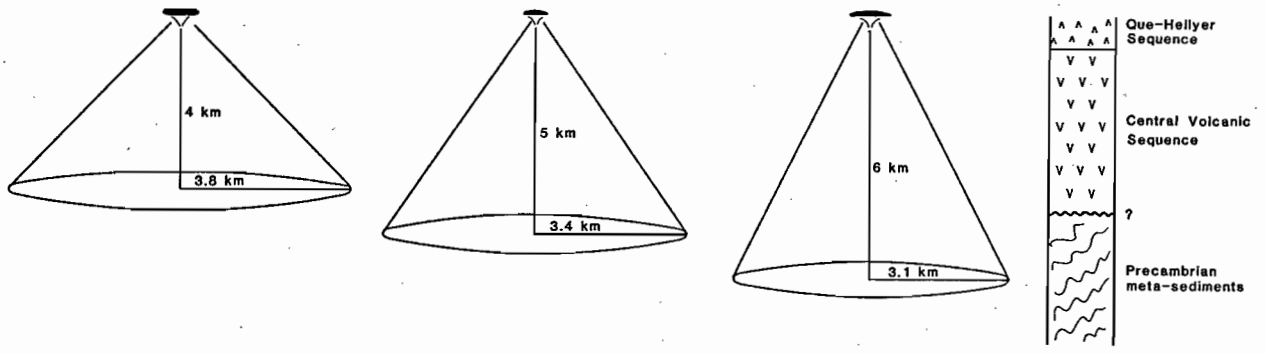

Figure 2 : Possible dimensions of cones of 60 km^3 of leachable rock below a massive sulphide. Note that the narrower cones would penetrate into the Precambrian basement.

thick. The dimensions of the narrow cones (fig. 2) indicate that in these cases metals would probably also be leached from 1-2 km of the Precambrian basement metamorphics. Lead isotope and strontium isotope studies (e.g. Gulson et al., 1987 and Whitford & Craven, 1986) support the concept of basement metal leaching.

Amounts of metals leached

A comparison of the average metal content of the Mt Read Volcanics, with the calculated metal leached is given below.

	Zn	Pb	Cu	Ag	Au
	ppm	ppm	ppm	ppm	ppb
Average Mount Read Volcanics*	80	10	35	0.5-1(?)	1-4(?)
Calculated amount required to be leached (from 60 km^3 of source rocks) to produce Hellyer	8	4	0.25	0.01	0.2

* from the Mount Read data base (Crawford, 1986, 1987).

It is obvious that the Mt Read Volcanics are an adequate source-rock for zinc, lead and copper. However, there is no reliable data on their silver and gold content. Crocket reports that the average gold content of rhyolites and dacites is 1.5 ppb whilst andesites and basalts average 3.6 ppb. Thus using a range for the Mount Read Volcanics of 1 to 4 ppb, they present an adequate source of leachable gold (calculated at 0.2 ppb - Table 1).

One conclusion from this discussion is that all volcanic rocks with greater than about 0.2 ppb leachable gold are an adequate source rock for gold-rich VMS deposits such as Hellyer and Rosebery, although high Mg basalts (with 3-4 ppb, Au) would theoretically be the best source rock.

Our present understanding of the volcanic stratigraphy of the Mount Read arc suggests that the only high Mg basalts occur toward the top of the Que-Hellyer Sequence, in fact immediately overlying the Hellyer ore position. The dominant lithologies in the footwall of Rosebery, Hercules and Mt Lyell are considered to be rhyolites, dacites and low Mg andesites, which are likely to contain low

levels (< 2 ppb) of gold. However, complete volcanic sections are not available, and our present knowledge of the basal part of the CVS is minimal.

Recent work by Ron Berry and Tony Crawford (this volume) suggests that high magnesium mafic and ultramafic rocks of the Early Cambrian Ophiotite sequence may be present as a thrust slice below the Central Volcanic Sequence. These rocks probably contain a high background of gold (> 3 ppb ?) and would constitute a very favourable source rock. This possibility requires further evaluation.

Water-Rock ratios

Using the simplistic concept of a convective fluid system with modified seawater flowing through the sides of an inverted cone and then funnelled upwards toward the apex of the cone (fig. 1), it is possible to roughly calculate water/rock ratios for different parts of the convective cone system.

Amount of ore fluid required to form Hellyer	=	1.4×10^{14} litres (kgms)
Assuming a discharge rate at the top of 10 kg/sec (Henley, 1986),		
Time for orebody formation	=	1.4×10^{13} seconds
	=	440,000 years
Mass of source rocks	=	1.6×10^{11} tonnes.
	=	1.6×10^{14} kgms.

Weigh for weight water/rock ratio over the lifetime of the system $= \frac{1.4 \times 10^{14}}{1.6 \times 10^{14}} \sim 1:1$

If all the fluid passing into the cone is channelled upwards and none is lost through the sides of the cone, then the water/rock ratio will increase dramatically passing up the system.

For example, the water/rock ratio in the top 500 m of the cone will be:

$$\frac{W}{R} \text{ top 500 m} = \frac{1.4 \times 10^{14}}{9.3 \times 10^{10}} = 1500:1.$$

Consequently the degree of metal leaching and hydrothermal alteration will increase dramatically up the convective cone system, along with the increasing Water/Rock ratio.

GOLD TRANSPORT FROM THE SOURCE REGION

The method of gold transport from the source region to the seafloor is controlled by buffer reactions between the heated seawater and the volcanic rocks.

Our previous studies (Huston and Large, 1987) show that for temperatures above 350°C, i.e. deep in the convective system, gold will be mobilised as the $AuCl_2^-$ complex. The switchover point between chloride transport and bisulphide transport will depend on temperature, pH and the a_{Cl^-}/a_{H_2S} ratio. In low temperature VMS systems generating Pb-Zn-rich ore, the switchover will be at about 350°C, which means that the upper and outer sections of the convective cone will promote $Au(HS)_2^-$ transport. However in high temperature copper-rich systems (e.g. Mt Chalmers or Mt Lyell), the switchover line will extend up into the orebody and roughly correspond to the boundary between copper ore and lead-zinc ore.

It is possible that under certain conditions (e.g. lower temperatures, low salinity, high pH), low grade gold ± copper veins or disseminations may be found deep in the convective channel due to saturation of the $AuCl_2^-$ complex before the switchover line is reached (fig. 3). This would cause a depletion of gold (and copper) in the fluids that reached the seafloor, and therefore a gold depleted VMS would result.

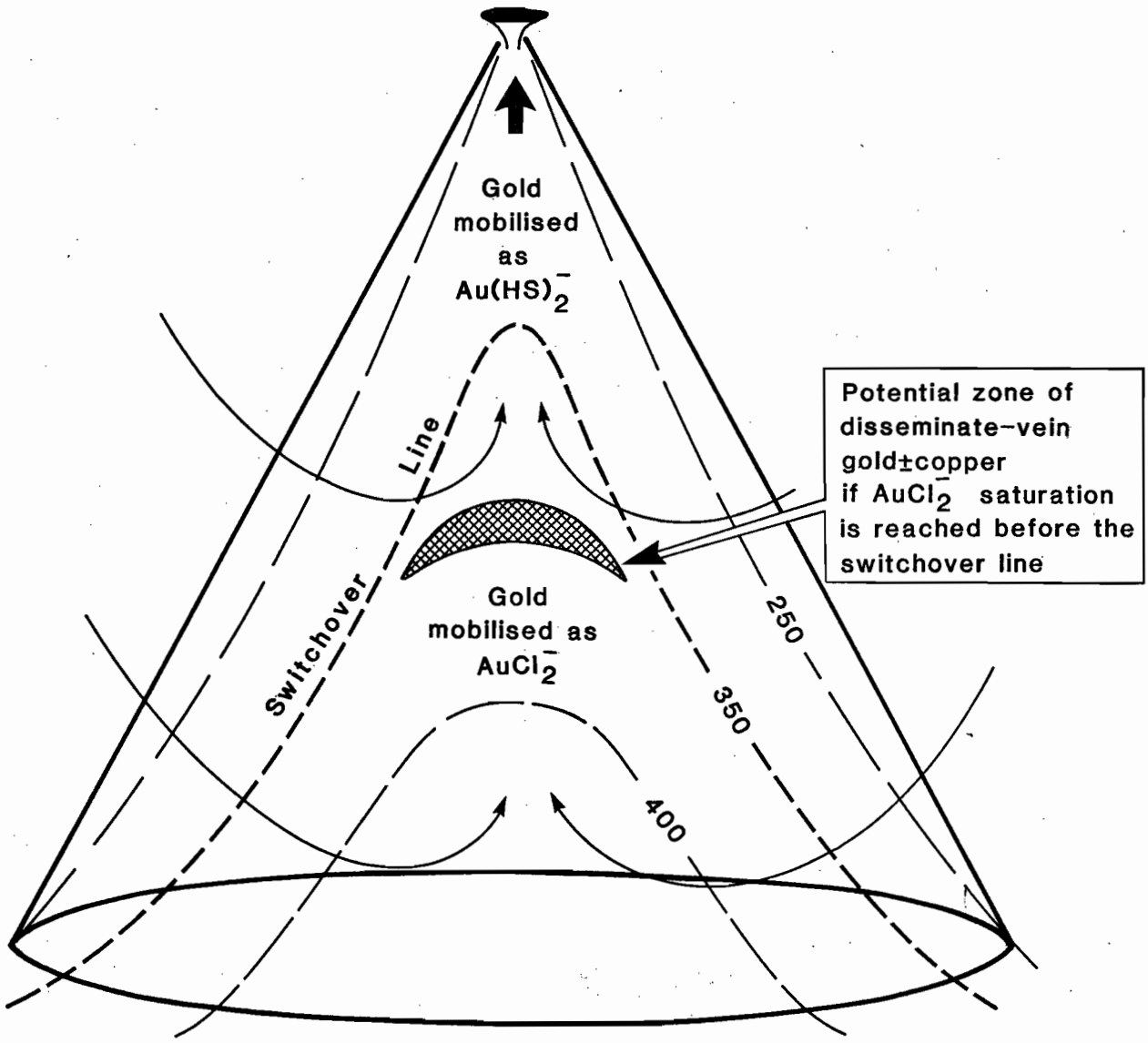

Figure 3 : Cone of metal leaching below a massive sulphide, with the switch-over line, separating $AuCl_2^-$ transport from $Au(HS)_2^-$ transport, equivalent to the 350^0C geotherm.

Effect of rock composition

Mafic volcanic rocks (basalt and andesite) contain a relatively high percentage of Fe^{2+}, Ca^{2+}, Mg^{2+} and sulphides compared to felsic volcanics (dacites and rhyolites). In mafic volcanics the following reactions will buffer the fO_2, pH and a_{H_2S} of the solution.

1. $4Fe^{2+} + 4H_2O + O_2 \leftrightarrow 2Fe_2O_3 + 8H^+$
   leads to a decrease in fluid fO_2.

2. $(Ca,Na_2)\ Al_2Si_6O_{16} + K^+ + 2H^+ \leftrightarrow KAl_3Si_3O_{10}(OH)_2 + 6SiO_2 + 3Na^+$
   plagioclase → muscovite
   leads to a decrease in fluid pH.

3. $FeS_2 + 2H^+ + H_2O \leftrightarrow Fe^{2+} + 2H_2S + \frac{1}{2} O_2$
   leads to an increase in a_{H_2S}.

These reactions will promote a depression of the switchover line and enhance gold mobilisation as $Au(HS)_2^-$. Thus low temperature convection in basaltic source rocks will promote gold mobilisation as $Au(HS)_2^-$ whilst high temperature convection in rhyolite source rocks will promote gold mobilsation as the $AuCl_2^-$ complex. In a pile composed of rhyolite followed by basalt, gold initially mobilisesd as $AuCl_2^-$ may be precipitated in a disseminated gold ± copper zone at the contact with the basalt, due to buffer reactions between the fluid and the basalt, which cause decreasing fO_2 and increasing pH.

FURTHER STUDIES

This preliminary discussion points to the need for future studies on:

a. the level of saturation of gold in the convective cone and its relation to gold in VMS deposits;

b. the effect of different source rock compositions on the convective cone;

c. the likelihood of disseminated gold ± copper deposits deep in the convective cone due to early saturation of $AuCl_2^-$ in the circulating fluid.

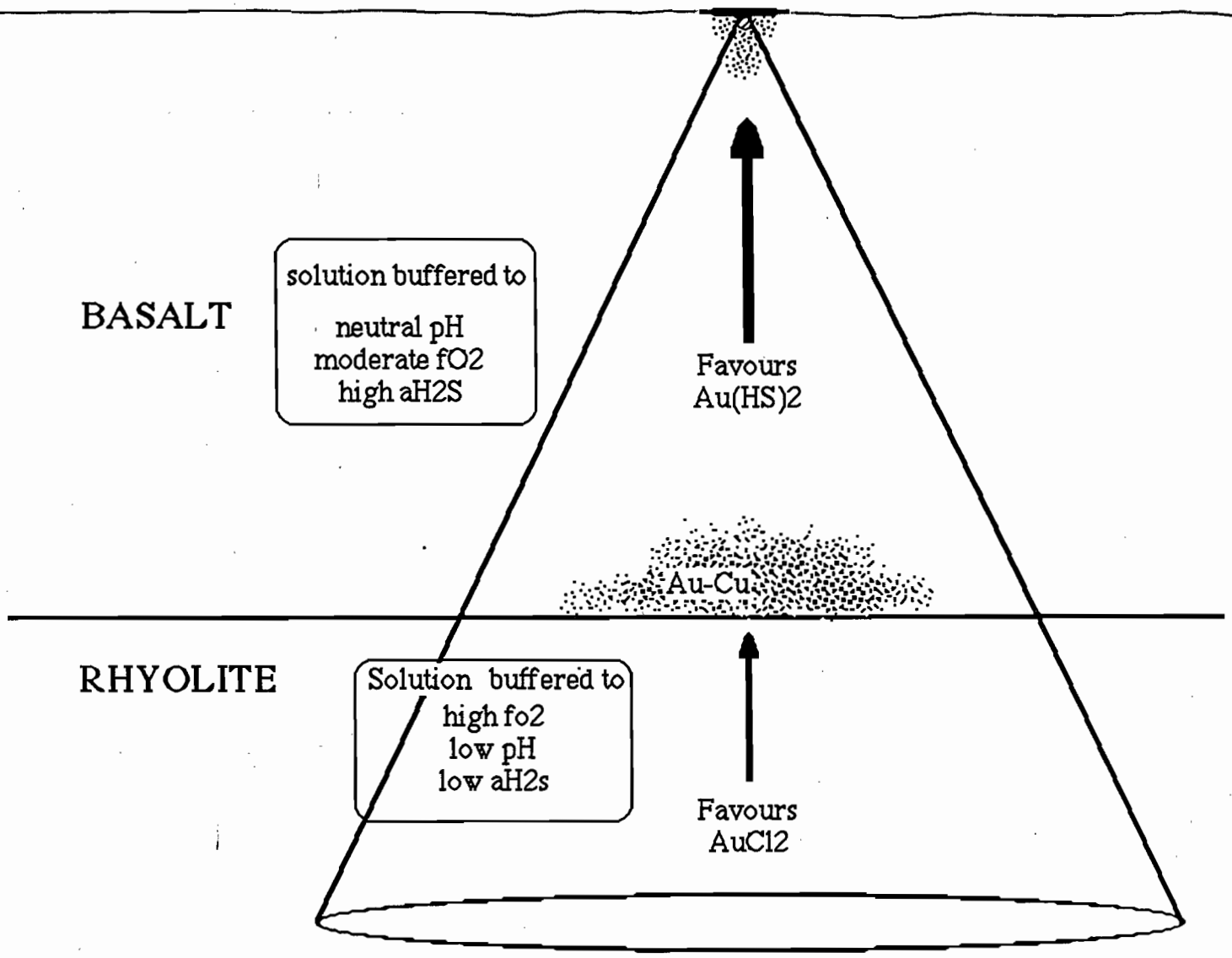

Figure 4 : Cone of metal leaching in a bimodal pile of volcanics. In the lower rhyolite dominated sequence gold would be mobilised as $AuCl_2^-$, whilst in the upper basalt dominated sequence gold is mobilised as $Au(HS)_2^-$. A zone of gold ± copper deposition may occur at the boundary of the rhyolite/basalt sequence.

REFERENCES

Crocket, J., 1974. Gold, Ch. 79. In Handbook of Geochemistry, K.H. Wedepohl (ed.). Springer-Verlag.

Gulson, B.L., Large, R.R. and Porritt, P.M., 1987. Base metal exploration of the Mount Read Volcanics, Western Tasmania: Pt. III. Application of lead isotopes at Elliott Bay. Econ. Geol., V.82, p.308-327.

Helgeson, H.C., 1969. Thermodynamics of hydrothermal systems at elevated temperatures and pressures. Am. Jour. Sci., V.267, p.729-804.

Henley, R.W., 1985. Geology and geochemistry of epithermal systems. Reviews in Econ. Geol., V.2, p.1-24.

Huston, D.L. and Large, R.R., 1987. A chemical model for the concentration of gold in volcanogenic massive sulphide deposits. Unpublished report, University of Tasmanua, July 1987, 36p.

Hutchinson, R.W., 1986. Precious metals in massive sulphide ores. Paper presented to S.E.G./A.I.M.E. meeting, New Orleans, March 1986.

Keays, R.R., 1987. Principles of mobilization (dissolution) of metals in mafic and ultramafic rocks - the role of immiscible magmatic sulphides in the generation of hydrothermal gold and volcanogenic massive sulphide deposits. Ore Geology Reviews, V.2, p.47-63.

Komyshan, P., 1986. Geology of the Hellyer-Mt Charter Area. In Large, R.R. (ed.). The Mount Read Volcanics and associated ore deposits. Geol. Soc. Aust. Tas. Div., Abs. Vol. p.53-56.

Whitford, D.J. and Craven, S.J. Strontium isotope studies at Que River and Hellyer. In Large, R.R. (ed.) the Mount Read Volcanics and associated ore deposits. Geol. Soc. Aust. Tas. Div., Abs. Vol. p.89-90.

APPENDIX 1

The following data has come to hand on an extremely gold-rich massive sulphide system in the Hokuroku district, Japan.

The Nurukawa deposit, which is quite small, contains the following approximate ore types and grades (Yamada et al., 1987, and Mining Journal, March, 1987):

	Au ppm	Cu %	Pb %	Zn %	Ag ppm
Lead-zinc black ore	7.5	0.9	5.0	10.0	150
Stockwork ore	13.5	2.0	2.0	3.0	40

Yamada et al. report that the gold has a strong affinity for copper and iron in the stockwork ore, i.e. similar to our observations at Mount Chalmers. Attempts are being made to have the paper translated.

Nurukawa Ore for Dowa Mining

Uchinotai Mining Co. Ltd., the wholly-owned subsidiary of Dowa Mining Co., will start underground production at the Nurukawa mine in April. This mine is located in northern Japan and was discovered in 1974 by Japan's Metal Mining Agency.

Dowa started underground drifting and drilling in 1982 and outlined large amounts of kuroko ore. In 1986, the company proved a lense of 50,000 t of siliceous ore grading 13.3 g/t gold.

The deposit contains five orebodies (No.1 to No.5) and initially the company will be mining the No.5 orebody at the rate of 5,000 t/month. This will comprise 3,700 t/month of kuroko ore (7.5 g/t gold, 150 g/t silver, 0.9% copper, 5.0% lead, 10.0% zinc) and 1,300 t/month of siliceous ore (10.0 g/t gold and 40 g/t silver).

A follow-up programme of underground drilling to increase the ore reserves will be continued.

鉱山地質 (Mining Geology), 37(2), 109～118, 1987

温川鉱床の高含金珪鉱について*

山田亮一**・須山俊明**・大串　融***

Gold-bearing siliceous ore of the Nurukawa kuroko deposit, Akita prefecture, Japan.

By Ryoichi Yamada**, Toshiaki Suyama** and Nagashi Ogushi***

Abstract: The Nurukawa deposit is of Kuroko type lately discovered in the northeastern extension of the Hokuroku district. The first discovery was made by surface diamond drilling in 1984 under thick cover of Quaternary pyroclastics about 2 km west of the lake Towada. An extensive exploration program has been carried out by combining construction of underground drifts and subsequent underground drillings.

The No. 5 and No. 3 ore bodies are now under exploration and exploitation. The characterisitcs of the deposit are nearly the same as those of known Kuroko deposits except its high gold content. It consists of polymetallic massive sulfide layer (black ore) and underlying silicified tuff breccia with network and dissemination of sulfides (siliceous ore). The siliceous orebody is classified into two types, namely, layered and stockwork, based on their shape and mode of occurrence. The latter type has cylindrical shape with a diameter of 20 to 40 meters and the vertical length of more than 50 meters. It has been revealed that gold content in the siliceous ore is extremely high especially in its core which ranges from 15 gram/ton to 100 gram/ton.

Gold and silver mineral in siliceous ore is identified as electrum which has 50-70 wt.% gold and 50-30 wt.% silver. In layered and stockwork siliceous ores, the electrum is concentrated in the chalcopyrite-pyrite-quartz veinlets as tiny grains about 10 microns in their diameter. These veinlets occur both on the margins of sphalerite and galena-bearing sulfide veinlets and within breccias in sphalerite and galena-bearing silicified pyroclastic rocks.

Statistical analysis of assays on gold, silver, lead, zinc, iron, and barium (sulfate) in the siliceous ore indicates that gold has strong affinity with copper and iron. Whereas, lead, zinc and barium which represent the elements enriched in black ore show good correlation each other. It is concluded, therefore, that the gold mineralization took place prior to that of the black ore.

1. はじめに

温川鉱山は金属鉱業事業団の地質構造調査と企業探鉱の連携により，昭和59年９月に発見された本邦で最も新しい黒鉱鉱床である．鉱床は第1～第５の５鉱体からなり，金銀の高い緻密質黒鉱，礫状黒鉱，石膏および黒鉱質珪鉱などで構成される(西谷ほか，1986)．

同和鉱業㈱は，昭和60年に金属鉱業事業団より温川構造坑道の譲渡を受け，当鉱山の開発に着手した．開発に当っては軌道と併用して，深沢・餌釣両鉱床の開発で成果をあげたトラックレスマイニング法がとり入れられ，主鉱体である第５鉱体と第３鉱体から着手された．現在，第５鉱体下盤基幹坑道と上盤探鉱坑道の一部，および第３鉱体下盤探鉱基幹坑道が完成，坑内試錐機３台を投入して鋭意探鉱中である．

この過程で，北鹿地域の黒鉱鉱床では例のない極めて金品位の高い珪鉱が発見された．当珪鉱は調査の進展にともない，経済的にも重要な量を占め，かつ温川鉱床の特性解明の重要な鍵になると予想されるに至った．現在なお探鉱継続中でもあり，その全体像は必ずしも明確ではないが，ここに現在まで判明した事実を紹介し，御意見，御批判を仰ぐ次第である．

2. 地質・鉱床の概要

2.1 地　質

当地域の地質は，下部より鍋倉沢層，早瀬森層，遠部層，および碇ヶ関層の第三系と，これらを不整合に覆う十和田火山堆積物からなる(第１図)．鉱山周辺では十和田火山堆積物が広く地表を覆い，第三系は谷沿いの低地に沿って細長く分布するにすぎない(第２図)．早瀬森層は凝灰角礫岩を主とする下部層と軽石凝灰岩からなる上

1987年２月13日受付，同年３月10日受理
* 1987年６月２日　日本鉱業協会第34回全国鉱山探査現場担当者会議で講演
** 同和鉱業㈱資源部北部探査室(Dowa Mining Co., Kosaka-cho, Kazuno-gun, Akita, 017-02)
*** 同和鉱業㈱資源部
Keywords: Nurukawa deposit (温川鉱床), Kuroko deposit, Gold-bearing siliceous ore

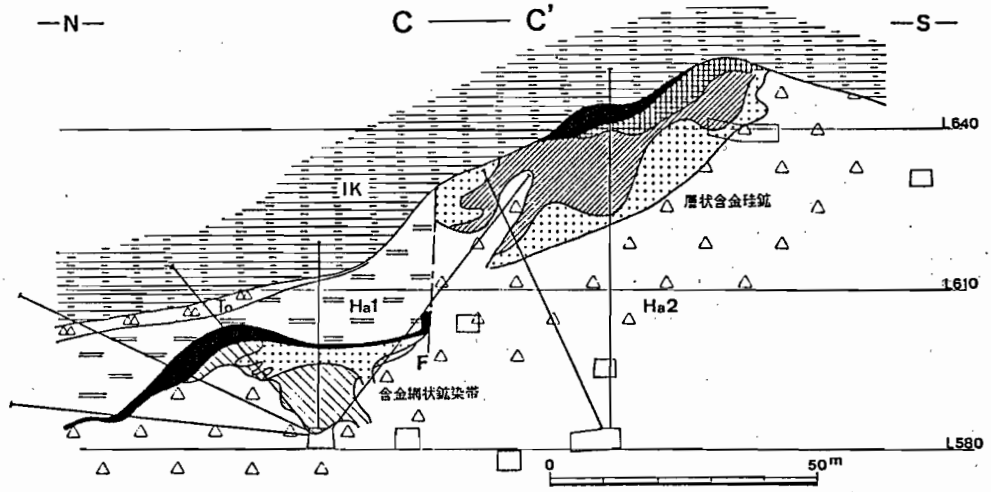

第7図-2　含金珪鉱の金品位分布(2)
F：断層（凡例は第1図に同じ，断面線位置は第4図C-C'）

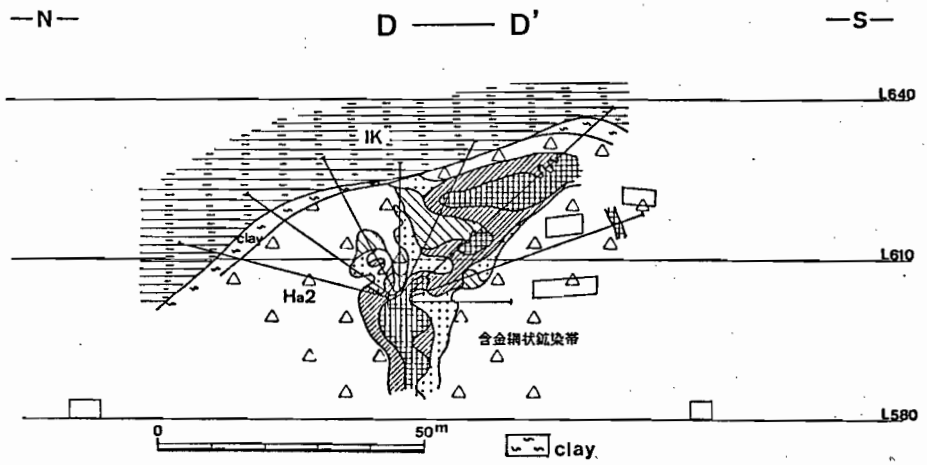

第7図-3　含金珪鉱の金品位分布(3)
（凡例は第1図に同じ，断面線位置は第4図D-D'）

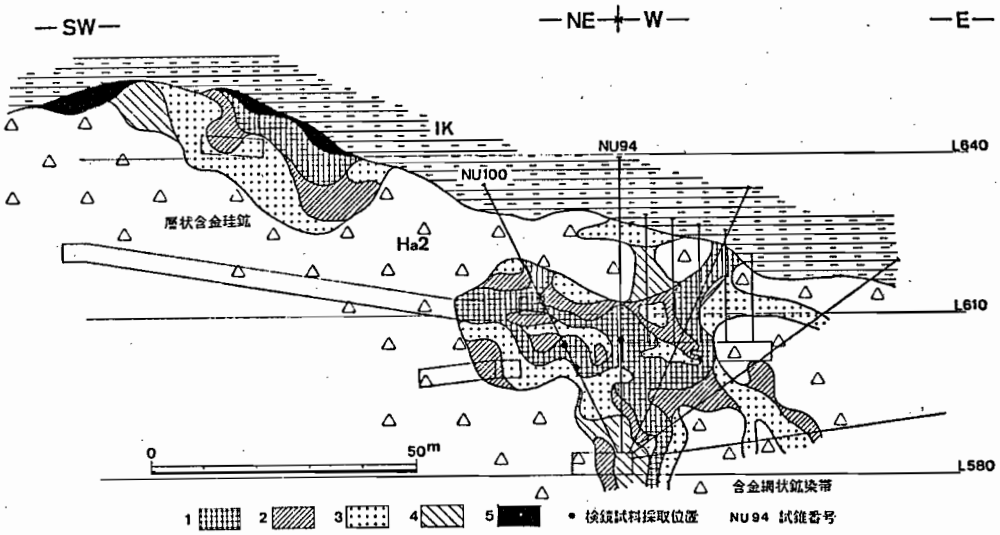

第7図-1　含金珪鉱の金品位分布(1)
1.Au 10 g/t 以上　2. Au 5～10 g/t　3. Au 2～5 g/t　4.黒鉱質珪鉱(Au 2 g/t 未満，Pb＋Zn 4%以上)　5.層状黒鉱
（凡例は第1図に同じ，断面線位置は第4図B-B'）